Discovery of novel Baeyer-Villiger monooxygenases and their application in organic synthesis

Inauguraldissertation

zur

Erlangung des akademischen Grades

doctor rerum naturalium (Dr. rer. nat.)

an der Mathematisch-Naturwissenschaftlichen Fakultät

der

Ernst-Moritz-Arndt-Universität Greifswald

vorgelegt von

Jessica Rehdorf

geboren am 22. August 1981

in Berlin

Greifswald, Dezember 2009

Dekan:	Prof. Dr. Klaus Fesser
1. Gutachter:	Prof. Dr. Uwe T. Bornscheuer
2. Gutachter:	Prof. Dr. Jörg Pietruszka
Tag der Promotion:	25. Januar 2010

Danksagung

Zuerst möchte ich mich allerherzlichst bei Professor Uwe T. Bornscheuer bedanken. Er hat es mir ermöglicht, meine Doktorarbeit über Baeyer-Villiger Monooxygenasen in seinem Arbeitskreis anzufertigen. Während dieser Zeit hat er mir stets mit seinem Rat, seinen Ideen, seiner Unterstützung und seinem uneingeschränkten Vertrauen zur Seite gestanden.

Weiterhin gilt mein besonderer Dank Professor Marko D. Mihovilovic von der Technischen Universität Wien. Während meiner Doktorarbeit ermöglichte er es mir, einen Teil der Forschung in seiner Arbeitsgruppe durchzuführen. Mein Dank gilt auch Thomas, Michi F., Michi S. und Saima, die mich während meines Aufenthalts in Wien unterstützt und für die nötige abendliche Abwechslung gesorgt haben. An meine Zeit in Wien werde ich mich noch lange erinnern.

Bedanken möchte ich mich auch bei Professor Jörg Pietruszka. Während der Förderzeit im Schwerpunkt „Nachhaltige Bioprozesse“ der Deutschen Bundestiftung Umwelt hat er mich als Co-Mentor betreut. Weiterhin übernahm er das Koreferat meiner Arbeit. Vielen Dank dafür.

Meinen besonderen Dank widme ich der gesamten Arbeitsgruppe Bornscheuer, in der ich mich in den letzten Jahren sehr wohl gefühlt habe. Vielen Dank an Anke, Radka, Christian und Andrew für das Korrekturlesen meiner Dissertation und die vielen hilfreichen Tips. Danke auch an Rainer und Matthias, mit denen ich in der ersten Zeit ein Labor geteilt habe. Dabei gab es oft interessante und anregende Diskussionen. Für die (fast) regelmäßigen Kartenabende nach der Arbeit möchte ich mich bei Marlen, Helge, Martin, Christian und Sebastian S. bedanken. An die Zeit in Greifswald werde ich oft zurück denken. Ich wünsche Euch alles Gute.

Meinen herzlichen Dank gilt auch der Deutschen Bundesstiftung Umwelt (DBU), die mich während der letzten drei Jahre nicht nur finanziell, sondern, durch die Aufnahme in den Schwerpunkt „Nachhaltige Bioprozesse“, auch ideell unterstützt hat. Vielen Dank an Frau Dr. H. Schlegel-Starmann für die persönliche Betreuung seitens der DBU. Bedanken möchte ich mich auch bei Professor A. Liese für die Koordination und Organisation innerhalb des Schwerpunktes.

Mama und Papa, auch bei Euch möchte ich mich bedanken. Ich widme Euch diese Arbeit, denn ohne Euch würde ich heute hier nicht stehen. Vielen Dank für Eure Liebe und Euer Vertrauen. An letzter Stelle, für mich aber immer an erster, bedanke ich mich bei Christoph, für seine Geduld, sein Verständnis, sein Zuhören und seine Motivation und dafür, dass er mich immer wieder daran erinnert hat, dass es neben Baeyer-Villiger Monooxygenasen auch andere wichtige Dinge im Leben gibt.

Für meine Eltern

Table of contents

List of abbreviations and symbols

A.	*Acinetobacter*
ADH	alcohol dehydrogenase
ADP	adenosin-5'-diphosphate
ATP	adenosin-5'-triphosphate
bp	base pair
BVMO	Baeyer-Villiger monooxygenase
BVO	Baeyer-Villiger oxidation
C.	*Comamonas*
c	conversion
CAL-A	lipase A from *Candida antarctica*
CAL-B	lipase B from *Candida antarctica*
CDMO	cyclododecanone monooxygenase
CHMO	cyclohexanone monooxygenase
CPMO	cyclopentanone monooxygenase
d	day(s)
DMF	N,N-dimethyl formamide
DMSO	dimethyl sulfoxide
DNA	desoxyribonucleic acid
E	enantioselectivity, E-value, enantiomeric ratio
E.C.	Enzyme Comission
E. coli	*Escherichia coli*
ee	enantiomeric excess
ee_P	enantiomeric excess of the product
ee_S	enantiomeric excess of the substrate
FAD	flavin adenine dinucleotide
FDH	formiate dehydrogenase
FMN	flavin adenine mononucleotide
g	gram
GC	gas chromatography
h	hour(s)
HAPMO	4-hydroxyacetophenone monooxygenase
i-Pr	isopropyl
IPTG	isopropyl-β-thio-D-galactopyranoside
K	equilibrium constant
k	reaction rate constant
kb	kilo base
k_{cat}	'turnover number'
kDa	kilo Dalton
kg	kilogram
K_M	Michaelis-Menten constant
K_S	dissociation constant
L	liter
LC	liquid chromatography
LB	Luria Bertani (medium)
M	mol per liter
mg	milligram
min	minute
mM	millimol per liter
mol	$6.022*10^{23}$ molecules
MS	mass spectroscopy
$NAD(P)^+$	nicotinamide adenosine diphosphate (oxidized)
NAD(P)H	nicotinamide adenosine diphosphate (reduced)
n-Bu	*n*-butyl
ng	nanogram
nm	nanometer
NMR	nuclear magnetic resonance
P.	*Pseudomonas*
PAGE	polyacrylamide gel electrophoresis
PAMO	phenylacetone monooxygenase
PCR	polymerase chain reaction
pH	*pondus hydrogenii*
R.	*Rhodococcus*
RT	room temperature
SDS	sodium dodecyl sulfate
sp.	species
T	temperature
T.	*Thermobifida*
U	unit (defined as 1 µmol/min)
v_{max}	maximal reaction rate in Michaelis-Menten kinetics
vol	volume
wt	wild-type
µg	microgram
µL	microliter
µmol	micromol
°C	degree celsius
%	percent
[α]	specific optical rotation
λ	wavelength
ρ	reaction constant
σ	substituent constant

Besides, also the common codes for amino acids and nucleotides as well as abbreviations for restriction enzymes were used.

List of articles sorted by topics

I. "Kinetic resolution of aliphatic acyclic β-hydroxy ketones by recombinant whole cell Baeyer-Villiger monooxygenases – Formation of enantiocomplementary regioisomeric esters."
Jessica Rehdorf, Alenka Lengar, Uwe T. Bornscheuer and Marko D. Mihovilovic (2009). *Bioorganic and Medical Chemistry Letters*, **19**, 3739-3743.

II. "Enzymatic synthesis of enantiomerically pure β-amino ketones, β-amino esters and β-amino alcohols with Baeyer-Villiger monooxygenases."
Jessica Rehdorf, Marko D. Mihovilovic, Marco W. Fraaije and Uwe T. Bornscheuer (2009). *Submitted*.

III. "Exploiting regioselectivity of Baeyer-Villiger monooxygenases: a route to the formation of β-amino acids."
Jessica Rehdorf, Marko D. Mihovilovic and Uwe T. Bornscheuer (2009). *Submitted*.

IV. "Enantioselective kinetic resolution of 3-phenyl-2-ketones using Baeyer-Villiger monooxygenases."
Kristian Geitner, Anett Kirschner, Jessica Rehdorf, Marlen Schmidt, Marko D. Mihovilovic and Uwe T. Bornscheuer (2007). *Tetrahedron Asymmetry*, **18**, 892-895.

V. "Cloning, expression and characterization of a Baeyer-Villiger monooxygenase from *Pseudomonas putida* KT2440."
Jessica Rehdorf, Anett Kirschner and Uwe T. Bornscheuer (2007). *Biotechnology Letters*, **29** (9), 1393-1398.

VI. "Cloning, expression, characterization, and biocatalytic investigation of the 4-hydroxyactophenone monooxygenase from *Pseudomonas putida* JD1."
Jessica Rehdorf, Christian L. Zimmer and Uwe T. Bornscheuer (2009). *Applied Environmental Microbiology*, **75** (10), 3106-3114.

Book chapter

I. "Monooxygenases, Baeyer-Villiger applications in organic synthesis."
Jessica Rehdorf and Uwe T. Bornscheuer (2009). In: *Encyclopedia of Industrial Biotechnology: bioprocess, bioseparation and cell technology*, VCH-Wiley & Sons, Inc., **Vol.1**, in press.

Preface

In this thesis the capabilities and possible industrial applications of Baeyer-Villiger monooxygenases (BVMOs) are presented, focusing on kinetic resolutions of racemic substituted linear and aryl aliphatic ketones to identify a new class of substrates for biooxidation. Furthermore, the search for other BVMOs to enlarge the enzymatic toolbox for biocatalytic investigation is outlined.

Enzymes are nature's biocatalyst equivalent of the chemical (metal)-catalysts usually used in synthetic organic chemistry. They not only meet the demands of sustainable and green chemistry, but they play a key role in industrial biotransformations today due to their advantages of often high chemo-, regio- and enantioselectivity. Their capacity to distinguish between two optically active biological compounds make enzymes powerful instruments in synthetic routes. Therefore, they offer the possibility to replace chemical reactions and thus contribute to the protection of nature and the environment. This led to their renaissance as tools for the pharmaceutical, food, textile, cosmetic and (agro)chemical industry.

However, mankind was already using enzymes for the production of food (cheese) and beverages (wine and beer) centuries ago. Today, enzymes can be isolated from plants and animals, where they are involved in a broad spectrum of biochemical reactions and the regulation of metabolism. The majority of industrially used enzymes is however of bacterial origin. The fact that enzymes catalyze reactions under mild conditions (e.g. physiological pH, room temperature) and in aqueous solutions makes them desirable for environmentally benign processes. Nevertheless, applications are still limited due to a restricted substrate spectrum combined with low enzyme-stability and high production costs. Recent advances in molecular biology, genomics and proteomics could help to overcome these obstacles. Methods of directed evolution and rational protein design allow access to enzymes with tailor-made properties and catalyzing the conversion of a broad range of substrates. Efficient high-throughput screening and selection methods have facilitated the identification of new and/or redesigned enzyme variants with higher solvent tolerance, better temperature and pH-stability, and combined with the heterologous expression of enzymes further increased the diversity of biocatalysts. Moreover, enzymes can be applied to catalyze the production of chemical substances that are still challenging or even not accessible using common chemical methods. All these features are essential to make enzymes competitive, profitable and sustainable alternatives to already established synthetic processes.

Among the discovered enzymes so far, Baeyer-Villiger monooxygenases belong to a comparatively young group of oxidizing enzymes. The oxidation of a ketone to its corresponding ester by introducing an oxygen atom between a carbon-carbon bond is one of the most powerful chemical reactions in organic synthesis today, and leads to valuable synthons and intermediates for the production of fine chemicals and pharmaceuticals. The following work will give an overview of the properties of BVMOs and their synthetic applications, both in analytical and large scale, to date.

1 Introduction

1.1 Baeyer-Villiger monooxygenases, properties and application in organic synthesis

1.1.1 The chemical Baeyer-Villiger oxidation

1.1.1.1 Mechanistic aspects

The discovery of the chemical Baeyer-Villiger oxidation dates back to 1899, when Adolf Baeyer and Victor Villiger first described an oxygen-inserting process between a carbon-carbon bond of cyclic ketones using persulfuric acid.[1] It is a typical peracid-catalyzed reaction, where a non-activated ketone is converted into the corresponding ester or lactone. The generally accepted mechanism for this Baeyer-Villiger oxidation, which was initially proposed by Criegee in 1948[2], is a two-step process and involves the formation and decay of the so-called Criegee-intermediate (Scheme 1.1).

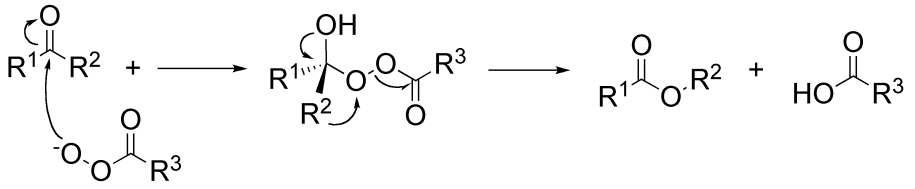

Scheme 1.1 Mechanism of the chemical Baeyer-Villiger oxidation proposed by Criegee.

For several decades the exact mechanism by which the oxygenation reaction proceeded was debated. Finally, it was elucidated in 1953, when W. Doering and E. Dorfmann published results on the study of the Baeyer-Villiger oxidation of ^{18}O-labeled benzophenone.[3] They proved that upon oxidation with perbenzoic acid, the labeled oxygen atom ended up as the carbonyl oxygen of the ester that was formed, as originally proposed by Criegee ((1) in Scheme 1.2). Formation of a dioxirane (2) postulated by Baeyer and Villiger[1] or the formation of a carboxyloxide by $^{+}$OH-transfer of the peracid to the oxygen of the carbonyl group[4] (3) did not occur.

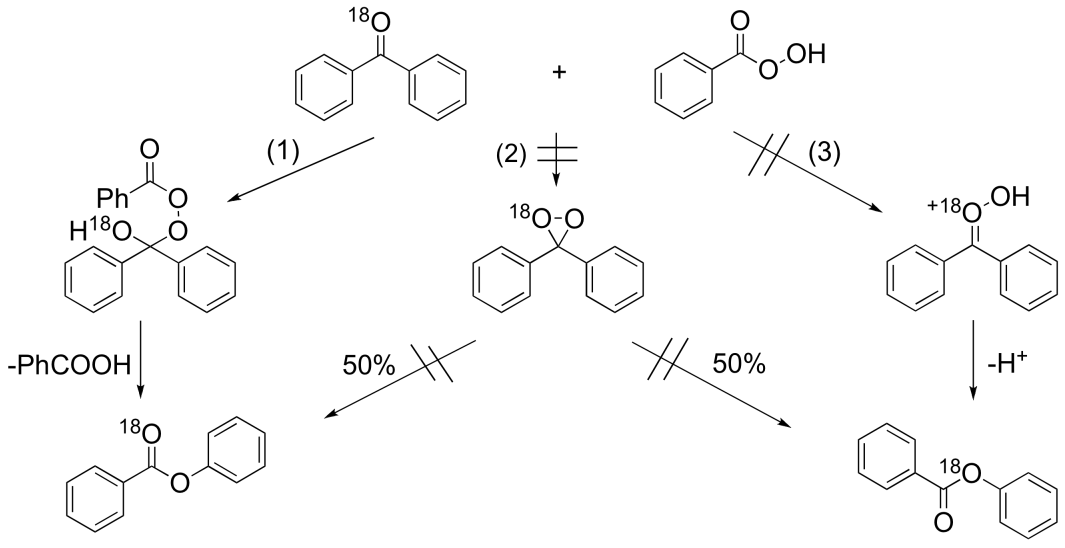

Scheme 1.2 Baeyer-Villiger oxidation with ^{18}O-labeled benzophenone confirmed the mechanism proposed by Criegee, performed in 1953 by Doering and Dorfmann.

1.1.1.2 Stereoselective Baeyer-Villiger oxidations

Peracids (e.g. hydrogen peroxide, *m*-chloroperbenzoic acid) are often toxic and explosive, thus requiring considerable safety precautions at high concentrations and in large-scale processes. Additionally, they are expensive and low yields often occur, which is detrimental towards ecological aspects of the reaction. The risk potential and high costs of using peracids have triggered the development of more gentle oxidants. Today, alternative and more stable compounds like bis(trimethysilyl)peroxide[5] and manganese monoperoxy phthalate are applied. In the 1990s, reactions were developed where molecular oxygen served as oxidizing and aldehydes as reducing agents.[6] Both transition metal- and main group element-based complexes were implemented for enantioselective Baeyer-Villiger oxidation. Pioneering work using hydrogen peroxide and molecular oxygen was done by the groups of Strukul and Bolm, respectively. Especially platinum(II)-complexes with chiral diphosphine ligands[7] and nickel(II)- or copper(II)-complexes[8] (Figure 1.1) were commonly used for stereoselective conversions of cyclohexanone and cyclopentanone derivatives, and gave moderate enantiomeric excesses (up to 58% ee).[9]

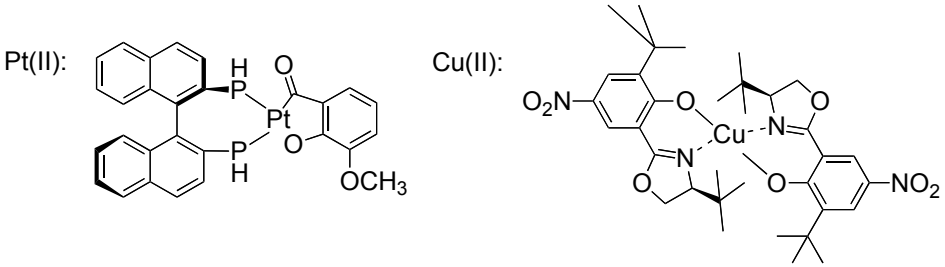

Figure 1.1 Platinum complex with phosphine ligand and copper complex used for stereoselective Baeyer-Villiger oxidations.

In 1995, Bolm and coworkers were able to convert racemic bicyclo[4.2.0]octanone in an enantiodivergent reaction. The use of a copper-complex catalyst and molecular oxygen yielded the regioisomeric lactone products in 92 and 67% ee (Scheme 1.3).[10]

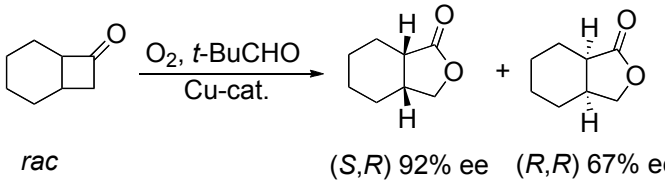

Scheme 1.3 Enantiodivergent Baeyer-Villiger oxidation of bicyclo[4.2.0]octanone using a chiral copper-complex and molecular oxygen.

1.1.2 The enzymatic Baeyer-Villiger oxidation

1.1.2.1 Discovery of Baeyer-Villiger monooxygenases and their physiological role

The first indication of the natural existence of Baeyer-Villiger oxidations was reported in the late 1940s. During their studies on the degradation pathway of cholesterone Turfitt and coworkers observed that several fungi were able to convert steroids *via* a Baeyer-Villiger oxidation.[11] Only a few years later, Murray and Peterson proposed that during conversion of progesterone and testosterone into Δ^1-dehydro-testololactone, Baeyer-Villiger oxidations might be involved[12] (Scheme 1.4). Hence, nature's equivalent of the previously known synthetic Baeyer-Villiger reaction was discovered. The enzymes that catalyzed these reactions were named Baeyer-Villiger monooxygenases.

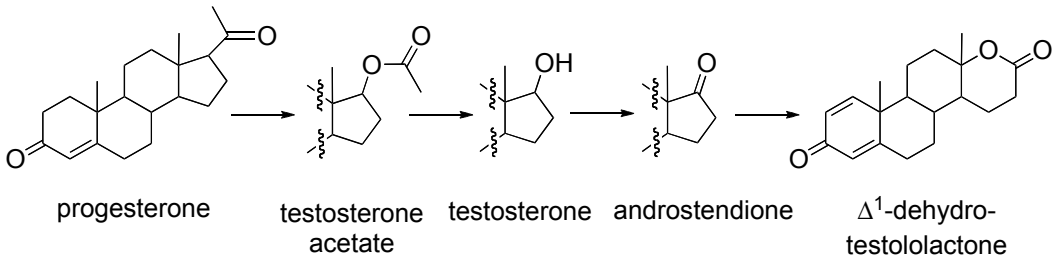

Scheme 1.4 Microbial degradation of progesterone into Δ^1-dehydro-testololactone presumably involves a BVO in the first and last step.

Besides steroid-converting enzymes, BVMOs involved in the degradation of aliphatic linear ketones were later discovered as well. It has been observed that various *Pseudomonas* strains were able to grow on tridecan-2-one.[13] Forney and Markovetz isolated undecyl acetate directly from growing cultures of *Pseudomonas aeroginosa*. Baeyer-Villiger oxidation is also a common reaction during the catabolic degradation of a variety of other compounds, including cyclic (mono-, bi- and polycyclic) and aromatic ketones. Also, it was observed that the Baeyer-Villiger reaction can be followed by an esterase-catalyzed hydrolysis. Indeed, genomic analyses showed that the gene encoding a BVMO is often located in the neighborhood of genes encoding for an esterase and an alcohol dehydrogenase.[14, Article V, Article VI] This co-localization demonstrates that BVMO, esterase/lactonase and dehydrogenase jointly play a key role in the degradation of natural compounds. One of the first reports describing lactone formation and ester bond cleavage was published in 1975[15] (Scheme 1.5) and details the degradation cyclohexanol as carbon source by various *Pseudomonas* sp. Further studies showed that other substrates, such as cyclopentanol[16], cyclohexane[17], cyclohexane-1,2-diol[18], cycloheptanone[19] and, more recently, cyclododecane[20], were degradated *via* analogous pathways.

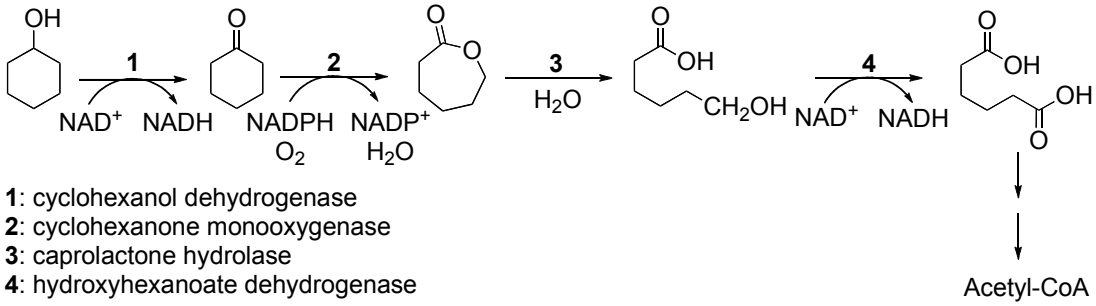

Scheme 1.5 Reaction sequence for the oxidation of cyclohexanone by *A. calcoaceticus* NCIMB 9871.

However, since the initial proposals of enzymatic-driven Baeyer-Villiger oxidations in 1948, it took more than two decades until the first BVMO was isolated and characterized. Today, more than 20 BVMOs have been cloned and functionally expressed in *E. coli*. They have been isolated from bacteria and fungi, where they are involved in the catabolism of organic compounds or are responsible for the switch between primary to secondary metabolism.[21]

1.1.2.2 Basic properties of Baeyer-Villiger monooxygenases (BVMOs)

Baeyer-Villiger monooxygenases (1.14.13.x) are flavoenzymes and belong to the class of oxidoreductases. They catalyze the oxidation of linear, cyclic and aromatic ketones to esters or lactones, respectively, highly similar to the chemical BVO (Scheme 1.6). During the enzymatic oxidation one atom of molecular oxygen is incorporated between a carbon-carbon bond of non-activated ketones, whereas the other oxygen atom ends up in a water molecule with the hydrogen atoms originating from the cofactor NAD(P)H. Compared to other monooxygenase systems (e.g. P450-monooxygenases), where oxygenases are membrane bound or at least membrane associated, BVMOs are typically soluble proteins and work without additional proteins (e.g. a reductase is required by most P450 enzymes).

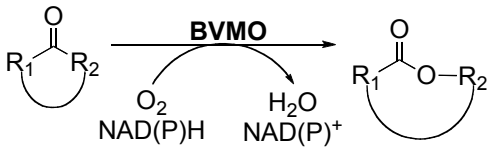

Scheme 1.6 Principle scheme of an enzymatic Baeyer-Villiger oxidation.

BVMOs contain a flavin cofactor (FAD or FMN), which is crucial for catalysis and is tightly, but not covalently, bound in the active site. Furthermore, these enzymes require stoichiometric reduction equivalents in order to reduce the flavin-cofactor and to activate it for molecular oxygen binding. Either NADH or NADPH act as the electron donors. Comparing some purified and well-characterized BVMOs revealed the existence of two subclasses[22]: Type I enzymes are the most intensively studied and are usually FAD-binding and NADPH-dependent. Both flavin reduction and substrate oxidation are carried out on one polypeptide chain. Some of these enzymes are monomeric, others have a homo-oligomeric structure

(homogeneous). On the contrary, type II BVMOs need FMN and NADH, while a substrate oxygenating subunit appears to require a separate flavin reductase, effectively serving as a NADH dehydrogenase, in order to generate reduced flavin (heterogeneous). The majority of discovered and described enzymes so far belong to type I BVMOs.

1.1.2.3 Enzymatic mechanism

The generally accepted enzymatic mechanism was initially proposed by Ryerson[23] and based on data obtained from the cyclohexanone monooxygenase (CHMO) from *A. calcoaceticus* NCIMB 9871. This enzyme was the only recombinantly available BVMO for a long time as it was cloned and overexpressed already in 1988.[24] Due to further investigation on the substrate profiles of other BVMOs, it was found out later that these enzymes not only catalyze a nucleophilic attack on a carbonyl atom of a ketone to yield the typical Baeyer-Villiger product, they are also able to perform an electrophilic reaction depending on the peroxygenated intermediate. Scheme 1.7 illustrates this catalytic cycle. The biocatalytic process is initiated by the reduction of the flavin moiety (1) mediated by the NADPH cofactor. In the second step $FADH_2$ (2) is then able to bind molecular oxygen to form the 4a-peroxyanion (3), which is in equilibrium with the corresponding 4a-hydroperoxyflavin[25] (4) and equivalent to the peroxy-group used in the chemical Baeyer-Villiger reaction. The presence of these two flavin species is suggested as responsible for either a nucleophilic or an electrophilic reaction process. The nucleophilic peroxyanion (3) facilitates Baeyer-Villiger oxidations as well as Michael-type addition on activated C-C double bonds, while the electrophilic hydroperoxide (4) is capable of heteroatom oxidation and epoxidation.[26] The nucleophilic attack at a carbonyl function generates the typical Criegee-intermediate (5), which decomposes after rearrangement to form the corresponding ester and 4a-hydroxyflavin (6). The catalytic cycle is closed with product release and elimination of water leading to FAD (1), which is now available for the next cycle.

The ability to stabilize a negatively charged peroxyflavin intermediate enables BVMOs to perform Baeyer-Villiger reactions. It is assumed that the consumed cofactor NADPH, which remains bound in the active site throughout the catalytic cycle[27], might be one reason for stabilization. Only after oxygenation and when the decay of the Criegee-intermediate occured, $NADP^+$ is released. Additionally, release of the oxidized cofactor $NADP^+$ limits the rate of catalysis, which indicates that the conversion rate is not always controlled by the nature of the substrate.[25]

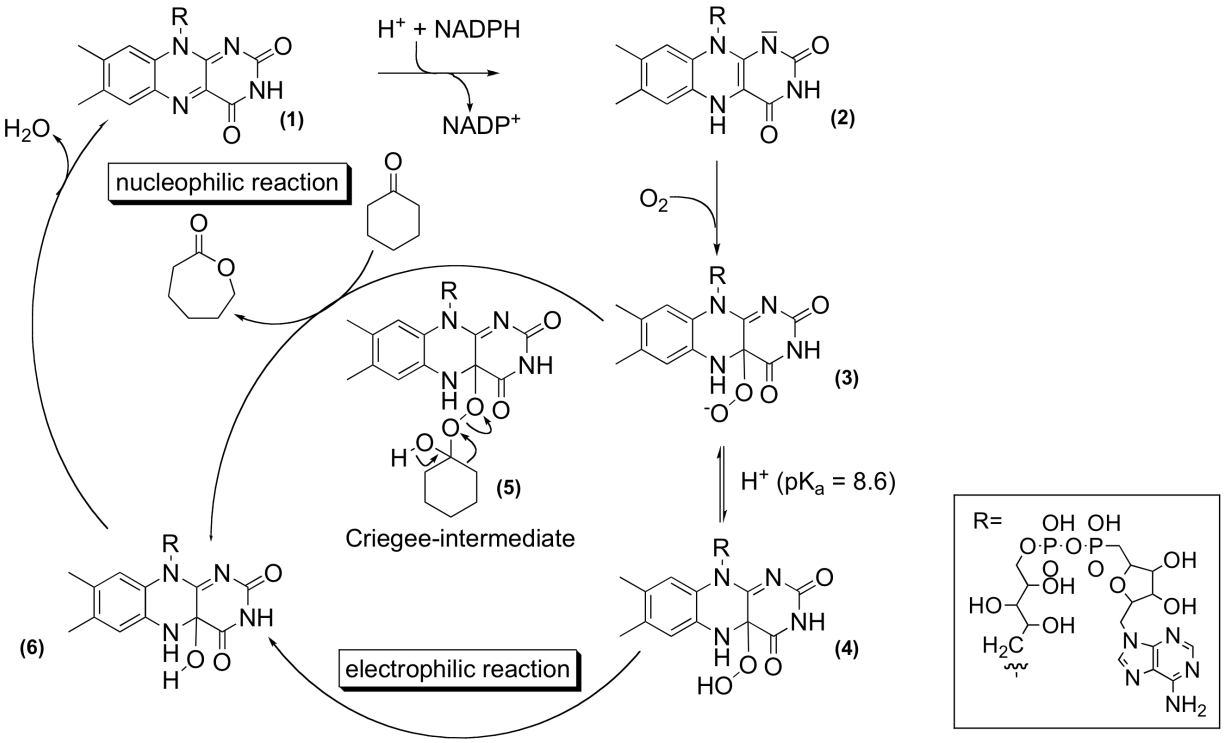

Scheme 1.7 Proposed mechanism for enzymatic Baeyer-Villiger oxidation type I.

1.1.2.4 Structural features

The first crystal structure of a BVMO was published in 2004.[28] Here, Malito *et al.* resolved the three dimensional structure of the phenylacetone monooxygenase (PAMO, pdb-code: 1W4X) originating from the thermophilic bacterium *Thermobifida fusca* (Figure 1.2). Until then, the cubic space model of CHMO from *A. calcoaceticus* NCIMB 9871 served as a model to describe enzymatic catalysis in the active site.[29] PAMO is a monomeric 62 kDa protein and so far the only thermostable among all characterized BVMOs. It has a two-domain architecture and the active site is located in a cleft at the domain interface. PAMO possesses two dinucleotide-binding motifs which are part of two Rossmann-folds: one for FAD, which binds at the bottom of the cleft between the two domains, and one for NADPH/NADP$^+$, which is coordinated by two conserved amino acids: R217 and K336. Both residues are crucial for recognition of the adenine and the 2'-phosphate moieties of NADPH, respectively. Replacement of R217 with Ala greatly reduced affinity to NADPH, while mutation of K336 into Ala switched the preference of cofactor towards NADH.[30] The highly conserved Lys336 explains the strict dependency on the phosphorylated cofactor form among Baeyer-Villiger type I monooxygenases.

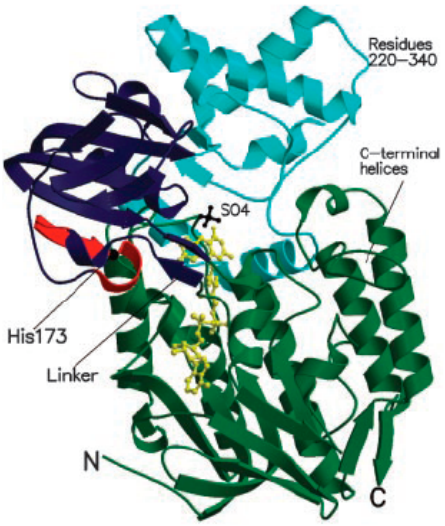

Figure 1.2 Ribbon diagram of the PAMO monomer (pdb-code: 1W4X).[28] The FAD-binding domain is shown in green, the NADP-binding domain is shown in blue. Residues 220-340, which form a subdomain inserted into the canonical NADP-binding domain topology, are depicted in cyan. The C-teminal helical extension found in the dinucleotide-binding fold of the FAD domain is labeled. The fingerprint residues (167-177), which characterize the Baeyer-Villiger monooxygenases[31], are outlined in red. His-173 is a strictly conserved residue of the fingerprint motif that has been shown to be crucial for cataylysis. The N- and C-terminal residues are labeled by N and C, respectively. The FAD cofactor and a bound sulfate ion are shown in yellow and black ball-and-stick representations, respectively.

Besides the structure of PAMO two other BVMO-structures were solved and published in 2009. One belongs to the BVMO MtmOIV from *Streptomyces argillaceus* (pdb-code: 3fmw), which is involved in the biosynthetic pathway of the natural anticancer drug mithramycin.[32, 21a] The second crystal structure is from a BVMO from *Rhodococcus* sp. strain HI-31[33] ($CHMO_{Rhodo}$; pdb-code: closed 3gwd, open 3wdf). It was shown that this enzyme belongs to the cyclohexanone-converting BVMOs and uses NADPH and oxygen as co-substrates. The three-dimensional architecture of $CHMO_{Rhodo}$, which mirrors that of PAMO, is highly modular in nature and can be separated into three domains and numerous loops (Figure 1.3). The FAD cofactor is buried deeply within the FAD domain, consistent with the observation that this cofactor does not dissociate from the enzyme, while the $NADP^+$ is sandwiched between the Rossmann fold of the NADP domain and a loop region of the FAD domain. The identification of two different $NADP^+$-dependent distinct conformations revealed domain shifts around multiple linkers and loop movements, involving the conserved Arg329 and Trp492, which affect translation of the nicotinamide resulting in a sliding cofactor. Consequently, the cofactor is ideally situated and subsequently repositioned during the catalytic cycle to first reduce the flavin moiety and later stabilize formation of the Criegee-intermediate. Concurrent movements of the loop adjacent to the active site demonstrate how this protein can effect large changes in the size and shape of the substrate binding pocket to accomodate a diverse range of substrates.

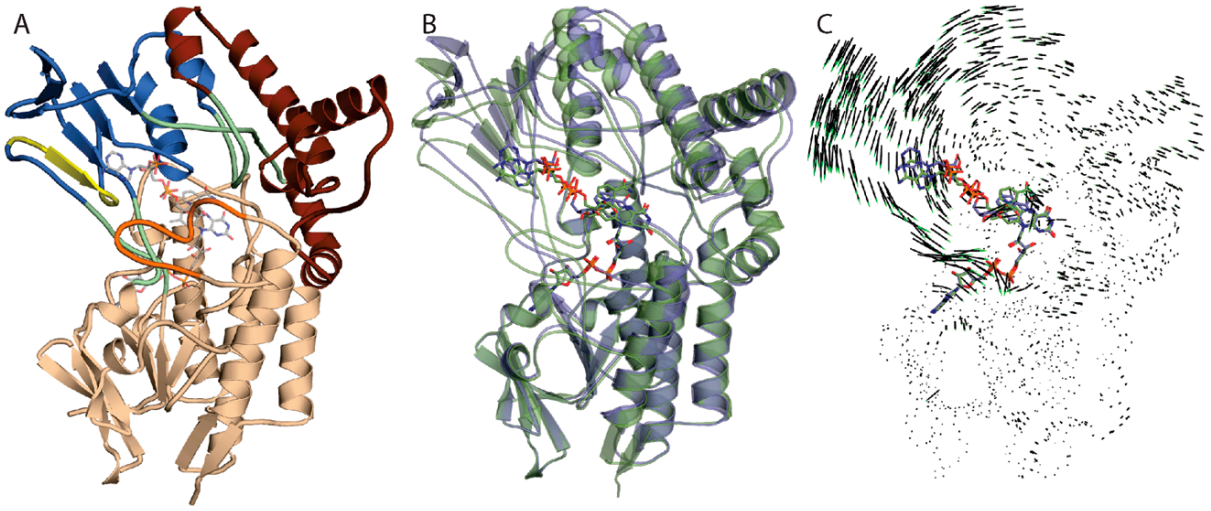

Figure 1.3 Color-coded representation of overall domain structure of CHMO from *Rhodococcus* sp. strain HI-31 and examination of conformational changes: (A) beige: FAD domain; dark blue: NADP domain; light green: linker region; red: helical domain; orange: mobile loop region; yellow: BVMO signature motif. (B) FAD domain-anchored structural superposition of $CHMO_{open}$ (blue) and $CHMO_{closed}$ (green). (C) Equivalent atoms vector diagram illustrating changes in relative backbone atom positions between $CHMO_{open}$ and $CHMO_{closed}$ (dark blue and purple regions from panel a). Notable is the large rotation of the NADP domain with a concurrent, albeit less pronounced, movement of the helical domain.[33]

Multiple sequence alignments of various BVMOs revealed that all possess these dinucleotide-binding domains for FAD and NADPH. Both domains incorporate GxGxxG-motifs, which are part of Rossmann folds and which enclose a BVMO-identifying sequence motif discovered a couple of years ago.[31] It could be shown that this fingerprint sequence (FXGXXXHXXXW-(P/D)) is critically involved in catalysis and contains several amino acids that are highly conserved in BVMOs (Figure 1.4). Thus, using this consensus sequence, new BVMOs could have been identified *via* genome mining.[34]

```
HAPMOACB      TAEEDLRAPRWHKDHVASGRDFKVVIIGAGESGMIAALRFK--QAGVPFVIYEKGNDVGG 178
HAPMOJD1      TAEEDPRAPRWHKDHVAAGREFKVVIIGAGVSGMIAALRFK--QAGVPFVVYEKGTDVGG 178
PAMO          MAGQT-----TVDSRRQPPEEVDVLVVGAGFSGLYALYRLR--ELGRSVHVIETAGDVGG 53
STMO          MNGQHPRSVVTAPDATTGTTSYDVVVVGAGIAGLYAIHRFR--SQGLTVRAFEAASGVGG 58
CHMOAcineto   ---------------MSQKMDFDAIVIGGGFGGLYAVKKLRD-ELELKVQAFDKATDVAG 44
CHMOBrevi1    -------------MPITQQLDHDAIVIGAGFSGLAILHHLR--EIGLDTQIVEATDGIGG 45
CHMOBrevi2    MTSTMPAPTAAQ-ANADETEVLDALIVGGGFSGPVSVDRLR--EDGFKVKVWDAAGGFGG 57
CPMO          MTTMTTMTTEQLGMNNSVNDKLDVLLIGAGFTGLYQLYHLR--KLGYKVHLVDAGADIGG 58
ATMO          --------------MDPANRPLRVVTIGTGISGILMAYQIQKQCPNVEHVLYEKNADVGG 46
SCMO          --------------MDPNNRRLRVITIGAGFSGILMAYQIQKQCANIEHVVYEKNHDIGG 46
EtaA          ----------MTEH-------LDVVIVGAGISGVSAAWHLQDRCPTKSYAILEKRESMGG 43
BVMOKT2440    ----------MSSHTALPVEPLDVLIMGAGVSGIGAAAYLRRNQPNKTFAILESRERMGG 50
CDMO          VDGWSHDPYMPITPREPKLDHVTFAFIGGGFSGLVTAARLRE-SGVESVRIIDKAGDFGG 94
                                       :* *  *      ::          :    ..*
```

```
HAPMOACB      IET-FKGPMFHSAQWDHD----------VDWSGKRVGVIGTGASATQFIPQLAQT-AAE 333
HAPMOJD1      KET-FQGPAFHSAQWDHN----------VDWSGKRVAVIGTGASAAQFIPQLAKT-AAD 333
PAMO          LKD-FAGNLYHTGNWPHEP----------VDFSGQRVGVIGTGSSGIQVSPQIAKQ-AAE 211
STMO          LDR-FTGDIVHTARWPHDG----------VDFTGKRVGVIGTGSSGIQSIPIIAEQ-AEQ 216
CHMOAcineto   INQ-FKGELHHTSRWPDD----------VSFEGKRVGVIGTGSTGVQVITAVAPL-AKH 201
CHMOBrevi1    IDE-FNGAKYHTAAWPADG----------VDFTGKKVGVIGVGASGIQIIPELAKL-AGE 203
CHMOBrevi2    LDS-FEGECHHTARWPQGG----------LDMTGKRVVVMGTGASGIQVIQEAAAV-AEH 214
CPMO          IET-FKGQWYHTALWPQEG----------VNMAGKRVAIIGTGSSGVQVAQEAALD-AKQ 215
ATMO          LHDRFQGRVIHTARWPDDYQE--------SQWKHDRVAVIGSGASSIQTVPGMQPT-VKH 211
SCMO          LHDRFKGRVIHTAAWPDDYGE--------VQWNSDRVAVIGSGASSIQAVAGIQPH-VGH 205
EtaA          SED-FVGPIIHPQHWPED----------LDYDAKNIVVIGSGATAVTLVPALADSGAKH 201
BVMOKT2440    SEQ-FKGQIIHPQHWPED----------LDYTGKRVVVIGSGATAVTLIPAMADK-VAS 209
CDMO          IES-FRGKSFHTSRWDYDYTGGDALGAPMDKLADKRVAVIGTGATAVQCVPELAKY-CRE 259
                .  * *   *.  *              .   ..: ::* *::.
```

Figure 1.4 Multiple sequence alignment of different flavoprotein monooxygenases including several BVMOs. FAD- and NADPH-binding domains are highlighted in yellow (Rossman fold), the fingerprint consensus sequence is highlighted in green. Conserved histidine and tryptophane of the fingerprint motif are written in bold letters. Protein explanation: HAPMOACB: 4-hydroxyacetophenone monooxygenase from *P. fluorescens* ACB, AF355751; HAPMOJD1: 4-hydroxyacetophenone monooxygenase from *P. putida* JD1, ACJ37423; PAMO: phenylacetone monooxygenase from *T. fusca*, 1W4X; STMO: steroid monooxygenase from *R. rhodochrous*, BAA24454; CHMOAcineto: cyclohexanone monooxygenase from *A. calcoaceticus* NCIMB 9871, AAG10021; CHMOBrevi1 and CHMOBrevi2: two cyclohexanone monooxygenases from *Brevibacterium* sp., AAG01289 and AAG01290; CPMO: cyclopentanone monooxygenase from *C. testosteronii* NCIMB 9872, CAD10798; ATMO: aflatoxin biosynthesis monooxygenase from *Aspergillus parasiticus*, AAF26281; SCMO: sterigmatocystein biosynthesis monooxygenase from *Aspergillus nidulans*, Q00730; EtaA: ethionamide-activating monooxygenase from *Mycobacterium tuberculosis* H37Rv, CAB06212; BVMOK2440: aliphatic open-chain ketone converting monooxygenase from *P. putida* KT2440, AAN68413; CDMO: cyclododecanone monooxygenase from *R. ruber*, AAL14233.

1.1.3 Baeyer-Villiger monooxygenases in organic synthesis

1.1.3.1 Available enzymes

The number of identified and heterologously expressed BVMOs has been enlarged significantly during the last ten years (Table 1.1). Not only the progress in molecular biological and genetic techniques, but also the discovery of highly conserved motifs of BVMO amino acid sequences has made it possible to explore enzymes with new properties either *via* genome mining of novel organism or protein redesign approaches. A large number of these BVMOs have cyclohexanone and its derivatives as preferred substrates (CHMOs). The isolation and cloning of cyclopentadecanone (CPDMO) and cyclododecanone (CDMO) monooxygenase, which oxidize larger and spatially more demanding ring-systems, created a toolbox of powerful oxygenating biocatalysts. A cyclopentanone monooxygenase (CPMO) that preferentially converts smaller ring-systems is also known. Except cycloketone-converting BVMOs, variants specific for aromatic (HAPMOs and PAMO) and aliphatic linear ketones (AOCMOs) are also described. Additionally, steroid-oxidizing monooxygenases (STMOs) have been reported. Interestingly, one of them originates from an eucaryotic organism.

Table 1.1 List of BVMOs that are described so far and of which the majority has already been cloned and overexpressed in *E. coli*.

BVMO/origin	acronym	primary substrate	year of cloning
Cyclohexanone monooxygenase from *A. calcoaceticus* NCIMB 9871 (1), *Arthrobacter* BP2 (2), *Brachymonas petroleovorans* (3), *Rhodococcus* sp. Phi1 & Phi2 (4), *Brevibacterium* sp. HCU (5) and *Xanthobacter* sp. ZL5 (6)	CHMO	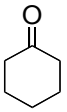	(1) – 1988[24] (2) – 2003[35] (3) – 2003[35] (4) – 2003[35] (5) – 2000[36] (6) – 2003[37]
Cyclopentanone monooxygenase from *C. testosteronii* NCIMB 9872	CPMO	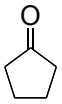	2002[14a]
Cyclododecanone monooxygenase from *R. ruber*	CDMO	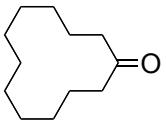	2001[38]
Cyclopentadecanone monooxygenase from *Pseudomonas* sp. HI-70	CPDMO	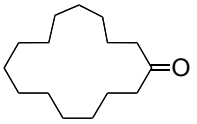	2006[39]
Phenylacetone monooxygenase from *T. fusca*	PAMO	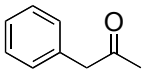	2005[34]
4-Hydroxyacetophenone monooxygenase from *P. putida* JD1 (1) and *P. fluorescens* ACB (2)	HAPMO	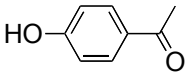	(1) – Article VI (2) – 2001[40]
Aliphatic open-chain monooxygenase from *P. fluorescens* DSM 50106 (1), *P. putida* KT2440 (2), *P. veronii* (3) and *P. cepacia* (4)	AOCMO	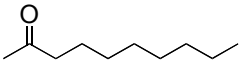	(1) – 2007[41] (2) – Article V (3) – 2008[42] (4) – 1977[13d]
Ethionamide monooxygenase from *Mycobacterium tuberculosis* H37Rv	EtaA	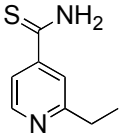	2004[43]
Steroid monooxygenase from *R. rhodochrous* IFO 3338 and *Cylindrocarpon radicicola* ATCC 11011	STMO	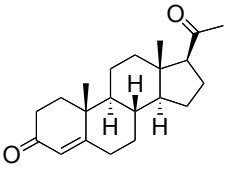	(1) – 1999[44] (2) – 1986[45] (identified)
2,5- & 3,6-Diketocamphane 1,2-monooxygenase from *P. putida* ATCC 17453	2,5- & 3,6-DKCMO	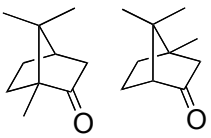	1986[46] (identified)
2-Oxo-Δ^3-4,5,5-trimethylcyclopentylacetyl coenzyme-A monooxygenase from *P. putida* ATCC 17453	MO2	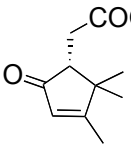	1983[47] (identified)
Monocyclic monoterpene ketone monooxygenase from *R. erythropolis* DCL14	MMKMO	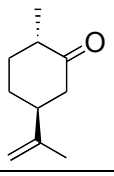	2000[48] (identified)

Although the Baeyer-Villiger oxidation is usually favored, BVMOs also showed their potential to perform oxidation on sulfur[49], nitrogen[50], selenium[51], organoboron[51, 52] and phosphor as well as to oxidize aldehydes and catalyze epoxidation of alkenyl-phosphonates[53] (Scheme 1.8). The ambivalent character of the peroxyflavin is responsible for the capability to convert both electron-rich and electron-deficient substrates. This promiscuity makes BVMOs a powerful tool in organic chemistry.

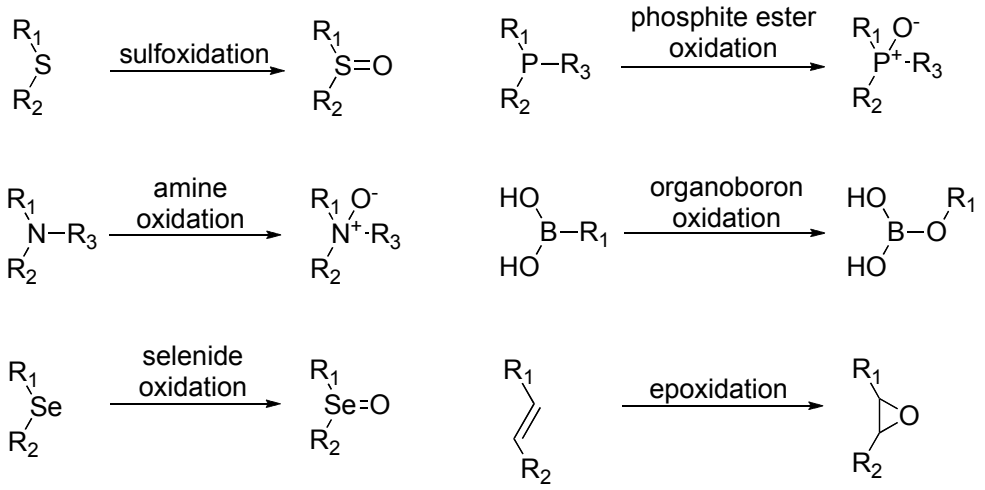

Scheme 1.8 Oxygenation of heteroatoms and oxidation of C-C double bonds by Baeyer-Villiger monooxygenases.

The most intensively studied type I BVMO so far is the cyclohexanone monooxygenase from *A. calcoaceticus* NCIMB 9871 (E.C. 1.14.13.22). This CHMO was shown to be active against a remarkable number of substrates exhibiting an exquisite chemo-, enantio- and/or regioselectivity.[54] Although this enzyme can be utilized in sulfoxidations, the Baeyer-Villiger process is usually favored, which is demonstrated by the chemoselective oxidation of the keto functionality in heterocyclic compounds.[55] This enzyme originally was discovered in 1976 by Donoghue[56] and later cloned and overexpressed in *E. coli*[24, 57] and *S. cerevisiae* ("designer-yeast").[58] Today, it is the predominantly used BVMO for desymmetrization processes, (dynamic) kinetic resolution and regiodivergent transformations in synthetic applications. Furthermore, this CHMO was also the first enzyme in large-scale preparations of *rac*-bicyclo[3.2.0]hept-2-en-6-one.[59] The obtained 2-oxabicyclooct-6-en-3-one lactones are valuable intermediates for synthesis of prostaglandins.[60] Until now, a lot more CHMOs from different bacterial origin have been reported. While sequence identity among them can be high, regioselectivity and enantiopreference can vary widely.[61]

Besides cyclohexanone-converting enzymes, BVMOs that preferentially convert smaller or larger ring-systems have also been intensively investigated. The most prominent representative is the cyclopentanone monooxygenase from *C. testosteronii* NCIMB 9872. Initial substrate specificity investigations showed acceptance for cyclic C_4 to C_8 ketones and norbornanone. Nowadays, CPMO has proven to be a promising biocatalyst in the production of functionalized chiral δ-valerolactones, which are biologically active compounds in natural product synthesis. The high chemoselectivity of CPMO was exploited in the biooxidation of a prochiral hetero-bicycloketone. In subsequent chemical operations, the Baeyer-Villiger pro-

duct can be converted to C-nucleosides like showdomycin, kumausyne and goniofufurone analogs, which are tetrahydrofuran natural products.[62]

Microbial degradation of acetophenone and its derivatives, initiated by Baeyer-Villiger monooxygenases, was reported for *Nocardia*[63], *Arthrobacter*[63,64], *Alcaligenes* and *Pseudomonas*[65] species. They are able to convert aryl ketone functions, which are generally less reactive than aliphatic carbonyl groups. Thus far, two enzymes have been isolated and characterized: one from *P. putida* JD1[66, Article VI], an organism growing on 4-ethylphenol, and one from *P. fluorescens* ACB[40], growing on 4-hydroxyacetophenone (4-HAP). Hydrolysis of the Baeyer-Villiger product 4-hydroxyphenyl acetate affords hydroquinone, which is an important intermediate in organic synthesis.[67] Due to carcinogenic benzene as starting material for the synthesis of hydroquinones, alternative routes to synthesize them is desirable. Furthermore, substituted catechols are valuable building blocks for pharmaceutical compounds.[68] As the chemical synthesis of phenol- or catechol-containing compounds requires protection of the hydroxy group(s) with ethers or *via* esterification, the HAPMO-catalyzed conversion of ring-substituted aryl ketones provides a biological alternative for the synthesis.

Besides monocyclic substrates also bicyclic and tricyclic ketones were subjected to enzymatic Baeyer-Villiger oxidation.[69] Among them camphor and its derivatives seem to be the most studied examples. First attempts to elucidate the degradation of (+)-camphor and the metabolism of (–)-camphor in *P. putida* ATCC 17453 were performed in the mid 1960s.[70] Later, it was found that there are three enzymes in *P. putida* that catalyze this Baeyer-Villiger reaction: 2,5-diketocamphane 1,2-monooxygenase, which forms the bicyclic lactone analog of (+)-camphor[46], 3,6-diketocamphane 1,6-monooxygenase, which forms the bicyclic lactone analog of (–)-camphor[71] and 2-oxo-Δ^3-4,5,5-trimethylcyclopentenyl-acetyl-Co-A monooxygenase, which catalyzes the lactonization of the monocyclic intermediate.[47] Both pathways can be induced by selective growth on either isomer. A similar behaviour was also reported from *Corynebacterium* sp. oxidizing racemic fenchone[72] and *Rhodococcus* sp. for biooxidation of 1,8-cineole or 6-oxo cineole[73], respectively.

Recent substrate profiling studies revealed that BVMOs have a rather broad substrate spectrum and often display overlapping specificities (Figure 1.5). Although several substrates can be converted by both CHMO and CPMO, enantioselectivity and enantiopreference can differ. Illustrative of the broad substrate acceptance is CHMO from *A. calcoaceticus* NCIMB 9871. Until 2002, more than 100 substrates have been reported to be accepted by this enzyme[54a], and since that time the impressive list of converted substrates has grown even further.

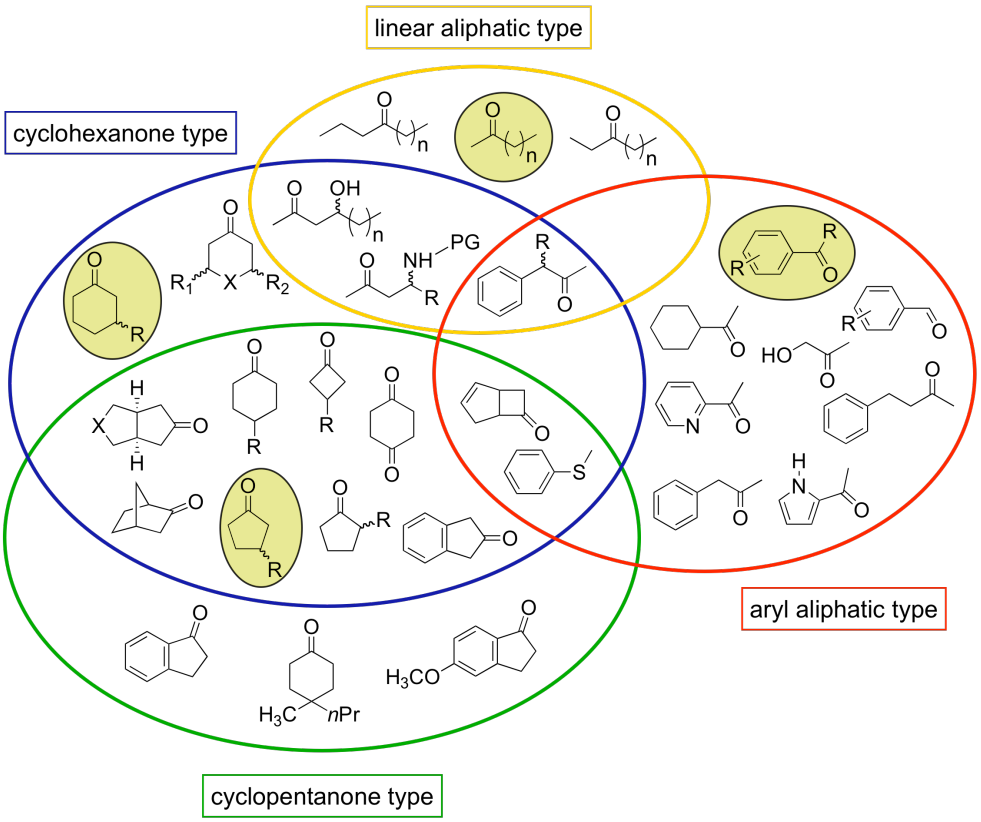

Figure 1.5 Overlapping substrate specificities of cyclohexanone, cyclopentanone, arylaliphatic and linear aliphatic BVMO type. Preferred substrates are highlighted in yellow (according to Kamerbeek[14b]).

1.1.4 Scale-up issues using Baeyer-Villiger monooxygenases

1.1.4.1 Isolated enzymes vs. whole cells – Cofactor recycling

With the identification of BVMOs as a versatile class of enzymes, their application as biocatalysts in organic chemistry significantly increased over recent years. However, the major drawback of these cofactor-dependent enzymes, especially in large-scale, is the necessity to regenerate the nicotinamide cofactor (NADPH), which is required in stoichiometric amounts and is ten times more expensive than the unphosphorylated NADH. One of the easiest means to circumvent the problem of *in situ* cofactor regeneration is to use whole cells, either growing or resting. Here, NAD(P)H recycling is provided *in vivo* by the recombinant cells themselves, overexpressing the BVMO. Nevertheless, implementing whole cells for biotransformations also has some disadvantages: productivity is limited by the growth rate, poor oxygen-transfer rates, cellular toxicity and substrate and/or product inhibition. Also, unwanted side-reactions can occur, either metabolizing the Baeyer-Villiger product or using the cofactor to dominantly maintain cell growth processes. Therefore, different strategies have been developed to facilitate the use of isolated enzymes and to solve the problem of cofactor-recycling, which are summarized in Table 1.2: (I) implemetation of a second enzymatic reaction, (II) chemical regeneration, (III) electrochemical cofactor recycling and (IV) photochemical regeneration.

Table 1.2 Summary of cofactor-recycling methods for flavin-containing oxidoreductases.

Cofactor-recycling system	
I - Implementation of a second enzyme 1) Recycling of NADPH by a) glucose-6-phosphate dehydrogenase (GPDH)[74], b) a mutant of formate dehydrogenase (FDH) from *Pseudomonas* sp. 101[75] and c) mutant of phosphite dehydrogenases from *P. stuzeri*.[76] Due to the expensive glucose-6-phosphate (a) different attempts were made to convert NADH-generating enzymes into NADPH-producing ones (b).	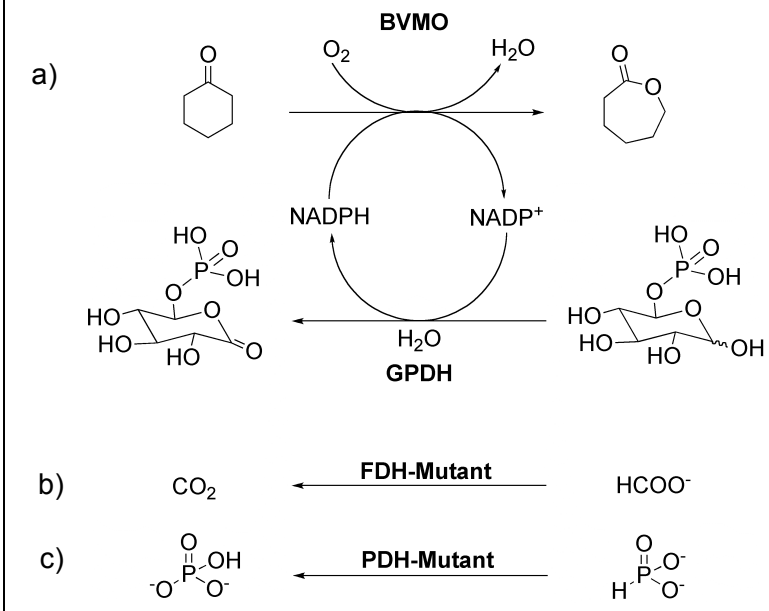
2) Closed-loop NADPH regeneration in a coupled enzyme system using alcohol dehydrogenase (ADH) from *Thermoanaerobium brockii* and cyclohexanone monooxygenase (CHMO) from *A. calcoaceticus* NCIMB 9871.[77]	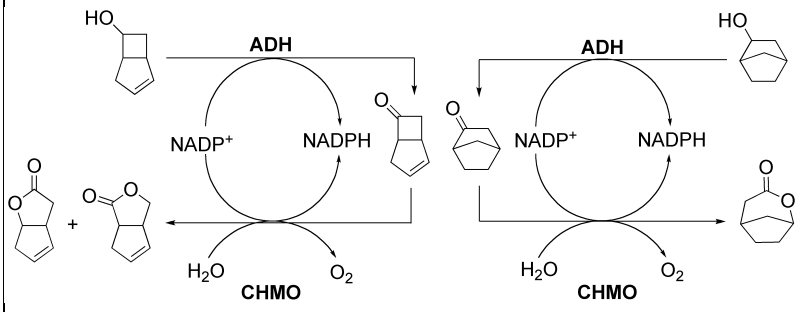
3) Coenzyme regeneration by phosphite dehydrogenase as CRE/BVMO fusion protein. Phosphite serves as cheap and sacrificial electron donor.[78]	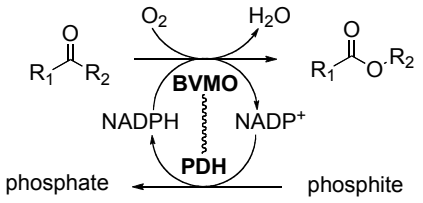
II - Chemical regeneration *In situ* cofactor regeneration with $[Cp^*Rh(bpy)(H_2O)]^{2+}$ in the chemoenzymatic system of tryptophane 7-halogenase.[79]	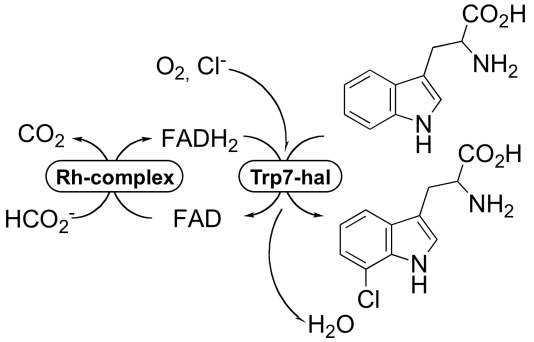

III - Electrochemical cofactor-recycling Cathodic reduction for the regeneration of FAD during epoxidation of styrene with styrene monooxygenase (StyAB) from *Pseudomonas* sp. VLB120. Here StyB (NADH-dependent reductase component) was replaced.[80]	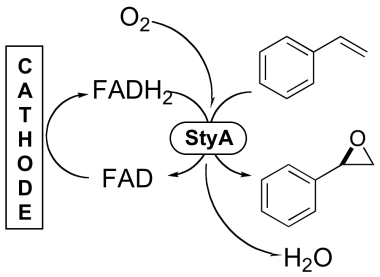
IV - Photochemical regeneration A "green" regeneration – light-driven cofactor recycling using EDTA as sacrificial electron donor.[81]	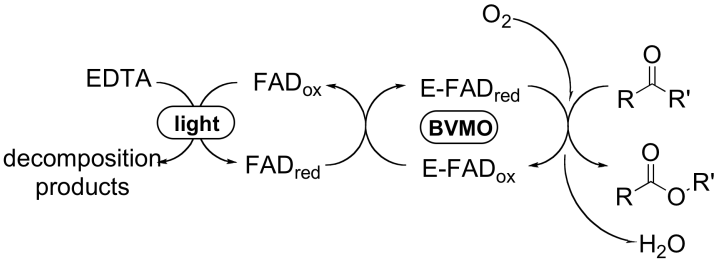

Due to lower efficiencies, systems II, III and IV can be considered as proofs of principle rather than good alternatives for cofactor-regeneration on a larger scale.

1.1.5 Large-scale application of Baeyer-Villiger monooxygenases

One of the primary goals of bioprocess engineering is to achieve kilogram-production levels of processes originally established on a bench-scale. Normally, an increase in reaction volume is combined with a decrease in the surface to volume ratio, thus prohibiting a direct scaling-up of a process because mass and energy transport limitations arise.[82] With respect to high space-time yields and high stability of the biocatalyst, which implies low production costs, optimization of several reaction parameters are often necessary: (a) pH and temperature, (b) utilization of whole cells (either resting or growing) or isolated biocatalysts (e.g. immobilized), which demands a sufficient cofactor-regeneration system, (c) optimal substrate- and product concentrations to circumvent enzyme inhibition, (d) addition of co-solvents and stabilizers, and (e) physical treatments like stirring or pumping to increase oxygen solubility and uptake. Only a handful of enzyme classes have been used at large-scale, and the majority of biocatalytic conversions have been carried out with isolated hydrolases resolving a stereogenic center. In recent years, much has been done to redress this imbalance by turning to enzymes for carbon-carbon bond synthesis and redox reactions.

In view of the potential of BVMOs for regio- and also enantioselective transformations of various substrates, intensive studies on the scale-up of these biooxidations began a couple of years ago. Another benefit of enzymatic Baeyer-Villiger oxygenation also includes the replacement of classical oxidants like peracids, which are flammable and explosive, thus difficult to handle especially in larger scale. Pioneering work on large-scale applications was done by Hilker and Woodley, who investigatied CHMO from *A. calcoaceticus* NCIMB 9871 ($CHMO_{Acineto}$). The major challenges were to ensure a sufficient oxygen supply and to over-

come the obstacle of cofactor-recycling by utilization of whole cells instead of isolated enzyme. Hereby, NAD(P)H-regeneration is provided by the cells themselves and work-intense enzyme purification and stabilization is no longer a limitation. Another bottleneck in BVMO-mediated oxidation processes was the low substrate concentration due to frequent inhibition or toxicity phenomena, but various techniques were developed to minimize these problems.

The first attempt of a Baeyer-Villiger biotransformation was performed with recombinant *E. coli* cells expressing the CHMO from *A. calcoaceticus* NCIMB 9871 using *rac*-bicyclo[3.2.0]hept-2-en-6-one as ketone substrate (Scheme 1.9). It was found out that the optimum ketone concentration was between 0.2-0.4 g L^{-1} and that of the combined regioisomeric lactones 3.5 g L^{-1}, both certainly not sufficient for commercial scale.[59]

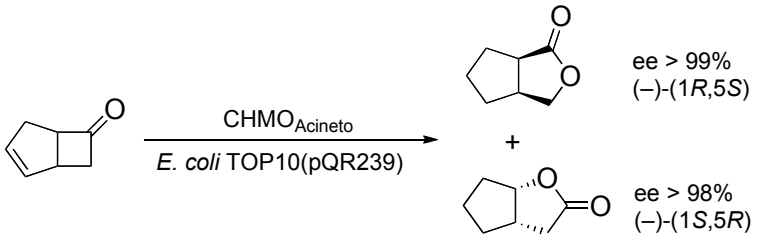

Scheme 1.9 Microbial Baeyer-Villiger oxidation of *rac*-bicyclo[3.2.0]hept-2-en-6-one.

Although the isolated product yield was 85-90%, accompanied with high enantiomeric excess of both regioisomers (> 98% ee), key limitations were substrate and product inhibition. In order to overcome these problems, strategies to control both the substrate and product concentrations, as well as mass transfer into and out of the cell are required. Some solutions include the use of a water-immiscible organic phase to serve as a substrate reservoir and a product sink up to a concentration of 5 g L^{-1}.[83] An even more effective technique would be the use of an *in situ* product removal (ISPR) on a selective adsorbent resin.[84] This technique has been optimized with respect to bottlenecks identified in downscaled experiments.[85] High productivity was obtained by combining the resin-based *in situ* substrate feeding with product removal (*in situ* SFPR). This helped to overcome the inherent limitation in productivity and space-time yield generated by the severe inhibition of the enzyme by substrate concentrations > 1 g L^{-1} and product concentrations > 3 g L^{-1}. Thereby, substrate ketone and product lactones were adsorbed onto a macroporous resin (Dowex Optipore L-493) prior to bioconversion, which was then added to the fermentation broth. Thus, a slow substrate release into the broth is assured, and after conversion into both regioisomeric lactones, products are re-adsorbed. Constant concentrations can be adjusted while avoiding product accumulation in the aqueous phase (Figure 1.6 A) and substrate concentration could be increased to 25 g L^{-1} (0.23 M) without affecting enzyme activity. Also downstream processing could be simplified by easy extraction of the lactones from the resin after complete conversion, making the resin reusable and therefore lowering the entire process costs.[86]

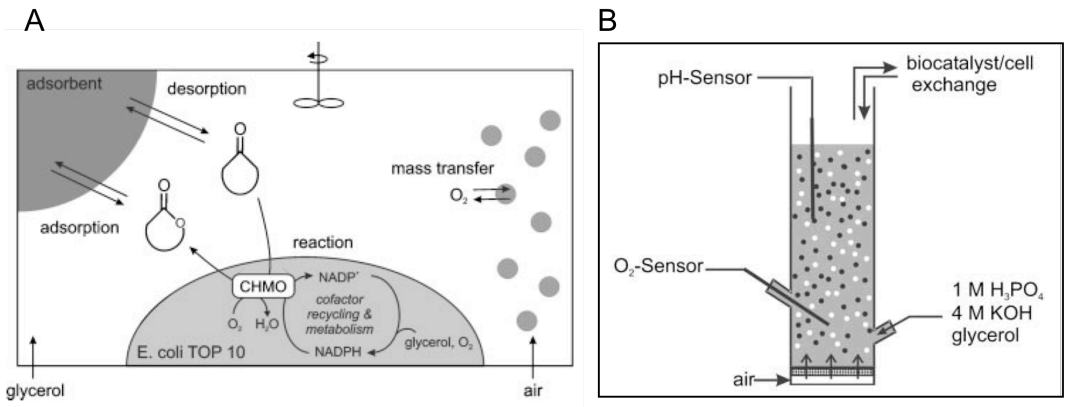

Figure 1.6 **A**) Principle of resin-based *in situ* SFPR methodology; **B**) "bubble reactor" set-up.[86]

In order to improve the oxygen input, which is crucial for catalysis, three different reactor types were investigated. A so-called "bubble-column", where aeration takes place through a sparger from the bottom, was found to be the best solution (Figure 1.6 B). Mixing of the liquid phase and dispersion of the resin is achieved by the rising air bubbles and mass transfer can be controlled by choosing an appropriate sparger porosity. Combined with a glycerol feed control, regiodivergent biotransformation of *rac*-bicyclo[3.2.0]hept-2-en-6-one was performed in a 50 L reactor using 900 g of racemic ketone and 6.3 kg of wet resin. After 20 h, both corresponding regioisomeric lactones [(–)-(1*S*,5*R*) and (–)-(1*R*,5*S*)], which were obtained in excellent enantiomeric purity (ee > 98%) and high preparative yield (84%), could be isolated resulting in a space-time yield of 8.2 mmol L^{-1} h^{-1} and a volumetric productivity of about 1 g lactones L^{-1} h^{-1}.[86] Although conversion of the ketone was complete, and despite the fact that loss of material in the liquid phase was only 10%, an unsatisfying overall yield of 58% of lactones was obtained. Hence, the total mass balance only accounted for 69% of the starting material, probably due to non-optimized extraction conditions. Recently, the bioconversion could be improved by overcoming limitations due to substrate and product inhibition. The described process was successfully applied to the preparative scale Baeyer-Villiger biooxidation of (–)-(1*S*,5*R*)-bicyclo[3.2.0]hepten-2-en-6-one (25 g). The corresponding lactone was obtained in 75-80% yield.[87] Nevertheless, these investigations and new methodologies facilitate the application of BVMOs for further industrial implementation.

1.1.6 Representative synthetic applications of Baeyer-Villiger monooxygenases

The relevance of oxygen inserting processes in organic chemistry and the need for stereo- and enantioselective oxidations have accelerated the development and the improvement of BVMO applications in synthetic chemistry during recent years. Important milestones in molecular biology made it possible to discover new enzymes with novel properties and specificities. However, the majority of synthetically interesting biooxidations have been performed with CHMO from *A. calcoaceticus* NCIMB 9871 only. Although this BVMO still plays a dominant role, an increasing number of other BVMOs became available during the last years, creating a toolbox of biocatalysts. Thus, sterically more demanding products can be synthesized and even those reactions that were not possible to be performed in a stereo- or enantioselective manner using chemical methods can now be conducted. Pioneering work in the field of desymmetrization processes and enantiodivergent biotransformations was done by Mihovilovic and coworkers[55, 62, 88], Taschner[69, 89], and Furstoss and Alphand.[60, 90]

1.1.6.1 Desymmetrization of prostereogenic ketones

Since desymmetrization of a prostereogenic compound (theoretically) provides 100% yield of optically pure product, this reaction is of high importance in organic chemistry and represents the most promising application of BVMOs. Especially, biooxidation of functionalized cycloalkanones gives access to corresponding ring-expanded lactones generating one or more new chiral centers in excellent stereoselectivity. A major contribution was the identification of BVMO subclusters, with sometimes overlapping substrate acceptance, that provided access to both regioisomeric lactones.[61] Upon comparison of protein sequences, phylogenetic relationship and biocatalytic performance, eight cycloketone converting BVMOs could be classified into two subclasses: CHMO-type and CPMO-type with $CHMO_{Acineto}$ and CPMO, respectively, as the most prominent representatives (Table 1.3).

Table 1.3 Desymmetrization of prostereogenic ketones to enantiocomplementary lactones by representatives of CHMO-type and CPMO-type BVMOs.[61]

	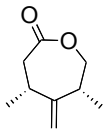	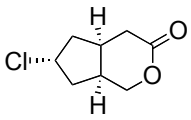	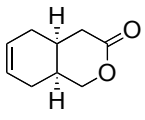
$CHMO_{Acineto}$	92% ee (+)	>99% ee (–)	5 %ee (–)
$CHMO_{Brevi1}$	>99% ee (+)	95% ee (–)	71 %ee (–)
CPMO	99% ee (–)	48% ee (+)	>99 %ee (+)
$CHMO_{Brevi2}$	>99% ee (–)	60% ee (+)	94 %ee (+)

This collection of BVMOs represents a complementary platform for diverse applications in chiral synthesis. Investigation of several 4-mono- and 4,4-disubstituted cyclohexanones and prochiral functionalized 3-cyclobutanones revealed that a vast variety of functionalized substrates are usually converted with high chemoselectivity. When the selectivity of BVMOs regarding the Baeyer-Villiger process *versus* a heteroatom oxidation is compared, usually the oxygenation of the carbonyl center is favored. Selected results of substituted

cyclohexanones and cyclobutanones oxidized by CHMO- and CPMO-type BVMOs are compiled in Figure 1.7.

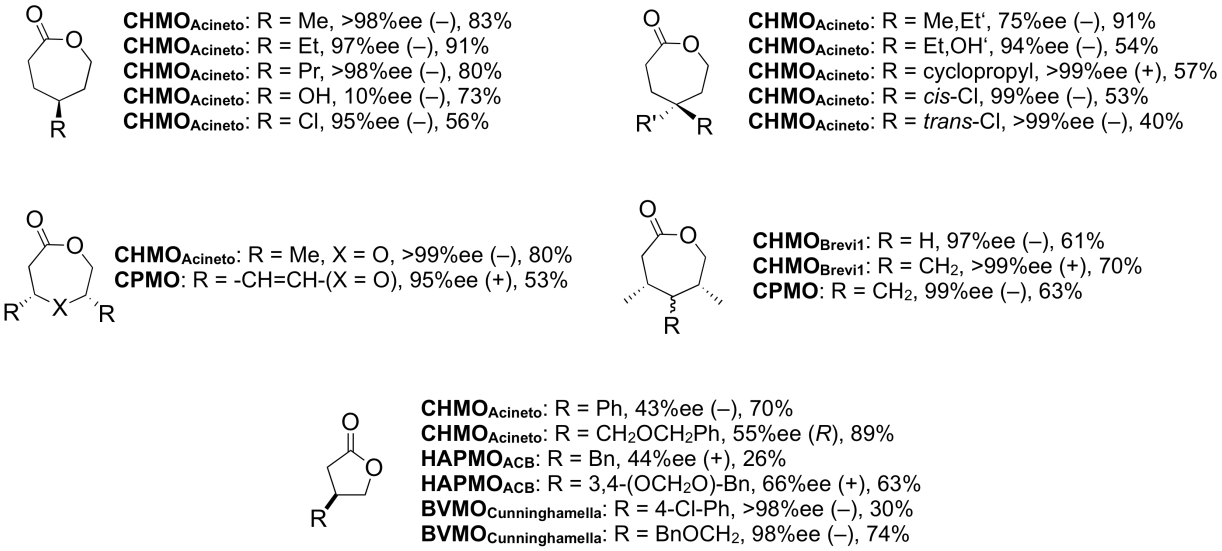

Figure 1.7 Selected examples of enzymatic stereoselective Baeyer-Villiger oxidation of functionalized cyclohexanones and cyclobutanones.[26, 91] $CHMO_{Acineto}$: *A. calcoaceticus* NCIMB 9871, CPMO: *C. testosteronii*; $HAPMO_{ACB}$: *P. fluorescens* ACB; $BVMO_{Cunninghamella}$: *Cunninghamella echinulata* NRRL 3655.

An interesting pharmaceutical application of BVMOs in desymmetrization processes is the chemoenzymatic synthesis of the γ-aminobutyric acid (GABA) inhibitor (*R*)-baclofen, which can be obtained from 3-(*p*-chlorophenyl)-γ-butyrolactone in excellent optical purity with biotransformation using wild-type cells of *Cunninghamella*.[92] Using whole cells of the same strain, 3-(benzyloxymethyl)-cyclobutanone can be oxidized to the corresponding (*R*)-(–)-γ-butyrolactone, another bioactive intermediate, which is further converted in a stereodivergent synthetic sequence to (*R*,*S*)-β-proline[93] (Scheme 1.10). Both compounds are of high interest due to pharmacological activity.

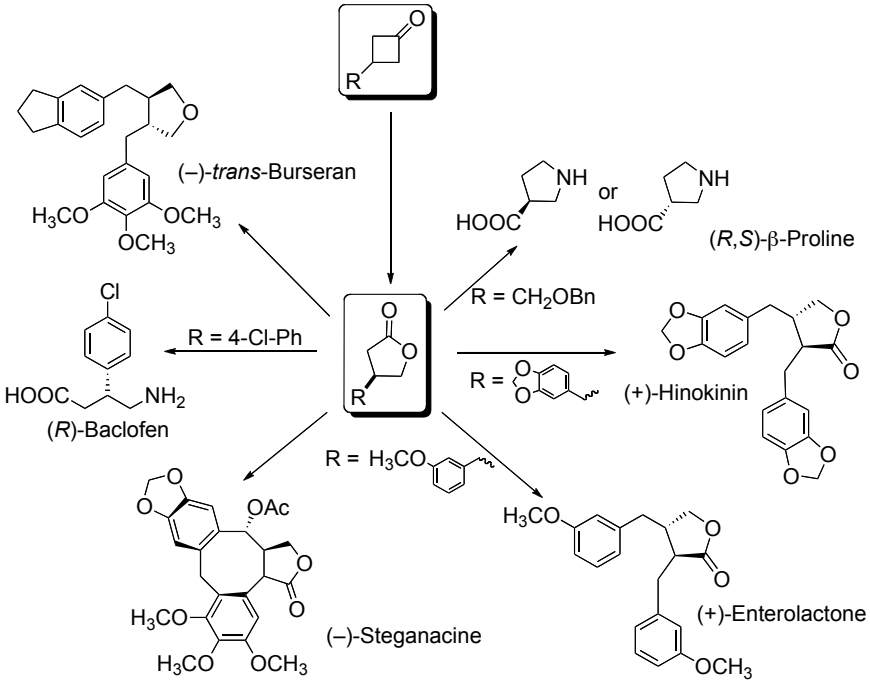

Scheme 1.10 Biooxidation of butyrolactones further converted to key intermediates for total synthesis.

1.1.6.2 Kinetic resolution of racemic ketones

Kinetic resolution of racemic starting material is a powerful tool in the synthesis of optically pure compounds. However, in comparison to desymmetrization processes of prostereogenic substances, the maximum conversion that can be achieved here is only 50%. Nevertheless, the major advantage of implementation of kinetic resolution is the access to both, enantiomerically pure product and substrate.

During recent years, a variety of BVMOs have been subjected to kinetic resolution processes in order to synthesize optically pure esters and ketones. Thereby, alkyl- mono- and di-substituted cyclohexanones and cyclopentanones have drawn major attention. The substituent spectrum of BVMOs included alkyl groups of different chain length, aromatic groups and substituents with additional functionality. Spatial constraints of the protein's active site seem to limit synthetic applications in the case of substrates with long substituents. Figure 1.8 compiles representative examples of kinetic resolutions with cyclopentanones and cyclohexanones using CHMO from *A. calcoaceticus* NCIMB 9871.

Some of these functionalized optically pure ketones or lactones can be used as precursors for the synthesis of natural and/or bioactive products. In one example, a BVMO from camphor-grown *P. putida* ATCC 17453 (MO2) was used to synthesize the corresponding lactone from 2-(2'-acetoxyethyl)cyclohexanone, which was further converted *via* Mitsunobu reaction to (*R*)-(–)-lipoic acid, a bioactive compound for the treatment of hepatitis, pancreatitis and induced carcinomas (Scheme 1.11).[94] Later, it was found that CPMO from *Comamonas* sp. displayed the opposite enantioselectivity suggesting that this enzyme can be used in place of MO2 to eliminate the use of the chemical Mitsunobu inversion.[95]

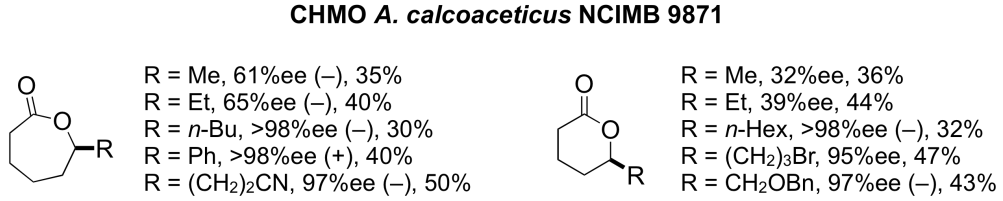

Figure 1.8 Selected examples of enzymatic kinetic resolutions of functionalized cyclohexanones and cyclopentanones catalyzed by CHMO from *A. calcoaceticus* NCIMB 9871.[26, 91]

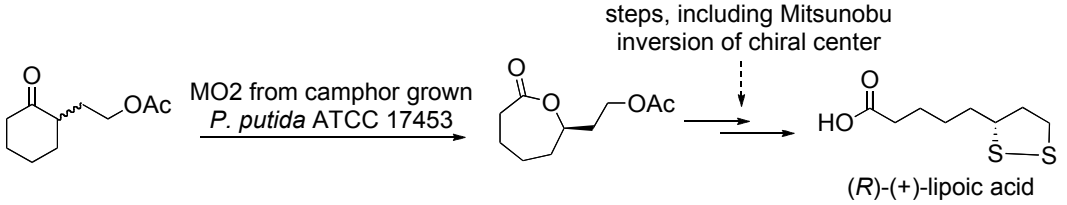

Scheme 1.11 Chemoenzymatic synthesis of (*R*)-(+)-lipoic acid using MO2 from *P. putida* ATCC 17453.

Besides the level of enantioselectivity, the major drawback of kinetic resolutions of racemic substrates is their maximal yield of 50%, since only one enantiomer is converted. Therefore, the most important contributation in recent years has been the development of a dynamic kinetic resolution (DKR), which allows conversions up to 100%. This approach requires a kinetic resolution coupled to an efficient *in situ* racemization of the non-converted ketone enantiomer, which should be faster than the desired enzymatic step. Moreover, conditions have to be selected carefully to prevent racemization of the obtained enantiomerically pure lactone. The first example of a BVMO-mediated DKR was performed for 2-benzyloxymethylcyclopentanone using engineered whole cells possessing CHMO from *A. calcoaceticus* NCIMB 9871 (Scheme 1.12).[96] Here, only the substrate showed pH-dependent racemization *via* keto-enol tautomerization, due to the increased acidity of the C2-proton. Increasing the pH to 9 resulted in a sufficient racemization, while the product lactone was not affected. After 24 h, 85% (*R*)-lactone was obtained with 96% ee (1.5 mM substrate concentration) and without compromising the stereoselectivity of the biooxidation. Implementing milder conditions (pH 7) using a weak anion exchanger (Lewatit MP62) led to higher substrate concentrations (up to 1 g L^{-1}) and improved racemization.[97]

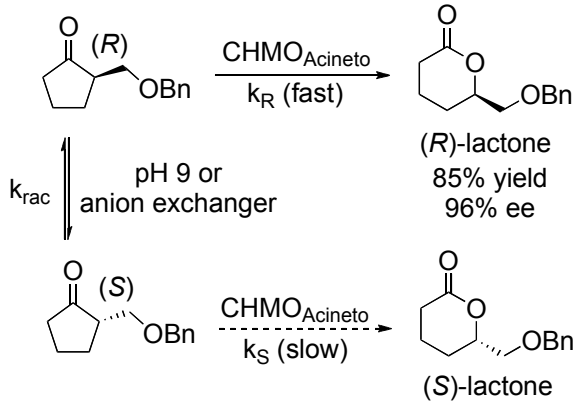

Scheme 1.12 Dynamic kinetic resolution of 2-benzyloxymethylcyclopentanone using CHMO from *A. calcoaceticus* NCIMB 9871.

1.1.6.3 Regiodivergent transformations

The regiodivergent Baeyer-Villiger biooxidation of antipodal cyclic ketones is considered as one of the most interesting transformations catalyzed by Baeyer-Villiger monooxygenases. In this reaction, both enantiomers of racemic starting material are converted into two separate regioisomers, where either the more substituted or less substituted carbon center undergoes migration. The reason is probably a different positioning of the antipodal ketones within the enzyme's active site. Thus, in the Criegee-intermediate, different bonds are situated antiperiplanar to the O-O bond of the leaving group.[26] While regioselectivity is governed predominantly by electronic effects leading to preferred migration of the more nucleophilic and more substituted carbon center, stereoelectronic effects also can influence enzymatic transformations. A mechanistic concept for the geometric situation of the transition state for both enantiomeric substrates within the active site was outlined previously.[98]

One of the most intensively studied BVMO-reactions is the biooxidation of fused bicycloketones bearing a cyclobutanone structural motif. As observed in desymmetrization processes, comparative studies suggest a similar clustering of BVMOs into CHMO-type and CPMO-type[99], which convert racemic starting material into "normal" (proximal) and "abnormal" (distal) lactones in different ratios (Scheme 1.13). While CHMO-type BVMOs oxidize both enantiomers into both antipodal lactones in equal ratio and high enantioselectivity, CPMO-type BVMOs predominanly generate the "normal" lactone with low enantioselectivity. Interestingly, a previously isolated BVMO from *Mycobacterium tuberculosis* H37Rv[100] ($BVMO_{Mtub5}$) selectively produces the "abnormal" lactone while the antipodal substrate remains unchanged.[101]

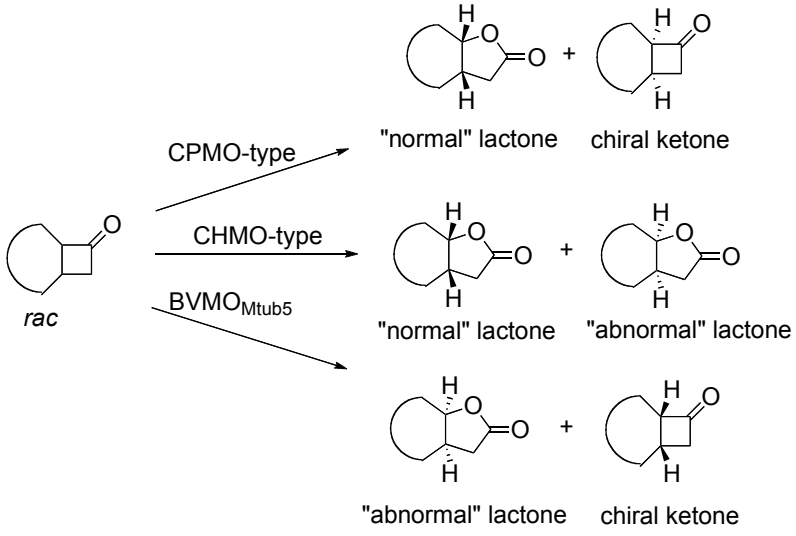

Scheme 1.13 Regiodivergent biooxidation of fused bicycloketones yielding the "normal" and "abnormal" Baeyer-Villiger lactone.

One of the benchmark reactions among fused oxa-cyclobutanones is the conversion of *rac*-bicyclo[3.2.0]hept-2-en-6-one. While the "normal" lactone product generated by CPMO-type BVMOs can be used as a precursor for the production of prostaglandins[60], the "abnormal" regioisomer obtained from *Cunninghamella* BVMO is a valuable intermediate in the synthesis of a series of brown algae pheromones (viridiene, multifene and caudoxirene) *via* an alcohol[102] and of cyclosarkomycin, which can be further converted into the cytostatic drug (*R*)-(–)-sarkomycin.[90d]

1.1.6.4 Heteroatom oxidation – sulfide and sulfoxide oxidation – epoxidation

Due to the ambivalent character of the reactive enzyme intermediate during biocatalysis, BVMOs are also capable of heteroatom oxidation. An asymmetric nitrogen oxidation has been reported for (hetero)aromatic tertiary amines, where high diastereoselectivity was observed for oxidation of (*S*)-nicotine by isolated CHMO from *A. calcoaceticus* NCIMB 9871. With a few other examples of nitrogen oxidations, conversion of boronic acids to borates[103], selenium BVMO-catalyzed oxidations[51] and in particular the conversion of organic sulfides to asymmetric sulfoxides, this has continued to be a highly active field. Because of the versatility of sulfoxides, they represent valuable synthons and chiral auxiliaries in synthetic chemistry and are also found in natural products and biologically active ingredients.[104]

Already in 1994, Willetts and coworkers showed that MO2 from *P. putida* ATCC 17453 stereoselectively converted a variety of aromatic sulfides.[105] Interestingly, it produced exclusively the (*S*)-enantiomer, while a comparison with CHMO from *A. calcoaceticus* NCIMB 9871 showed, that this enzyme often oxidized the (*R*)-enantiomer of the same substrates. Later, also HAPMO from *P. fluorescens* ACB and PAMO from *T. fusca* have been studied intensively and showed high enantioselectivities in the sulfoxidation of alkyl aryl sulfides, dialkyl sulfides, and cyclic and acyclic 1,3-dithioacetals. The high enantioselectivity of PAMO could be exploited in a kinetic resolution of ethyl benzyl sulfide. Here, only the (*R*)-sulfoxide reacted to the corresponding non-chiral sulfones, yielding the (*S*)-sulfoxide in high optical purity (E = 110)[52] (Scheme 1.14).

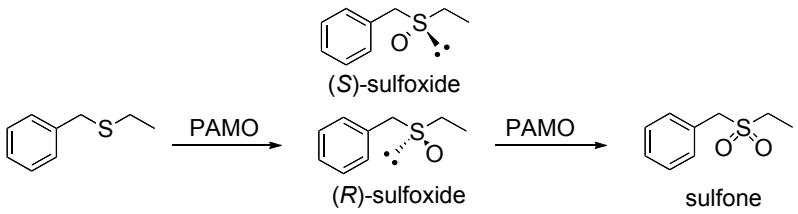

Scheme 1.14 Stereoselective oxidation of ethyl benzyl sulfide to chiral sulfoxides and non-chiral sulfones by phenylacetone monooxygenase from *T. fusca*.

Besides bacterial systems being applied to sulfide oxidations, several fungal systems possess broad substrate acceptance and provide access to antipodal sulfoxides.[49c] Here, bio-oxidation of functionalized dialkyl sulfides was utilized in a direct synthesis of sulphoraphane and analogs.[106]

In case a ketone substrate is not available, BVMOs are able to perform enantioselective epoxidation since the 4a-hydroperoxyflavin can act as an electrophile. Colonna and coworkers showed that dimethyl and diethyl vinyl phosphonates were converted by $CHMO_{Acineto}$ (ee_P > 98%) into fosfomycin precursors.[53] A similar enzymatic mechanism is also observed for FAD-dependent styrene monooxygenase.[107] Nevertheless, in presence of a keto-group the nucleophilic Baeyer-Villiger oxidation is always preferred.

1.2 Natural compounds and pharmacological ingredients accessible by Baeyer-Villiger monooxygenases

The application of Baeyer-Villiger monooxygenases as biocatalysts for environmentally benign syntheses of drugs, natural compounds and bioactive additives has been utilized and improved during recent decades. Indeed, several enzymatic routes are known to show a higher productivity combined with a reduction of synthetic steps compared to non-enzymatic reactions. The production of (*R*)-lipoic acid using a BVMO from camphor-grown *P. putida* ATCC 17453 or CPMO from *Comamonas* sp. belongs to the most prominent examples. Implementation of the latter enzyme simplified the synthesis even further since tedious chemical Mitsunobu inversion was not longer necessary.[95] Another example is the synthesis of the cytostatic drug (*R*)-(–)-sarkomycin[90d] *via* a regiodivergent transformation of the fused oxacyclobutanone *rac*-bicyclo[3.2.0]hept-2-en-6-one. Moreover, the possibility to perform heteroatom oxidation and sulfoxidation using Baeyer-Villiger monooxygenases broadens the applicability, since sulfoxides serve as important chiral building blocks for the synthesis of biologically active products and pharmaceutical ingredients.
Within this work, BVMOs once more proved to be powerful tools for the synthesis of optically active valuable substances. Here, mainly β-substituted linear aliphatic compounds were subjected to investigation (**Articles I-III**). Several enantiopure β-hydroxy or β-amino esters could be synthesized, which also served as the precursors for the production of optically active 1,2-diols, *N*-protected 2-amino alcohols and β-amino acids. The following chapter will introduce the major properties, important chemical and enzymatic pathways and possible application fields of these compounds.

1.2.1 Chiral 1,2-diols

Optically active 1,2-diols are important building blocks for the asymmetric synthesis of bioactive compounds. For instance, several patents describe the application of pentane-1,2-diol as an ingredient in cosmetic products such as skin moisturisers and sun blocks. Dodecane-1,2-diol is known to show antimicrobial activity and is therefore applied as an additive in antiperspirants.[108] Moreover, 1,2-diols are used as diluents in the synthesis of plastics and polyesters for packaging materials. The classical chemical synthetic routes to prepare 1,2-diols are based on the ring opening of epoxides using water or alcohols as nucleophiles. Other synthetic steps describe the formation of 1,2-diols by aldol condensation or dihydroxylations of olefins (e.g. Sharpless asymmetric dihydroxylation using OsO_4). Some examples are summarized in Table 1.4. These approaches, however, are laborious and often accompanied with unsatisfactory yields and selectivities. Far more elegant methods proceed enzymatically, where 1,2-diols can either be obtained *via* the asymmetric hydrolysis of epoxides using epoxide hydrolases[109] (enzymatic pendant to chemical alternatives) or aldolases[110], or the reduction of 2,4-diketones with regio- and enantioselective ketoreductases[111] or transesterification methods implementing lipases in chemoenzymatic approaches[112] (Scheme 1.15). Also, dioxygenases have been reported to dihydroxylate aromatic compounds to yield 1,2-diols. Hudlicky desribed an *in situ* enzymatic dihydroxylation of aromatics by toluene and naphthalene dioxygenases, respectively, yielding optically active 1,2-diols.[113]

However, vicinal 1,2-diols are extensively employed high-value intermediates in the synthesis of chiral compounds because of their ability to react with a broad variety of nucleophiles[114] (Scheme 1.16). Additionally, 1,2-diols can be further oxidized to furnish α-hydroxy carboxylic acids, another valuable synthon whose chemical synthesis is challenging.

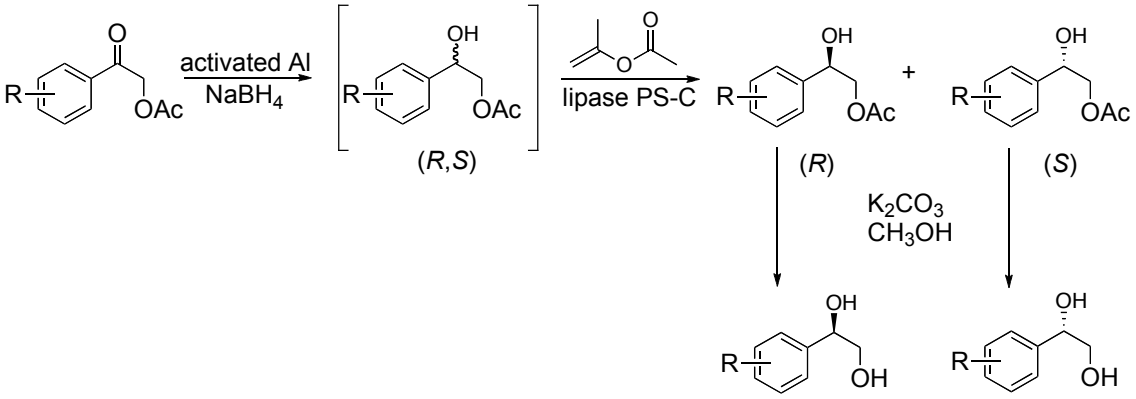

Scheme 1.15 Chemoenzymatic synthesis of enantiomerically pure 1,2-diols using lipases in an one-pot reaction procedure.[112d]

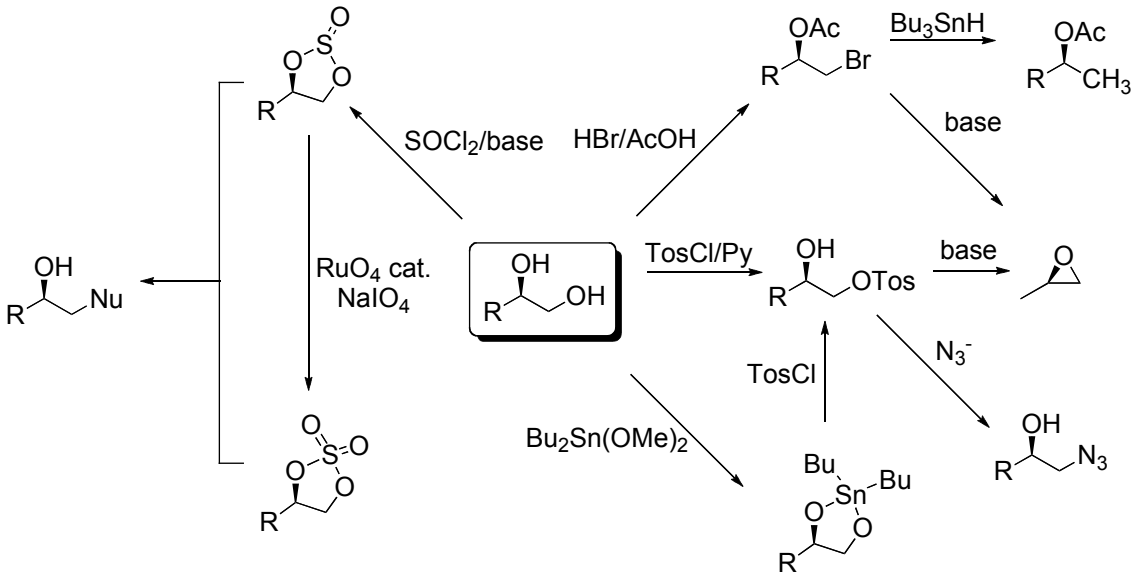

Scheme 1.16 Synthetic steps from chiral 1,2-diols.[115]

Table 1.4 Chemical synthesis of 1,2-diols.

Synthetic route	reaction scheme
Hot water-promoted ring opening of epoxides and aziridines by water and other nucleophiles.[116]	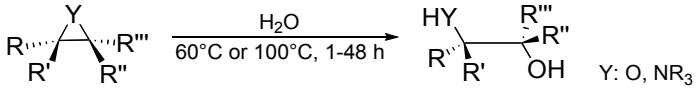
Carbon tetrabromide as an efficient catalyst for regioselective ring opening of epoxides with alcohols and water.[117]	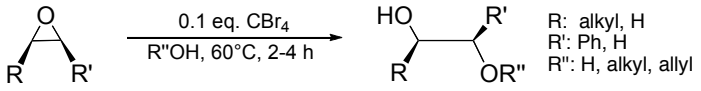
Efficient regio- and stereoselective ring opening of epoxides with alcohols, acetic acid and water catalyzed by NH_4^+-decatungstocerate (IV).[118]	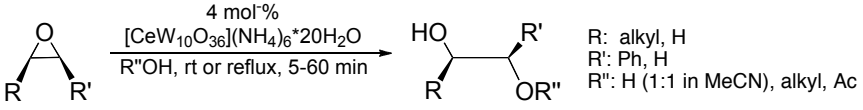
Organocatalyzed direct aldol condensation using BINAM-prolinamides: regio-, diastereo- and enantioselective controlled synthesis of 1,2-diols.[119]	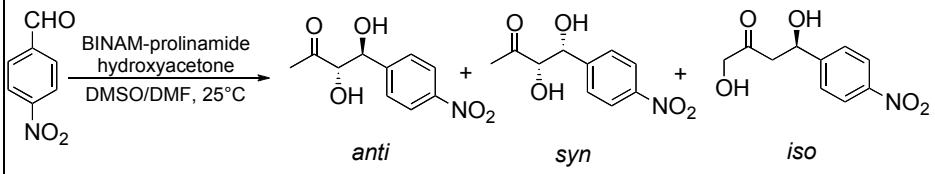
Asymmetric synthesis of 1,2-diols by single-pot allene boration/ hydroboration/cross-coupling.[120]	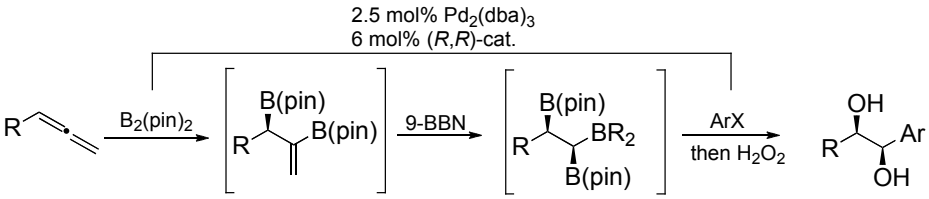
Asymmetric dihydroxylation using permanganate in the presence of a chiral phase-transfer reagent.[121]	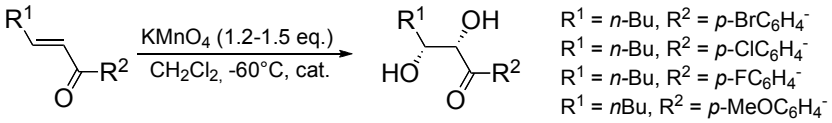

1.2.2 Optically active 2-amino alcohols

Enantiomerically pure 2-amino alcohols play an increasingly important role in both the treatment of a wide variety of human disorders, for example ophthalmic diseases[122], and as chiral auxiliaries in asymmetric carbon-carbon bond formation. The importance of enantiomeric purity in pharmaceuticals has been demonstrated by the debilitating and sometimes harmful side-effects caused by the presence of the non-therapeutic enantiomer of an otherwise beneficial drug. The application field of amino alcohols is wide and ranges from pharmaceutical intermediates, biological buffers and cosmetic ingredients to paintings, coatings and metalworking fluids. The simplest representative is ethanolamine, a head group for phospholipids found in biological membranes. This non-chiral compound is used as feedstock in the production of detergents, emulsifiers, polishes, chemical intermediates and pharmaceuticals. Moreover, the amino alcohol motif does not only occur in drugs, such as ephedrine, chloramphenicol or pronethalol, but is also present in hormones, for example adrenaline and noradrenaline. Furthermore, a large variety of 2,6-disubstituted piperidine-3-ols can be isolated from the West African savanna tree *prosopis africana*, whose leaves are traditionally used as treatment against toothache. One derivative is (+)-prosopine, which showed analgetic, anesthetic and antibiotic properties.[123] Also, some membrane lipids like sphingosine possess the amino alcohol motif (Figure 1.9).

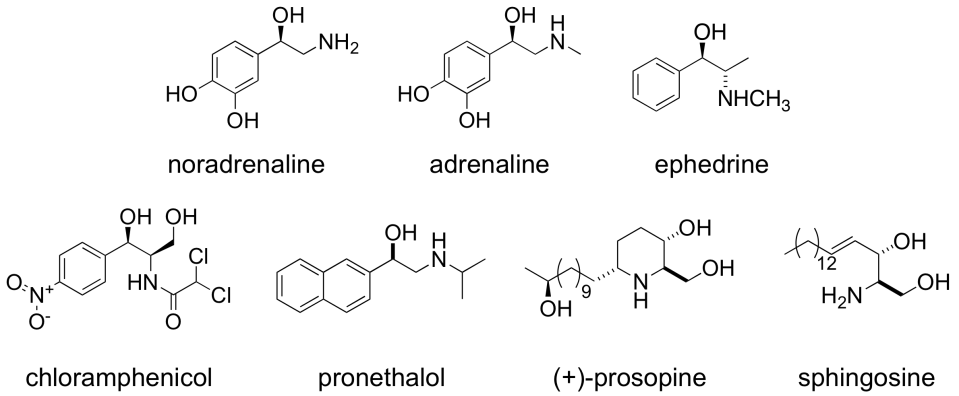

Figure 1.9 Amino alcohols of high pharmacological and toxicological value.

Among the few chemical methods for synthesizing racemic mixtures of 2-amino alcohols, enantiomerically pure compounds are available only through the reduction of amino acids or by kinetic resolution of racemic mixtures of 2-amino alcohols or amino alkyl acetates, often requiring expensive metal-catalysts. Furthermore, the reduction of amino acids to the corresponding amino alcohols is economically feasible only for the naturally occurring L-amino acids. The only synthetic methodologies available for the direct synthesis of 1,2- or 1,3-amino alcohols in high yields are the enantioselective amination of chiral epoxides[124], the directed reductive amination of β-hydroxy ketones[125], the aminoacetoxylation of alkylenes[126] and the asymmetric hydrogenation or reduction of prochiral β-amino ketones. While aminolysis of epoxides suffers from the limitations that chiral epoxides are not readily available, are expensive, and that only mono-substituted and *trans*-symmetrically substituted epoxides can

be used, metal-based reactions require expensive transition metals (rhodium[127], palladium or ruthenium).
Thus far, only a few enzyme-catalyzed methodologies have been described for the synthesis of enantiomerically pure 2-amino alcohols. In the late 1990s the protease subtilisin was subjected to the synthesis of peptidyl amino alcohols as potential specific serine protease inhibitors.[128] Another enzymatic approach was the synthesis of enantiopure *N*-aryl amino alcohols in the kinetic resolution of racemic acetates with pig liver esterase (PLE).[129] Recently, an immobilized lipase from *Arthrobacter* sp. was used for the preparation of enantiopure masked amino alcohols.[130]

1.2.3 Enantiopure β-amino acids

In contrast to α-amino acids, which are essential prerequisites for life, β-amino acids mostly occur as building blocks for natural products and pharmacological ingredients such as β-peptides, alkaloids, terpenoids or β-lactam antibiotics. Furthermore, they are valuable precursors for medical products like the anti-cancer drug taxol or the potent anti-tumor depsipeptide cryptophycin.[131] As biologically and physiologically active compounds, β-peptides have an auspicious potential due to their enhanced stability towards proteolytic enzymes. This offers new possibilities for creating drugs that are not rejected or degraded by the human body. Therefore, a plethora of chemical methods for the preparation of β-amino acids focussing on asymmetric synthesis have been developed[132] (Scheme 1.17). However, chemical syntheses often lack the advantages of stereo- and enantioselectivity usually achieved when utilizing enzymes. So far, the main enzymatic paths for obtaining highly enantiopure β-amino acids are based on kinetic resolutions exploiting enzymes either acting on C-N bonds (for example acylases[133], amidases[134] or aminopeptidases[135]) or C-O bonds (for example hydrolytic enzymes like lipases[136] or esterases[137]). Besides kinetic resolutions, optically pure β-amino acids can also be obtained by using aminomutases[138] or *via* reductive amination of ketones with β-aminotransferases[139] (Scheme 1.18). The simplest β-amino acid is β-aminopropionic acid, also called β-alanine, which is an essential component, although not proteinogenic, for many relevant biologically active compounds, like vitamin B3 (pantothenic acid).

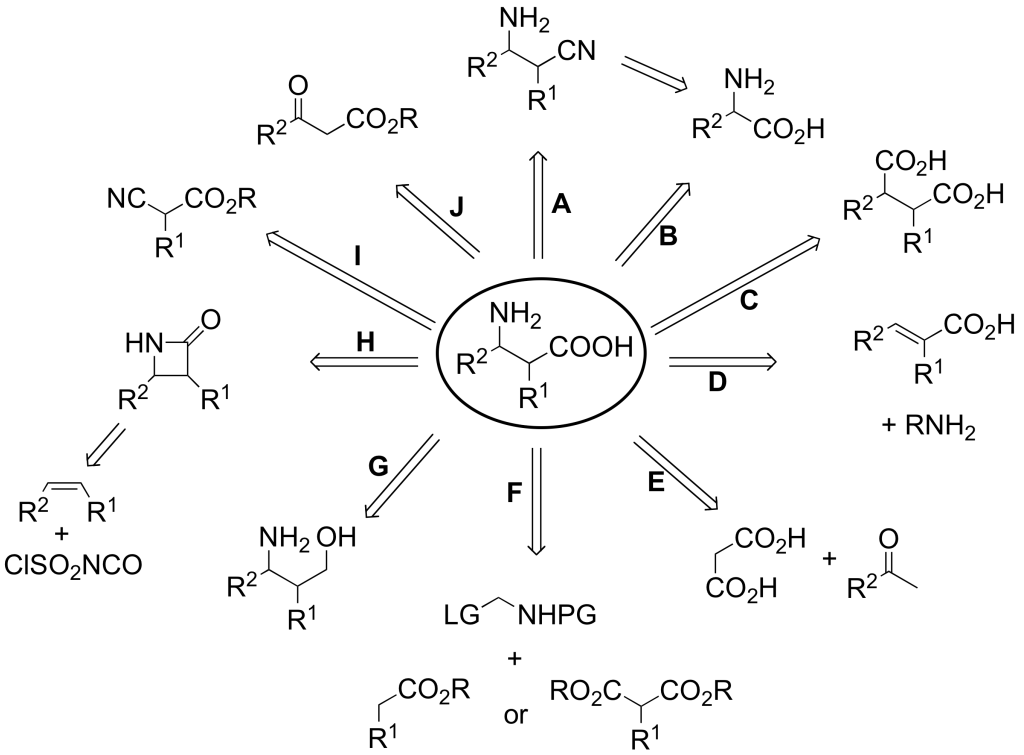

Scheme 1.17 Retrosynthetic analysis for the synthesis of β^3- and $\beta^{2,3}$-amino acids.[137] A: nitrile hydrolysis; B: homologation of α-amino acids; C: rearrangement; D: Michael-addition; E: modified Knoevenagel condensation; F: amido methylation; G: oxidation; H: β-lactam opening; I: nitrile reduction; J: reductive amination.

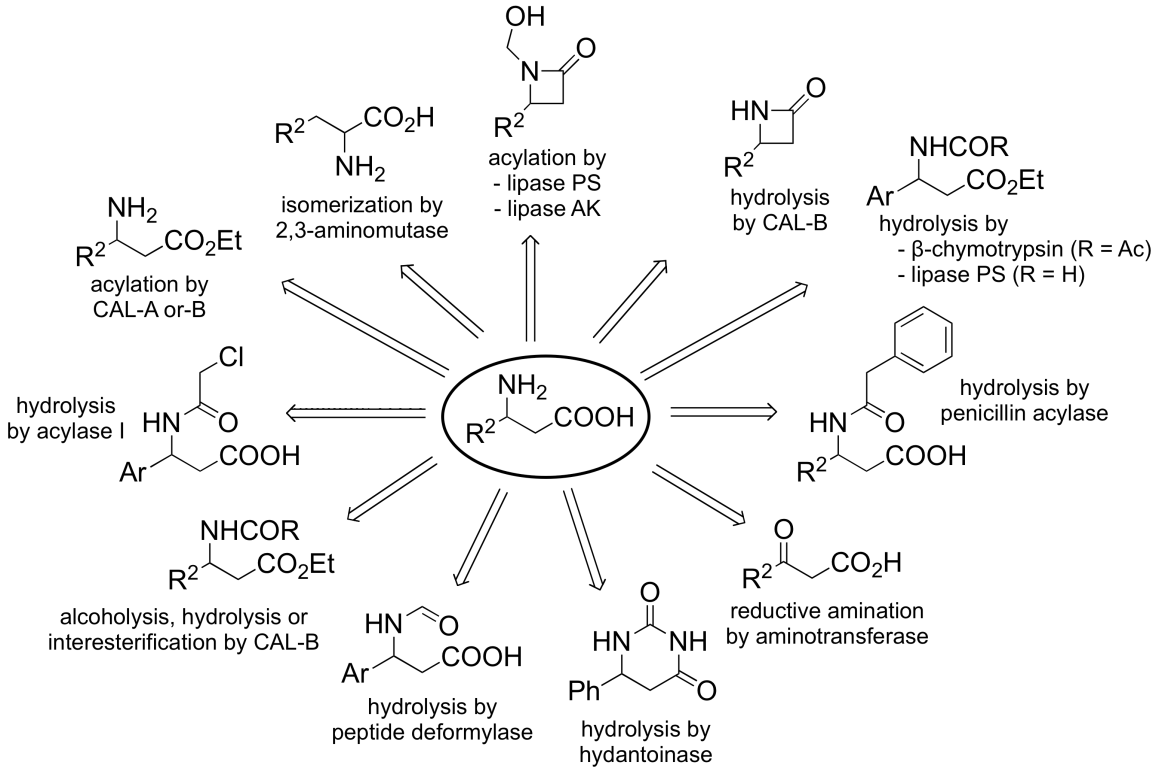

Scheme 1.18 Synthesis of enantiopure β^3-amino acid derivatives by enzymatic resolution.[137]

1.3 The stereoelectronic influence of polar substituents on the reaction rate: induction and resonance effects

Within the studies on kinetic parameters of $HAPMO_{JD1}$ a broad range of *para*, *meta*- and *ortho*-substituted acetophenone derivatives were examined. Besides enzymatic activity also binding capacities and reaction rates were determined (K_M and k_{cat}). The influence of substituents at the benzene ring of acetophenone on the formation of the transition state can be evaluated using the Hammett relationship (**Article VI**), according which these substituents can either accelerate or decelerate reaction rate depending on the sum of their inductive and mesomeric effects. The following paragraph provides an introduction into the Hammett equation.

1.3.1 The Hammett equation

Empirically it was found that polar substituents influence the reactivity of arylic organic compounds in a similar way to the acidity of acids and the alkalinity of bases. A quantitative correlation can be described in the case of *meta*- and *para*-substituted benzene derivatives. There, the logarithm of the reaction rate constant *k* has a linear relationship with the logarithm of the dissociation constant K_S (= $-pK_S$). The *ortho*-substituents must be left out due to steric interactions between substituent and reaction center, masking electronic factors.[140]

$$\lg k = \rho \lg K_S + b \quad (\rho \text{ reaction constant}) \tag{1}$$

The slope of the linear correlation line is referred to as ρ, the reaction constant. It measures the sensitivity of the reaction to electronic effects. Generally, side chain reactivity of *meta*- and *para*-substituted benzenes correlate linearly with σ values. Thus, for a reaction the following equation can be described

$$\lg k/k_0 = \sigma\rho \quad \text{(Hammett equation)} \tag{2}$$

with:

$$\sigma = \log K/K_0 \quad (\sigma \text{ substituent constant, } K \text{ equilibrium constant}) \tag{3}$$

where *k* is the rate constant for the reaction of *meta*- and *para*-substituted benzene derivatives and k_0 is the rate constant for the unsubstituted compound.[141] The Hammett postulation represents a linear free energy relationship. If ρ for a reaction is positive, that reaction is accelerated by electron-withdrawing substituents and slowed down by electron-donating substituents. A negative ρ value obviously implies the opposite of this.[142] The size of ρ is also an indication of the extent of charge development at the atom of the reaction center ring in passing from ground to transition state. Thus, when the atom is directly involved in the bond making and breaking process (α-substitition), ρ is relatively large. When the reacting side chain is insulated from the ring by an additional CH_2-group (β-substitution), ρ is smaller (Scheme 1.19).

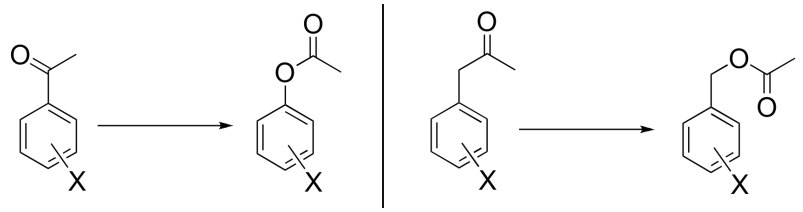

Scheme 1.19 Influence of the side chain length on reaction constant ρ.

On the other hand, σ values represent the measurement of the charge distribution by attachment of the reacting side chain to the *meta*- and *para*-positions. If $\sigma = 0$ the substituent has no effect and is electronically the same as H. If σ is positive, the substituent is electron-withdrawing, a negative σ value means electron donation. The electronic influence of a substituent is expressed by its σ_m and σ_p values and can be quantitatively described as the sum of independent inductive and resonance contributions. Inductive effects from polarization of σ bonds are greater for σ_m than for σ_p because the substituent is nearer.[142]
The resonance effect of a substituent involves interaction between orbitals in the substituent which are in the same plane as the π electron orbitals of the benzene ring. Therefore, conjugation is generally more effective in the *para*-position. Indeed, the NH_2 group has a large negative σ_p and a zero σ_m. It donates electrons strongly to the carbonyl group of acetophenone from the *para*-position but does not conjugate in the *meta*-position where its donation happens just to balance the effect of electronegative nitrogen (Figure 1.10).

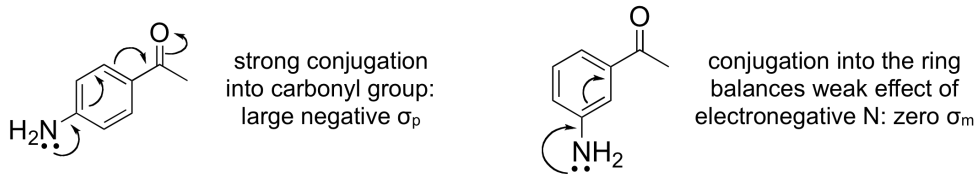

Figure 1.10 Conjugation of *para*- and *meta*-aminoacetophenone.

The OCH_3 group has a negative σ_p but a positive σ_m because a weaker electron donation from the lone pairs is more important in the *para*-position. But the effect of the very electronegative oxygen on the σ framework of the ring in the *meta*-position is more important than lone pair donation that does not reach the carbonyl group. Groups such as CHO, CN or NO_2 are of dipolar type, with the positive end of the dipole attached to the benzene ring. They exert their influence on the ring by combination of inductive and mesomeric effects, while the former effect outweighs the latter. The halogens have a powerful negative inductive effect due to their electronegativity which more than compensates a positive resonance, arising from the donation of the halogen lone pair into the ring. Alkyl substituents are the only common ones with a positive inductive effect. Since the σ_p values are more negative than the σ_m values, there must be a contribution from the positive resonance effect also. Thus, taking into consideration the assumption that the inductive effect is transmitted equally to the *meta*- and *para*-positions, σ_m is an approximate measure of the size of the inductive effect, and σ_p - σ_m an approximate measure of the resonance effect of a given substituent.

1.4 Molecular biology

1.4.1 Amplification of unknown flanking genomic regions using PCR-methods

This chapter deals with two PCR-methods that were used to amplify the gene of the 4-hydroxyacetophenone monooxygenase from *P. putida* JD1 (**Article VI**). The protein was first described in 2000, when Tanner and Hopper purified and sequenced it using Edman-degradation.[66] They identified three peptides, of which one was the N-terminus. This information provided the basis for a *gradient*-PCR using degenerate primers and genomic DNA from *P. putida* JD1 as template. This approach helped to identify 600 amino acids. Since this BVMO was described as a 70 kDa protein, it was assumed that there were still 40 amino acids missing. Various PCR-methods have been designed so far to overcome this challenge, including LAM-PCR (linear amplification mediated) (Figure 1.11) and vectorette-PCR (Figure 1.12). Another more cost-saving strategy to amplify unknown regions of a known sequence is inverse-PCR. A far more elegant and recently introduced method is the *SiteFinding*-PCR, which was originally developed to perform chromosome-walking.[143]

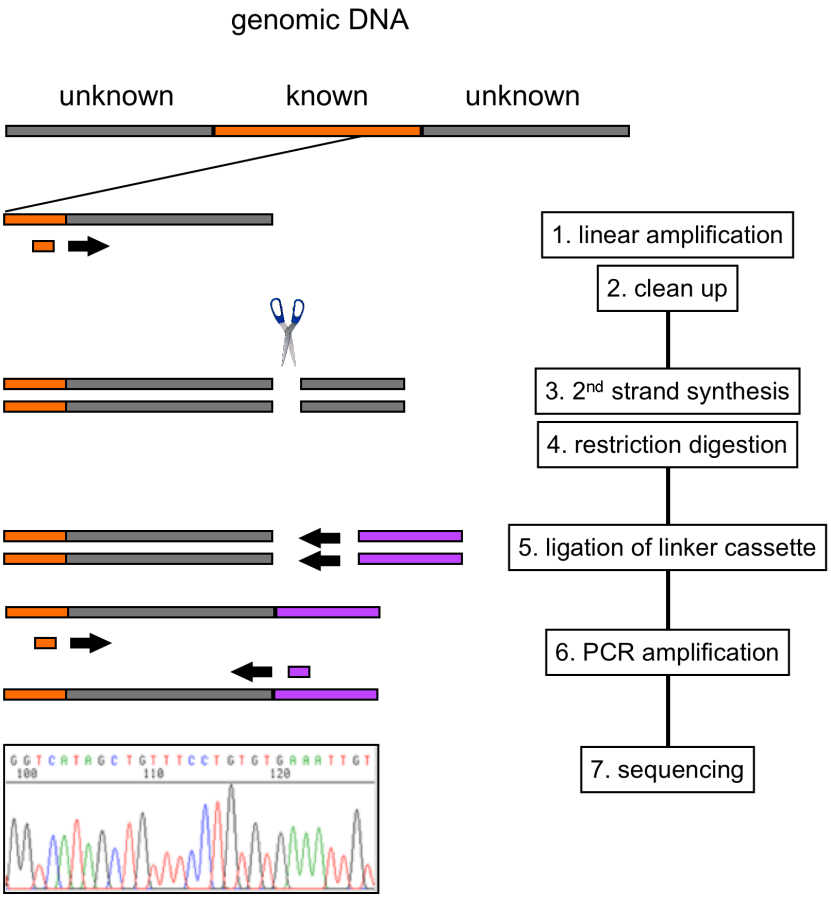

Figure 1.11 Principle of the LAM-PCR (linear amplification mediated).

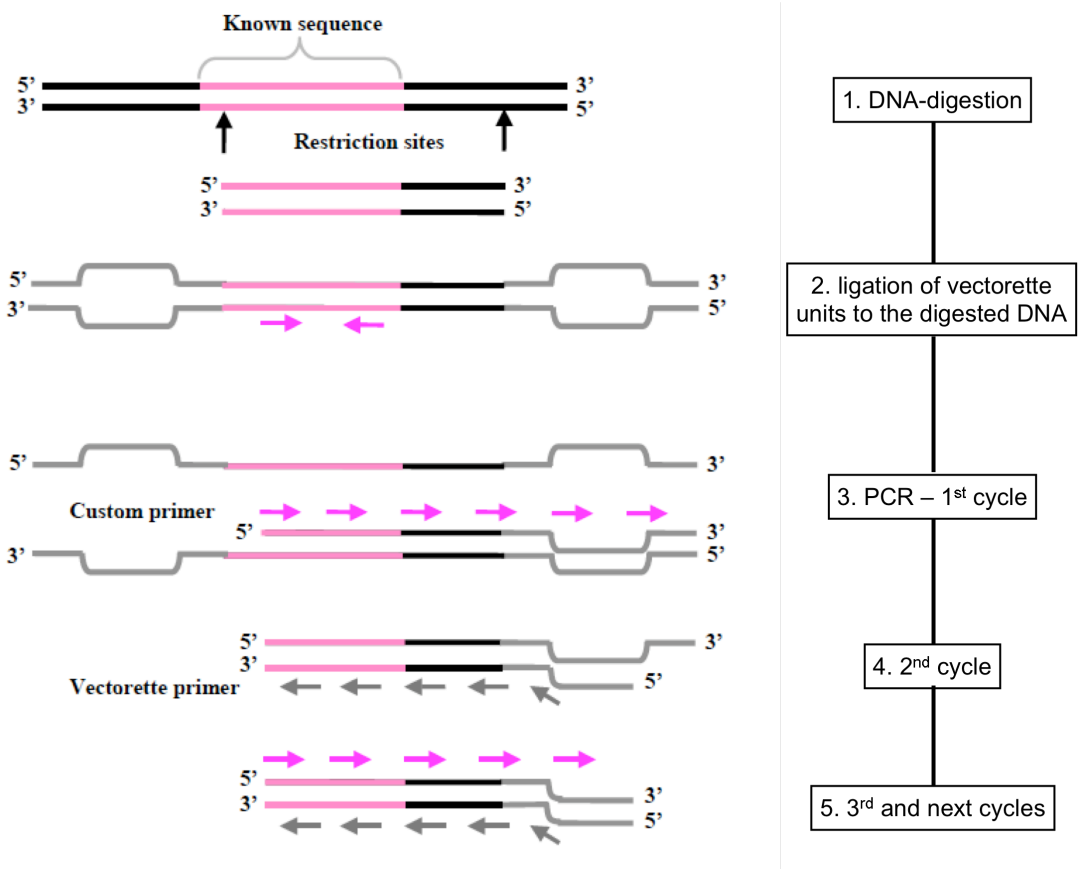

Figure 1.12 Principle of the vectorette-PCR.

1.4.1.1 Inverse-PCR

The literature details numerous techniques for amplification of unknown flanking regions, such as promotor and ribosome binding sites. The most frequently used technique is the inverse-PCR[144] (iPCR), typically proceeding in three steps: (i) first, the genomic DNA is digested with an appropriate restriction enzyme that does not cleave within the known sequence, followed by a self-ligation step to circularize the fragments in order to (ii) generate a plasmid-like structure converting flanking DNA to interior regions. Finally, (iii) a *nested*-PCR is performed using primers that bind up- and downstream of the known sequence, thus not oriented towards each other. Due to the self-circularization, both primers are addressed towards each other and a "normal" PCR can be conducted (Figure 1.13).
Implementing a *nested*-PCR, also known as interlaced-PCR, has two advantages: using an outer and an inner primer pair increases the specificity and sensitivity of the reaction. The outer primers generate a larger amplificate in the first PCR that serves as template for the second PCR with the inner primers, thus reducing the production of side-products.[145] However, digestion and ligation steps prior to the PCR makes this method rather tedious compared to the following strategy.

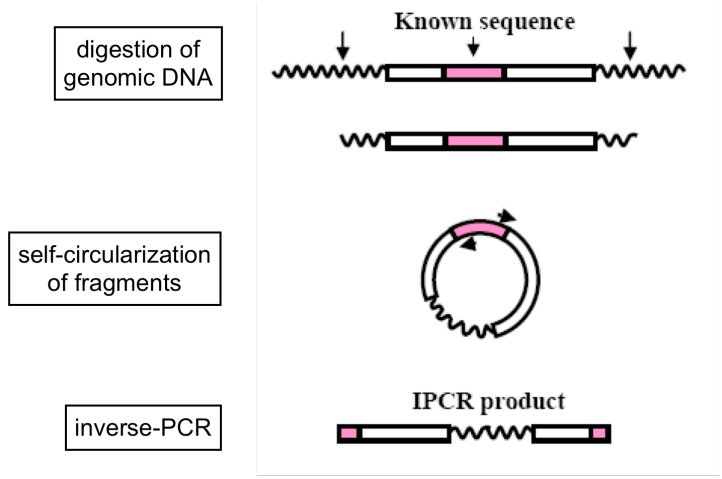

Figure 1.13 Principle of the inverse-PCR (iPCR).

1.4.1.2 *SiteFinding*-PCR

Most of the previously mentioned PCR-methods require complicated manipulations such as restriction cleavage, Southern blotting, and ligation or tailing before PCR amplification. Furthermore, arbitrary priming produces amplification of non-target molecules, thus increasing the bulk of unwanted side-products. The *SiteFinding*-PCR[143] consists of two PCR-based steps only: (i) priming of the genomic DNA using a sitefinder and (ii) a *nested*-PCR with sitefinder-specific (SFP) and gene-specific primers (GSP). The sitefinder consists of approximately 60 nucleotides with a 4-6 bp recognition site at the 3'-terminus, for example 5'-...NNNNNGCCT-3' or 5'-...NNNNNGCCTA-3'. This construct can then prime the DNA at low temperatures (25°C) annealing at the recognition sites. During the following *nested*-PCRs two GSPs and two SFPs are utilized. While the GSPs bind within the known sequence, the SFPs anneal within the sitefinder. Normally, the ends of individual DNA-strands, where the SFPs bind, form a stem-loop structure following every cycle due to the presence of inverted terminal repeats. Stem-loop structures are more stable than primer template hybrids, suppressing exponential amplification of non-target molecules. The target molecule contains the sitefinder sequence only at one side. Furthermore, the distance GSP extends the DNA through the sitefinder and the stem-loop structure cannot be generated. Therefore, the amount of non-target molecules theoretically should be very low. The method of the *SiteFinding*-PCR as well as stem-loop formation are shown in Figure 1.14.

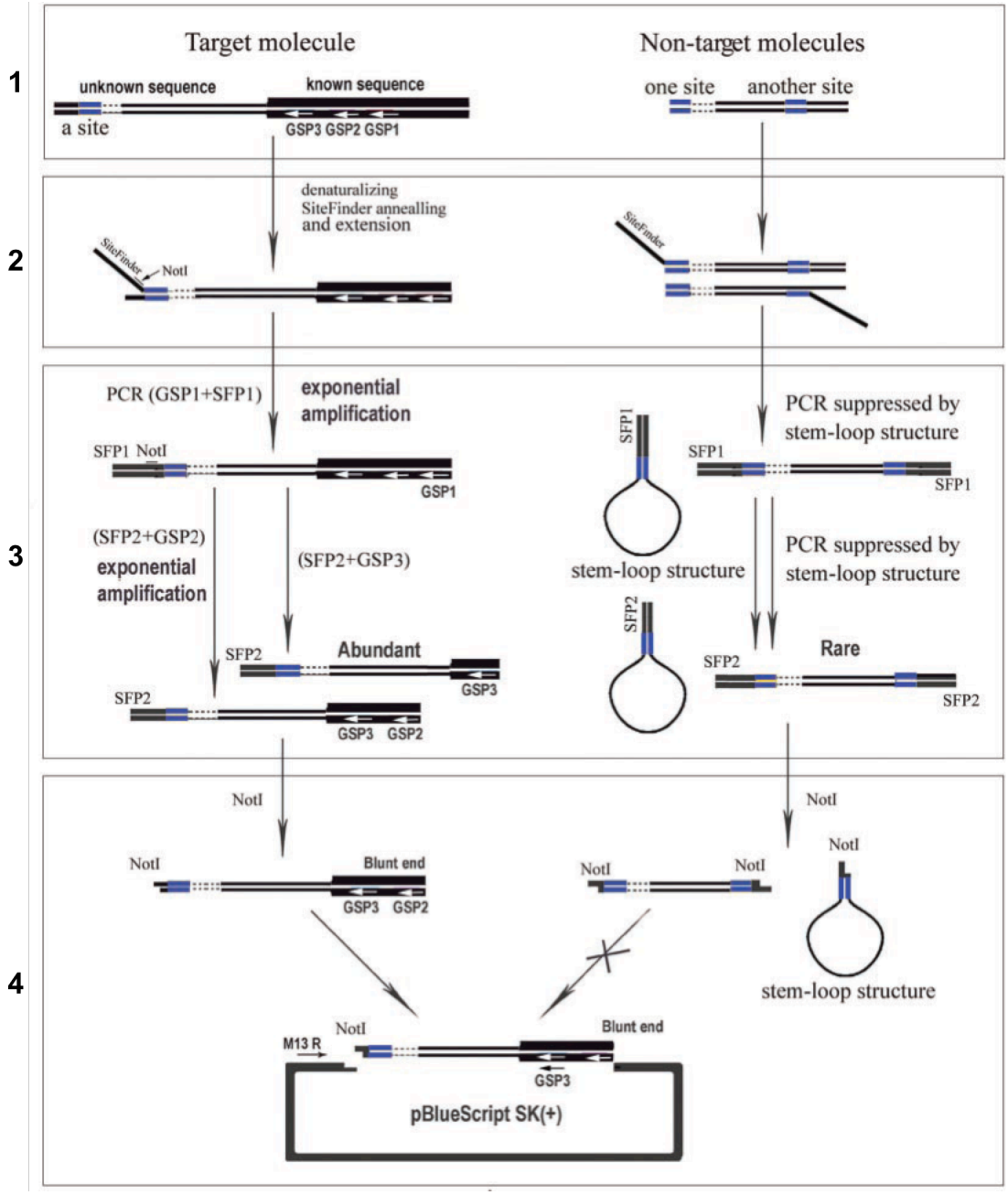

Figure 1.14 Schematic outline of *SiteFinding*-PCR.[143] 1) Original genomic double-strand templates showing target and non-target molecules. 2) *SiteFinding* reaction: after low temperature priming by a sitefinder, one strand of the target gene was replaced by *Taq* DNA polymerase. 3) *Nested*-PCR: the target DNA was exponentially amplified by *nested*-PCR with gene-specific (GSP) and sitefinder-specific (SFP) primers , while non-target gene amplification was suppressed by the stem-loop structure formation. 4) Cloning target molecules: PCR-products were purified by agarose gel electrophoresis, and purified DNA can be either cloned into a pBluescript SK(+) vector or, as performed in this work, directly into the TOPO pCRII® vector using a topoisomerase.

Compared to other PCR-methods, the *SiteFinding*-PCR provides some advantages: a) simplicity – it does not require additional manipulations; b) specificity – because of the stem-loop structure suppression effect co-amplification of non-specific products is very weak; c) sensitivity – only 10 ng of genomic DNA is enough; d) efficiency – low costs and time-saving. Within this work, the *SiteFinding*-PCR has been successfully applied to amplify the unknown gene of the 4-hydroxyacetophenone monooxygenase from *P. putida* JD1.

2 Goals and Outline

The main aim of this thesis was the identification of linear aliphatic or aryl aliphatic substrates with different substituents in β-position as novel substrates for Baeyer-Villiger monooxygenases. Besides the hydroxy ketones, also linear ketones bearing an amino group, a halogeno function or an aromatic ring in vicinity should be investigated. Moreover, the diversity of substrates should be enlarged further by varying the chain length and the carbonyl position, respectively. Since all substrates were not commercially available, they had to be synthesized chemically prior biotransformations. Then, all 20 substrates were subjected to kinetic resolutions using growing cells of *E. coli* expressing various BVMOs. Until now, 22 BVMOs with different substrate scopes and preferences are recombinantly available. Within these studies, the following 15 were examined concerning their potential of enantiomerically oxidizing linear and aryl aliphatic ketones with high conversions: $CHMO_{Acineto}$ (cyclohexanone monooxygenase from *A. calcoaceticus* NCIMB 9871), $CHMO_{Xantho}$ (cyclohexanone monooxygenase from *Xanthobacter* sp. ZL5), $CHMO_{Rhodo1}$ and $CHMO_{Rhodo2}$ (cyclohexanone monooxygenases from *Rhodococcus* sp. Phi1 and Phi2), $CHMO_{Brevi1}$ and $CHMO_{Brevi2}$ (cyclohexanone monooxygenases from *Brevibacterium* sp. HCU), $CHMO_{Arthro}$ (cyclohexanone monooxygenase from *Arthrobacter* sp.), $CHMO_{Brachy}$ (cyclohexanone monooxygenase from *Brachymonas* sp.), $BVMO_{Psfl}$ (BVMO from *P. fluorescens* DSM 50106), $BVMO_{KT2440}$ (BVMO from *P. putida* KT2440), CPMO (cyclopentanone monooxygenase from *Comamonas* sp. NCIMB 9872), CDMO (cyclododecanone monooxygenase from *R. ruber*), $HAPMO_{JD1}$ (4-hydroxyacetophenone monooxygenase from *P. putida* JD1), $HAPMO_{ACB}$ (4-hydroxyacetophenone monooxygenase from *P. fluorescens* ACB) and PAMO (phenylacetone monooxygenase from *T. fusca*).
Biotransformations using β-halogenic ketones are not further presented, since these substrates were instable and not converted by BVMOs.

Article I describes kinetic resolutions of β-hydroxy ketones which differ in chain length and carbonyl position. Here, influence of steric hindrance and regioselectivity were discussed in detail. It was observed, that by using an enzymatic Baeyer-Villiger oxidation also the “abnormal“ ester can be synthesized, depending on the structure of the substrate. The article further outlines formation of enantiopure 1,2-diols due to the hydrolysis of the 2-hydroxy alkyl acetates. Examination of β-amino ketones on the other hand are presented in **Articles II** and **III**. So far, only a few nitrogen bearing compounds, mainly of cyclic constitution, were investigated in enzymatic Baeyer-Villiger oxidations. Thus, this article provides the first examples, where linear aliphatic β-amino ketones were used as substrates for BVMOs. Similar to hydroxy ketones, the cleavage of the ester bond could be observed *in vivo* yielding enantiopure 2-amino alcohols. The indroduction of oxygen *via* migration of the less-favored carbon atom led to formation of the “abnormal“ ester, which opened up an alternative route to enantiopure β-amino acids as described in **Article III**. Kinetic resolutions of aryl aliphatic ketones are discussed in **Article IV**. Large-scale biotransformations were also performed.

The second aim within this thesis was the amplification, cloning, expression and biocatalytical characterization of two other BVMOs from *Pseudomonas* sp., namely $BVMO_{KT2440}$ and $HAPMO_{JD1}$. While **Article V** presents expression optimization and biocatalyis of $BVMO_{KT2440}$,

revaeling that this enzyme preferentially converts linear aliphatic ketones, **Article VI** dominantly refers to the amplification method and the purification of $HAPMO_{JD1}$ followed by the examination of kinetic parameters of acetophenone and its derivatives, aldehydes and heteroaromatic compounds. Furthermore, the physiological role of BVMOs is demonstrated. Figure 2.1 displays the relationship between molecular biology, chemical synthesis and biocatalysis as part of this work.

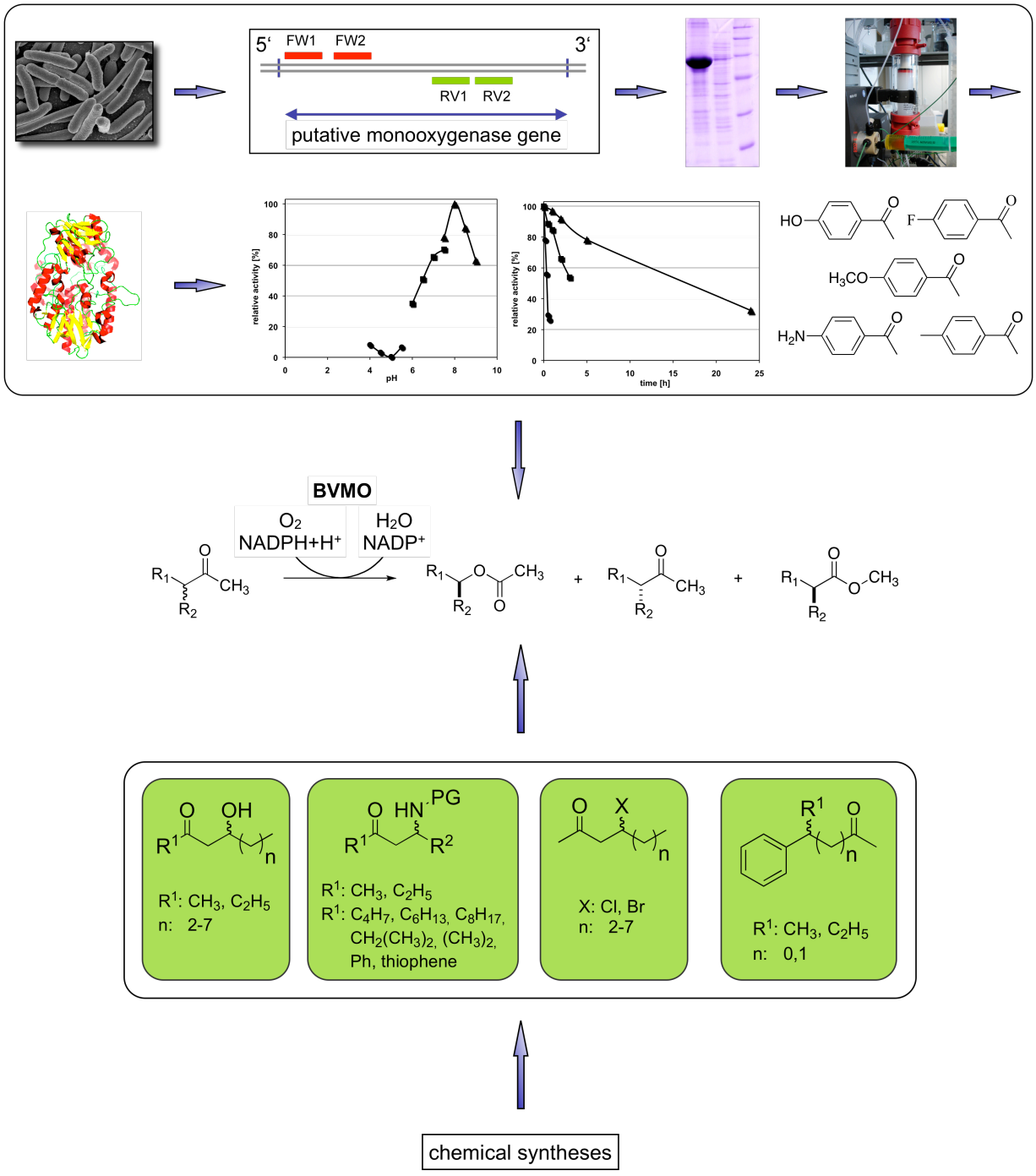

Figure 2.1 Relation between molecular biology, chemical synthesis and biocatalysis.

3 Results and Discussion

3.1 Synthetic application – Enlarging the platform of substrates for Baeyer-Villiger monooxygenases

A large toolbox of characterized and recombinantly available BVMOs of various bacterial origin have been subjected to kinetic resolution. Further emphasis was put on reaction rate and enantioselectivity. The main goal beyond was to establish a new substrate class and thus enlarge the platform of optically active ketones and esters accessible with BVMOs. Thus far, mainly cyclic cyclohexanone and cyclopentanone derivatives have been investigated in kinetic resolution processes.[90c, 146] Recently it was discovered that also linear aliphatic 2- and 3-ketones possessing either a hydroxy[147] or an amino group in the β-position can be very good substrates, yielding high optical purities with almost maximum conversions (50%). The possible enantiomerically pure products are of high pharmaceutical interest and serve as chiral building blocks in synthetic chemistry. Moreover, kinetic resolution opens up access to three chemically different compounds: the Baeyer-Villiger ester, the enantiopure non-converted ketone enantiomer and the hydrolytic product resulting from the ester bond cleavage.

In these examinations, defined BVMOs with different substrate scopes (Scheme 3.1) were subjected to kinetic resolutions with β-hydroxy (**Article I**) and β-amino ketones (**Articles II** and **III**). All products were of high optical purity. Corresponding esters could be hydrolyzed to yield either 1,2-diols or 2-amino alcohols, both enantiomerically pure. When the "abnormal" ester was generated, access to β-amino acids and β-hydroxy carboxylic acids was possible.

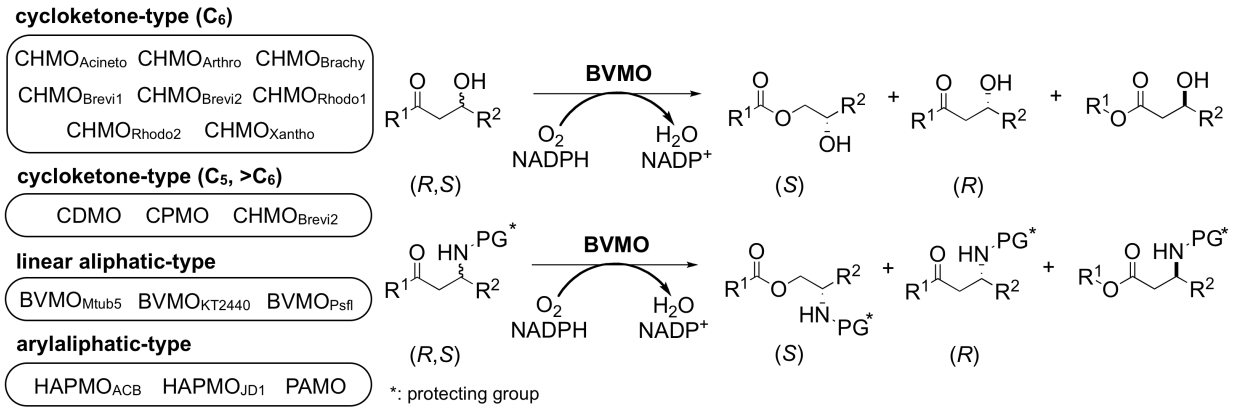

Scheme 3.1 Biocatalytic toolbox of Baeyer-Villiger monooxygenases for the kinetic resolution of β-hydroxy and β-amino ketones.

All biotransformations were carried out using growing *E. coli* cells overexpressing the desired BVMO. Therefore, addition of the expensive cofactor NADPH during reaction was not required, as it is provided endogenously by the cell metabolism. Furthermore, enzyme stability was ensured by the native physiological environment. The next chapter will summarize and discuss the most important results from kinetic resolutions of aliphatic open-chain β-hydroxy, β-amino ketones and aryl aliphatic ketones of various structure.

3.1.1 Kinetic resolution of β-hydroxy ketones – Access to optically active 1,2-diols

Using Baeyer-Villiger monooxygenases in kinetic resolutions of racemic linear aliphatic β-hydroxy ketones, different optically active compounds can be generated. For example, hydrolysis of the corresponding 2-hydroxy alkyl acetates, either chemically or enzymatically using lipases or esterases in the latter case, yield enantiomerically pure 1,2-diols. Thus, BVMOs can disclose a new environmentally benign possibility for the synthesis of highly valuable 1,2-diols as building blocks for the pharmaceutical industry (**Article I**).
The chemical synthesis of various linear aliphatic β-hydroxy ketones as substrates for biotransformations was performed by a regioselective aldol addition using ethyl acetoacetate or ethyl propionylacetate and the respective aldehyde.[148] All isolated yields are shown in Scheme 3.2.

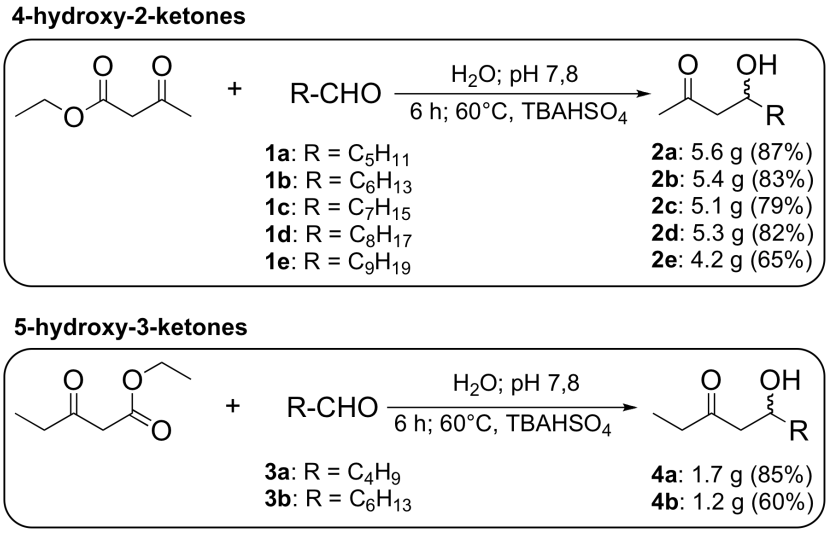

Scheme 3.2 Chemical synthesis of linear β-hydroxy ketones *via* a regioselective aldol-addition.

The majority of the investigated BVMOs proved to be highly active against linear aliphatic 4-hydroxy-2-ketones. The previously described discrimination among BVMOs based on substrate preferences discovered so far also reflected within this study, since aryl aliphatic-converting enzymes, such as $HAPMO_{JD1}$, PAMO and $HAPMO_{ACB}$, showed either no or only a very weak activity against these substrates. On the contrary, cycloketone-converting enzymes like $CHMO_{Acineto}$, $CHMO_{Arthro}$, $CHMO_{Brachy}$ and $CHMO_{Xantho}$ and linear ketone-converting $BVMO_{Psfl}$ oxidized middle-chain hydroxyketones showing moderate to high enantioselectivities (**Article I**, **Table 1**). All enzymes examined exclusively converted the (*S*)-enantiomer. While selectivity was not influenced by the substrate structure, activity decreased with growing chain length (Figure 3.1). Obviously, larger substrates are too bulky to be properly positioned in the active site and a combined higher hydrophobicity may lead to repulsion within the access tunnel.

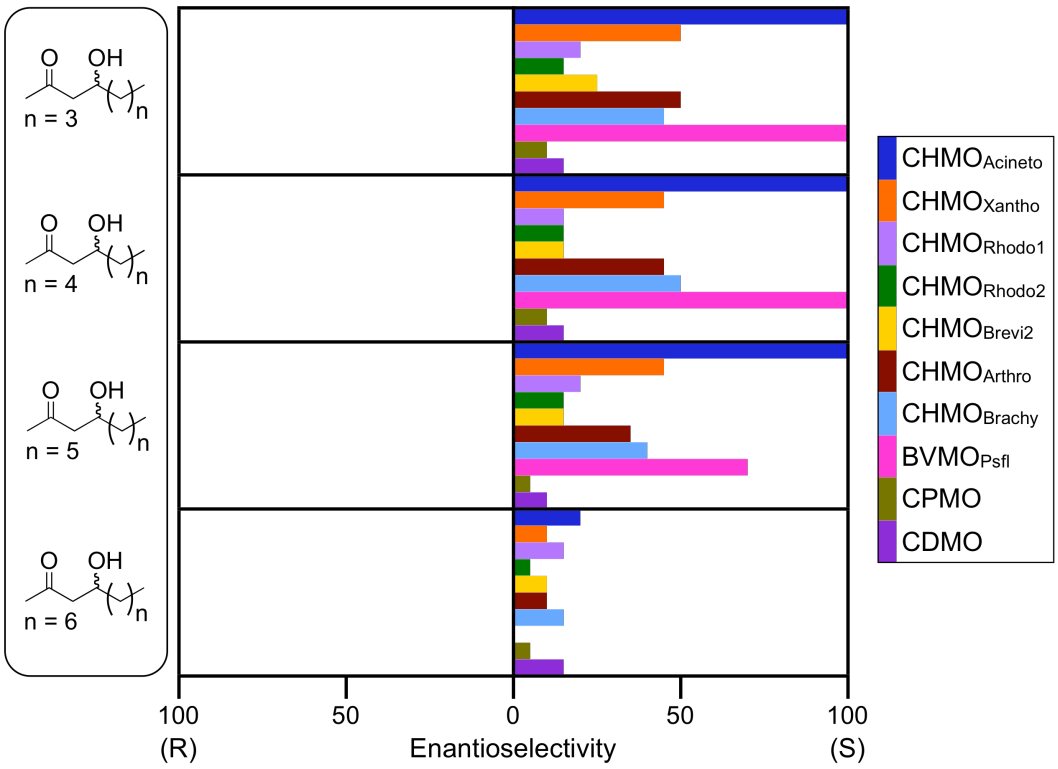

Figure 3.1 Enantioselectivities and enantiopreferences of investigated BVMOs in kinetic resolutions of 4-hydroxy-2-ketones. All E-values refer to the "normal" ester.

The formation of enantiopure β-hydroxy ketones and 2-hydroxy alkyl acetates is chemically challenging and, additionally, enzymatic approaches based on selective ketoreductases[111] or esterases are still rare. Therefore, the oxidation of these ketones using highly selective BVMOs would open up an attractive alternative for already established methods. Furthermore, these enzymes would allow access to a third interesting and valuable compound: enantiomerically pure 1,2-diols. During these studies it could be observed that some 2-hydroxy alkyl esters were hydrolyzed *in situ*, probably due to a decreasing pH resulting from cell metabolism (**Article I**, **Figure 1**). Since the chirality is not altered during hydrolysis, all 1,2-diols display the same optical purity as their ester counterparts. Formation of these 1,2-diols was especially observed for $CHMO_{Acineto}$ from *A. calcoaceticus* NCIMB 9871 and $BVMO_{Psfl}$ from *P. fluorescens* DSM 50106 (Figure 3.2).

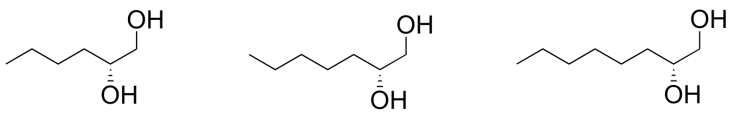

$CHMO_{Acineto}$: 50%
$BVMO_{Psfl}$: 8%

$CHMO_{Acineto}$: 21%
$BVMO_{Psfl}$: 34%

$CHMO_{Acineto}$: 28%
$BVMO_{Psfl}$: 50%

Figure 3.2 Yields of optically active 1,2-diols resulting from the *in situ* hydrolysis of the corresponding Baeyer-Villiger 2-hydroxy alkyl acetates after oxidation of the respective β-hydroxy ketones.

Besides the observation of the 1,2-diol formation, production of the "abnormal" Baeyer-Villiger ester was observed using 5-hydroxy-3-ketones as substrates (**Article I**, **Table 2** and **Figure 2**). In the case of 4-hydroxy-2-ketones formation of the "abnormal" ester was

observed to a very low extent (c < 10%). Due to enzyme's regioselectivity, the oxygen atom can also be introduced on the other side adjacent to the carbonyl group thus migrating the less-favored carbon-center. This feature is of particularly high value since chemical synthesis of this "abnormal" ester is still very challenging. Indeed, movement of the reactive site into the center of the molecule increased the amount of "abnormal" ester drastically. Enlarging the residue next to the carbonyl function from methyl to ethyl lowered enzymatic regioselectivity. Therefore, the likelihood of both residues migrating became similar, since both were able to stabilize the charge of the intermediate during catalysis. Nevertheless, enantioselectivity was not impaired (Figure 3.3).

	Acineto	Rhodo1	Rhodo2	Brevi2	Arthro	Brachy	Xantho	BVMO	CPMO	CDMO
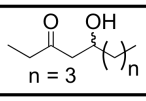 n = 3	+	+	+		+	+		+		+
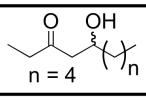 n = 4		+			+	+		+		+

white: E <30
light grey: E >30<70
dark grey: E >70<100
black: E >100
+: abnormal ester is generated

Figure 3.3 Summary of enantioselectivites of various BVMOs from kinetic resolutions of 5-hydroxy-3-ketones and formation of the "abnormal" ester (indicated by +). Acineto: cyclohexanone monooxygenase from *A. calcoaceticus* NCIMB 9871; Rhodo1 and Rhodo2: cyclohexanone monooxygenases from *Rhodococcus* sp. Phi1 and Phi2; Brevi2: cyclohexanone monooxygenase from *Brevibacterium* sp. HCU; Arthro: cyclohexanone monooxygenase from *Arthrobacter* sp.; Brachy: cyclohexanone monooxygenase from *Brachymonas* sp.; Xantho: cyclohexanone monooxygenase from *Xanthobacter* sp. ZL5; BVMO: BVMO from *P. fluorescens* DSM 50106; CPMO: cyclopentanone monooxygenase from *C. testosteronii* NCIMB 9872; CDMO: cyclododecanone monooxygenase from *R. ruber*.

3.1.2 Left or right waltz? – Regioselectivity of BVMOs offers alternative synthetic pathways for 2-amino alcohols and β-amino acids

The application of enzymatic reactions from prostereogenic compounds or kinetic resolution of racemic starting material is restricted to the enzyme's substrate specificity and therefore limits diversity of enzymatically synthesized natural compounds. Nevertheless, especially substances bearing an amino group in β-position to a hydroxy-, a carbonyl- or a carboxyl-function are indeed very important intermediates. Implementing Baeyer-Villiger monooxygenases may enlarge the platform of available and easy accessible amino compounds. Compared to a chemical Baeyer-Villiger oxidation, BVMOs show a regioselectivity correlated with the ketone's structure. Thus, they are able to introduce oxygen onto a carbon-carbon bond by enabling the less-substituted carbon-center to migrate yielding the "abnormal" Baeyer-Villiger ester. Using a broad set of linear aliphatic β-amino ketones as substrates would lead to β-amino esters which can be cleaved to give free β-amino acids. On the other hand, hydrolysis of the "normal" ester, generated by oxygen incorporation adjacent to the higher

substituted carbon atom, would furnish the synthesis of highly valuable 2-amino alcohols. Investigation of ketones containing a nitrogen motif in β-position to the carbonyl group as substrates for BVMOs is subject of **Articles II** and **III**. In a two-step enzymatic approach the Baeyer-Villiger ester can be hydrolized to yield optically active *N*-protected 2-amino alcohols or β-amino acids (Scheme 3.3).

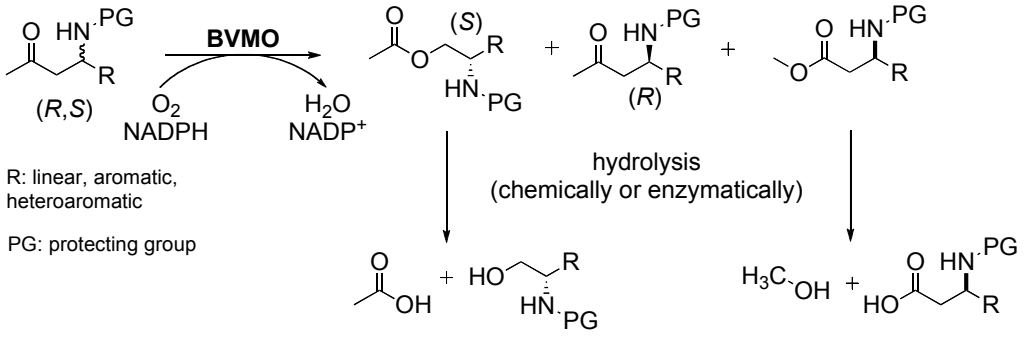

Scheme 3.3 BVMO-mediated kinetic resolutions of β-amino ketones yielding enantiomerically pure 2-amino alkyl acetates and β-amino esters which undergo hydrolysis to give *N*-protected 2-amino alcohols or *N*-protected β-amino acids.

Chemical syntheses of the precursors for the biotransformations was accomplished by an *aza*-Michael-addition[149] of methylcarbamate onto an α,β-unsaturated linear ketone in dichloromethane using TMSCl as Lewis-acid catalyst and *n*-tributylphosphine as phase-transfer catalyst. Since the majority of alkenones were not commercially available, those had to be synthesized first by an aldol addition similar to the synthesis of β-hydroxy ketones. All isolated yields are shown in Schemes 3.4 and 3.5.

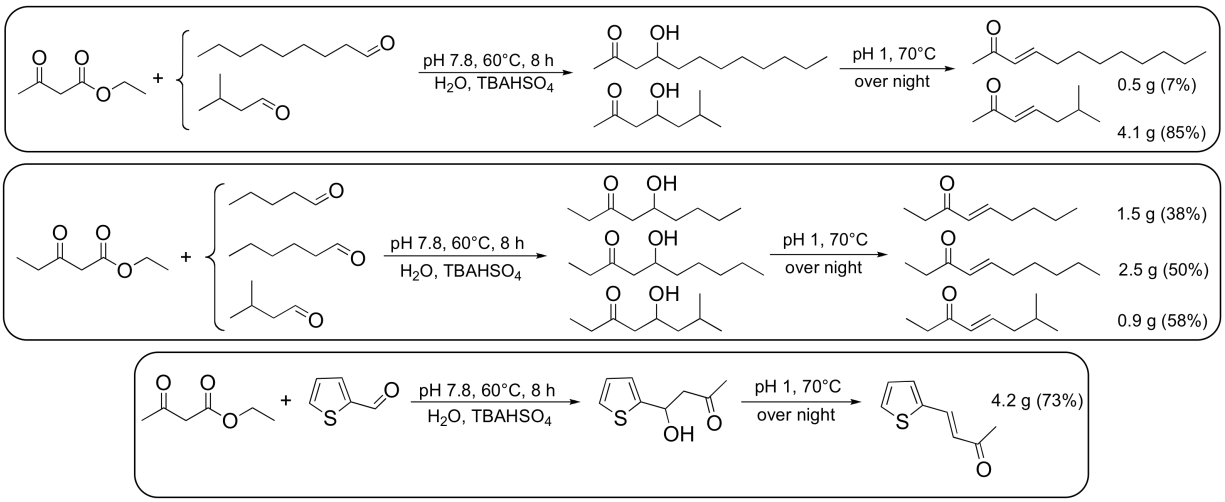

Scheme 3.4 Aldol-addition to synthesize α,β-unsaturated ketones.

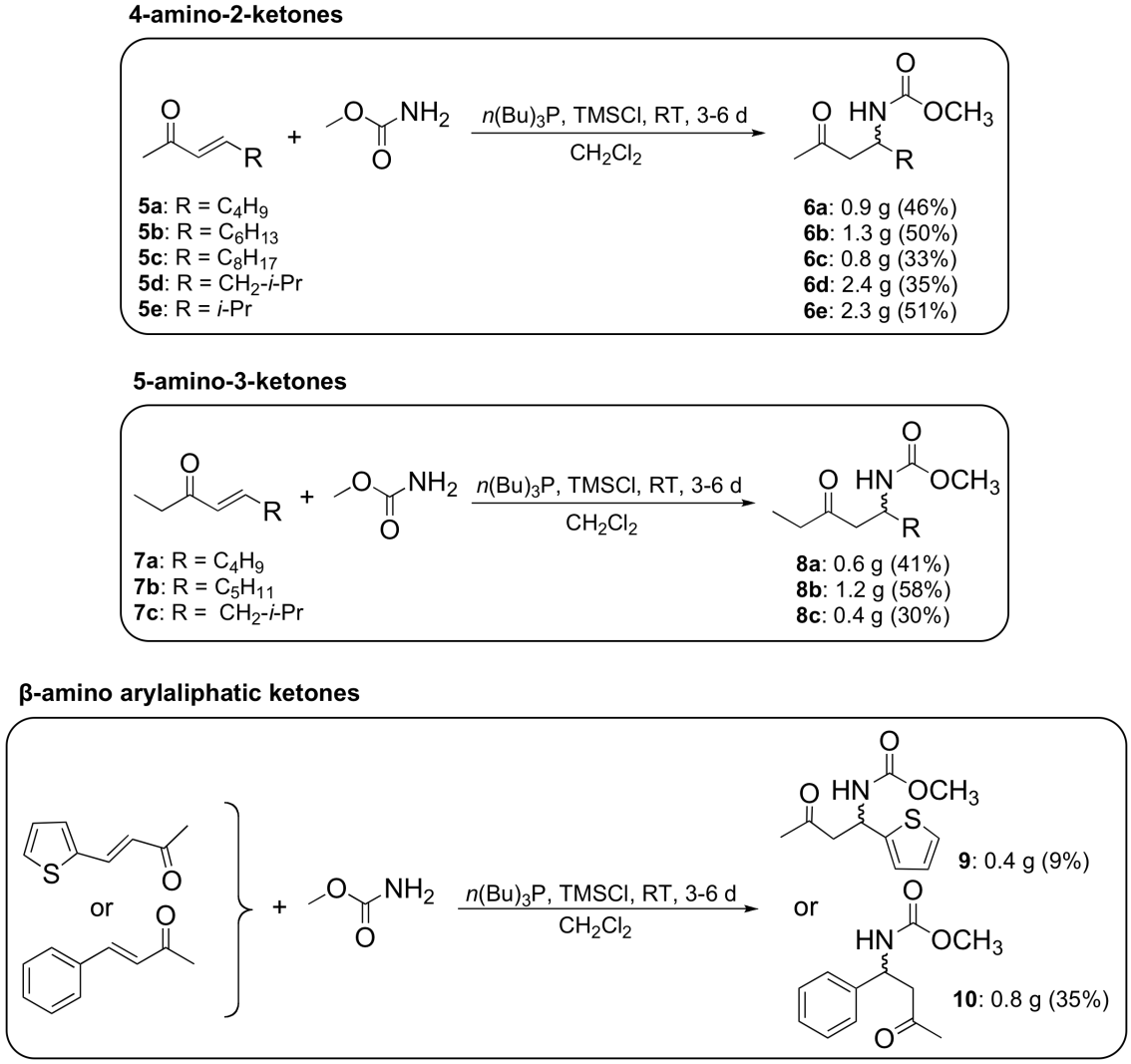

Scheme 3.5 Synthesis of linear and aryl aliphatic β-amino ketones *via aza*-Michael-addition.

Due to the different electronic environment of a nitrogen atom compared to an oxygen atom, the exchange of the β-hydroxyl group into an β-amino substituent can influence selectivity and enantiopreference of BVMOs. Several β-amino ketones with different structures (linear and linear-branched) were analyzed (**Article II**). Comparing the linear substrates **1**-**3** (Figure 3.4) revealed that the enantiopreference of $CHMO_{Arthro}$, $CHMO_{Brachy}$ and $CHMO_{Xantho}$ correlated with the substrate's chain length. While all three enzymes oxidized (+)-**1** (C_8), in the case of **2** (C_{10}) and **3** (C_{12}) the (–)-enantiomer was converted. A similar preference was observed for $HAPMO_{ACB}$ from *P. fluorescens* ACB, although enantioselectivity was rather low. Regarding enantioselectivities of linear-branched β-amino ketones **4** and **5**, selectivity was not only decreased drastically (E < 15), also the enantiopreference changed from (–)-**4** to (+)-**5**, with the exception of $CHMO_{Brevi1}$. Moreover, the latter BVMO is an example of how the substrate's structure can influence enantioselectivity. Decreasing the chain-length about a methylene group led to an increase of selectivity (E = 68). Obviously, the additional CH_2-group adjacent to the reaction center leads to a spatially more demanding substrate structure, thus increasing steric hindrance. Therefore, enantioselectivity of $CHMO_{Brevi1}$ for **4** might be very low compared to **5** (compiled results in **Article II**, **Table 1**).

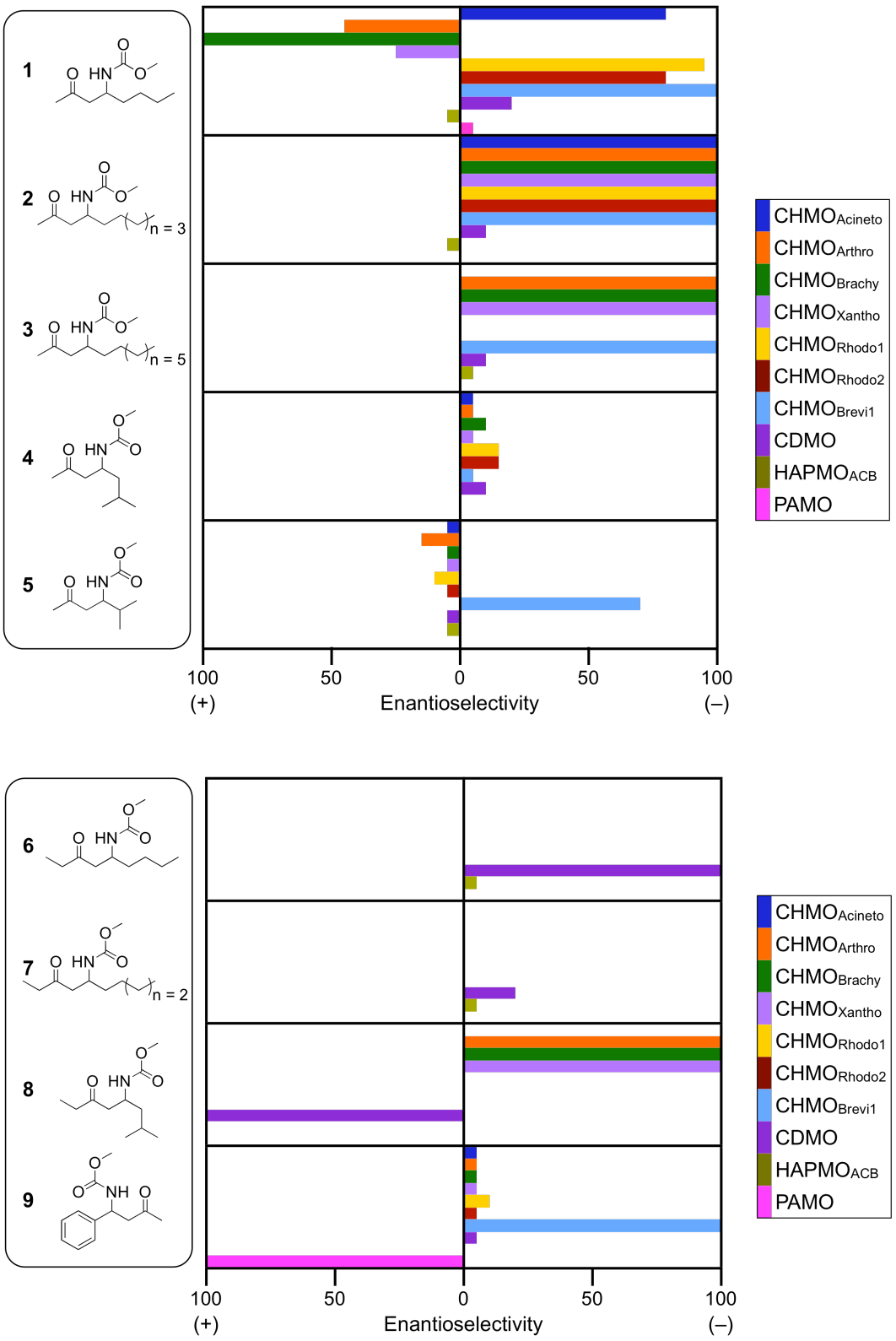

Figure 3.4 Enantioselectivities and enantiopreferences of examined BVMOs in kinetic resolution of β-amino ketones (shown are E-values of the "normal" ester synthesis).

Considering the results for the β-hydroxy ketones, it was also assumed that hydrolysis of the 2-amino alkyl acetates might be observed *in situ*. Indeed, production of enantiopure 2-amino alcohols could be obtained for **1** (20%), **2** (52%), **4** (50%), **5** (38%), **7** (9%) and **8** (6%) using different BVMOs (**Article II**, **Figure 3**). Therefore, regioselectivities of BVMOs during oxidation of **6**-**8** (Figure 3.4) were investigated in detail. As already described for

5-hydroxy-3-ketones, regioselectivity can be lowered exchanging the methyl group adjacent to the carbonyl function into an ethyl residue. Hydrolysis of the “abnormal“ ester yielded enantiomerically pure β-amino acids. This synthetic pathway offers an alternative access route to β-amino acids compared to established (enzymatic) methods so far. Several enzymes oxidized **6**-**8** yielding enantiopure “abnormal“ esters (E > 100), which additionally differed in their absolute configuration (**Article III**). While CDMO exclusively oxidized (+)-**8**, $CHMO_{Arthro}$, $CHMO_{Brachy}$ and $CHMO_{Xantho}$ on the other hand converted (–)-**8** only. Due to the aliphatic residue (CH_2-*i*Pr) in the vicinity of the chiral center, formation of *N*-protected (+)- and (–)-β-leucine would be possible. In a coupled enzyme reaction using enantioselective CDMO for Baeyer-Villiger oxidation followed by ester hydrolysis catalyzed by CAL-B, formation of *N*-protected (+)-β-leucine could be successfully demonstrated (Scheme 3.6, detailed results in **Article III**, **Table 1** and **Scheme 2**). These synthetic steps can offer new possibilities for the enantioselective synthesis of a large variety of natural and non-natural β-amino acids.

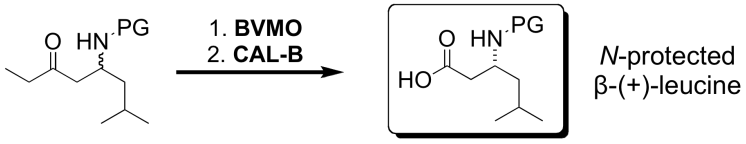

Scheme 3.6 Formation of enantiopure *N*-protected (+)-β-leucine in a coupled enzymatic kinetic resolution using CDMO from *R. ruber* and CAL-B from *Candida antarctica*.

3.1.3 Aryl aliphatic ketones: large-scale application of Baeyer-Villiger monooxygenases

Among the various linear aliphatic ketones, five aryl aliphatic substrates with methyl, ethyl, hydroxyl or phenyl substituents within the side chain have also been examined. High E-values were achieved with arylketone-preferring BVMOs like PAMO, $HAPMO_{ACB}$ and $HAPMO_{JD1}$. Cycloketone-converting BVMOs were also highly active, but showed a lower enantioselectivity (Figure 3.5). While the majority of enzymes showed (*S*)-selectivity towards **1**, $BVMO_{KT2440}$ preferred the (*R*)-enantiomer, although enantioselectivity was quite low (E = 13). Increasing the chain length of the alkyl residue from methyl (**1**) to ethyl (**2**) changed the enantiopreference of CPMO (**Article IV**). However, selectivity was not impaired. Investigations of the reduced counterpart 2-phenylpropionaldehyde using $HAPMO_{ACB}$ and PAMO, yielding phenylethyl methanoate, revealed that indeed BVMOs are able to oxidize aldehydes, but accompanied with a lower enantioselectivity compared to a ketone reaction center.[150] Substrates bearing either an additional methylene group adjacent to the carbonyl group (**3**) and/or possessing a hydroxyl residue (**4**) led to reduced activity and enantioselectivity. Spatially more demanding substrates like **5** were not oxidized anymore. It was believed that the substrate cannot enter the active site due to increased steric hindrance resulting from the neighboring second phenyl ring.

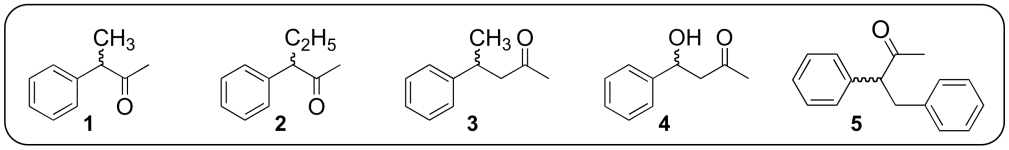

HAPMO$_{JD1}$	**E > 200 (*S*)**	**n.c.**	**n.d.**	**n.c.**	
HAPMO$_{ACB}$	**E = 127 (*S*)**	**E = 156 (*S*)**	**E = 1**	**n.c.**	
PAMO*	**E > 100 (*S*)**	**E > 200 (S)**	**n.d.**	**n.d.**	
CHMO$_{Acineto}$	**E < 3 (*S*)**	**E = 4.5 (S)**	**E = 3**	**n.c.**	
CHMO$_{Brevi2}$	**E = 9 (*S*)**	**E = 9 (*S*)**	**E = 18**	**n.c.**	**n.c.**
CHMO$_{Xantho}$	**E = 34 (*S*)**	**E = 3 (*S*)**	**E = 3**	**E > 100**	
CPMO	**E = 6 (*S*)**	**E = 4 (*R*)**	**E = 11**	**n.c.**	
BVMO$_{Psfl}$	**E = 42 (*S*)**	**n.c.**	**traces**	**n.c.**	
BVMO$_{KT2440}$	**E = 13 (*R*)**	**n.c.**	**n.c.**	**n.c.**	

*: results from Rodriguez *et al*. (2007)
n.c.: no conversion; n.d.: not determined

Figure 3.5 Summarized enantioselectivities of selected BVMOs for various aryl aliphatic ketones. Results refer to time-course experiments performed in plastic dishes or reactions vials with whole cells of *E. coli*.

One important goal of a bioprocess originally developed on an analytical scale is the transfer into a large-scale production by increasing substrate and enzyme concentration and reaction volume. Implementing an enzymatic Baeyer-Villiger reaction, which is strictly dependent on molecular oxygen, the increase in reaction volume is often combined with the major drawback of mass and energy transport limitations. A challenge that has to be considered crucially, is the enzyme's cofactor-dependency, which can increase economic expenses drastically when no appropriate recycling-system is available. Another bottleneck are the often very low substrate amounts required to avoid enzyme inhibition or toxicity phenomena. In order to demonstrate a possible industrial application, biotransformation of **1** was also performed in larger scale (1 mmol) in a baffled erlenmeyer flask using resting cells of *E. coli* JM109 pGro7 expressing BVMO$_{Psfl}$ (**Article IV**). It was assumed that a better oxygen supply, due to an enlarged surface to volume ratio compared to the experiments in reaction vials or plastic dishes, may influence reaction rate. Oxygen is not only a necessary co-substrate of catalysis, it is also severely important for the cell growth and metabolism, since living cells used in all experiments provide the necessary cofactor NADPH. Besides the improvement of oxygen input, the better mixing in a baffled flask also ensured an equal substrate distribution. Therefore, limitations concerning substrate diffusion in the media are not longer a problem. To ensure a sufficient substrate uptake into the cells, 0.5 eqiv. of β-cyclodextrin were added.[151] Interestingly, enantioselectivity could be increased nearly two fold from $E_{analytic}$ = 43 to $E_{preparativ}$ = 82 (46% conversion).

Another important bottleneck that has to be considered is the downstream-processing of the product and residual ketone. The isolated yield of 1-phenylethyl acetate, the Baeyer-Villiger product of **1**, was 35% (93% ee_P, determined from the corresponding alcohol after ester hydrolysis with unselective CAL-A) and can be improved. In order to overcome this obstacle and therefore "to hit two birds with one stone", namely product recovery and substrate inhibition, one can either add a second organic phase or make use of the well-established resin-based *in situ* substrate feeding and product removel technique[86, 87] (*in situ* SFPR). However, the first choice has the disadvantage of probable toxicity problems especially when working

with whole cell biocatalysts. Furthermore, it has to be ensured that both substrate and product have similar solubilities within the organic solvent. Anyway, this approach was successfully applied in stereospecific biotransformation of styrene using whole cells of *E. coli* JM101 expressing the styrene monooxygenase from *Pseudomonas* sp. VLB120.[107] This system was successfuly scaled-up (30 L fed-batch cultivation, 400 g styrene oxide[152]) and introduction of an apolar organic solvent reduced toxic effects of substrate and/or product. Later, using a biofilm of *Pseudomonas* sp. VLB120 it was also possible to utilize pure styrene in a two-liquid-phase application (ee_P > 99%).[153] The second possibility to use the SFPR-technique may be more elegant and was already successfully applied in the regiodivergent transformation of *rac*-bicyclo[3.2.0]hept-2-en-6-one using $CHMO_{Acineto}$ from *A. calcoaceticus* NCIMB 9871 as biocatalyst.[59] The application of several resins to set up an equilibrium to guarantee constant substrate and product concentrations within the flask or reactor and therefore enhance productivity and space-time yield has been examined recently for 3-phenyl-2-butanone.[154]

3.2 Cloning of novel Baeyer-Villiger monooxygenases, expression optimization in *E. coli*, characterization and biocatalytical investigation

3.2.1 Identification of novel Baeyer-Villiger monooxygenases and their putative physiological role

The discovery of the enzymatic Baeyer-Villiger oxidation in 1948[11] and the isolation of the first Baeyer-Villiger monooxygenase in 1976[56] accelerated exploration and investigation of these enzymes during recent decades. Since the oxygen inserting process is one of the most powerful reactions in organic chemistry, seeking for new enzymes with different properties to enlarge the platform of available biocatalysts is still one of the main goals of the biotechnological industry. Nature exhibits a huge diversity of these biocatalysts, with different substrate specificities waiting to be discovered.

For a long time, however, mainly cyclic ketone-converting BVMOs were known and still today they cover the majority of characterized BVMOs implemented in enzymatic-driven Baeyer-Villiger oxidations. Within this work, two additional Baeyer-Villiger monooxygenases from *Pseudomonas* sp. were identified, which preferentially oxidized linear aliphatic and aryl aliphatic ketones, respectively. The first BVMO ($BVMO_{KT2440}$) originated from *P. putida* KT2440. In a complete genome sequencing project of the strain in 2002[155] this BVMO was suggested to be a FAD-dependent monooxygenase. Investigation of the substrate scope quickly revealed that this enzyme converted short- and middle-chain linear aliphatic ketones, while cyclic ketones were only poorly oxidized and aromatic substrates were not accepted at all (**Article V**). In contrast, the second BVMO ($HAPMO_{JD1}$), identified in *P. putida* JD1 in 2000[66], revealed a different substrate specificity. Here, mainly aryl aliphatic ketones with substituents in *para*- and *meta*-position were preferred (**Article VI**) (Figure 3.6).

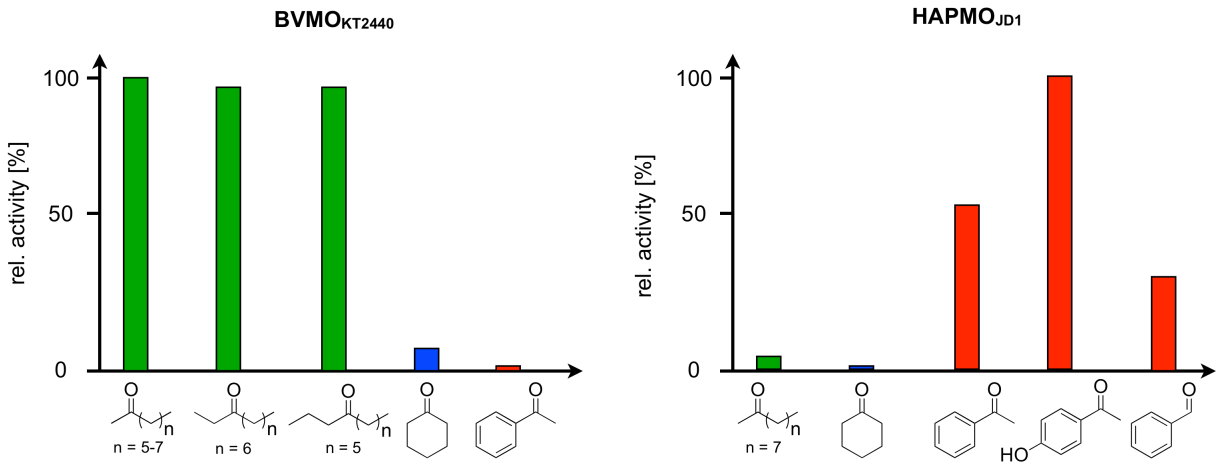

Figure 3.6 Substrate scope of BVMO from *P. putida* KT2440 (left) and *P. putida* JD1 (right).

Since the nucleotide sequence of HAPMO$_{JD1}$ was not available, amplification of this gene was rather sophisticated. Utilizing *SiteFinding*-PCR, the amplification from genomic DNA was successful. Moreover, this method allowed the amplification of other open reading frames up- and downstream of the BVMO-gene. For this reason, four other genes could be identified, encoding an esterase, a dioxygenase, a dehydrogenase and a reductase. It was assumed that all five enzymes were metabolically connected in the degradation of 4-hydroxyacetophenone (**Article VI**, **Figure 4**), the key substrate of this BVMO and an intermediate in the catabolism of 4-ethylphenol. This gene-cluster might be controlled by a LysR regulator protein that was also identified by *SiteFinding*-PCR. The co-localization of a BVMO, a hydrolase and a dehydrogenase in the genome (Figure 3.7) was also described in previous studies.[14b,156] The interaction of these enzymes in the degradation of (chlorinated) acetophenones[157], cyclic (cyclohexanone or camphor[15a, 46]) and linear hydrocarbons (2-tridecanone[13d]) and progesterone[158] was also observed for other microorganisms.[63-65]

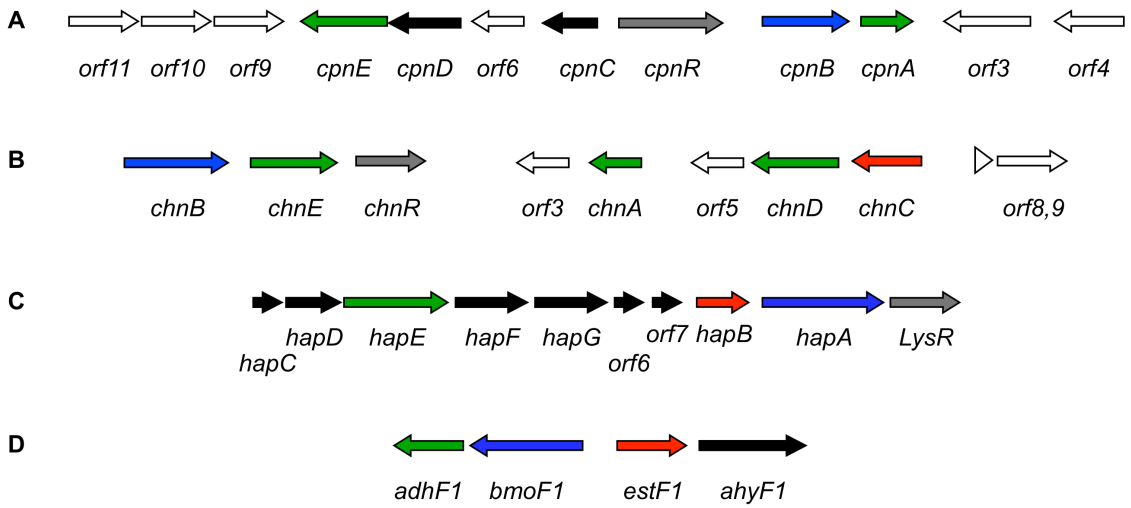

Figure 3.7 Physical map of (A) the *cpn* cluster in *Comamonas* sp. NCIMB 9872[14a], (B) the *chn* cluster in *A. calcoaceticus* NCIMB 9871[15a], (C) the *hap*-Operon in *P. putida* JD1 (Article VI) and (D) the cluster in *P. fluorescens* DSM 50106.[41] Genes encoding a BVMO are colored in blue, genes encoding a hydrolase (e.g. esterase) are highlighted in red, and genes encoding a dehydrogenase are marked in green.

In order to classify these two novel BVMOs within other characterized and recombinantly available BVMOs, a phylogentic tree on the basis of the protein sequences was generated (**Article VI**, **Figure 2**). Remarkably, $HAPMO_{JD1}$ showed a very high sequence homology (83%) towards a BVMO from *P. fluorescens* ACB ($HAPMO_{ACB}$), which is rarely observed for enzymes originating from different bacteria. Furthermore, both enzymes possess a similar substrate spectrum and belong to an operon crucially involved in the catabolism of acetophenone derivatives. One possible hypothesis for this relation could be found in evolution itself: either the operon was transferred by horizontal gene transfer or both *Pseudomonas* strains evolved from the same parental organism. Also, the suggestion for the existence of two isomers has been illustrated.[40] Normally, sequence homology on the nucleotide level is rather low among BVMOs which makes it more difficult to predict any substrate scope or preferences.

3.2.2 Optimization of protein expression: influence of temperature, co-expression of chaperones and codon bias

Both enzymes, $BVMO_{KT2440}$ and $HAPMO_{JD1}$, were functionally expressed in *E. coli*. Bacterial systems, like *E. coli*, have the advantage that they can be genetically engineered easily and produce large quantities of recombinant proteins in rapid, often inexpensive, fermentation processes. Among the many systems available for heterologous protein production (plants, mammalian cell lines, insect and yeast cells) bacteria still remain the most attractive.[159] Different expression strains, namely *E. coli* BL21 (DE3), BL21 CodonPlus®, BL21 C41 (DE3), Rosetta™ (DE3) and JM109, were implemented and expression levels were compared visually using SDS-PAGE and, if possible, Western blot analysis as well as by measuring the activity. *E. coli* BL21 CodonPlus® and Rosetta™ (DE3) have been designed to express proteins with an increased number of rare amino acid codons in *E. coli*. Most amino acids are encoded by more than one codon, and each organism carries its own bias in the usage of codons.[160] Thus, when the mRNA of heterologous target genes is overexpressed in *E. coli*, differences in codon usage can impede translation due to the demand for one or more tRNAs that may be rare or lacking.[161] Insufficient tRNA pools can lead to translational stalling, premature translation termination, translation frameshifting and amino acid misincorporation[162], possibly yielding inclusion bodies. While *E. coli* BL21 CodonPlus® can deliver four rare codons for protein translation (*argU*, *ileY*, *proL* and *leuW*), Rosetta™ (DE3) possesses a pRARE plasmid (Figure 3.8) encoding ten rare amino acids tRNAs (*argU*, *ileX*, *thrU*, *tyrU*, *glyT*, *thrT*, *argW*, *metT*, *leuW* and *proL*).[163] Therefore, the pRARE plasmid encodes tRNA genes for all “problematic” rarely used codons encoding Arg, Leu, Gly, Pro and Ile. *E. coli* BL21 C41 (DE3) is known from literature as a mutant strain that overcomes the toxicity associated with the overexpression of recombinant proteins.[164]

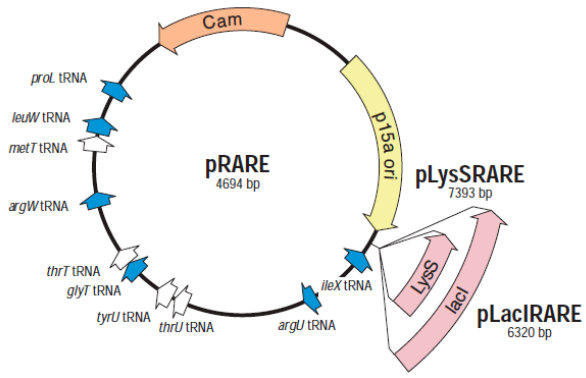

Figure 3.8 Map of pRARE plasmid family. (The basic structure of pRARE is indicated.) pLysSRARE and pLacIRARE contain the genes encoding T7 lysozyme (LysS) and lac repressor (lacI), respectively. Also indicated are chloramphenicol resistance gene (Cam), origin of replication (p15a ori) and tRNA genes. tRNA genes corresponding to rare codons in *E. coli* are indicated in blue. pRARE is derived from pRIG.[165])

It turned out that for $HAPMO_{JD1}$ the expression in *E. coli* Rosetta™ (DE3) gave best results, while for $BVMO_{KT2440}$ the best expression levels could be achieved with *E. coli* JM109. Nevertheless, the overall amount of soluble active protein still was in inclusion bodies. Optimization strategies using either different media compositions (addition of glucose and potassium phosphate in a complex-medium or increasing yeast-tryptone portions in LB-medium) or adding FMN, a prerequisite for FAD, which is a BVMO cofactor and might be crucial for native protein folding, could not overcome the problem of solubility. In order to reduce the production of inclusion bodies, the influence of different expression temperatures (37, 30 and 20°C) were investigated. At lower cultivation temperatures cell growth is decreased, resulting in lower expression levels due to a slower transcription and translation machinery. Consequently, protein stress is reduced and endogenous chaperones have more time to assist correct protein folding. Indeed, the best results were achieved at 20°C expression temperature. Figure 3.9 illustrates the activities measured during protein expression of $HAPMO_{JD1}$ in *E. coli* Rosetta™ (DE3). Clearly visible is the two-fold higher activity when comparing 20 and 37°C nine and eleven hours after induction.

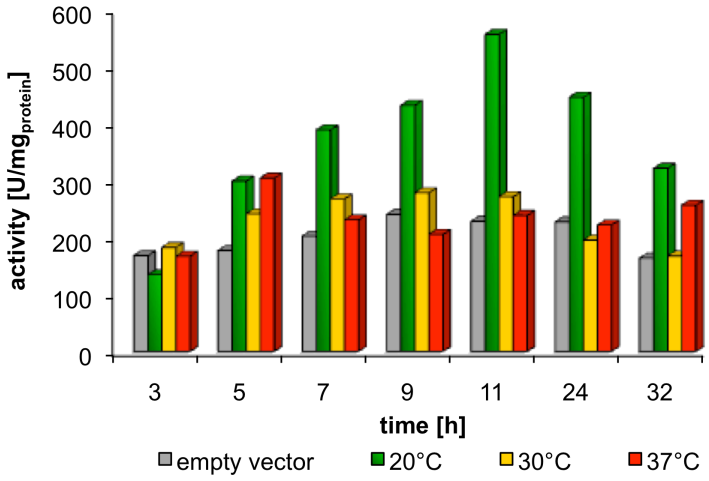

Figure 3.9 Temperature-dependent protein expression of $HAPMO_{JD1}$.

Furthermore, the influence of the plasmid itself was investigated. Both, $HAPMO_{JD1}$ and $BVMO_{KT2440}$ were cloned into pJOE4072.6[166] and pET22b(+) and both constructs were expressed in *E. coli* Rosetta™ (DE3), BL21 (DE3) or JM109 at 20°C. The best results for $BVMO_{KT2440}$ were achieved with pJOE4072.6 in *E. coli* JM109, while for $HAPMO_{JD1}$ the highest activity could be obtained with pET22b(+) in *E. coli* Rosetta™ (DE3), a low-copy plasmid sufficient for expression in *E. coli* (Figure 3.10).

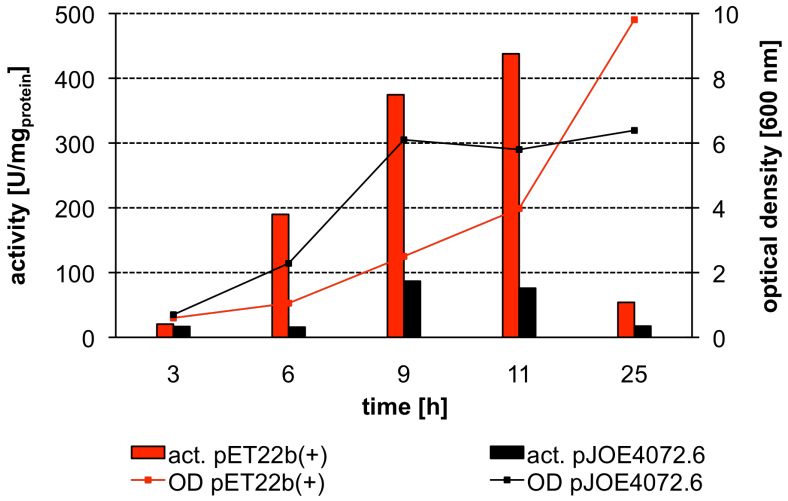

Figure 3.10 Vector-dependent protein expression of $HAPMO_{JD1}$ in *E. coli* Rosetta™ (DE3).

Besides optimization by varying the expression vector, media composition, additives like FMN and expression temperature, also co-expression of molecular chaperones was investigated. Therefore, a commercial chaperone plasmid set from TaKaRa Bio Inc. (Outsu, Japan) was implemented, which consisted of five different plasmids bearing different molecular chaperones (Table 3.1). Chaperones assist folding of proteins into their correct three-dimensional structure. Futhermore, they are able to unfold incorrectly folded proteins and solubilize protein aggregates that are toxic for the cell.[167] Chaperones can be divided into different families: some are permanently present in the cell (e.g. GroES/EL-system), while others are produced as a stress-induced response (e.g. heat-shock proteins, DnaK/DnaJ-system).[168] Application of these chaperones to increase the yield of soluble and active recombinant proteins was described for CHMO from *A. calcoaceticus* NCIMB 9871.[169] However, for both BVMOs, $HAPMO_{JD1}$ and $BVMO_{KT2440}$, the pGro7 and pG-Tf2 plasmids providing GroES/EL chaperones alone or with trigger factor led to the best results (**Articles V** and **VI**). Here, production of soluble protein in *E. coli* Rosetta™ (DE3) and JM109 could be slightly increased. That indicates that the beneficial effect of chaperones may depend on the target and, even more importantly, on the concentration and mixture of chaperones provided. Nevertheless, the majority of protein was still in inclusion bodies.

Table 3.1 Chaperone properties (chaperone plasmid set, TaKaRa Bio Inc.) and expression levels of $BVMO_{KT2440}$ (in *E. coli* JM109) and $HAPMO_{JD1}$ (in *E. coli* Rosetta™ (DE3)), at 20°C.

No.	plasmid	chaperone	mass [kDa]	inducer	expression level $BVMO_{KT2440}$	expression level $HAPMO_{JD1}$
1	pKJE7	DnaK DnaJ GrpE	70 40 22	L-arabinose	–	+/–
2	pG-KJE8	DnaK DnaJ GrpE	70 40 22	L-arabinose	+	+/–
		GroES GroEL	60 10	tetracycline		
3	pTf16	Tf*	56	L-arabinose	+/–	+/–
4	pG-Tf2	GroES GroEL Tf*	60 10 56	tetracycline	+	+
5	pGro7	GroES GroEL	60 10	L-arabinose	+	+

* Tf: trigger factor
+: expression is higher compared to that without chaperone co-expression
+/–: expression level is similar to the expression without chaperone co-expression
–: no soluble expression

Another approach to enhance the amount of soluble $HAPMO_{JD1}$ was the exchange of amino acid codons on the nucleotide level using QuikChange™ site-directed mutagenesis, in order to overcome codon bias in *E. coli*. Investigations concerning amino acid triplets that are lacking in *E. coli* determined that especially arginine and leucine codons may lead to translation stagnation due to insufficient tRNA supply (Figure 3.11). Therefore, two nucleotide exchanges, Leu350 and Arg628, were performed to adapt the codon usage for *E. coli*. Expression in *E. coli* Rosetta™ (DE3) at 20°C followed by SDS-PAGE analysis and activity measurements revealed that both single mutations had no influence on protein expression compared to the wild-type (Figure 3.12).

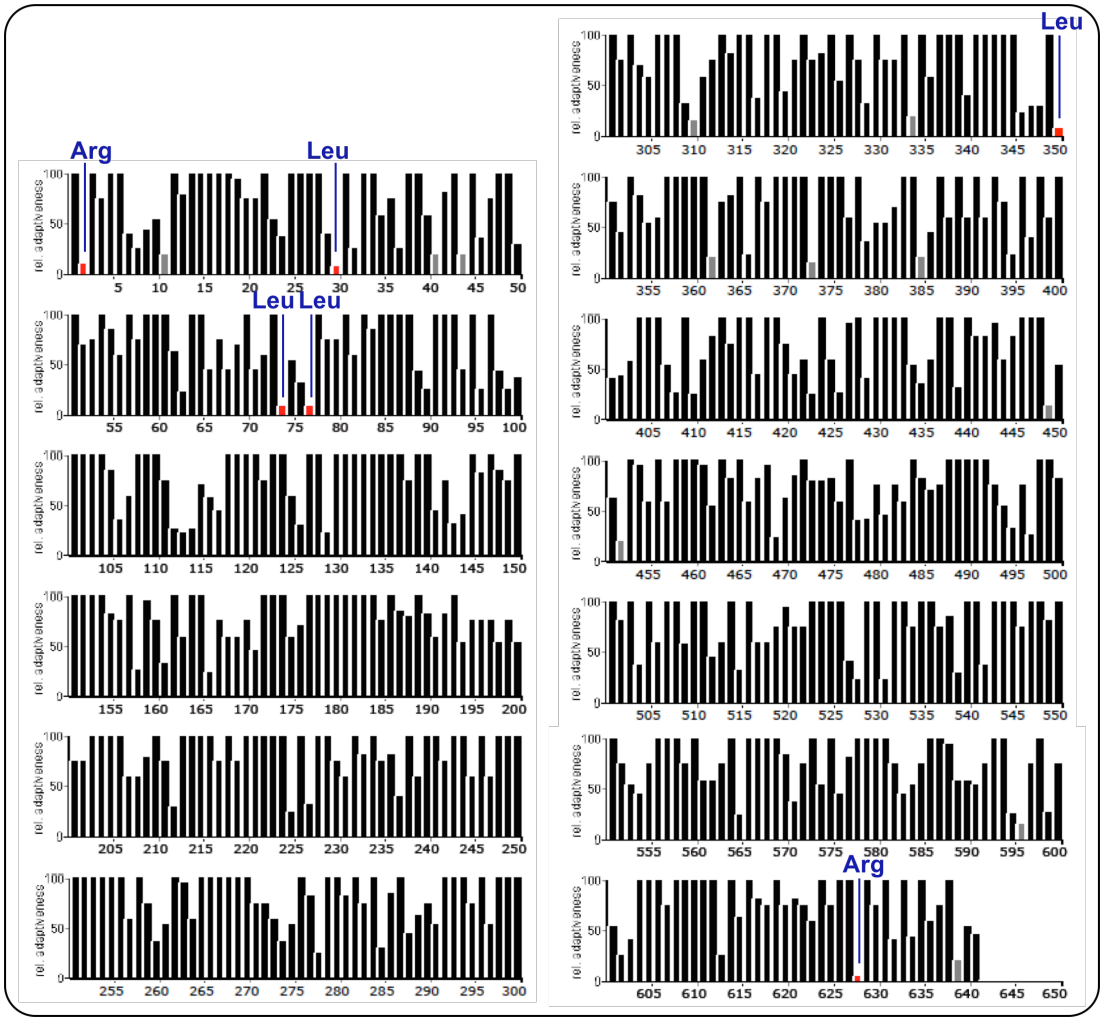

Figure 3.11 Graphical codon usage analysis of *E. coli* K12 using HAPMO$_{JD1}$ from *P. putida* JD1 as template (powered by geneart: www.gcua.de). Red columns show amino acids (Arg and Leu) whose codon usage in *E. coli* is below 10%, gray beams refer to a codon usage below 20%.

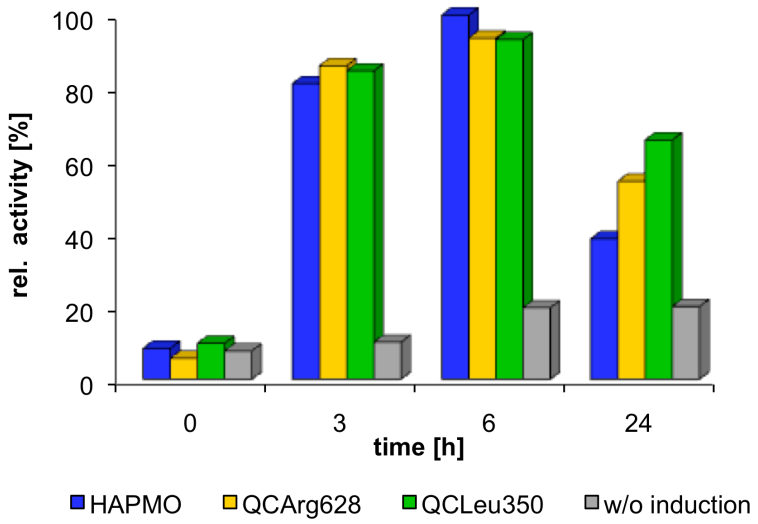

Figure 3.12 Comparison of activities of wt-HAPMO$_{JD1}$ with Leu350 and Arg628 mutants and negative control without induction at 20°C expression temperature in *E. coli* Rosetta™ (DE3).

3.2.3 Biotransformation: isolated enzyme vs. whole cells

Investigation of the substrate scope of $HAPMO_{JD1}$ and $BVMO_{KT2440}$ revealed that $HAPMO_{JD1}$ predominantly oxidized arylic compounds while for $BVMO_{KT2440}$ linear aliphatic ketones seemed to be the preferred substrate class. Both enzymes were subjected to biotransformations and kinetic resolutions using isolated biocatalysts or whole cells, either growing or resting. The advantage of isolated enzymes is that the substrate does not have to overcome cell-based barriers (for example cell wall or cell membrane) and that substrate and/or product cannot be further metabolized by the cell itself. On the other hand, using isolated enzyme neccesitates the addition of the expensive cofactor NADPH, which does not make this strategy feasible from an economic point of view. In order to reduce additional costs, whole cells can be used. Here, NADPH is provided by endogenous cell metabolism. Nevertheless, space-time yields can be hampered due to diffusion barriers of both substrate and oxygen within the medium and the cytoplasm. For $BVMO_{KT2440}$ a detailed comparison of both systems at different tempartures using linear aliphatic short- and middle-chain ketones was performed (**Article V**). In contrast to whole cell experiments, conversion of linear ketones did not exceed 15% using the cell-free extract. This could be explained using the following argument: the loss of the cellular environment can be accompanied by a decreased protein stability and activity. Therfore, the half-life of the enzyme can decline drastically. The decrease in stability and activity of BVMOs when using isolated enzyme has already been described[41] and may be correlated with protein degradation that may occur when losing cell environment. An intact cell possesses a defined redox potential and pH value, both helping to form disulfide bonds in immature proteins and stabilize (hydrophobic) interactions. Lacking this physiological environment might influence protein structure due to incorrect orientation of surface amino acids. To attempt to improve the isolated system in terms of stability and activity, the enzyme can either be immobilized on a proper matrix or reducing agents like DTT or mercaptoethanol can be added to mimic a cell-like environment. However, the disadvantage of cofactor-addition still has to be faced.

Growing cells provide NADPH due to intracellular regeneration, while for resting cells the addition of glucose for cofactor recycling is necessary, but glucose displays a cheap alternative to NADPH. Comparing both system of whole cell applications it can be observed that conversion of resting cells is much higher than that of growing cells after the same time interval (8 h) (**Article V**, **Table 1**). This advantage can be explained by the proceedure itself. While for growing cells the substrate is added at the same timepoint as the inducer for protein expression, resting cells have already expressed the desired BVMO by the time biotransformation is started. Therefore, the time until full conversion is reached can be reduced. Another disadvantage of growing cells is the high dilution due to the medium. An attractive solution, therefore, is the implementation of resting cells where volumes of buffer are decreased while conversion per volumetric content is increased. Another advantage of resting cells is the storage possibility at 4°C without significant loss of activity. One obstacle of whole cells that has to be solved however, is a possible metabolization of substrate or product due to side-reactions within the cell. For applications in large-scale “bothersome” genes should be deleted in order to increase conversion and space-time yields. One prominent example for such a deletion mutant is the “designer-yeast”. Here, the gene of an alcohol dehydrogenase was deleted to circumvent the reduction of the BVMO substrate cyclohexanone to

cyclohexanol.[147b, 170] Also, for biotransformation of cyclohexanone using $BVMO_{KT2440}$, the production of cyclohexanol was observed, although only to a low extent (7% in growing cells). Hence, it remains to be verified that a deletion mutant can increase conversion of cyclic ketones using whole cells of *E. coli* expressing $BVMO_{KT2440}$.

3.2.4 Exploration of the substrate spectrum of 4-hydroxyacetophenone monooxygenase from *P. putida* JD1

For the exploration of the substrate scope of $HAPMO_{JD1}$ 36 ketones of different structure and electronic nature were investigated. A broad range of acetophenone derivatives bearing substituents in *ortho-, meta-* and *para*-position, and also aldehydes, sulfur-containing compounds, heteroaromatic ketones, steroids, cyclic and bicyclic ketones were subjected to oxidation. Due to the "flexible" catalytic mechanism caused by the equilibrium between the reactive peroxy-intermediate and the hydroperoxide form, BVMOs are able to perform both an electrophilic and a nucleophilic attack, whereas the nucleophilic Baeyer-Villiger oxidation is always preferred when a ketone is available. Within this study, it should be clarified which aromatic substrates are preferred and whether $HAPMO_{JD1}$ is able to perform sulfoxidation or oxidation of heteroaromatic compounds *via* an electrophilic attack. Furthermore, the induction and mesomeric effects of substituents of the aromatic ring-system of different acetophenone compounds and the resulting influence on reaction rate were investigated (**Article VI**).

Comparing kinetic parameters for acetophenone derivatives with substituents in *ortho*-, *meta*- or *para*-positions revealed that *para*-substituted compounds were preferentially converted (**Article VI**, **Table 2**). This indicated that the functional position at the aromatic ring is crucial for substrate recognition and that the *para*-position might aid binding in the active site. A similar tendency was observed for $HAPMO_{ACB}$ from *P. fluorescens* ACB[30], a close homolog to $HAPMO_{JD1}$. Among *para*-substituted aryl aliphatic ketones, *p*-hydroxy- and *p*-aminoacetophenone showed the lowest K_M-values (38.1 µM and 5.6 µM, respectively) indicating a strong substrate binding. Both substituents display a negative inductive effect, while the resonance effect is positive. Halogens, like chloro- and fluoro-substituents, also have a positive resonance effect arising from the donation of the lone electron pair into the ring, but they also bear a powerful negative inductive effect that compensates the resonance. Thus, their influence on reaction rate is attenuated resulting in lower k_{cat}-values (*p*-F: 1.3 s^{-1}, *p*-Cl: 1.6 s^{-1}) compared to *p*-hydroxy- (9.8 s^{-1}) and *p*-aminoacetophenone (8.2 s^{-1}). Among all the investigated *para*-substituted compounds with a positive resonance effect, the *para*-alkyl-substituted compound 4-methylacetophenone is the only substituent with a positive induction effect. With a K_M of 241 µM it seems to be a rather moderate substrate for $HAPMO_{JD1}$. 4-Nitroacetophenone was the only substrate with a negative resonance effect. Although it revealed a low substrate binding capacitiy (K_M: 313 µM), the turnover number (k_{cat}: 2.6 s^{-1}) was above that of *p*-chloro-, *p*-fluoro and *p*-methoxyacetophenone. Within the *meta*-substituted substrates *m*-hydroxy-, *m*-amino-, *m*-methoxy- and *m*-nitroacetophenone were examined. It turned out that *m*-methoxyacetophenone is the best substrate, since the K_M was rather low (88.5 µM). Nevertheless, besides electronic effects, sterical effects that influence the reaction center may also be considered. The increased steric hindrance compared to

para-substituted substrates is reflected in the low k_{cat}-values of *m*-amino-, *m*-methoxy- and *m*-nitroacetophenone. In order to determine the influence of *para*- and *meta*-substituted acetophenone derivatives on the formation of the transition state and thus reaction rate, a Hammett-plot was investigated (Figure 3.13).

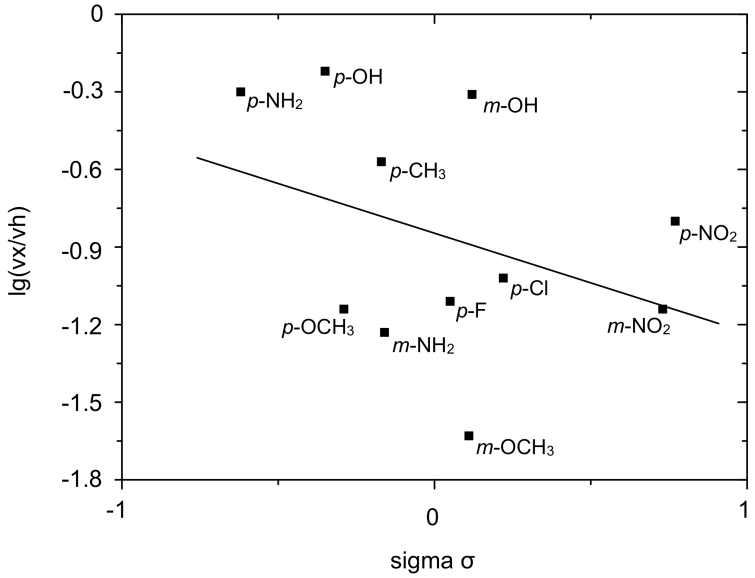

Figure 3.13 Hammett-plot of enzymatic Baeyer-Villiger oxidation with $HAPMO_{JD1}$ for *p*ara- and *m*-substituted acetophenone derivatives.

The slope of the linear regression, which correlates with the reaction constant ρ, was negative which means electrons flow away from the aromatic ring and a positive charge is built up during the rate-determining step. Thus, electron-donating substituents ($\sigma < 0$) like for example NH_2, OH and OCH_3 can accelerate oxidation, while electron-withdrawing substituents ($\sigma > 0$) like NO_2 and Cl decelerate reaction rate. This was also observed for the oxidation of cyclohexanone using CHMO from *A. calcoaceticus* NCIMB 9871.[25] According the migration tendency of the Baeyer-Villiger rearrangement the aromatic ring migrates. During the formation of the transition state the decrease of electron density could be stabilized by electron-donating groups attached to the ring. Presumably, the rate-limiting step of a Baeyer-Villiger oxidation might not be oxygen binding or the formation of the tetrahedral Criegee-intermediate but the migration of the higher-substituted carbon-center and the release of $NADP^+$, which remains tightly bound during catalysis. Anyway, since the coefficient of determination, which provides a measure of goodness-of-fit, was very low ($R^2 < 0.3$) no significant evidence of the mechanism can be made.

The structure of the side chain of aceto-, propio- and butyrophenone revealed an influence on affinity and rate of catalysis. It seemed that increasing the aliphatic hydrophobic chain adjacent to the reaction site by an additional methylene (propiophenone) or even ethylene (butyrophenone) groups decreased the catalytic turnover dramatically. Substitution of the methyl group in acetophenone into a trifluoro-group led to a lower K_M for trifluoroacetophenone, representative of better substrate binding, probably due to an increased inductive effect triggered through the high electronegativity of the fluorine (**Article VI**, **Table 2**).

Interestingly, $HAPMO_{JD1}$ is capable of oxidizing aldehydes. Moreover, K_M- and k_{cat} lay in the same range as some *para*-substituted acetophenones. Besides aldehyde oxidation, sulfoxi-

dation was also observed. As indicated before, this reaction is catalyzed by the reactive hydroperoxide-species in the enzyme's active site and a kind of promiscous reaction among BVMOs. This capability was described previously for cyclohexanone monooxygenase from *A. calcoaceticus* NCIMB 9871[49a] and phenylacetone monooxygenase from *T. fusca*[52] using alkyl aryl-sulfides as substrates. Although the substrate concentration of methyl-4-tolyl sulfide must be very high for $HAPMO_{JD1}$ to perform sulfoxidation (K_M: 21241 µM), this type of reaction is quite interesting since the corresponding chemical synthesis is often challenging, especially regarding optically pure compounds

Within the class of heteroaromatic ketones 2-, 3- and 4-acetylpyridine, acetylindol and 2-acetylpyrrole were investigated, but $HAPMO_{JD1}$ showed activity only towards the latter compound. Obviously, the pyrrole ring was preferred to the pyridine. Similar to sulfoxidation, heteroaromatic ketones are oxidized *via* an electrophilic attack of the hydroperoxide flavin. The low K_M of 2-acetylpyrrole (103 µM) indicated that affinity might be higher than for acetophenone.

Determining kinetic parameters of some cyclic and linear aliphatic ketones as well as diketones once more illustrated that $HAPMO_{JD1}$ preferrentially converts aromatic and arylaliphatic compounds. This is also consistent with the phylogenetic comparison of characterized BVMOs and their substrate specificities on the basis of their amino acid sequences. While cyclic ketones are not accepted, affinity towards linear ketones is relatively low and thus K_M-values quite high. Obviously, the aromatic system is a prerequisite for a Baeyer-Villiger reaction catalyzed by this BVMO.

4 Summary and Conclusion

The application of BVMOs in kinetic resolution is a versatile alternative for the synthesis of optically pure esters. Within this thesis BVMOs proved to be highly active against a broad range of linear and aryl aliphatic ketones yielding a variety of enantiopure products.
Among the β-hydroxy ketones several CHMOs and $BVMO_{Psfl}$ showed the best results (E > 100), whereas the application of the latter enzyme also allowed access to the abnormal esters (regioisomeric excess > 40%). Interestingly, some enzymes showed a reduced activity and selectivity with a growing chain length of the ketone, suggesting that middle-chain ketones (C_8-C_{10}) might be preferred. Moreover, the production of optically pure 1,2-diols was observed (yields 8-50%), resulting from an *in vivo* hydrolysis of the 2-hydroxy alkyl acetates.
Regarding the *N*-protected β-amino ketones, results were different. While the majority of CHMOs catalyzed linear substrates showing high enantioselectivities (for $CHMO_{Brevi1}$ and $CHMO_{Brachy}$ E > 100, c = 40-50%), $BVMO_{Psfl}$ did not convert nitrogen bearing linear ketones, although this might also be justified with the methylcarbamate protecting group. Interestingly, the number of BVMOs catalyzing oxidation of spatially more demanding linear branched β amino ketones was greatly reduced, indicating steric hindrance that was also combined with a decrease in selectivity. Similar to the observation for β-hydroxy ketones, also the 2 amino alkyl acetates hydrolyzed furnishing 2-amino alcohols (yields 9-52%). Moreover, hydrolysis of the “abnormal“ esters allowed an alternative access to valuable native and non-native β-amino acids. In a two step process, using CDMO from *R. ruber* and CAL-B, it was possible to generate *N*-protected (+)-β-leucine.
During kinetic resolutions of aryl aliphatic ketones it was observed that the highest enantioselectivities could be achieved utilizing $HAPMO_{JD1}$, $HAPMO_{ACB}$ and PAMO, enzymes typically preferring aromatic substrates. Biotransformation with 3-phenyl-2-butanone revealed an E-value > 100 for $HAPMO_{JD1}$ (*S*-selective). Nevertheless, also $BVMO_{Psfl}$ converted this substrate (E = 43), and also $CHMO_{Acineto}$ and CPMO oxidized it, although selectivity was rather low (E < 5). Interestingly, $BVMO_{KT2440}$ was the only examined enzyme showing *R*-selectivity (E = 13). Additionally, increasing the scale and performing biotransformation in a baffled flask could increase enantioselectivity of $BVMO_{Psfl}$ from E = 43 to 82.

The discovery of novel enzymes with diverse properties is still a main goal of the biotechnological industry. Within these studies, two BVMOs ($BVMO_{KT2440}$ and $HAPMO_{JD1}$) could be successfully amplified from genomic DNA using different PCR-methods. Then, expression in *E. coli* was optimized, revealing that the reduction of expression temperature, implementation of *E. coli* JM109 or Rosetta™ (DE3), possessing the pRARE plasmid to facilitate translation of rare codons in the latter case, and/or co-expression of chaperones (pGro7: GroEL/ES-familiy) could increase the amount of soluble and active protein. Both enzymes were subjected to biocatalysis and it was found that $BVMO_{KT2440}$ preferentially oxidized linear ketones, while $HAPMO_{JD1}$ dominantly converted aryl aliphatic ketones. The latter enzyme could be purified by anion exchange and affinity chromatography allowing examination of kinetic parameters. Thereby, $HAPMO_{JD1}$ displayed lowest K_M-values for acetophenone derivatives bearing their substituent in *para*-position (K_M < 320 µM). Moreover, also aldehydes and heteroaromatic compounds were oxidized and also sulfoxidation was observed. Interestingly it was found, that both BVMO genes are located in the direct neighborhood of a

dehydrogenase and a hydrolase. This led to the suggestion that these enzymes may be metabolically connected in the degradation of their natural substrate.

The number of BVMOs that can be exploited for biocatalytic purposes is still relatively low. Databases (like NCBI or 'Sargasso sea') reveal that there is a large number of genomic sequences of over 600 microbes currently available, which comprise 174 putative BVMOs waiting to be described and investigate. Thus, ambitious reasearch is demanded implying interaction of organic chemistry, molecular biology and molecular modeling as well as (bio-)chemical engineering to achieve substantial advances in the toolbox enlargement of tailor-made robust enzymes applicable in biocatalysis in the near future.

5 References

1. A. Baeyer and V. Villiger (1899). *Ber. Dtsch. Chem. Ges.,* **32**, 3625-3633.
2. R. Criegee (1948). *Justus Liebig Ann. Chem.,* **560**, 127-135.
3. W. v. E. Doering and E. Dorfmann (1953). *J. Am. Chem. Soc.,* **75**, 5595-5598.
4. M. Renz and B. Meunier (1999). *Eur. J. Org. Chem.,* 737-750.
5. M. Suzuki, H. Takada and R. Noyori (1982). *J. Org. Chem.,* **47**, 903-904.
6. S.-I. Murahashi, Y. Oda and T. Naota (1992). *Tetrahedron Lett.,* **33**, 7557-7560.
7. G. Strukul, A. Varagnolo and F. Pinna (1997). *J. Mol. Catal. A: Chemical,* **117**, 413-423.
8. C. Bolm, G. Schlinghoff and K. Weickhardt (1994). *Angew. Chem. Int. Ed.,* **33**, 1848-1849.
9. A. Gusso, C. Baccin, F. Pinna, *et al*. (1994). *Organometallics,* **13**, 3442-3451.
10. C. Bolm and G. Schlinghoff (1995). *Chem. Soc. Chem. Commun.,* 1247-1248.
11. G. E. Turfitt (1948). *Biochem. J.,* **42**, 376-383.
12. a) D. J. Peterson, S. H. Eppstein, P. D. Meister, *et al*. (1953). *J. Am. Chem. Soc.,* **75**, 5768-5769; b) J. Fried, R. W. Thoma and A. Klingsberg (1953). *J. Am. Chem. Soc.*, **75**, 5764-5765.
13. a) F. W. Forney and A. J. Markovetz (1968). *J. Bacteriol.,* **96**, 1055-1064; b) F. W. Forney and A. J. Markovetz (1969). *Biochem. Biophys. Res. Commun*., **37**, 31-38; c) A. C. Shum and A. J. Markovetz (1974). *J. Bacteriol.,***118**, 890-897; d) L. N. Britton and A. J. Markovetz (1977). *J. Biol. Chem*., **252**, 8561-8566.
14. a) H. Iwaki, Y. Hasegawa, S. Wang, *et al.* (2002). *Appl. Environ. Microbiol.,* **68**, 5671-5684; b) N. M. Kamerbeek (2004). *Thesis*, University of Groningen.
15. a) N. A. Donoghue and P. W. Trudgill (1975). *Eur. J. Biochem.,* **60**, 1-7; b) D. B. Norris and P. W. Trudgill (1971). *Biochem. J*., **121**, 363-370.
16. R. Shaw (1966). *Nature,* **209**, 1369.
17. a) M. S. Anderson, R. A. Hall and M. Griffin (1980). *J. Gen. Microbiol.,* **120**, 89-94; b) L. A. Stirling, R. J. Watkinson and I. J. Higgins (1977). *J. Gen. Microbiol*., **99**, 119-125; c) M. K. Trower, R. M. Buckland, R. Higgins, *et al.* (1985). *Appl. Environ. Microbiol*., **49**, 1282-1289; d) A. M. Magor, J. Warburton, M. K. Trower, *et al.* (1986). *Appl. Environ. Microbiol*., **52**, 665-671.
18. a) J. F. Davey and P. W. Trudgill (1977). *Eur. J. Biochem.,* **74**, 115-127; b) N. A. Donoghue and P. W. Trudgill (1973). *Biochem. Soc. Trans. 1*, 1287-1290.
19. Y. Hasegawa, K. Hamano, H. Obata, *et al.* (1982). *Agric. Biol. Chem.,* **46**, 1139-1143.
20. J. D. Schumacher and R. M. Fakoussa (1999). *Appl. Microbiol. Biotechnol.,* **52**, 85-90.
21. a) M. Gibson, M. Nur-e-alam, F. Lipata, *et al.* (2005). *J. Am. Chem. Soc.,* **127**, 17594-17595; b) K. M. Henry and C. A. Townsend (2005). *J. Am. Chem. Soc*., **127**, 3300-3309.
22. a) A. Willetts (1997). *Trends Biotechnol.,* **15**, 55-62; b) G. Grogan (1995). *Thesis*, Department of Biological Sciences, University of Exceter.
23. C. C. Ryerson, D. P. Ballou and C. T. Walsh (1982). *Biochemistry,* **21**, 2644-2655.
24. Y.-C. J. Chen, O. P. Peoples and C. T. Walsh (1988). *J. Bacteriol.,* **170**, 781-789.
25. D. Sheng, D. P. Ballou and V. Massey (2001). *Biochemistry,* **40**, 11156-11167.
26. M. D. Mihovilovic (2006). *Curr. Opin. Chem.,* **10**, 1265-1287.

27. R. H. H. van den Heuvel, N. Tahallah, N. M. Kamerbeek, *et al.* (2005). *J. Biol. Chem.,* **280**, 32115-32121.
28. E. Malito, A. Alfieri, M. W. Fraaije, *et al.* (2004). *Proc. Nat. Acad. Sci. USA,* **101**, 13157-13162.
29. G. Ottolina, G. Carrea, S. Colonna, *et al.* (1996). *Tetrahedron: Asymmetry,* **7**, 1123-1136.
30. N. M. Kamerbeek, M. W. Fraajie and D. B. Janssen (2004). *Eur. J. Biochem.,* **217**, 2107-2116.
31. M. W. Fraaije, N. M. Kamerbeek, W. J. H. van Berkel, *et al.* (2002). *FEBS Lett.,* **518**, 43-47.
32. M. Beams, P., M. A. Bosserman, N. Noinaj, *et al.* (2009). *Biochemistry,* **48**, 4476-4487.
33. I. A. Mirza, B. J. Yachin, S. Wang, *et al.* (2009). *J. Am. Chem. Soc.,* **131**, 8848-8854.
34. M. W. Fraaije, J. Wu, D. P. H. M. Heuts, *et al.* (2005). *Appl. Microbiol. Biotechnol.,* **66**, 393-400.
35. P. C. Brzostowicz, D. M. Walters, S. M. Thomas, *et al.* (2003). *Appl. Environ. Microbiol.,* **69**, 334-342.
36. P. C. Brzostowicz, K. a. L. Gibson, S. M. Thomas, *et al.* (2000). *J. Bacteriol.,* **18215**, 4241-4248.
37. J. B. van Beilen, F. Mourlane, M. A. Seeger, *et al.* (2003). *Environ. Microbiol.,* **5**, 174-182.
38. K. Kostichka, S. M. Thomas, K. J. Gibson, *et al.* (2001). *J. Bacteriol.,* **183**, 6478-6486.
39. H. Iwaki, S. Wang, S. Grosse, *et al.* (2006). *Appl. Environ. Microbiol.,* **72**, 2707-2720.
40. N. M. Kamerbeek, M. J. H. Moonen, J. G. M. van der Ven, *et al.* (2001). *Eur. J. Biochem.,* **268**, 2547-2557.
41. A. Kirschner, J. Altenbuchner and U. T. Bornscheuer (2007). *Appl. Microbiol. Biotechnol.,* **73**, 1065-1075.
42. A. Völker, A. Kirschner, U. T. Bornscheuer, *et al.* (2008). *Appl. Microbiol. Biotechnol.,* **77**, 1251-1260.
43. M. W. Fraaije, N. M. Kamerbeek, A. J. Heidekamp, *et al.* (2004). *J. Biol. Chem.,* **279**, 3354-3360.
44. S. Morii, S. Sawamoto, Y. Yamauchi, *et al.* (1999). *J. Biochem.,* **126**, 624-631.
45. E. Itagaki (1986). *J. Biochem.,* **99**, 815-824.
46. D. G. Taylor and P. W. Trudgill (1986). *J. Bacteriol.,* **165**, 489-497.
47. H. J. Ougham, D. G. Taylor and P. W. Trudgill (1983). *J. Bacteriol.,* **153**, 140-152.
48. M. J. van der Werf (2000). *Biochem. J.,* **347**, 693-701.
49. a) S. Colonna, N. Gaggero, G. Carrea, *et al.* (1998). *Chem. Commun.,* **3**, 415-416; b) D. R. Kelly, C. J. Knowles, J. G. Mahdi, *et al.* (1996). *Tetrahefron Asymm.*, **7**, 365-368; c) H. L. Holland, J.-X. Gu, Kerridge, *et al.* (1999). *Biocatal. Biotrans.*, **17**, 305-317.
50. G. Ottolina, S. Bianchi, B. Belloni, *et al.* (1999). *Tetrahedron Lett.,* **40**, 8483-8486.
51. J. Latham, J. A., B. P. Branchaud, Y.-C. J. Chen, *et al.* (1986). *J. Chem. Soc., Chem. Commun.,* 528-530.
52. G. de Gonzalo, D. E. Torres Pazmiño, G. Ottolina, *et al.* (2006). *Tetrahedron Asymm.,* **17**, 130-135.
53. S. Colonna, N. Gaggero, G. Carrea, *et al.* (2002). *Tetrahedron Lett.,* **43**, 1797-1799.

54. a) M. D. Mihovilovic, B. Müller and P. Stanetty (2002). *Eur. J. Org. Chem.,* **22**, 3711-3730; b) S. M. Roberts and P. W. H. Wan (1998). *J. Mol. Catal. B: Enzym*, **4**, 111-136.

55. M. D. Mihovilovic, B. Müller, M. M. Kayser, *et al.* (2001). *J. Mol. Catal. B: Enzym,* **11**, 349-353.

56. N. A. Donoghue, D. B. Norris and P. W. Trudgill (1976). *Eur. J. Biochem.,* **63**, 175-192.

57. S. D. Doig, L. M. O'Sullivan, S. Patel, *et al.* (2001). *Enz. Microb. Technol.,* **28**, 265-274.

58. M. M. Kayser, G. Chen and J. D. Stewart (1999). *Synlett,* **1**, 153-158.

59. V. Alphand, G. Carrea, R. Wohlgemuth, *et al.* (2003). *Trends Biotechnol.,* **21** 318-323.

60. a) V. Alphand, A. Archelas and R. Furstoss (1989). *Tetrahedron Lett.,* **30**, 3663-3664; b) R. F. Newton and S. M. Roberts (1980). *Tetrahedron*, **36**, 2163-2196.

61. M. D. Mihovilovic, F. Rudroff, B. Grötzl, *et al.* (2005). *Angew. Chem. Int. Ed.,* **44**, 3609-3613.

62. M. D. Mihovilovic, D. A. Bianchi and F. Rudroff (2006). *Chem. Commun.,* **14**, 3214-3216.

63. R. E. Cripps, P. W. Trudgill and J. G. Whateley (1978). *Eur. J. Biochem.,* **86**, 175-186.

64. R. E. Cripps (1975). *Biochem. J.,* **152**, 233-241.

65. F. K. Higson and D. D. Focht (1990). *Appl. Environ. Microbiol.,* **56**, 3678-3685.

66. A. Tanner and D. J. Hopper (2000). *J. Bacteriol.,* **182**, 6565-6569.

67. D. P. Ivanov, V. I. Sobolev, L. V. Pirutko, *et al.* (2002). *Adv. Synth. Catal.,* **344**, 986-995.

68. a) M. Held, A. Schmid, H.-P. Kohler, *et al.* (1999). *Biotechnol. Bioeng.,* **62**, 641-648; b) L. E. Hüsken, M. C. Dalm, J. Tramper, *et al.* (2001). *J. Biotechnol*., **88**, 11-19; c) W. Wouters, M. T. Tulp and P. Bevan (1988). *Eur. J. Pharmacol*., **149**, 213-223.

69. M. J. Taschner and L. Peddada (1992). *J. Chem. Soc., Chem. Commun*., 1384-1385.

70. H. E. Conrad, R. Dubus, M. J. Namtvedt, *et al.* (1965). *J. Biol. Chem.,* **240**, 495-503.

71. K. H. Jones, R. T. Smith and P. W. Trudgill (1993). *J. Gen. Microbiol.,* **139**, 797-805.

72. P. J. Chapman, G. Meermann and I. C. Gunsalus (1965). *Biochem. Biophys. Res. Commun.,* **20**, 104-108.

73. D. R. Williams, P. W. Trudgill and D. G. Taylor (1989). *J. Gen. Microbiol.,* **135**, 1957-1967.

74. C.-H. Wong and G. M. Whitesides (1981). *J. Am. Chem. Soc.,* **103**, 4890-4899.

75. a) U. Schwarz-Linek, A. Krödel, F.-A. Ludwig, *et al.* (2001). *Synthesis,* **6**, 947-951; b) S. Rissom, U. Schwarz-Linek, M. Vogel, *et al.* (1997). *Tetrahedron Asymm*., **8**, 2523-2526; c) K. Seelbach, B. Riebel, W. Hummel, *et al.* (1996). *Tetrahedron Lett*., **37**, 1377-1380.

76. R. Woodyer, W. A. van der Donk and H. Zhao (2003). *Biochemistry,* **42**, 11604-11614.

77. a) A. J. Willetts, C. J. Knowles, M. S. Levitt, *et al.* (1991). *J. Chem. Soc., Perkin Trans 1,* 1608-1610; b) F. Secundo, G. Carrea, S. Riva, *et al.* (1993). *Biotechnol. Lett*., **15**, 865-870.

78. D. E. Torres Pazmiño, R. Snajdrova, B.-J. Baas, *et al.* (2008). *Angew. Chem. Int. Ed.,* **47**, 2275-2278.

79. a) H. Christine Lo, O. Buriez, J. B. Kerr, *et al.* (1999). *Angew. Chem. Int. Ed.,* **38**, 1429-1432; b) F. Hollmann, A. Schmid and E. Steckhan (2001). *Angew. Chem. Int. Ed*., **40**, 169-171; c) J. Lutz, F. Hollmann, T. V. Ho, *et al.* (2004). *J. Organomet. Chem*., **689**, 4783-4790.

80. a) F. Hollmann, K. Hofstetter, T. Habicher, *et al.* (2005). *J. Am. Chem. Soc*., **127**, 6540-6541.81; b) V. Reipa, M. P. Mayhew and V. L. Vilker (1997). *Proc. Nat. Acad. Sci. USA,* **94**, 13554-13558; c) E. Katz and I. Willner (2004). *Angew. Chem. Int. Ed*., **43**, 6042-6108; d) Y. Xiao, F. Patolsky, E. Katz, *et al.* (2003). *Science*, **229**, 1877-1881

81. F. Hollmann, A. Taglieber, F. Schulz, *et al.* (2007). *Angew. Chem. Int. Ed.,* **46**, 2903-2906.

82. A. Liese, K. Seelbach and C. Wandrey (2000), *Industrial biotransformations: a comprehensive handbook.* Wiley-VCH Weinheim; Vol. 2.

83. F. Schulz, F. Leca, F. Hollmann, *et al.* (2005). *Beilstein J. Org. Chem.,* **1**, 1-10.

84. G. J. Lye and J. M. Woodley (1999). *Trends Biotechnol.,* **17**, 395-402.

85. I. Hilker, V. Alphand, R. Wohlgemuth, *et al.* (2004). *Org. Lett.,* **6**, 1955-1958.

86. I. Hilker, R. Wohlgemuth, V. Alphand, *et al.* (2005). *Biotechnol. Bioeng.,* **92**, 702-710.

87. I. Hilker, M. C. Gutierrez, R. Furstoss, *et al.* (2008). *Nature Protocols,* **3**, 546-554.

88. a) M. D. Mihovilovic, G. Chen, S. Wang, *et al.* (2001). *J. Org. Chem.,* **66**, 733-738; b) M. D. Mihovilovic and P. Kapitan (2004). *Tetrahedron Lett.,* **45**, 2751-2754; c) M. D. Mihovilovic, P. Kapitán and P. Kapitánová (2008). *ChemSusChem,* **1**, 143-148; d) M. D. Mihovilovic, B. Müller, A. Schulze, *et al.* (2003). *Eur. J. Org. Chem.,* DOI: 10.1002/ejoc.200300023, 2243-2249; e) M. D. Mihovilovic, F. Rudroff, B. Müller, *et al.* (2003). *Bioorg. Med. Chem. Lett.,* **13**, 1479-1482; f) M. D. Mihovilovic, R. Snajdrova and B. Grötzel (2006). *J. Mol. Catal. B: Enzym,* **39**, 135-140; g) M. D. Mihovilovic, R. Snajdrova, A. Winninger, *et al.* (2005). *Synlett,* **18**, 2751-2754; h) M. D. Mihovilovic, F. Rudroff, A. Winninger, *et al.* (2006). *Org. Lett.,* **8**, 1221-1224.

89. a) M. J. Taschner and D. J. Black (1988). *J. Am. Chem. Soc.,* **110**, 6892-6893; b) M. J. Taschner, D. J. Black and Q.-Z. Chen (1993). *Tetrahedron Asymm.,* **4**, 1387-1390.

90. a) V. Alphand, A. Archelas and R. Furstoss (1990). *Biocatalysis,* **3**, 73-83; b) V. Alphand and R. Furstoss (1992). *J. Org. Chem.*, **57**, 1306-1309; c) V. Alphand, R. Furstoss, S. Pedragosa-Moreau, *et al.* (1996). *J. Am. Soc., Perkin Trans 1*, 1867-1872; d) L. Andrau, J. Lebreton, P. Viazzo, *et al.* (1997). *Tetrahedron Lett.,* **38**, 825-826.

91. J. Rehdorf and U. T. Bornscheuer (2009). Monooxygenases, Baeyer-Villiger applications in organic synthesis. In: *Encyclopedia of industrial biotechnology: bioprocess, bioseparation and cell technology*, Ed.: M. Flickinger, Wiley-VCH; Vol. 1.

92. C. Mazzini, J. Lebreton, V. Alphand, *et al.* (1997). *Tetrahedron Lett.,* **38**, 1195-1196.

93. C. Mazzini, J. Lebreton, V. Alphand, *et al.* (1997). *J. Org. Chem.,* **62**, 5215-5218.

94. B. Adger, M. T. Bes, G. Grogan, *et al.* (1995). *J. Chem. Soc., Chem. Commun.,* 1563-1564.

95. B. Adger, M. T. Bes, G. Grogan, *et al.* (1997). *Bioorg. Med. Chem.,* **5**, 253-261.

96. N. Berezina, V. Alphand and R. Furstoss (2002). *Tetrahedron Asymm.,* **13**, 1953-1955.

97. M. C. Gutiérrez, R. Furstoss and V. Alphand (2005). *Adv. Synth. Catal.,* **347**, 1051-1059.

98. D. R. Kelly, C. J. Knowles, J. G. Mahdi, *et al.* (1995). *Chem. Soc. Chem. Commun.,* 729-730.

99. M. D. Mihovilovic, P. Kapitán, J. Rydz, *et al.* (2005). *J. Mol. Catal. B: Enzym,* **32**, 135-140.

100. D. Bonsor, S. F. Butz, J. Solomons, *et al.* (2006). *Org. Biomol. Chem.,* **4**, 1252-1260.

101. R. Snajdrova, G. Grogan and M. D. Mihovilovic (2006). *Bioorg. Med. Chem. Lett.,* **16**, 4813-4817.

102. a) J. Lebreton, V. Alphand and R. Furstoss (1996). *Tetrahedron Lett.,* **37**, 1011-1014; b) J. Lebreton, V. Alphand and R. Furstoss (1997). *Tetrahedron*, **53**, 145-160.

103. B. J. Branchaud and C. T. Walsh (1985). *J. Am. Chem. Soc.,* **107**, 2153-2161.

104. K. Kyung, D. C. Han and H. P. Fleming (1997). *Journal of Food Science,* **62**, 406-409.

105. J. Beecher, P. Richardson and A. J. Willetts (1994). *Biotechnol. Lett.,* **16**, 909-912.

106. H. L. Holland, F. M. Brown, B. G. Larsen, *et al.* (1995). *Tetrahedron Asymm.,* **6**, 1569-1574.

107. a) S. Panke, B. Witholt, A. Schmid, *et al.* (1998). *Appl. Environ. Microbiol.,* **64**, 2032-2043; b) S. Panke, M. G. Wubbolts, A. Schmid, *et al.* (2000). *Biotechnol. Bioeng*., **69**, 91-100.

108. G. Schmaus, M. Herrmann and H. Joppe (2003). PCT/EP2002/006751, WO/2003/000220.

109. a) A. L. Botes, C. A. G. M. Weijers, P. J. Botes, *et al.* (1999). *Tetrahedron,* **10**, 3327-3336; b) M. J. van der Werf, K. M. Overkamp and J. A. M. de Bont (1998). *J. Bacteriol.*, **180**, 5052-5057; c) L. Zhao, B. Han, Z. Huang, *et al.* (2004). *J. Am. Chem. Soc.*, **126**, 11156-11157.

110. S. M. Dean, W. A. Greenberg and C.-H. Wong (2007). *Adv. Synth. Catal.,* **349**, 1308-1320.

111. a) G.-J. Shen, Y.-F. Wang, C. Bradshaw, *et al.* (1990). *J. Chem. Soc., Chem. Commum.,* 677-679; b) A. Fauve and H. Veschambre (1990). *Biocatalysis*, **3**, 95-109.

112. a) F. Theil, S. Ballschuh, A. Kunath, *et al.* (1991). *Tetrahedron Asymm.,* **2**, 1031-1034; b) F. Theil, J. Weidner, S. Ballschuh, *et al.* (1993). *Tetrahedron Lett.*, **34**, 305-306; c) A. J. M. Janssen, A. J. H. Klunder and B. Zwanenburg (1991). *Tetrahedron*, **47**, 7409-7416; d) A. Kamal, M. Sandbhor, K. Ahmed, *et al.* (2003). *Tetrahedron Asymm.*, **14**, 3861-3866.

113. a) T. Hudlicky, D. Gonzales and D. T. Gibson (1999). *Adrichimica Acta,* **32**, 1999; b) D. S. Torok, S. M. resnick, J. M. Brand, *et al.* (1995). *J. Bacteriol.*, **177**, 5799-5805.

114. S. Flitsch and G. Grogan (2002). Baeyer-Villiger applications. In: *Enzyme catalysis in organic synthesis*, Eds.: K. Drauz and H. Waldmann, Wiley-VCH, Weinheim; Vol. 3, 1202-1245.

115. K. Faber and R. V. A. Orru (2002). Hydrolysis of epoxides. In: *Enzyme catalysis in organic synthesis*, Eds.: K. Drauz and H. Waldmann, Wiley-VCH, Weinheim; Vol. 2, 579-605.

116. Z. Wang, Y.-T. Cui, Z.-B. Xu, *et al.* (2007). *J. Org. Chem.,* **73**, 2270-2274.

117. J. S. Yadav, B. V. S. Reddy, K. Harikishan, *et al.* (2005). *Synthesis,* **17**, 2897-2900.

118. V. Mirkhani, S. Tangestaninejad, B. Yadollahi, *et al.* (2003). *Tetrahedron,* **59**, 8213-8218.

119. G. Guillena, M. del Carmen Hita and C. Nájera (2006). *Tetrahedron: Asymm.,* **17**, 1027-1031.

120. N. F. Pelz and J. P. Morken (2006). *Org. Lett.,* **8**, 4557-4559.

121. R. A. Bhunnoo, Y. Hu, D. I. Lainé, *et al.* (2002). *Angew. Chem. Int. Ed.,* **41**, 3479-3480.

122. A. Rothaul and J. Brew (2007). WO/2007/060458, PCT/GB2006/004410.

123. a) G. Ratle, X. Monseur, B. C. Das, *et al.* (1966). *Bull. Soc. Chim. Fr.,* **9**, 2945-2947; b) Q. Khuong-Huu, G. Ratle, X. Monseur, *et al.* (1972). *Bull. Soc. Chim. Belges*, **81**, 425-441.

124. a) Shivani, B. Pujala and A. K. Chakraborti (2007). *J. Org. Chem.,* **72**, 3713-3722; b) A. Heydari, M. Mehred, A. Maleki, *et al.* (2004). *Synthesis*, **10**, 1557-1558.

125. D. Menche, F. Arikan, J. Li, *et al.* (2007). *Org. Lett.,* **9**, 267-270.

126. G. Liu and S. S. Stahl (2006). *J. Am. Chem. Soc.,* **128**, 7179-7181.

127. L. Dahlenburg, H. Treffert, F. Christian, *et al.* (2007). *Eur. J. Inorg. Chem.,* **12***,* 1738-1751.

128. J. V. Potetinova, T. L. Voyushina and V. M. Stepanov (1997). *Bioorg. Med. Chem. Lett.,* **7**, 705-710.

129. G. Sekar, R. M. Kamble and V. K. Singh (1999). *Tetrahedron Asymm.,* **10**, 3663-3666.

130. A. Chaubey, R. Parshad, P. Gupta, *et al.* (2009). *Bioorg. Med. Chem.,* **17**, 29-34.

131. E. Juaristi and V. A. Soloshonok (2005). *Enantioselective synthesis of β-amino acids*, Wiley-VCH, New York; Vol. 2.

132. a) E. Juaristi and H. López-Riuz (1999). *Curr. Med. Chem.,* **6**, 983-1004; b) S. Abele and D. Seebach (2000). *Eur. J. Org. Chem.*, **1**, 1-15; c) F. Fülöp (2001). *Chem. Rev.*, **101**, 2181-2204; d) M. Liu and M. P. Sibi (2002). *Tetrahedron*, **58**, 7991-8035; e) G. Lelais and D. Seebach (2004). *Bioploymers*, **76**, 206-243.

133. H. Gröger, H. Trauthwein, S. Buchholz, *et al.* (2004). *Org. Biomol. Chem.,* **2**, 1977-1978.

134. a) V. A. Soloshonok, N. A. Fokina, A. V. Rybakova, *et al.* (1995). *Tetrahedron Asymm.,* **6**, 1601-1610; b) D. Li, S. Cheng, D. Wie, *et al.* (2007). *Biotechnol. Lett*., **29**, 1825-1830.

135. T. Heck, D. Seebach, S. Osswald, *et al.* (2009). *ChemBioChem,* **10**, 1558-1561.

136. a) S. Gedey, A. Liljeblad, L. Lázár, *et al.* (2001). *Tetrahedron Asymm.,* **12**, 105-110; b) S. Gedey, A. Liljeblad, L. Lázár, *et al.* (2002). *Can. J. Chem*., **80**, 565-570.

137. A. Liljeblad and L. T. Kanerva (2006). *Tetrahedron,* **62**, 5831-5854.

138. a) P. A. Frey and O. T. Magnusson (2003). *Chem. Rev.,* **103**, 2129-2148; b) B. Wu, W. Szymanski, P. Wietzes, *et al.* (2009). *ChemBioChem*, **10**, 338-344.

139. A. Banerjee, M. Chase, R. A. Clayton, *et al.* (2006). EP20040743849/20040630, WO2005005633.

140. H. G. O. Becker, W. Berger and G. Domschke (2004). *Organikum*; Wiley-VCH, Weinheim; Vol. 22.

141. a) H. H. Jaffé (1953). *Chem. Rev.,* **53**, 191-261; b) D. H. McDaniel and H. C. Brown (1958). *J. Org. Chem*., **23**, 420-427.

142. J. Claydon, N. Greeves, S. Warren, *et al.* (2001). *Organic Chemistry,* Oxford University Press; Vol 1.

143. G. Tan, Y. Gao, M. Shi, *et al.* (2005). *Nucl. Acids Res.,* **33**, doi:10.1093/nar/gni124.

144. H. Ochman, A. S. Gerber and D. L. Hartl (1988). *Genetics,* **120**, 621-623.

145. F. Lottspeich and H. Zorbas (1998). *Bioanalytik*, Spektrum Akademischer Verlag Heidelberg, Berlin; Vol. 1.

146. a) J. D. Stewart, K. W. Reed, J. Zhu, *et al.* (1996). *J. Org. Chem.,* **61**, 7652-7653; b) J. D. Stewart, K. W. Reed, C. A. Martinez, *et al.* (1998). *J. Am. Chem. Soc.*, **120**, 3541-3548; c) M. M. Kayser, G. Chen and J. D. Stewart (1998). *J. Org. Chem.*, **63**, 7103-7106; d) M. T. Bes, R. Villa, S. M. Roberts, *et al.* (1996). *J. Mol. Catal. B: Enzyme*, **1**, 127-134.

147. A. Kirschner and U. T. Bornscheuer (2006). *Angew. Chem. Int. Ed.,* **45**, 7004-7006.

148. T. Kourouli, P. Kefalas, N. Ragoussis, *et al.* (2002). *J. Org. Chem.,* **67**, 4615-4618.

149. L.-W. Xu and C.-G. Xia (2004). *Tetrahedron Lett.,* **45**, 4507-4510.

150. C. Rodríguez, G. de Gonzalo, M. W. Fraaije, *et al.* (2007). *Tetrahedron Asymm.,* **18**, 1338-1344.

151. a) A. R. Hedges (1998). *Chem. Rev.,* **98**, 2035-2044; b) W. Saenger (1980). *Angew. Chem. Int. Ed.*, **19**, 344-362.

152. S. Panke, M. Held, M. G. Wubbolts, *et al.* (2002). *Biotechnol. Bioeng.,* **80**, 33-41.

153. R. Gross, B. Hauer, K. Otto, *et al.* (2007). *Biotechnol. Bioeng.,* **98**, 1123-1134.

154. K. Geitner, J. Rehdorf, R. Snajdrova, *et al.* (2009). *Proc. Biochem.,* submitted.

155. K. E. Nelson, C. Weinel, I. T. Paulsen, *et al.* (2002). *Environ. Microbiol.,* **4**, 799-808.

156. A. Kirschner, J. Altenbuchner and U. T. Bornscheuer (2007). *Appl. Microbiol. Biotechnol.,* **75**, 1095-1101.

157. a) M. J. H. Moonen, N. M. Kamerbeek, A. H. Westphal, *et al.* (2008). *J. Bacteriol.,* **190**, 5190-5198; b) J. M. Darby, D. G. Taylor and D. J. Hopper (1987). *J. Gen. Microbiol.*, **133**, 2137-2146.

158. M. A. Rahim and C. J. Sik (1966). *J. Biol. Chem.,* **241**, 3615-3623.

159. A. Mogk, M. P. Mayer and E. Deuerling (2002). *ChemBioChem,* **3**, 807-814.

160. H. Dong, L. Nilsson and C. G. Kurland (1996). *J. Mol. Biol.,* **260**, 649-663.

161. a) J. F. Kane (1995). *Curr. Opin. Biotechnol.,* **6**, 494-500; b) C. G. Kurland and J. Gallant (1996). *Curr. Opin. Biotechnol.*, **7**, 489-493; c) E. Goldman, A. H. Rosenberg, G. Zubay, *et al.* (1995). *J. Mol. Biol.*, **245**, 467-473.

162. Y. Nakamura, T. Gojobori and T. Ikemura (2000). *Nucl. Acids Res.,* **28**, 292.

163. Newsletter of Novagene Inc. (2001). Advanced products and protocols for molecular biology research; No. **12**, 1-3.

164. a) B. Miroux and J. E. Walker (1996). *J. Mol. Biol.,* **260**, 289-296; b) L. Dumon-Seignovert, G. Cariot and L. Vuillard (2004). *Protein Expression Purif.*, **37**, 203-206.

165. A. M. Baca and W. G. J. Hol (2000). *Int. J. Parasitology,* **30**, 113-118.

166. T. Stumpp, B. Wilms and J. Altenbuchner (2000). *Biospektrum,* **1**, 33-36.

167. N. K. Nagradova (2004). *Biochemistry (Moscow),* **69**, 830-843.

168. S. Walter and J. Buchner (2002). *Angew. Chem. Int. Ed.,* **41**, 1098-1113.

169. D. H. Lee, M. D. Kim, W. H. Lee, *et al.* (2004). *Appl. Microbiol. Biotechnol.,* **63**, 549-552.

170. J. D. Stewart, K. W. Reed and M. M. Kayser (1996). *J. Chem. Soc. Perkin Trans. 1,* 755-757.

Zusammenfassung

6 Zusammenfassung

6.1 Einleitung und Ziele dieser Doktorarbeit

Biotechnologie ist das Bemühen, zwei außerordentlich erfolgreiche Entwicklungen, die Evolution des Lebens und die vom Menschen aufgebaute Technik, zu verbinden und nutzbar zu machen. Nur wenige Beschäftigungsfelder des Menschen sind älter als die Biotechnologie und dennoch wird sie allgemein als die Schlüsseltechnologie des 20sten Jahrhunderts angesehen. Die Wurzeln biotechnologischer Verfahren reichen bis in die Frühzeit der Menschengeschichte. Bereits vor Jahrtausenden nutzten zahlreiche Kulturen biotechnologische Prozesse wie z. B. die Milchsäuregärung oder die Essigsäuregärung zur Herstellung von Speisen (Käse, Milchprodukte und Brot) und Getränken (Bier und Wein). Moderne Biotechnologie ist jedoch mehr als die Produktion von Bier und Brot. Mit der Entdeckung der ersten Antibiotika durch Alexander Fleming (1928) und dem Einsatz von Pilzen zur Herstellung von Zitronensäure (1923), ist eine entscheidene Phase der Biotechnologie eingeleitet worden. Sie gipfelte schließlich in der Geburtsstunde der Gentechnologie mit der Entdeckung α-helikaler DNA durch Watson und Crick im Jahre 1953.
Neben der heute etablierten grünen (Landwirtschaft) und roten Biotechnologie (Medizin, Pharmazeutik) gehört die weiße Biotechnologie, oder auch industrielle Biotechnologie, zu einer der bedeutendsten Technolgien der Naturwissenschaften, was nicht zuletzt auf die Entdeckung der Mikroorganismen und deren Enzyme zurückzuführen ist. Der Einsatz von nachwachsenden Rohstoffen kombiniert mit enzymatischen Biotransformationen zur Herstellung wichtiger chemischer Intermediate und optisch aktiver Pharmazeutika macht die weiße Biotechnologie zu einer attraktiven und umweltschonenden Alternative zur chemischen Synthese.
Somit gewannen Enzyme in den letzten Jahrzehnten im Bereich Forschung und Entwicklung immer mehr an Bedeutung. Die Fähigkeit, zwischen zwei optisch aktiven Verbindungen unterscheiden zu können, macht sie zu einem ausgesprochen starken Werkzeug vieler industrieller Syntheseschritte. Auf Grund ihrer ökologischen und auch ökonomischen Vorteile, erfuhren Enzyme eine regelrechte Renaissance in der Herstellung von medizinischen Produkten und Feinchemikalien in der Pharmazeutischen und der Chemischen Industrie.
Enzyme sind natürliche Biokatalysatoren, die in allen Lebensformen vorkommen. Dort steuern sie sämtliche Stoffwechselvorgänge und katalysieren biochemische Reaktionen. Indem sie die Aktivierungsenergie senken, sind sie in der Lage, die Reaktionsgeschwindigkeit zu erhöhen. Außerdem arbeiten Enzyme meist unter milden physiologischen Reaktionsbedingungen (pH, Temperatur) und oftmals kann auf den Einsatz organischer (toxischer) Lösungsmittel verzichtet werden. Enzyme können aus Pflanzen und Tieren isoliert werden; der überwiegende Teil der industriell genutzten Enzyme ist jedoch bakteriellen Ursprungs. Heute sind sie ein wesentlicher Bestandteil vieler (bio)technologischer Prozesse, bei denen man sich die Vorteile gegenüber chemischen Reaktionen zu Nutze macht. Diese Überlegenheit ist auch auf die hohe Chemo-, Regio- und Enantioselektivität zurückzuführen, wodurch Enzyme ein hohes Potenzial für den Einsatz in der Industrie aufweisen. Dabei spielen jedoch nicht nur ökonomische Aspekte eine Rolle: durch die oftmals Ressourcen-schonende Anwendung von Enzymen einhergehend mit der Möglichkeit, chemische Syntheseverfahren durch enzymatische ersetzten zu können, kann ein wesentlicher und nachhaltiger Beitrag

zum Umwelt- und Naturschutz geleistet werden. Daher bezeichnet man den Einsatz von Enzymen in organischen Synthesen auch als „Green Chemistry“ (umweltfreundliche Chemie).
Die Mehrheit der industriell genutzten Enzyme sind Hydrolasen (E.C.3; z.B. Lipasen, Esterasen und Proteasen), die durch die Bildung und Spaltung von C-O und C-N-Bindungen eine sehr wichtige Anwendung in der Biokatalyse zur Herstellung optisch reiner Ester und Alkohole darstellen. Innerhalb der Klasse der Oxidoreduktasen (E.C.1) beschränken sich die Anwendungen bisher auf Redoxreaktionen, die durch Ketoreduktasen und Alkoholdehydrogenasen katalysiert werden. Einen beträchtlichen Fortschritt hat der Einsatz von solchen Enzymen gemacht, die Redoxreaktionen katylsieren. Zu dieser wichtigen Gruppe von Biokatalysatoren gehören die Baeyer-Villiger Monooxygenasen (E.C.1.14.13.x), die in der Lage sind, Sauerstoff zwischen eine C-C-Bindung einer nicht-aktivierten Kohlenstoffverbindung einzuführen.

Die erste Baeyer-Villiger Monooxygenase (BVMO) wurde im Jahre 1976 isoliert, kloniert und charakterisiert. Durch den rasanten Fortschritt molekularbiologischer und gentechnischer Methoden sind bis heute zwanzig weitere bakterielle BVMOs kloniert und rekombinant erhältlich. Darunter befindet sich eine Steroid-modifizierende Monooxygenase, sowie BVMOs, die bevorzugt zyklische, arylaliphatische oder lineare Ketone zu Estern bzw. Lactonen umsetzen. Untersuchungen hinsichtlich der jeweiligen Substratprofile haben gezeigt, dass die Mehrzahl dieser BVMOs bevorzugt zyklische Ketone der Kettenlängen C_5 bis C_{16} umsetzen (Abbildung 1).

Abbildung 1. Prozentuale Verteilung der Substratpräferenzen aller bisherigen Baeyer-Villiger Monooxygenasen, deren Nukleotidsequenz bekannt ist.

Um das Substratspektrum und damit die Einsatzmöglichkeiten von BVMOs in biotechnologischen Prozessen zu erweitern, kann z. B. mit traditionellen Methoden nach neuen BVMOs gesucht werden (Screening von Bodenkulturen aus der Natur). Hier können entweder die Enzyme besonderer Habitate erschlossen werden oder Stammsammlungen hinsichtlich Monooxygenase-Aktivitäten durchmustert werden. Da jedoch nur etwa 1% aller Mikroorganismen unter normalen Laborbedingungen kultivierbar ist, ermöglicht die effiziente Metagenom-Analyse auch die Identifizierung und den Zugang zu Enzymen aus nicht-kultivierbaren Organismen. Eine weitere elegante Methode, Enzyme mit modifizierten Eigenschaften zu finden, ist die Veränderung bereits bekannter Enzyme. Hierfür stehen zwei verschiedene Strategien zur Verfügung: 1) Ist die detaillierte Struktur und der Mechanismus des Enzyms bekannt, so können mittels rationalem Proteindesign Vorhersagen über einhergehende Substratspezifitäten und Selektivitäten durch Änderungen in der Proteinsequenz getroffen wer-

den. 2) Fehlen diese Informationen und ist lediglich die Nukleotidsequenz des Enzyms bekannt, bedient man sich den Mitteln der klassischen gerichteten Evolution.

Die Synthese optisch reiner Verbindungen ist besonders für die Pharma-, die Kosmetik- und die Lebensmittelindustrie von Interesse. Mit herkömmlichen chemischen Methoden sind enantiomerenreine Stoffe oft gar nicht oder nur bedingt synthetisierbar. Verbunden mit meist effizienteren Ausbeuten, geringeren Risiken durch Verzicht auf toxische und umweltschädliche Komponenten und mit einem verringerten ökonomischen Aufwand, stellen enzymatische Reaktion eine attraktive Alternative dar. In den letzten Jahren sind für eine Vielzahl zyklischer und arylaliphatischer Ketone eine ganze Reihe enzymatischer Biotransformationen mittels BVMOs zur Darstellung optisch aktiver Verbindungen untersucht worden. Im Mittelpunkt standen dabei asymmetrische Synthesen prochiraler Ketone, kinetische Racematspaltungen und enantiodivergente Transformationen. Die erste BVMO, die bevorzugt lineare mittelkettige Ketone umsetzte, war die 2-Tridecanon Monooxygenase aus *P. cepacia*. In den vergangenden Jahren wurden auch in der Arbeitsgruppe von Prof. Bornscheuer BVMOs gefunden, die lineare aliphatische Ketone oxidieren, während zyklische Ketone sehr schlecht und aromatische gar nicht umgesetzt wurden. Eine dieser BVMOs stammte aus *P. fluorescens* DSM 50106 ($BVMO_{Psfl}$), die andere aus *P. putida* KT2440 ($BVMO_{KT2440}$). Dabei zeigte sich, dass die Aktivität beider Enzyme vor allem von der Kettenlänge des Substrates abhängig war (Abbildung 2).

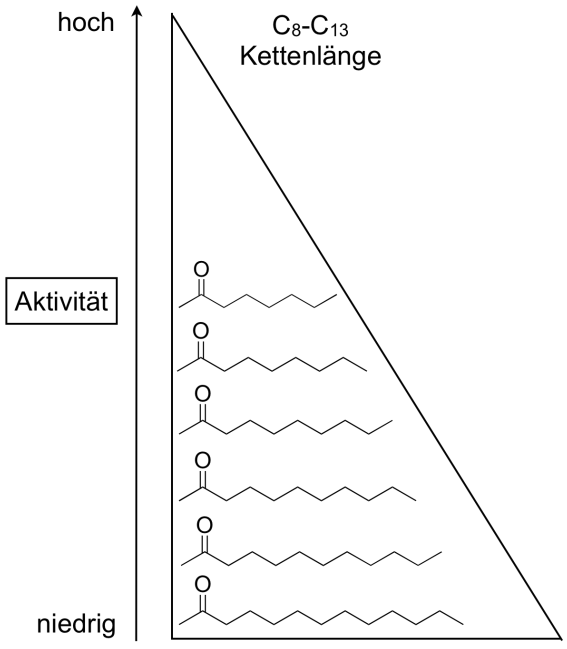

Abbildung 2. Graphischer Zusammenhang der Aktivitäten der BVMOs aus *P. fluorescens* DSM 50106 und *P. putida* KT2440 gegenüber linearen aliphatischen 2-Ketonen der Kettenlängen C_8-C_{13}.

Diese Ergebnisse lieferten die Grundlage für weitere Untersuchungen mit linearen aliphatischen Ketonen als potenzielle Substrate für BVMOs und die Voraussetzung für diese Doktorarbeit. Ziel war es nun, mit verschiedenen linearen Ketonen kinetische Racematspaltungen durchzuführen, die in β-Position zur Carbonylgruppe einen Substituenten haben und damit Chiralität aufweisen. Im Mittelpunkt standen dabei β-Hydroxyketone und β-Aminoketone sowie halogen-substituierte lineare Ketone und arylaliphatische Ketone (Abbildung 3). Im Gegensatz zu den Hydroxy- und den Aminoketonen zeigten die Biotransformationen mit halogen-substituierten Ketonen sowohl im Ganzzell-System als auch mit isoliertem Enzym keinen Umsatz. Daher wird auf diese Verbindungsklasse hier nicht weiter eingegangen.

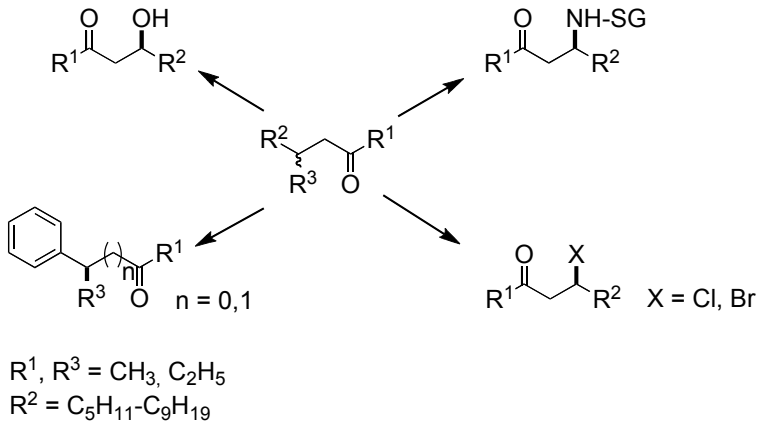

Abbildung 3. Darstellung der racemischen Substrate für die kinetische Racematspaltung mit BVMOs (SG = Schutzgruppe).

Die maximale theoretische Ausbeute einer kinetischen Racematspaltung ist 50%. Im Falle einer hochselektiven BVMO würde diese Reaktion den Zugang zu zwei optischen aktiven Verbindungen ermöglichen: dem Enantiomer des Baeyer-Villiger Esters und dem nicht umgesetzten Enantiomer des Ketons. Damit sollten lineare β-substituierte Ketone als neue Substratklasse für BVMOs etabliert werden. Warum diese Verbindungen von besonderen Interesse sind, soll am Beispiel der 4-Hydroxy-2-ketone erläutert werden: in Abhängigkeit von der Regioselektivität des Enzyms sind bei einer kinetischen Racemtspaltung theoretisch zwei verschiedene Ester zu erwarten, je nachdem auf welcher Seite der Carbonlygruppe das Sauerstoffatom eingebaut wird bzw. je nach Wanderungstendenz der beiden Reste am Carbonylkohlenstoff. Zum einen entsteht der sog. normale Baeyer-Villiger Ester, in diesem Fall das Acetat bzw. das Propylat, zum anderen der sog. abnormale Ester, der hier ein Methyl- bzw. Ethylester ist. Alle Produkte können nach enzymatischer, chemischer oder spontaner Hydrolyse entweder in ein 1,2-Diol oder eine β-Hydroxycarbonsäure umgewandelt werden, wobei beide enantiomerenrein vorliegen (Abbildung 4).

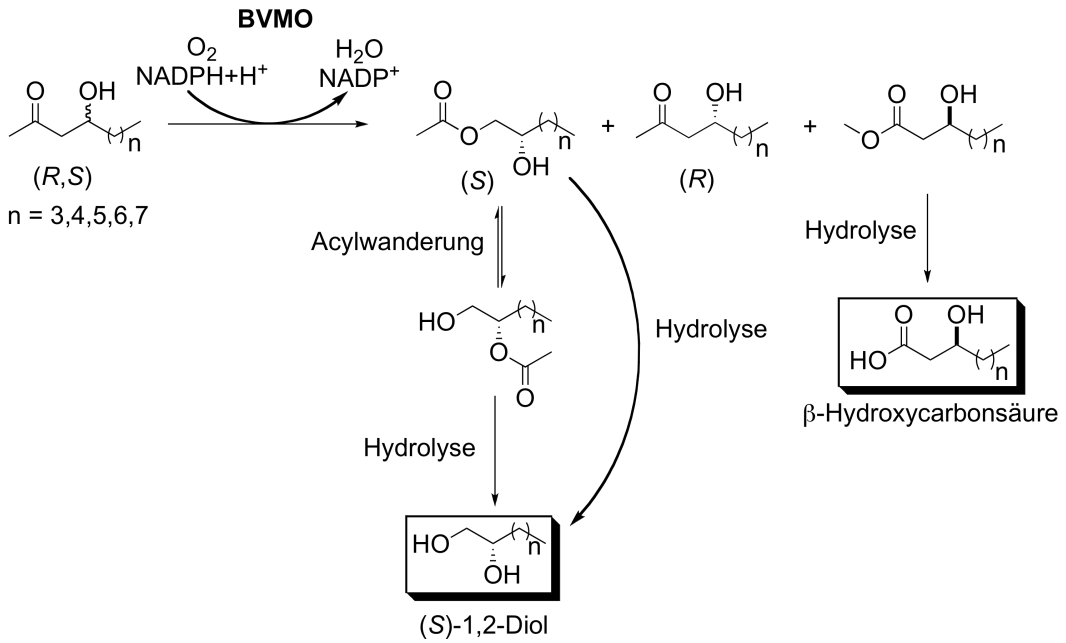

Abbildung 4. Enzymatische Baeyer-Villiger Oxidation von 4-Hydroxy-2-ketonen mit anschließender Hydrolyse der Baeyer-Villiger Ester.

Neben den Biotransformationen linearer aliphatischer Ketone sollte mit Hilfe molekularbiologischer Methoden das Gen einer weiteren BVMO aus *P. putida* JD1 amplifiziert und kloniert werden. Nach Optimierung der Proteinexpression in *E. coli* sollte diese BVMO aufgereinigt und hinsichtlich ihres Substratspektrums charakterisiert werden.

6.2 Synthesen der Substrate für die Biokatalysen

Da die zu untersuchenden Substrate nicht kommerziell erhältlich sind, mussten alle Verbindungen mittels chemischer Synthese hergestellt werden. Die Synthese der β-Hydroxyketone erfolgte mittels einer regioselektiven Aldol-Addition ausgehend von Ethylacetoacetat bzw. Ethyl-3-oxopentanoat und dem jeweiligen Aldehyd. Die entstandenen β-Hydroxyketone dienten dann als Ausgangssubstanzen für die Darstellung der halogen-substituierten Ketone (Cl und Br) in einer nukleophilen Substitution (S_N1) mit Thionylchlorid bzw. Tetrabrommethan. Alle β-Aminoketone wurden durch eine Michael-Addition an einem α,β-ungesättigtem Keton mit Methylcarbamat als Stickstoffdonor und TMSCl als Lewissäure Katalysator durchgeführt. Die Synthese der Alkenone, die kommerziell nicht erhältlich sind, erfolgte mittels Aldol-Addition analog zur Synthese der β-Hydroxyketone, wobei die Hydroxygruppe durch Erhitzen bei pH 1 eliminiert wurde. Die arylaliphatischen Ketone wurden zum einen ebenfalls mittels Aldol-Addition, zum anderen durch die Umsetzung von Phenylcarbonsäuren mit Methyllithium hergestellt. Ein biarylaliphatisches optisch aktives Substrat wurde durch Acylierung von *trans*-Stilben hergestellt. Alle Produkte wurde mittels Säulenchromatographie (Kieselgel) aufgereinigt und die Struktur mit $^{1}H/^{13}C$-NMR und GC/GCMS verifiziert. Nach Etablierung der Enantiomerenanalytik mittels chiraler GC wurde anschließend mit den Biotransformationen im Ganzzell-System sowie mit isoliertem Enzym begonnen (Abbildungen 5, 6 und 7).

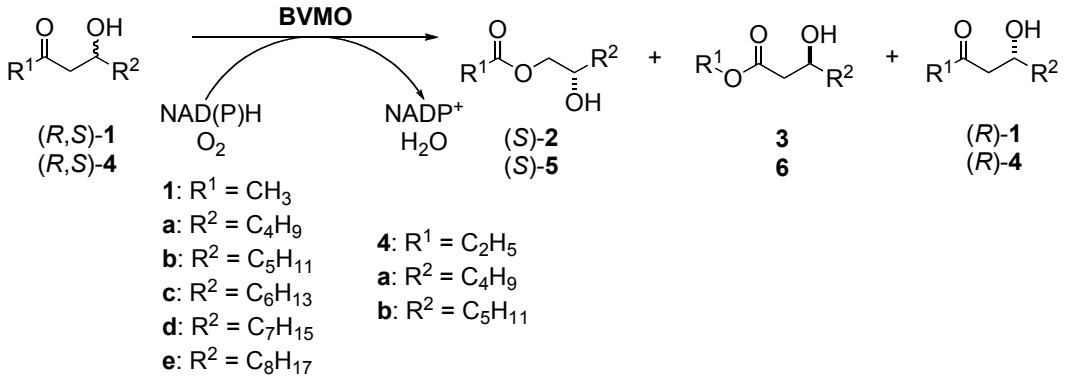

Abbildung 5. Kinetische Racematspaltung linearer 4-Hydroxy-2-ketone sowie 5-Hydroxy-3-ketone mittels BVMOs verschiedenen bakteriellen Ursprungs.

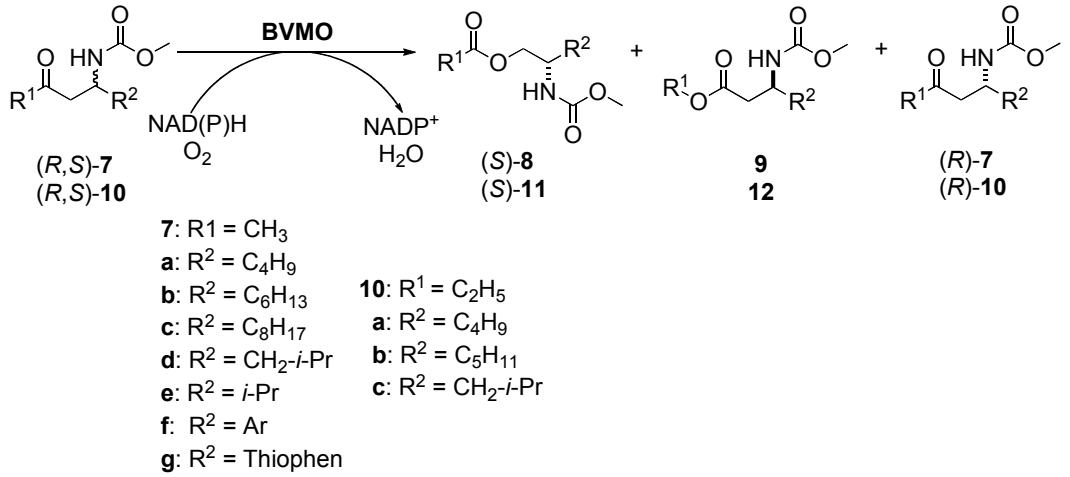

Abbildung 6. Enzymatische Baeyer-Villiger Oxidation linearer und arylaliphatischer *N*-geschützter β-Aminoketone.

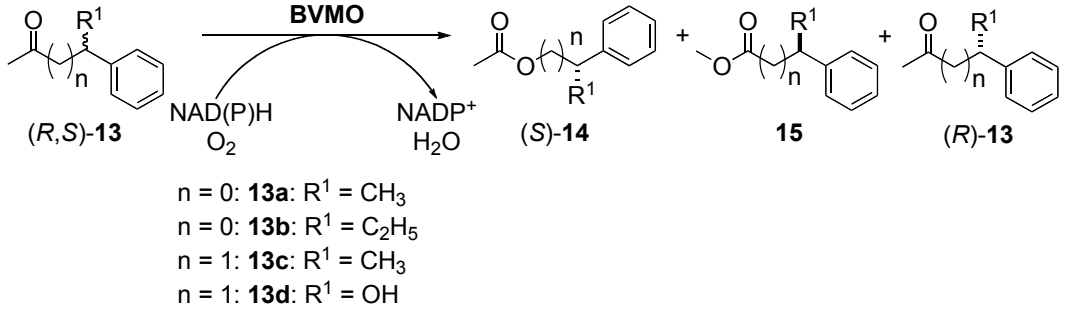

Abbildung 7. Enzymatische Baeyer-Villiger Oxidation arylaliphatischer Ketone.

6.3 Biotransformationen von β-Hydroxyketonen mit Baeyer-Villiger Monooxygenasen im Ganzzell-System und Untersuchungen der enzymatischen Regioselektivität

Alle Umsetzungen wurden mit wachsenden *E. coli* Zellen durchgeführt, welche die gewünschte BVMO exprimierten. Das hat den Vorteil, dass der benötigte Cofaktor NAD(P)H bereits endogen durch den Zellstoffwechsel zur Verfügung gestellt wird und somit nicht von außen hinzugefügt werden muss. Dadurch kann auf ein (aufwendiges) Regenerierungssystem verzichtet werden. Außerdem sind die meisten BVMOs intrazellulär stabiler.
Es stellte sich heraus, dass die β-Hydroxyketone sehr gute Substrate für eine ganze Reihe der 15 untersuchten BVMOs verschiedener Susbtratpräferenzen darstellen. So zeigten neben den beiden beschriebenen BVMOs ($BVMO_{Psfl}$ und $BVMO_{KT2440}$), die bevorzugt lineare Ketone umsetzen, auch viele Cyclohexanon-Monooxygenasen (CHMOs) hohe Aktivitäten und gute Selektivitäten (E > 80) gegenüber **1a**-**e**, obwohl sie als Cycloketon-umsetztende Monooxygenasen charakterisiert sind. Überraschenderweise setzte sich auch bei den CHMOs die Präferenz gegenüber mittelkettigen Ketonen (C_8-C_{10}) fort, die auch schon für die aliphatischen Ketone in den Vorversuchen beobachtet wurde (Abbildung 8). Vermutlich erschwert zum einen der lange Alkylrest die richtige Positionierung des Substrats im aktiven Zentrum, zum anderen könnte es zu elektrostatischen Abstoßungsreaktionen aufgrund der erhöhten Hydrophobizität kommen. Interessanterweise konnte auch die postulierte Bildung optisch reiner 1,2-Diole aus den jeweiligen Acetaten durch Hydrolyse von **2a**-**c** *in vivo* beobachtet werden. Auf diese Weise konnten 1,2-Hexandiol, 1,2-Heptandiol und 1,2-Octandiol dargestellt werden, die z.B. als Weichmacher in der Plastikindustrie oder als Zusatzstoff für Kosmetikprodukte Einsatz finden.
Bei den Biotransformationen der 5-Hydroxy-3-ketone **4a** und **4b** wurde die enzymatische Regioselektivität genauer untersucht. Tatsächlich senkte eine Kettenverlängerung von Methyl auf Ethyl benachbart zur Ketogruppe die Regioselektivität der Enzyme, so dass neben dem zu erwartenden normalen Ester auch der Ethylester zu größeren Anteilen gebildet wurde. Für die $BVMO_{Psfl}$ aus *P. fluorescens* DSM 50106 konnten sogar Verhältnisse von 50:50 und 40:60 für Propylat zu Ethylester beobachtet werden. Die Darstellung des abnormalen Baeyer-Villiger Esters ist bisher mit herkömmlichen chemischen Methoden nur schwer zugänglich, was die enzymatische Baeyer-Villiger Oxidation für diese Anwendungen besonders attraktiv macht.

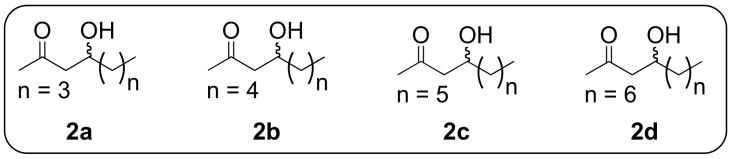

$CHMO_{Acineto}$	**E = 156**	**E > 200**	**E = 90**	**E = 4**
$BVMO_{Psfl}$	**E > 200**	**E > 200**	**E = 100**	**k.U.[a]**
CPMO	**E = 7**	**E = 7**	**E = 4**	**E = 2**

[a] k.U.: kein Umsatz

Abbildung 8. Enantioselektivitäten verschiedener BVMOs ($CHMO_{Acineto}$: Cyclohexanon-Monooxygenase aus *A. calcoaceticus* NCIMB 9871, $BVMO_{Psfl}$: Alkylketon-Monooxygenase aus *P. fluorescens* DSM 50106, CPMO: Cyclopentanon-Monooxygenase aus *C. testosteroni* NCIMB 9872). Deutlich zu erkennen ist der Abfall der Selektivitäten mit wachsender Alkylkette des Substrats.

6.4 Enzymatische Synthese optisch aktiver β-Aminoketone, β-Aminoalkylacetate und 2-Aminoalkohole mittels Baeyer-Villiger Monooxygenasen

Innerhalb der Substratklasse der (aryl)aliphatischen 4-Amino-2-ketone kann man zwischen i) linearen (**7a**-**c**), ii) linear-verzweigten (**7d**, **7e**) und iii) arylaliphatischen Ketonen (**7f**, **7g**) unterscheiden. Die Untersuchungen von i) und ii) zeigten, dass einige BVMOs ausschließlich die mittelkettigen Ketone (C_8-C_{10}) umsetzten und andere eher C_{12}-kettige Ketone oxidierten. In einigen Fällen konnte keine eindeutige Kettenlängenpräferenz erkannt werden (CDMO, $CHMO_{Xantho}$ und $CHMO_{Brevi1}$, Abbildung 9).

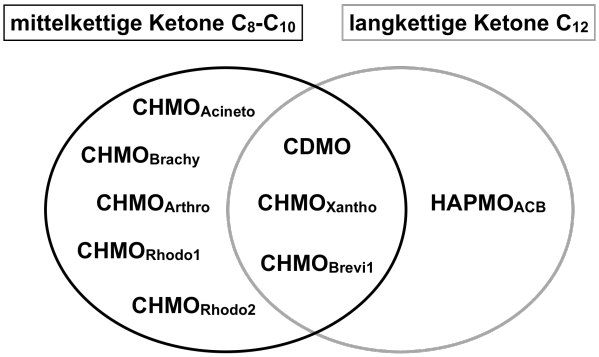

Abbildung 9. Darstellung der Kettenlängenspezifitäten verschiedener BVMOs ($CHMO_{Acineto}$: Cyclohexanon-Monooxygenase (CHMO) aus *A. calcoaceticus* NCIMB 9871, $CHMO_{Brachy}$: CHMO aus *Brachymonas* sp., $CHMO_{Arthro}$: CHMO aus *Arthrobacter* sp., $CHMO_{Rhodo1}$ und $CHMO_{Rhodo2}$: CHMOs aus *Rhodococcus* sp. Phi1 und Phi2, CDMO: Cyclododecanon-Monooxygenase aus *R. ruber*, $CHMO_{Xantho}$: CHMO aus *Xanthobacter* sp. ZL5, $CHMO_{Brevi1}$: CHMO aus *Brevibacterium* sp. und $HAPMO_{ACB}$: 4-Hydroxyacetophenon Monooxygenase aus *P. fluorescens* ACB) bezüglich linearer und linear-verzweigter *N*-geschützter β-Aminoketone.

Von den zehn untersuchten Substraten zeigten **7a** und **7b** die besten Ergebnisse in der kinetischen Racematspaltung**.** Hier konnten Enantioselektivitäten von E > 100 bei nahezu 50% Umsatz erzielt werden. Besonders auffällig war auch, dass einige Enzyme die enantiokom-

plementären Ketone oxidierten, was den Zugang zu beiden Substrat- und Produkt-Enantiomeren mit jeweils hoher optischer Reinheit ermöglichte. Mit wachsender Kettenlänge (**7c**) sank die Anzahl der BVMOs, die diese Substrate umsetzen, deutlich. Die Mehrheit der untersuchten Enzyme (80%) oxidierte auch die linear-verzweigten Substrate **7d** und **7e**, jedoch waren die Enantioselektivitäten in den meisten Fällen gering (E = 68 für **7e** mit $CHMO_{Brevi1}$, sonst E < 20). Während alle untersuchten BVMOs bevorzugt (–)-**7d** oxidierten kehrte sich diese Präferenz bei **7e** um. Hier wurde ausschließlich der (+)-Ester gebildet, was auf die unterschiedlichen sterischen Gegebenheiten durch die zusätzliche Methylengruppe in **7d** zurückzuführen sein könnte. Eine Ausnahme bildete die $CHMO_{Brevi1}$ aus *Brevibacterium* sp., die sowohl für **7d** als auch **7e** das (–)-Keton oxidierte. Interessanterweise konnte auch im Falle der β-Aminoketone eine spontane Hydrolyse der 2-Aminoalkylacetate *in vivo* beobachtet werden. Dabei entstanden enantiomerenreine 2-Aminoalkohole, die besonders für die Pharmaindustrie als hochwertige Vorstufen für die Synthese von Medikamenten von Bedeutung sind.

Bei der Oxidation der arylaliphatischen β-Aminoketone **7f** und **7g** zeigte sich, dass das heteroaromatische Substrat **7g** gar nicht oxidiert wurde, während **7f** ein sehr gutes Substrat für die BVMOs darzustellte. Mit Ausnahme der CPMO, der $HAPMO_{ACB}$ und der Alkylketon-umsetzenden BVMOs oxidierten alle anderen untersuchten BVMOs **7f** mit vergleichbar hohen Reaktionsgeschwindigkeiten. Die Enantioselektivitäten waren dabei aber bis auf zwei Ausnahmen sehr gering (E < 10). Lediglich die $CHMO_{Brevi1}$ und die PAMO (Phenylaceton-Monooxygenase aus *T. fusca*) wiesen bei etwa 50% Umsatz sehr gute Selektivitäten auf (E > 200). Hervorzuheben sei hier noch, dass beide Enzyme eine enantiokonvergente Selektivität zeigten.

6.5 Ausnutzung der enzymatischen Regioselektivität zur Darstellung von *N*-geschütztem β-Leucin

Um die enzymatische Regioselektivität der BVMOs genauer zu untersuchen, wurden neben den β-Amino-2-ketonen, welche die Carbonylgruppe am zweiten Kohlenstoffatom tragen, auch β-Amino-3-ketone synthetisiert. Damit verlängert sich der aliphatische Rest an der endständigen Seite des Moleküls von Methyl auf Ethyl. Wie bereits die Ergebnisse der β-Hydroxyketone zeigten, kann diese Strukturänderung des Substrats einen entscheidenden Einfluss auf die Wanderungstendenz der Reste und die Regioselektivität des Enzyms haben. Es zeigte sich, dass vier BVMOs ($CHMO_{Arthro}$, $CHMO_{Brachy}$, $CHMO_{Xantho}$ und die CDMO) in der Lage sind, im Falle von **10a**-**c** den Sauerstoff auf beiden Seiten der Carbonylgruppe einzubauen (Abbildung 10). Erfolgt die (enzymatische) Hydrolyse des entstandenen Ethylesters, so können enantiomerenreine *N*-geschützte β-Aminosäuren generiert werden (Abbildung 11).

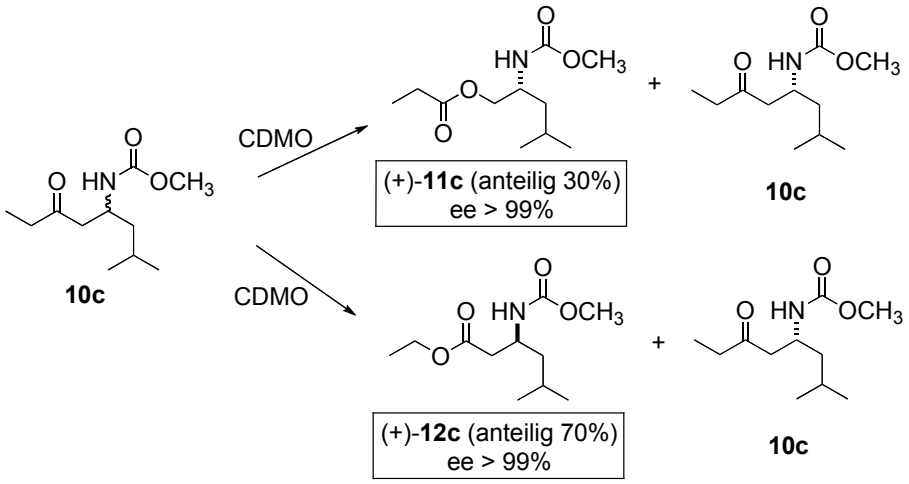

Abbildung 10. Darstellung der enzymatischen Regioselektivität der CDMO (Cyclododecanon-Monooxygenase aus *R. ruber*) am Beispiel **10c**. Eine CH_2-Verlängerung des endständigen Alkylrestes am Carbonylkohlenstoffatom führt zur Bildung des normalen (30%) und des abnormalen (70%) Baeyer-Villiger Esters.

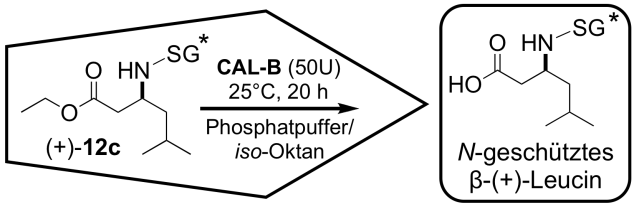

*SG: Schutzgruppe

Abbildung 11. Enzymatische Hydrolyse (CAL-B, *Candida antarctica* Lipase) des β-Aminoethylesters und Bildung von *N*-geschütztem β-Leucin.

6.6 Biotransformation mit arylaliphatischen Ketonen

Neben den linearen Ketonen wurden auch arylaliphatische Substrate untersucht, welche die Carbonylgruppe in der aliphatischen Seitenkette tragen. Erwartungsgemäß zeigten gerade $HAPMO_{JD1}$, $HAPMO_{ACB}$ und PAMO, die bevorzugt aromatische und arylaliphatische Ketone umsetzen, die besten Enantioselektivitäten (**13a** und **13b** in Abbildung 12). Erhöht man jedoch den Abstand zwischen Carbonylgruppe (Reaktionszentrum) und dem aromatischem Ring durch eine zusätzliche Methylengruppe (**13c**, **13d**), sinkt die Aktivität und die Enantioselektivität stark ab. Ein Grund hierfür können der wachsende sterische Anspruch sowie die Rotationsflexibilität durch die CH_2-Gruppe sein. Möglicherweise ist die Ausrichtung für eine enantioselektive Oxidation im aktiven Zentrum daher nicht mehr möglich. Wird ein zweiter Phenylring benachbart zur Ketogruppe eingeführt, entsteht ein Substrat, das vermutlich zu sperrig ist und daher nicht mehr in das aktive Zentrum passt. Für dieses Substrat wurde bei keiner der untersuchten BVMOs Aktivtät gefunden.

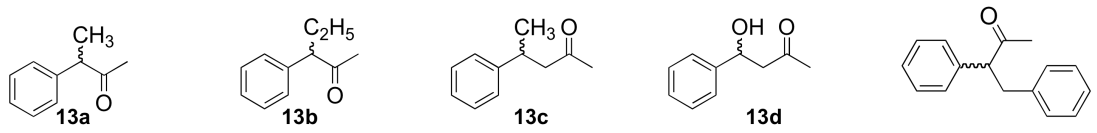

HAPMO$_{JD1}$: E > 200 c = 48% **HAPMO$_{ACB}$: E > 200 c = 50%** **CHMO$_{Brevi2}$: E = 18 c = 32%** **CHMO$_{Xantho}$: E > 100 c = 22%** **n.c.**

Abbildung 12. Enantioselektivitäten und Umsätze der arylaliphtaischen Ketone nach kinetischer Racematspaltung mit ausgewählten BVMOs.

Ein weiteres Ziel war es, die Biotransformationen nach Abschluss der Untersuchungen im analytischen Maßstab in einen präparativen Maßstab zu überführen. Hierfür wurden Experimente im Schüttelkolben (500 mL, 1 mmol Substratkonzentration) mit 3-Phenyl-2-butanon als Substrat und der BVMO$_{Psfl}$ aus *P. fluorescens* DSM 50106 als Biokatalysator mit ruhenden *E. coli* JM109 pGro7 Zellen durchgeführt. Für eine verbesserte Substrataufnahme in die Zellen wurden 0,5 Äquivalente β-Cyclodextrin hinzugegeben. Überraschenderweise konnte eine fast doppelt so hohe Enantioselektivität im Vergleich zu den analytischen Versuchen festgestellt werden ($E_{analytisch}$ = 43, $E_{präparativ}$ = 82). Nach Extraktion des Produkts aus dem Reaktionsansatz konnte eine Ausbeute von 35% (ee_P > 93%) festgestellt werden.
Ein wichtiges Problem, das die Ausbeute von enzymatischen Baeyer-Villiger Oxidationen oft mindert, ist die geringe Substrat- und Produkttoleranz. Um dieses Hindernis zu umgehen, wurden bereits erste Verfahren entwickelt, in denen man Substrat und Produkt auf ein geeignetes Trägermaterial adsorbiert hat. Dadurch stellt sich ein Gleichgewicht innerhalb des Reaktionsmediums ein und auch die Aufarbeitung und Produktextraktion kann wesentlich erleichtert werden. Die Erhöhung Ausbeute von 3-Phenyl-2-butanon durch den gezielten Einsatz solcher Trägermaterialien ist Gegenstand weiterer Untersuchungen.

6.7 Amplifikation der 4-Hydroxyacetophenon Monooxygenase aus *P. putida* JD1 mittels *SiteFinding*-PCR

Ebenfalls Ziel dieser Arbeit war es, das Gen der 4-Hydroxyacetophenon Monooxygenase aus *P. putida* JD1 zu amplifizieren und zu klonieren. Nach Optimierung der Proteinexpression in *E. coli* sollte das Substratspektrum charakterisiert werden. Die Amplifikation aus genomischer DNA (gDNA) stellte sich als anspruchsvoll heraus, da bis auf drei Peptidfragmente die Sequenz dieser BVMO ($HAPMO_{JD1}$, 70 kDa, 1920 bp) nicht bekannt war. Mit Hilfe von degenerierten Primern und einer Gradienten-PCR konnte schließlich ein etwa 1600 bp langes Oligonukleotid amplifiziert werden. Um die unbekannten flankierenden Bereiche dieser Teilsequenz zu amplifizieren, wurde zunächst mit einer Inversen-PCR gearbeitet. Eine weitaus elegantere Methode, die dann auch zum Erfolg führte, ist die *SiteFinding*-PCR. Diese PCR-Methode wurde ursprünglich für das *Genome*- oder *Chromosome-Walking* entwickelt, und eignet sich daher sehr gut, um unbekannte Sequenzen benachbart zu einer bekannten Sequenz zu amplifizieren. Der Vorteil dieser Methode gegenüber z.B. der Inversen-PCR ist, dass auf sämtliche Restriktions- und Ligationsschritte verzichtet werden kann (Abbildung 13).

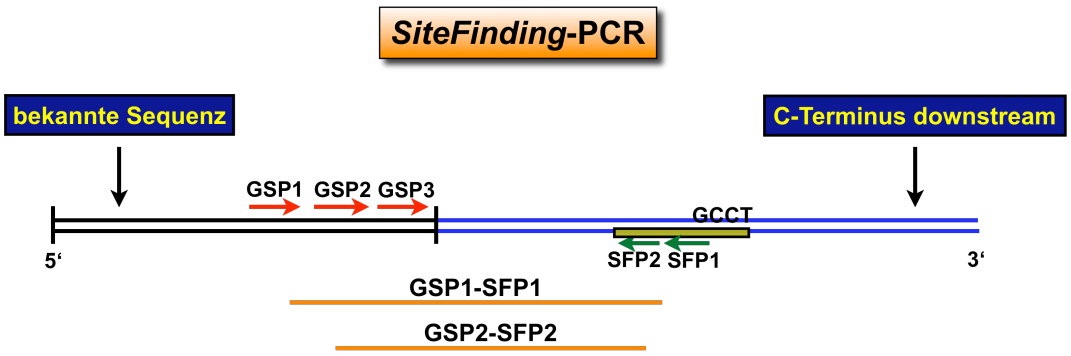

Abbildung 13. Prinzip der *SiteFinding*-PCR. GSP = genspezifischer Primer; SFP = *SiteFinding*-Primer. Zunächst bindet ein ca. 60 bp langes Oligonukleotid (SiteFinder) bei niedrigen Temperaturen mit der Priming-Sequenz GCCT am 5'-Ende an das Template (gDNA). Anschließend erfolgt eine *Nested*-PCR, wobei im ersten Schritt der GSP1 (bindet in der bekannten Sequenz) und der SFP1 (bindet im SiteFinder) als Primerpaar eingesetzt werden. Es entsteht das Amplifikat GSP1-SFP1, das dann als Template für die zweite PCR dient. In dieser werden der GSP2 und der SFP2 als Primerpaar eingesetzt und es entsteht das GSP2-SFP2 Amplifikat. Der GSP3 kann dann zur Sequenzierung der neuen Sequenz eingesetzt werden.

Die *SiteFinding*-PCR ermöglichte es, neben dem Gen der gesuchten $HAPMO_{JD1}$ sieben weitere offene Leserahmen in unmittelbarer Nachbarschaft zur Monooxygenase zu identifizieren. Darunter befanden sich eine Esterase, eine Dioxygenase, eine Reduktase, eine Dehydrogenase, ein Regulatorgen (LysR-Familie) sowie die kleine und die große Untereinheit einer weiteren Dioxygenase (Abbildung 14). Da 4-Hydroxyacetophenon das bevorzugte Substrat der BVMO ist, wurde postuliert, dass diese Proteine zu einem Operon gehören (*hap*-Operon), das am Abbau von Acetophenon-Derivaten beteiligt ist. Dabei katalysiert die $HAPMO_{JD1}$ den Einbau eines Sauerstoffatoms in das Substrat. Der entstandene Ester wird durch die Esterase gespalten, gefolgt von einer Ringöffnung durch die Dioxygenase. Nach Dehydrierung und Reduktion kann die β-Ketodicarbonsäure über den β-Ketoadipatabbauweg

in den Fettsäurestoffwechsel des Organismus eingeschleust werden. Proteinsequenzvergleiche der einzelnen Enzyme haben gezeigt, dass diese eine hohe Homologie zu denen aus *P. fluorescens* ACB zeigen. Auch hier wurde das vollständige Operon zum Abbau von 4-Hydroxyacetophenon amplifiziert und der postulierte Abbauweg verifiziert (Abbildung 15).

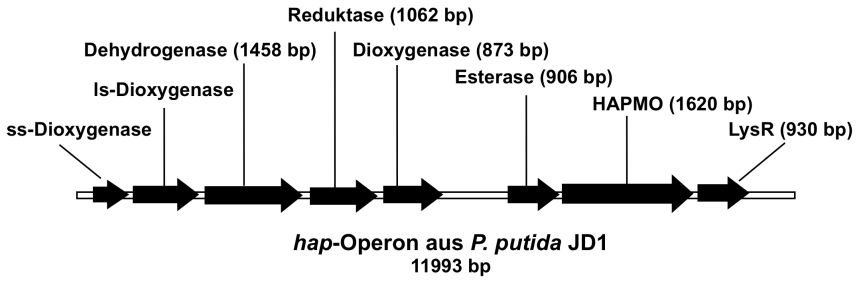

Abbildung 14. Operon aus *P. putida* JD1 (amplifiziert mittels der *SiteFinding*-PCR).

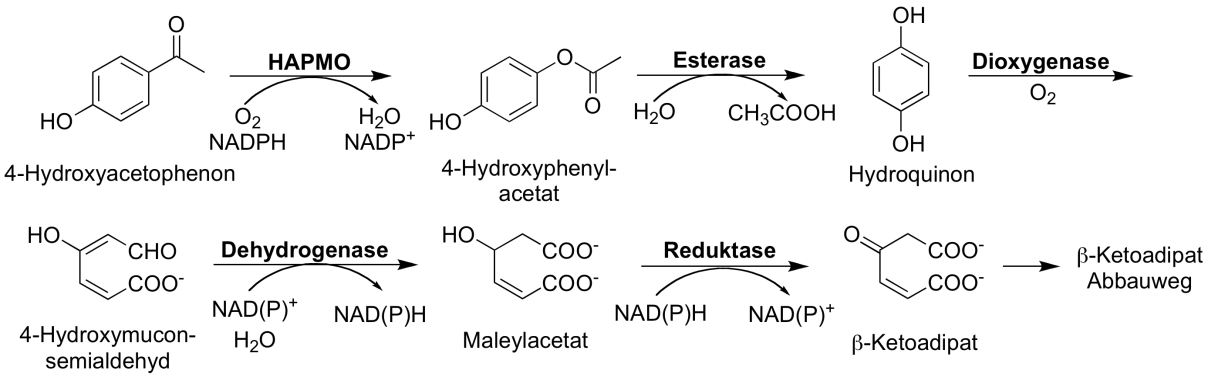

Abbildung 15. Postulierter Abbauweg von 4-Hydroxyacetophenon katalysiert durch die Enzyme der *hap*-Operons aus *P. putida* JD1.

6.8 Biochemische Charakterisierung der 4-Hydroxyacetophenon Monooxygenase aus *P. putida* JD1

Nachdem das Gen der $HAPMO_{JD1}$ erfolgreich amplifiziert wurde, konnte mit der rekombinanten Expression in *E. coli* begonnen werden. Zu den Optimierungsstrategien gehörten eine Variation der Induktorkonzentration (0,05-1 mM IPTG) und des Induktionszeitpunktes, die Expression in verschiedenen *E. coli*-Stämmen (BL21 (DE3), Rosetta™ (DE3), JM109, BL21 (DE3) CodonPlus® und BL21 (DE3) C41) sowie Änderung der Expressionstemperatur. Außerdem wurde eine Co-Expression von molekularen Chaperonen als Faltungshelfer in *E. coli* BL21 (DE3) sowie die Zugabe von FMN (Vorstufe von FAD, prosthetische Gruppe im aktiven Zentrum) und verschiedene Kultivierungsmedien untersucht. Dabei stellte sich heraus, dass die optimale Expressionstemperatur bei 20°C liegt und der Anteil an aktivem Protein in *E. coli* Rosetta™ (DE3) am höchsten ist. Die Proteinexpression wurde mit 0,1 mM IPTG bei OD_{600nm} 0,8-1 induziert. Die Zugabe von FMN oder die Co-Expression von Chaperonen konnte die Expression von löslichem aktivem Protein nicht wesentlich steigern.
Anschließend erfolgte die Proteinaufreinigung mittels Anionenaustauscher (DEAE, Kaliumphosphatpuffer, 50 mM, pH 7,5) und einer 2'ADP-basierenden Affinititätschromatographie (Elution mit $NADP^+$), gefolgt von der biochemischen Charakterisierung des Proteins. Neben der Bestimmung von pH- und Temperaturmaxima (pH 8.0 Tris-HCl, 30°C) wurden insgesamt 22 Substrate (arylaliphatische Acetophenon-Derivate, aromatische Aldehyde, heteroaromatische Ketone, lineare Ketone) hinsichtlich der kinetischen Parameter K_M und k_{cat} untersucht. Dabei stellte sich heraus, dass unter den Acetophenon-Derivaten solche bevorzugt umgesetzt werden, die den Substituenten in *para*-Position haben. Neben den arylaliphtaischen Ketonen wurden aber auch Aldehyde (Benzaldehyd, 2-Phenylpropionylaldehyd), sowie heteroaromatische Ketone (2-Acetylpyrrol) und Sulfide (Methyl-4-tolylsulfid) oxidiert (Abbildung 16).

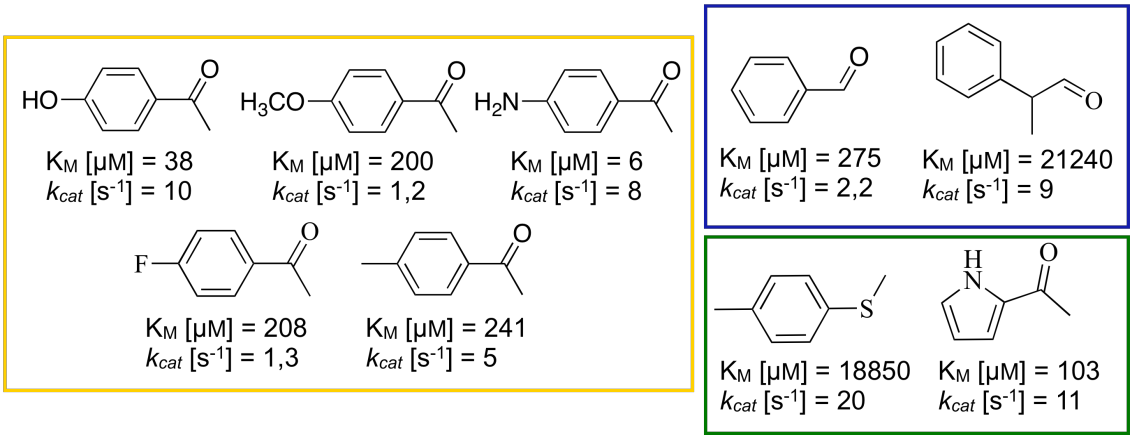

Abbildung 16. Kinetische Parameter der bevorzugten arylaliphatischen Substrate der 4-Hydroxyacetophenon Monooxygenase aus *P. putida* JD1. Gelb: arylaliphatische Ketone; blau: Aldehyde; grün: heteroaromatische Ketone und Sulfide.

Article I

Bioorganic & Medicinal Chemistry Letters 19 (2009) 3739–3743

Contents lists available at ScienceDirect

Bioorganic & Medicinal Chemistry Letters

journal homepage: www.elsevier.com/locate/bmcl

Kinetic resolution of aliphatic acyclic β-hydroxyketones by recombinant whole-cell Baeyer–Villiger monooxygenases—Formation of enantiocomplementary regioisomeric esters

Jessica Rehdorf [a], Alenka Lengar [b], Uwe T. Bornscheuer [a,*], Marko D. Mihovilovic [b,*]

[a] University of Greifswald, Institute of Biochemistry, Department of Biotechnology and Enzyme Catalysis, Felix-Hausdorff-Str. 4, 17487 Greifswald, Germany
[b] Vienna University of Technology, Institute of Applied Synthetic Chemistry, Getreidemarkt 9/163-OC, 1060 Vienna, Austria

ARTICLE INFO

Article history:
Received 16 February 2009
Revised 4 May 2009
Accepted 6 May 2009
Available online 9 May 2009

Keywords:
Biocatalysis
Biotransformation
Biooxygenation
Asymmetric synthesis
Chiral compounds

ABSTRACT

A set of various linear aliphatic β-hydroxyketones was investigated as substrates in the enzymatic kinetic and regioselective Baeyer–Villiger oxidation catalyzed by 12 Baeyer–Villiger monooxygenases from different bacterial origin. Excellent enantioselectivities (E >100) could be observed with 4-hydroxy-2-ketones. After acyl migration, the ester undergoes hydrolysis followed by the formation of optically active 1,2-diols. Furthermore, resolution of 5-hydroxy-3-ketones gave access to the 'abnormal' esters, which broadens applicability of these enzymes in organic chemistry. Additionally, it was noticed, that several substrates were converted by different enzymes in an enantiocomplementary way and with high optical purities.

As a powerful methodology in synthesis to break carbon–carbon bonds in an oxygen insertion process,[1] the Baeyer–Villiger oxidation is an appealing reaction in organic synthesis.[2] The transformation of ketones into the corresponding esters or lactones, respectively, gives access to valuable intermediates in organic chemistry on both bulk and fine chemical scale. The enzyme-mediated Baeyer–Villiger oxidation has received increasing attention in recent years.[1,3] Key advantages are chemo-, regio- and stereoselectivity combined with utilization of molecular oxygen as primary oxidant compared to metal-based mediated catalytic strategies.[4,5] Such biocatalytic strategies offer sustainable access to chiral compounds of pharmaceutical, nutritional and industrial interest.[6] During the last years, the number of recombinantly available Baeyer–Villiger monooxygenases (BVMOs) has increased, leading to an enzyme platform representing novel substrate specificities and complementary properties. The exploitation of whole-cell biotransformations using recombinant expression hosts for such NAD(P)H-dependent flavoenzymes[7] is currently of particular popularity in both laboratory and industrial scale applications, as the operational aspects are simple and facile, hence, enabling straight forward utilization in synthetic chemistry.[8]

Recently, we have reported on the first BVMO-catalyzed kinetic resolution of aliphatic acyclic ketones with racemic 4-hydroxy-2-ketones serving as model substrates.[9] We discovered that a BVMO from *Pseudomonas fluorescens* DSM 50106 ($BVMO_{Pfl}$)[10] oxidizes 4-hydroxy-2-octanone-, decanone- and dodecanone with moderate enantioselectivities, giving access to both optically active acetates and hydroxyketones (Scheme 1). Reports on biooxygenations of linear ketones by BVMOs are remarkably limited; only few precendences for the conversion of aryl-aliphatic compounds bearing the carbonyl group in a side chain have been published for arylketone accepting enzymes.[11,12]

In this study we enlarge the number of aliphatic acyclic β-hydroxyketones including 4-hydroxy-2-nonanone and -undecanone as well as the structurally more demanding compounds 5-hydroxy-3-nonanone and -decanone (synthesized after Kourouli

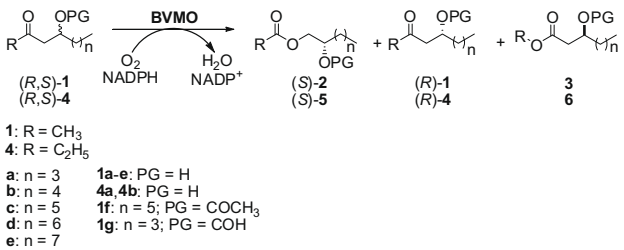

Scheme 1. Kinetic resolution of β-substituted linear ketones using recombinant BVMOs.

* Corresponding authors.
E-mail addresses: uwe.bornscheuer@uni-greifswald.de (U.T. Bornscheuer), mmihovil@pop.tuwien.ac.at (M.D. Mihovilovic).

0960-894X/$ - see front matter © 2009 Elsevier Ltd. All rights reserved.
doi:10.1016/j.bmcl.2009.05.014

et al.[13]). Furthermore, we extended the toolbox of linear-ketone accepting BVMOs by eleven additional enzymes of various bacterial origin: cyclohexanone monooxygenase ($CHMO_{Acineto}$) from *Acinetobacter calcoaceticus* NCIMB 9871[14] and seven other cyclohexanone monooxygenases ($CHMO_{Arthro}$ from *Arthrobacter* sp.,[15] $CHMO_{Brachy}$ from *Brachymonas* sp.,[16] $CHMO_{Brevi1}$ and $CHMO_{Brevi2}$ from *Brevibacterium* sp.,[17] $CHMO_{Rhodo1}$ and $CHMO_{Rhodo2}$ from *Rhodococcus* sp.[15] and $CHMO_{Xantho}$ from *Xanthobacter* sp. ZL5[18]), as well as cyclopentanone monooxygenase (CPMO) from *Comamonas* sp. NCIMB 9872,[19] 4-hydroxyacetophenone monooxygenase from *Pseudomonas putida* JD1 ($HAPMO_{PpJD1}$)[20] and alkylketone-converting BVMO from *P. putida* KT2440[21] ($BVMO_{PpKT2440}$).

BVMO-mediated oxidations were initially accomplished on screening scale using 24-well plastic dishes in parallel format.[22] On the basis of screening results, individual biotransformations were conducted as time-course experiments with selected biocatalysts in order to investigate the relationship between time, conversion and enantiomeric excess in detail.[23] Enantioselectivity values (*E*; determined by computer fitting)[24] and regioisomeric excess (% re)[25] were calculated to evaluate the efficiency of kinetic resolution and the regioselectivity of the oxygen insertion process.

With the exception of $CHMO_{Brevi1}$ and $HAPMO_{PpJD1}$ ketones **1a**–**e** were almost fully converted (*c* >70%) in most cases to the product esters **2a**–**e** within 24 h at 24 °C (data not shown) and short- and middle-chain ketones **1a**–**c** seem to be preferred. This is consistent with the discovered clustering of BVMOs into two distinct groups, the cyclohexanone- and cyclopentanone-type monooxygenases.[26] $CHMO_{Acineto}$ and $BVMO_{Pfl}$ showed best results with conversions between 40% and 60% and ee_P >80% for **1a**–**d**, while for the other BVMOs it seemed that the 'better-fitting' enantiomer is only converted with a slightly higher velocity than the 'less-fitting' enantiomer. Surprisingly, $CHMO_{Acineto}$ and $BVMO_{Pfl}$ showed only low activity against **1e**. The longer chain is possibly too bulky for BVMO active sites. Substrate **1e** was therefore excluded from further experiments.

We also found that in the case of a protection of the free hydroxyl group prior to the biotransformation (incorporation of acetyl **1f** and formyl protecting groups **1g**), substrate acceptance of CHMO-type enzymes decreased significantly. However, CPMO-type BVMOs (CPMO and $CHMO_{Brevi2}$) now display good kinetic resolutions providing access to enantiocomplementary esters compared to the above biooxygenations of the hydroxyl-substrates.

Similar results could be obtained using 5-hydroxy-3-ketones as substrates. Ketones **4a** and **4b** were almost fully oxidized (*c* >70%), but again $CHMO_{Brevi1}$ showed no and $CHMO_{Brevi2}$ only very low conversion. Conversion of **4a** by CPMO stopped at 53% suggesting a higher enantioselectivity compared to **1a**–**d**. Interestingly, the formation of two regioisomers could be observed with $BVMO_{Pfl}$. Either the more substituted or the less substituted carbon center undergoes migration, leading consequently to 'normal' esters **5a** and **5b** and 'abnormal' esters **6a** and **6b** ester (Scheme 1). Such regiodivergent biooxygenations have been observed in previous studies on cyclic systems.[27–30] A mechanistic relationship has been proposed for this behavior based on stereoelectronic effects.[31]

In order to optimize enantiomeric excesses and enantioselectivities of products **2a**–**d**, **5a** and **5b** within the kinetic resolution process, time-course experiments were performed to stop conversion close to 50% (for optimized resolution results). For these experiments selected biocatalysts were used that showed satisfactory results in pre-screening experiments as described above: $CHMO_{Acineto}$

Table 1
Microbial Baeyer–Villiger oxidations of β-hydroxy-2-ketones **1a**–**d** and β-protected ketones **1f** and **1g** using recombinant whole-cells of *E. coli* expressing BVMOs from different bacterial origin

Substrate	BVMO	*t* (h)	*c*[a] (%)	ee_S[b] (%)	ee_P[b] (%)	abs. conf.[c]	*E*[d]
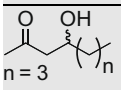 **1a**	$CHMO_{Acineto}$	8	49	91	96	(*S*)	156
	CPMO	3	53	64	56	(*S*)	7
	$BVMO_{Pfl}$	24	46	85	>99	(*S*)	>200
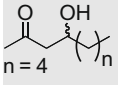 **1b**	$CHMO_{Acineto}$	20	49	96	>99	(*S*)	>200
	$CHMO_{Xantho}$	10	47	84	95	(*S*)	103
	CPMO	2	44	48	62	(*S*)	7
	$BVMO_{Pfl}$	8	48	89	98	(*S*)	>200
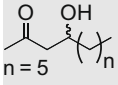 **1c**	$CHMO_{Acineto}$	20	50	92	93	(*S*)	90
	CPMO	2	44	39	50	(*S*)	4
	$BVMO_{Pfl}$	6	41	68	96	(*S*)	100
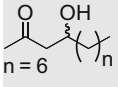 **1d**	$CHMO_{Acineto}$	30	20	13	52	(*S*)	4
	$CHMO_{Arthro}$	20	55	62	50	(*S*)	6
	$CHMO_{Rhodo2}$	10	18	17	80	(*S*)	10
	CPMO	2	65	37	20	(*S*)	2
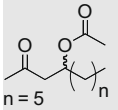 **1f**	$CHMO_{Acineto}$	24	<5	n.d.	n.d.	n.a.	n.d.
	CPMO	24	25	45	>99	(*R*)	>200
	$CHMO_{Brevi2}$	20	23	41	91	(*R*)	31
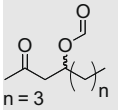 **1g**	$CHMO_{Acineto}$	24	42	25	33	(*S*)	3
	$CHMO_{Xantho}$	24	57	73	66	(*S*)	10
	CPMO	24	50	99	99	(*R*)	>200
	$CHMO_{Brevi2}$	24	28	27	>99	(*R*)	>200

Reactions were monitored over 48 h. Syntheses of **2a** and **2c** as standards for GC analysis were performed enzymatically by esterification of 1,2-diols with vinyl acetate by immobilized *Candida antarctica* lipase B as described by Kirschner and Bornscheuer.[9] Syntheses of **2b** and **2d** was accomplished as described in Ref. 2. Spectral data are shown in Ref. 33. Syntheses of **1f** and **1g** were performed from β-hydroxyketones according standard procedures.
n.d. = not determined; n.a. = not applicable.

[a] Conversion calculated from % ee_S (enantiomeric excess of substrate) and % ee_P (enantiomeric excess of product).

[b] % ee_S and % ee_P were determined by chiral phase GC and calculated according to Chen et al.[34]

[c] Absolute configurations of hydroxyalkyl acetates **2a**–**d** were determined by comparison with (*R*)-2-hydroxydecyl acetate ((*R*)-**2e**), which was synthesized from (*R*)-1,2-decandiol by using lipase-catalyzed transesterification. Since **2a**–**d** are structurally related (homologue series) the same configuration is assumed for **2a**–**c**.[9]

[d] Enantioselectivity values were determined by computer fitting of GC data from % ee_S and % ee_P.

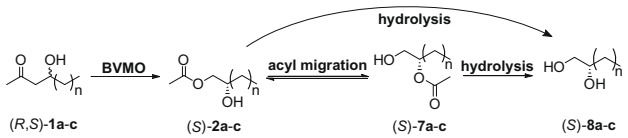

Scheme 2. Kinetic resolution of **1a–c** followed by direct ester hydrolysis or via acyl migration and ester bond cleavage releasing optically active 1,2-diols **8a–c**.

and CPMO as two 'benchmark' catalysts, reflecting the key features of the two family clusters among BVMOs, CHMO$_{Xantho}$, CHMO$_{Rhodo2}$, CHMO$_{Brachy}$, CHMO$_{Arthro}$, CHMO$_{Brevi1}$ and BVMO$_{Pfl}$. Results obtained from biotransformations with **1a–d** are compiled in Table 1.

All investigated enzymes oxidized the (*S*)-enantiomer of **1a–d,** whereas biotransformations of **1a–c** with CHMO$_{Acineto}$ and BVMO$_{Pfl}$ lead to very high enantioselectivities. Even after 48 h the (*R*)-hydroxyketone is not converted at all and reaction rate is stopped at 50%. In comparison, CPMO oxidized ketones very fast (less than 3 h for 50% conversion), but showed nearly no selectivity. The highest *E*-value of 7 could be achieved for **2a** and **2b**. Investigating the effect of chain-length indicated that enantioselectivity decreases (compare CHMO$_{Acineto}$ in Table 1) from **1a** with eight carbon atoms to **1d** with eleven carbon atoms. Tentatively, the chain-length and therefore the increase in hydrophobicity are criteria for selectivity.

Interestingly, kinetic resolution of 4-hydroxy-2-ketones can be used to generate two different chemical species, which additionally differ in their configuration. Besides the residual optically active hydroxyketones (*R*)-**1a–d**, optically active hydroxyalkyl esters (*S*)-**2a–d** are formed, which in case of **2a**, **2b** and **2c** undergo acyl migration to form optically pure acetates of 1,2-diols **7a–c** (Scheme 2).

The equilibrium between **2a–c** and **7a–c** is shifted towards the production of the acylated 1,2-diol after 24 h reaction time followed by hydrolysis of the ester bond yielding in enantiomerically pure 1,2-diols **8a–c**. Since acyl migration proceeds without any conformational changes, all 1,2-diols possess the same configuration as the hydroxyalkyl acetates. The maximum amount of generated 1,2-diol was 55% after 48 h using **1c** as starting material and BVMO$_{Pfl}$ as biocatalyst (compare Fig. 1).

Indeed, this feature makes this biotransformation especially useful and complementary to bioreductions by highly regio- and stereospecific ketoreductases.[35,36] The alternative kinetic resolution of 1,2-diols using lipases or esterases proceeds so far with low selectivity.[37–39]

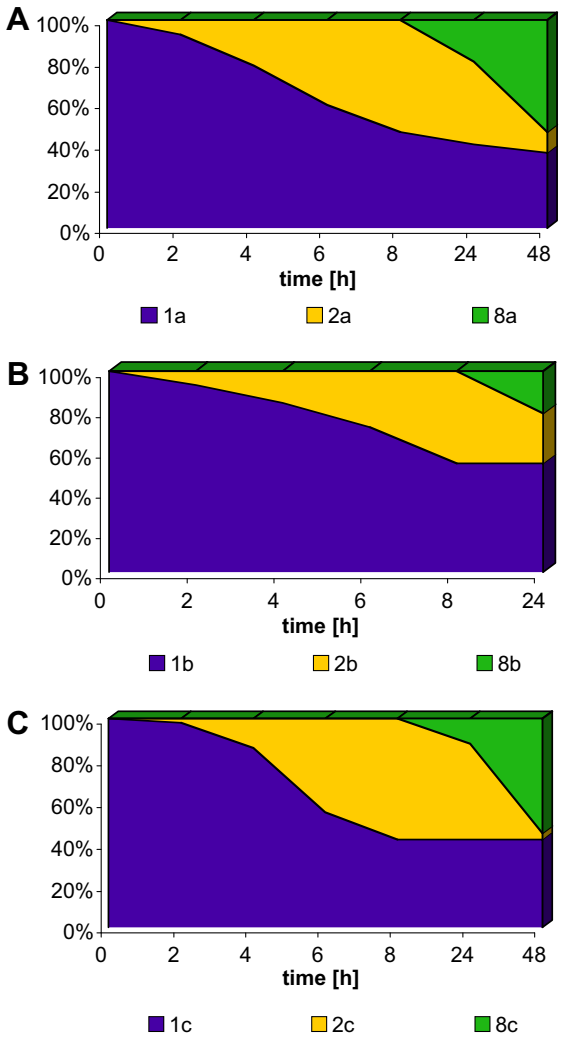

Figure 1. Enzymatic formation of 1,2-diols **8a–c** via kinetic resolution of 4-hydroxy-2-ketones **1a–c** at 24 °C after 24 and 48 h with (A) **1a** and CHMO from *A. calcoaceticus* NCIMB 9871, (B) **1b** an CHMO from *A. calcoaceticus* NCIMB 9871 and (C) **1c** and BVMO from *P. fluorescens* DSM 50106, both enzymes expressed in *E. coli*.

Oxidation of **4a** and **4b** showed different results (summarized in Table 2). In this case, enantioselectivity among utilized BVMOs is opposite compared to **1a–d**. While for CHMO$_{Acineto}$ and BVMO$_{Pfl}$

Table 2
Microbial Baeyer–Villiger oxidations of β-hydroxy-3-ketones **4a** and 4**b** using recombinant whole-cells of *E. coli* expressing BVMOs from different bacterial origin

Substrate		BVMO	*t* (h)	*c*[a] (%)	ee$_S$[b] (%)	ee$_P$[b] (%)	*E*[c]	re[d] (%)
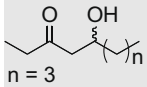 n = 3	**4a**	CHMO$_{Acineto}$	10	46	75	88	35	–
		CHMO$_{Xantho}$	10	53	81	72	15	–
		CHMO$_{Brachy}$	8	58	>99	70	40	–
		CPMO	24	50	>99	96	>200	–
		BVMO$_{Pfl}$	10	32	25	53	4	64
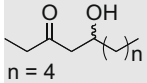 n = 4	**4b**	CHMO$_{Acineto}$	8	40	46	69	8	–
		CHMO$_{Xantho}$	8	44	61	78	14	–
		CHMO$_{Brachy}$	6	42	57	75	12	–
		CPMO	10	48	81	87	35	–
		BVMO$_{Pfl}$	24	55	>99	82	74	40

Reactions were monitored over 48 h. For syntheses of product standards see Ref. 32. Spectral data are shown in Ref. 33.
[a] Conversion calculated from % ee$_S$ (enantiomeric excess of substrate) and % ee$_P$ (enantiomeric excess of product).
[b] % ee$_S$ and % ee$_P$ were determined by chiral phase GC and calculated according to Chen et al.[34]
[c] Enantioselectivity values were determined by computer fitting of GC data from % ee$_S$ and % ee$_P$.
[d] Percent regioisomeric excess in favor of 'abnormal' ester determined by chiral phase GC.

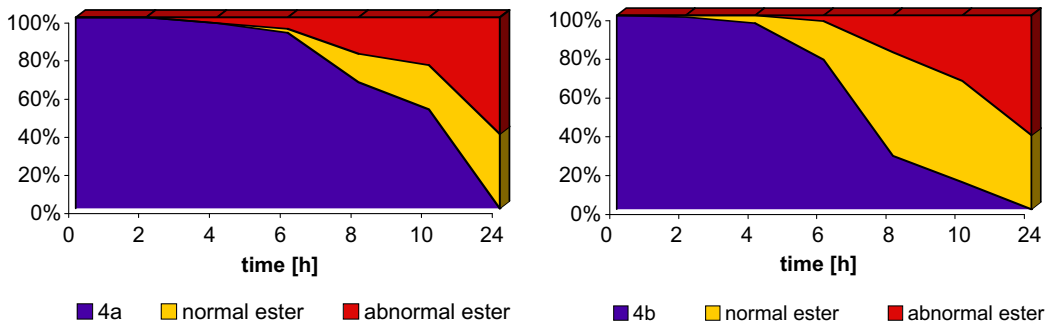

Figure 2. Regioselective Baeyer–Villiger oxidation of 5-hydroxy-3-ketones **4a** and **4b** using engineered *E. coli* cells expressing BVMO from *P. fluorescens* DSM 50106.

E-values are between 4 and 40, CPMO now showed a very high and even reverse selectivity for **4a** (*E* >200). Thus, implementing $CHMO_{Brachy}$ and CPMO for kinetic resolution of **4a** gives access to both enantiomers of **5a** in high optically purity. This fact makes this reaction a powerful and interesting tool in organic chemistry.

Furthermore, it could be observed that the location of the keto group in the molecule influences regioselectivity of the enzymes. While the methyl ester ('abnormal' product) was formed only up to 10% (data not shown) for 4-hydroxy-2-ketones this fact changed using 5-hydroxy-3-ketones. $BVMO_{Pfl}$ even generated 64% or 40% in favor of the 'abnormal' ester in case of **4a** and **4b**, respectively (Fig. 2). This is the only option to synthesize 'abnormal' esters enzymatically to our knowledge until now. This observation underscores the powerful capabilities of BVMOs and not only broadens their synthetic applicability, but also provides a synthetically useful alternative to already established chemical reactions in organic chemistry.

Based on our observations, aliphatic open-chain β-hydroxyketones are good substrates for most of the BVMOs recombinantly available so far, especially for those previously described as cycloketone converting enzymes. The possibility to synthesize enantiopure 1,2-diols enzymatically is noteworthy, since these compounds are of special interest for example, in organic industry for the synthesis of polyesters but also in medical treatment as antimicrobial agents.[40] Furthermore, 1,2-diols are predominantly synthesized chemically, so far; thus, kinetic resolution of 4-hydroxy-2-ketones using BVMOs can accomplish a considerable contribution for environmental protection.

The fact that some BVMOs are capable to generate the 'abnormal' Baeyer–Villiger product with high enantioselectivity offers new possibilities for the synthesis of natural products. Together with the enantiocomplementary conversion of ketones by different enzymes it displays the potential of the natural diversity to provide suites of catalysts for chemical operations. Currently, further studies on the regioselectivity of BVMOs are in progress in our laboratories.

Acknowledgements

We thank the German Federal Foundation of Environment (Deutsche Bundesstiftung Umwelt, DBU) for a stipend to Jessica Rehdorf. Part of this research was funded by the Austrian Science Fund FWF (P19845). Furthermore, we thank Dr. Pierre Rouviere (DuPont USA) for providing six recombinantly expressed BVMOs.

References and notes

1. Mihovilovic, M. D. *Curr. Opin. Chem.* **2006**, *10*, 1265.
2. Krow, G. R. *Org. React.* **1993**, *43*, 251.
3. Kamerbeek, N. M.; Janssen, D. B.; van Berkel, W. J. H.; Fraaije, M. W. *Adv. Synth. Catal.* **2003**, *345*, 667.
4. Gusso, A.; Baccin, C.; Pinna, F.; Strukul, G. *Organometallics* **1994**, *13*, 3442.
5. Strukul, G.; Varagnolo, A.; Pinna, F. *J. Mol. Catal. A: Chem.* **1997**, *117*, 413.
6. Kawamoto, M.; Utsukihara, T.; Abe, C.; Sato, M.; Saito, M.; Koshimura, M.; Kato, N.; Horiuchi, A. C. *Biotechnol. Lett.* **2008**, *30*, 1655.
7. van Berkel, W. J. H.; Kamerbeek, N. W.; Fraaije, M. W. *J. Biotechnol.* **2006**, *124*, 670.
8. Mihovilovic, M. D.; Rudroff, F.; Müller, B.; Stanetty, P. *Bioorg. Med. Chem. Lett.* **2003**, *13*, 1479.
9. Kirschner, A.; Bornscheuer, U. T. *Angew. Chem., Int. Ed.* **2006**, *45*, 7004.
10. Kirschner, A.; Altenbuchner, J.; Bornscheuer, U. T. *Appl. Microbiol. Biotechnol.* **2007**, *73*, 1065.
11. Geitner, K.; Kirschner, A.; Rehdorf, J.; Schmidt, M.; Mihovilovic, M. D.; Bornscheuer, U. T. *Tetrahedron: Asymmetry* **2007**, *18*, 892.
12. Rodríguez, C.; de Gonzalo, G.; Fraaije, M. W.; Gotor, V. *Tetrahedron: Asymmetry* **2007**, *18*, 1338.
13. Kourouli, T.; Kefalas, P.; Ragoussis, N.; Ragoussis, V. J. *Org. Chem.* **2002**, *67*, 4615.
14. Chen, Y.-C. J.; Peoples, O. P.; Walsh, C. T. *J. Bacteriol.* **1988**, *170*, 781.
15. Brzostowicz, P. C.; Walters, D. M.; Thomas, S. M.; Nagarajan, V.; Rouvière, P. E. *Appl. Environ. Microbiol.* **2003**, *69*, 334.
16. Bramucci, M. G.; Brzostowicz, P. C.; Kostichka, K.; Nagarajan, V.; Rouvière, P. E., Thomas, S. M. 2003 Genes encoding Baeyer–Villiger monooxygenases. P. I. Appl. WO/2003/020890; **2003**, *138*, 233997.
17. Brzostowicz, P. C.; Gibson, K. a. L.; Thomas, S. M.; Blasko, M. S.; Rouvière, P. E. *J. Bacteriol.* **2000**, *18215*, 4241.
18. van Beilen, J. B.; Mourlane, F.; Seeger, M. A.; Kovac, J.; Li, Z.; Smits, T. H. M.; Fritsche, U.; Witholt, B. *Environ. Microbiol.* **2003**, *5*, 174.
19. Iwaki, H.; Hasegawa, Y.; Wang, S.; Kayser, M. M.; Lau, P. C. K. *Appl. Environ. Microbiol.* **2002**, *68*, 5671.
20. Rehdorf, J.; Zimmer, C. L.; Bornscheuer, U. T. *Appl. Environ. Microbiol.* **2009**, *75*, 3106.
21. Rehdorf, J.; Kirschner, A.; Bornscheuer, U. T. *Biotechnol. Lett.* **2007**, *29*, 1393.
22. *Typical procedure for screening experiments*—Precultures were inoculated with a single colony from a plate and incubated at 37 °C overnight (in case of CHMO from *Xanthobacter* sp. at 30 °C) in an orbital shaker in a baffled Erlenmeyer flask. LB_{amp} ($LB_{amp/chl}$ for HAPMO from *P. putida* JD1) was inoculated with 1% of the overnight preculture and incubated at 37 or 30 °C, respectively, until OD_{600nm} reached 0.5–0.7. Then, protein expression was induced with either IPTG (0.1 mM final concentration) or in case of BVMO from *P. putida* KT2440 with L-rhamnose (0.2% final concentration). Protein expression was performed at 24 °C for 2 h. Screening was performed in 24-well plastic plates (*Greiner BioOne company*). 1 mL bacterial culture was transfered into each well (max. volume of 2 mL) and substrate was added (2.5 mM final concentration). Biotransformations were carried out at 24 °C and analyzed after 24 h. Therefore, samples were extracted with ethyl acetate supplemented with 1.2 mM of an internal standard (benzoic acid methylester) and dried over sodium sulfate.
23. *Typical procedure for time-course experiments*—Biotransformations were performed as described for screening experiments, but here samples were taken at certain time intervals (2, 4, 6, 8, 10, 24, 30 and 48 h), extracted and analyzed via GC.
24. Faber, K.; Hönig, H., and Kleewein, A. Free shareware programs ('Selectivity-1.0') for calculation of the enantiomeric ratio. Available on the authors website: <http://borgc182.kfunigraz.ac.at./>.
25. Percent regioisomeric excess (% re) is defined as the percentage of the major regioisomer (both enantiomers) minus the percentage of the minor regioisomer (both enantiomers).
26. Mihovilovic, M. D.; Rudroff, F.; Grötzl, B.; Kapitan, P.; Snajdrova, R.; Rydz, J. *Angew. Chem., Int. Ed.* **2005**, *44*, 3609.
27. Snajdrova, R.; Grogan, G.; Mihovilovic, M. D. *Bioorg. Med. Chem. Lett.* **2006**, *16*, 4813.
28. Mihovilovic, M. D.; Kapitan, P.; Kapitanova, P. *ChemSusChem* **2008**, *1*, 143.
29. Cernuchová, P.; Mihovilovic, M. D. *Org. Biomol. Chem.* **2007**, *5*, 1715.
30. Kyte, B. G.; Rouvière, P. E.; Cheng, Q.; Stewart, J. D. J. *Org. Chem.* **2004**, *69*, 12.

31. Kelly, D. R.; Knowles, C. J.; Mahdi, J. G.; Taylor, I. N.; Wright, M. A. *Chem. Soc., Chem. Commun.* **1995**, *12*, 729.
32. *Preparative scale biotransformations and enzymatic synthesis of **2b**, **2d**, **5a**, **5b**, **6a** and **6b***—Baffled Erlenmeyer flask with LB_{amp} (500 mL) was inoculated with an overnight bacterial culture, IPTG was added at OD 0.6 (0.1 mM final concentration) together with substrate (50 mg). Flasks were shaken at 24 °C for 24 h, then biomass was removed by centrifugation, the aqueous phase was saturated with sodium chloride and extracted five times with ethyl acetate. Organic layers were combined, dried over sodium sulfate and concentrated. Esters were purified by silica gel chromatography.
33. *Physical and spectral data of* **4a**: Obtained from 3-oxoheptanoate and *n*-valeraldehyde as a colorless liquid (685 mg, 84%); δ_H (300 MHz, $CDCl_3$) 0.90 (t, *J* = 6.9 Hz, 3H), 1.07 (t, *J* = 6.6 Hz, 3H), 1.23–1.55 (m, 6H), 2.42–2.58 (m, 2H), 2.59 (q, *J* = 3 Hz, 2H), 4.0–4.07 (m, 1H); δ_C (50 Hz, $CDCl_3$) 7.5 (q), 14.0 (q), 22.6 (t), 27.6 (t), 36.1 (t), 36.8 (t), 48.6 (t), 67.7 (d), 212.8 (s). Physical and spectral data of **4b**: obtained from 3-oxoheptanoate and capronaldehyde as a colorless liquid (220 mg, 60%); specific rotation of sample obtained in enzyme mediated kinetic resolution: $[\alpha]_D^{20} = -34.8$ (*c* 0.34, $CHCl_3$; ee = 93%); δ_H (300 MHz, $CDCl_3$) 0.89 (t, *J* = 7 Hz, 3H), 1.06 (t, *J* = 7.4 Hz, 3H), 1.25–1.52 (m, 8H), 2.48–2.67 (m, 2H), 2.55 (q, *J* = 4 Hz, 2H), 4.0–4.07 (m, 1H); δ_C (50 MHz, $CDCl_3$) 7.9 (q), 14.1 (q), 22.7 (t), 24.8 (t), 31.4 (t), 32.1 (t), 36.2 (t), 48.6 (t), 67.6 (d), 211.6 (s). Physical and spectral data of **2b**: colorless liquid (15 mg, 30%); δ_H (200 MHz, $CDCl_3$) 0.85 (t, *J* = 8 Hz, 3H), 1.29-1.45 (m, 8H), 2.09 (s, 3H), 3.83-3.95 (m, 1H), 3.98-4.1 (m, 2H); δ_C (50 MHz, $CDCl_3$) 14.1 (q), 21.0 (q), 22.7 (t), 25.1 (t), 31.9 (t), 33.4 (t), 68.9 (d), 70.0 (t), 171.4 (s). Physical and spectral data of **2d:** colorless liquid (20 mg, 40%); δ_H (200 MHz, $CDCl_3$) 0.86 (t, *J* = 9 Hz, 3H), 1.26–1.49 (m, 12H), 2.1 (s, 3H), 3.81–3.90 (m, 1H), 4.0–4.18 (m, 2H); δ_C (50 MHz, $CDCl_3$) 14.3 (q), 21.1 (q), 22.8 (t), 25.5 (t), 29.3 (t), 29.7 (t), 31.9 (t), 33.5 (t), 68.9 (d), 70.1 (t), 171.4 (s). Physical and spectral data of **5a**: colorless liquid (24 mg, 48%); δ_H (200 MHz, $CDCl_3$) 0.9 (t, *J* = 10 Hz, 3H), 1.14 (t, *J* = 8 Hz, 3H), 1.25–1.44 (m, 6H), 2.29 (q, 18 Hz, 2H), 3.74–3.87 (m, 1H), 4.0–4.36 (m, 2H); δ_C (50 MHz, $CDCl_3$) 9.4 (q), 14.1 (q), 23.1 (t), 27.2 (t), 27.6 (t), 32.2 (t), 70.9 (d), 71.2 (t), 171.4 (s). Physical and spectral data of **6a**: colorless liquid (23 mg, 46%); specific rotation of sample obtained in enzyme mediated kinetic resolution: $[\alpha]_D^{20}$ = -18.2 (c 0.43, $CHCl_3$; ee = 93%); δ_H (200 MHz, $CDCl_3$) 0.91 (t, *J* = 11 Hz, 3H), 1.24 (t, *J* = 7.2 Hz, 3H), 1.31–1.46 (m, 6H), 2.32–2.56 (m, 2H), 3.89–4.0 (m, 1H), 4.12–4.23 (q, *J* = 7.4 Hz, 2H); δ_C (50 MHz, $CDCl_3$) 12.9 (q), 13.2 (q), 21.6 (t), 26.6 (t), 35.2 (t), 40.3 (t), 59.7 (d), 67.0 (t), 172.1 (s). Physical and spectral data of **5b**: colorless liquid (17 mg, 34%); specific rotation of sample obtained in enzyme mediated kinetic resolution: $[\alpha]_D^{20}$ = +2.2 (*c* 0.74, $CHCl_3$; ee = 93%); δ_H (200 MHz, $CDCl_3$) *J* = 0.91 (t, 6 Hz, 3H), 1.15 (t, *J* = 7.6 Hz, 3H), 1.24–1.45 (m, 8H), 2.35 (q, *J* = 5.4 Hz, 2H), 3.8–3.92 (m, 1H), 3.91–4.19 (m, 2H); δ_C (50 MHz, $CDCl_3$) 9.4 (q), 14.1 (q), 22.7 (t), 24.8 (t), 27.6 (t), 32.1 (t), 32.5 (t), 70.8 (d), 71.2 (t), 174,1 (s). Physical and spectral data of **6b**: colorless liquid (25 mg, 50%); specific rotation of sample obtained in enzyme mediated kinetic resolution: $[\alpha]_D^{20} = -20.5$ (*c* 0.69, $CHCl_3$; ee >99%); δ_H (200 MHz, $CDCl_3$) 0.88 (t, *J* = 6.4 Hz, 3H), 1.27 (t, *J* = 7.2 Hz, 3H), 1.31–1.43 (m, 8H), 2.4–2.48 (m, 2H), 3.95–4.03 (m, 1H), 4.06–4.19 (m, 2H). δ_C (50 MHz, $CDCl_3$) 14.0 (q), 14.2 (q), 21.0 (t), 22.6 (t), 25.1 (t), 31.7 (t), 36.5 (t), 41.3 (t), 60.7 (d), 173.1 (s).
34. Chen, C.-S.; Fujimoto, Y.; Girdaukas, G.; Sih, C. J. *J. Am. Chem. Soc.* **1982**, *104*, 7294.
35. Kaluzna, I. A.; Matsuda, T.; Sewell, A. K.; Stewart, J. D. *J. Am. Chem. Soc.* **2004**, *126*, 12827.
36. Moore, J. C.; Pollard, D. J.; Kosjek, B.; Devine, P. N. *Acc. Chem. Res.* **2007**, *40*, 1412.
37. Theil, F.; Weidner, J.; Ballschuh, S.; Kunath, A.; Schick, H. *Tetrahedron Lett.* **1993**, *34*, 305.
38. Theil, F.; Ballschuh, S.; Kunath, A.; Schick, H. *Tetrahedron: Asymmetry* **1991**, *2*, 1031.
39. Janssen, A. M.; Klunder, A. J. H.; Zwanenburg, B. *Tetrahedron* **1991**, *47*, 7409.
40. Schmaus, G.; Herrmann, M., Joppe, H., Use of 1,2-decandiol for combating germs causing body odour. WO/2003/000220; PCT/EP2002/006751, 2003.

Article II

Enzymatic Synthesis of Enantiomerically Pure β-Amino Ketones, β-Amino Esters and β-Amino Alcohols with Baeyer-Villiger Monooxygenases

Jessica Rehdorf[a], Marko D. Mihovilovic[b], Marco W. Fraaije[c] and Uwe T. Bornscheuer[a*]

[a]University of Greifswald, Institute of Biochemistry, Department of Biotechnology & Enzyme Catalysis, Felix-Hausdorff-Str. 4, 17487 Greifswald, Germany
Fax: (+49)-3834-86-80066, e-mail: uwe.bornscheuer@uni-greifswald.de
[b]Vienna University of Technology, Institute of Applied Synthetic Chemistry, Getreidemarkt 9/163-OC, 1060 Vienna, Austria
[c]Rijksuniversiteit Groningen, Department of Biochemistry, Nijenborgh 4, 9747 AG Groningen, The Netherlands

Submitted to Advanced Synthesis & Catalysis 2009

Abstract

The enzymatic kinetic resolution of a broad set of linear aliphatic β-amino ketones was investigated using a collection of 16 Baeyer-Villiger monooxygenases originating from different bacterial origin displaying various substrate specificities. Within this platform of enzymes excellent enantioselectivities (E > 100) could be found towards linear and linear-branched aliphatic 4-amino-2-ketones and some enzymes even showed opposite enantioselectivity. The intermediate β-aminoalkyl acetates underwent autohydrolysis to yield optically pure β-amino alcohols, which are key intermediates in the synthesis of natural products and bioactive compounds of high interest for the pharmaceutical industry. Furthermore, in some cases the abnormal esters were formed.

Keywords – β-Amino alcohols, β-amino ketones, Baeyer-Villiger monooxygenases, kinetic resolution, whole cell biotransformation.

Introduction

Biotransformations have become a frequently applied strategy in synthetic routes due to the advantages of enzyme-mediated conversions, which are usually highly stereospecific and compatible with the concepts of green and sustainable chemistry. Among oxygenation processes the Baeyer-Villiger reaction is one of the most powerful and widely appreciated tool used in synthetic chemistry today.[1-3] The chemical reaction was already discovered more than 100 years ago by Adolf Baeyer and Victor Villiger[4] and describes the oxygen insertion process into a carbon-carbon bond with strict retention of configuration. With the discovery of the first Baeyer-Villiger monooxygenase (BVMO) in 1948[5], nature's enzymatic equivalent of the chemical Baeyer-Villiger oxidation was found. Compared to metal-based mediated catalytic strategies[6, 7], key advantages of enzymatic-driven Baeyer-Villiger reactions are chemo-, regio-, and stereoselectivity combined with the utilization of cheap and safe molecular oxygen as primary oxidant. Recent advances in molecular biology and gene technology accelerated exploration and investigation of new BVMOs and offered possibilities to modify and optimize the performance of a biocatalytical entity.[8-11] Therefore, the number of

recombinantly available BVMOs heavily increased during the last years, leading to an enzyme platform with a large variety of substrate specificities and complementary properties.[12, 13] The most intensively studied BVMO is the cyclohexanone monooxygenase from *A. calcoaceticus* NCIMB 9871[14] with over 100 substrates reported[15, 16], illustrative for a broad substrate profile including desymmetrization of prochiral ketones, enantiodivergent reactions and kinetic resolution[13, 16], whereas the latter one is a particularly powerful approach, since two chemically different species are generated. Today, cyclic[15, 17-20], aromatic[21, 22] as well as linear aliphatic[23-26] and aryl-aliphatic ketones[21, 27, 28], respectively, are known to be good substrates for BVMOs. However, thus far cycloketone-converting enzymes seem to be the most widespread. Recently, we investigated a set of various linear aliphatic β-hydroxy ketones as substrates in the enzymatic kinetic resolution and regioselective Baeyer-Villiger oxidation using a collection of several BVMOs originating from different bacterial origin with overlapping substrate specificity as biocatalysts[29, 30]; it seems noteworthy, that these enzymes were previously reported as mainly cycloketone converting proteins. We reported that the majority of enzymes showed high activity towards these model substrates generating optically pure 2-hydroxy alkyl acetates, which again undergo ester hydrolysis to give enantiomerically pure 1,2-diols as final product. The exchange of the hydroxyl group in beta-position to the carboxylic function into an electronically different and more demanding amino group followed by subsequent kinetic resolution, would consequently lead to β-amino alcohols, the chemical pendant to 1,2-diols, after cleavage of the β-aminoalkyl acetate intermediate. Enantiomerically pure β-amino alcohols play an increasingly important role in both the treatment of a wide variety of human disorders, e.g. ophthalmic diseases[31], and as chiral auxiliaries in asymmetric carbon-carbon bond formation. The application field of these compounds is wide and ranges from pharmaceutical intermediates, biological buffers as well as cosmetic ingredients to paintings, coatings and metalworking fluids. Moreover, the β-amino alcohol motif does not only occur in drugs, such as ephedrine, chloramphenicol or pronethalol, but is also present in e.g., adrenaline and noradrenaline. The importance of enantiomeric purity in pharmaceuticals has been demonstrated by the debilitating and sometimes harmful side-effects caused by the presence of the non-therapeutic enantiomer of an otherwise beneficial drug.

Among the few chemical methods for synthesizing racemic mixtures of β-amino alcohols, enantiomerically pure compounds are available only through the reduction of amino acids or kinetic resolution of racemic mixtures of amino alcohols or aminoalkyl acetates, often requiring expensive metal-catalysts. Furthermore, the reduction of amino acids to the corresponding amino alcohols is economically feasible only for the naturally occurring L-amino acids. The only synthetic methodologies available for the direct synthesis of amino alcohols in high yields are the enantioselective amination of chiral epoxides[32-34], the directed reductive amination of β-hydroxy ketones[35], the aminoacetoxylation of alkylenes[36] and the asymmetric hydrogenation or reduction of prochiral β-amino ketones. While aminolysis of epoxides suffers from the limitations that chiral epoxides are not readily available, are expensive, and that only mono-substituted and *trans*-symmetrically substituted epoxides can be used, metal-based reactions on the other hand require expensive transition elements (rhodium[37], palladium or ruthenium) and ligands such as BINAP. Thus far, only a few enzyme-catalyzed methodologies have been described for the synthesis of enantiomerically pure β-amino

alcohols. In the late 1990s the protease subtilisin has been subjected to the synthesis of peptidyl amino alcohols as potential specific serine proteinase inhibitors.[38] Another enzymatic approach was the synthesis of enantiopure *N*-aryl-β-amino alcohols in the kinetic resolution of racemic acetates with pig liver esterase (PLE) as shown by Sekar *et al*.[39]

In this report, we introduce an efficient approach for the enzymatic synthesis of linear aliphatic β-aminoalkyl acetates and β-amino alcohols using racemic *N*-protected β-amino ketones as starting materials and Baeyer-Villiger monooxygenases as biocatalysts (Scheme 1). Combined with the fact, that successful conversions of nitrogen containing substrates by BVMOs were reported in the literature only in a very limited number of cases[40], the possibility to form optically active β-amino alcohols via a Baeyer-Villiger oxidation is an ambitious and challenging approach. It highlights the potential of enzymatic oxygen insertion processes and demonstrates a new application of Baeyer-Villiger monooxygenases in organic chemistry.

Results and Discussion

In the present study we utilized a toolbox consisting of 16 BVMOs recombinantly expressed in *E. coli* for the kinetic resolution of β-amino ketones (for further details see experimental section). Racemic linear aliphatic *N*-protected β-amino ketones **1a**,**c**-**g** and **5a**,**b** and **5e** were synthesized by an *aza*-Michael addition with methylcarbamate as nitrogen source[41] from the corresponding α,β-unsaturated ketones generated by an aldol-addition.[42] Enzymatic kinetic resolution was performed as outlined in Scheme 1 using living *E. coli* cells bearing a plasmid with the respective BVMO-gene.

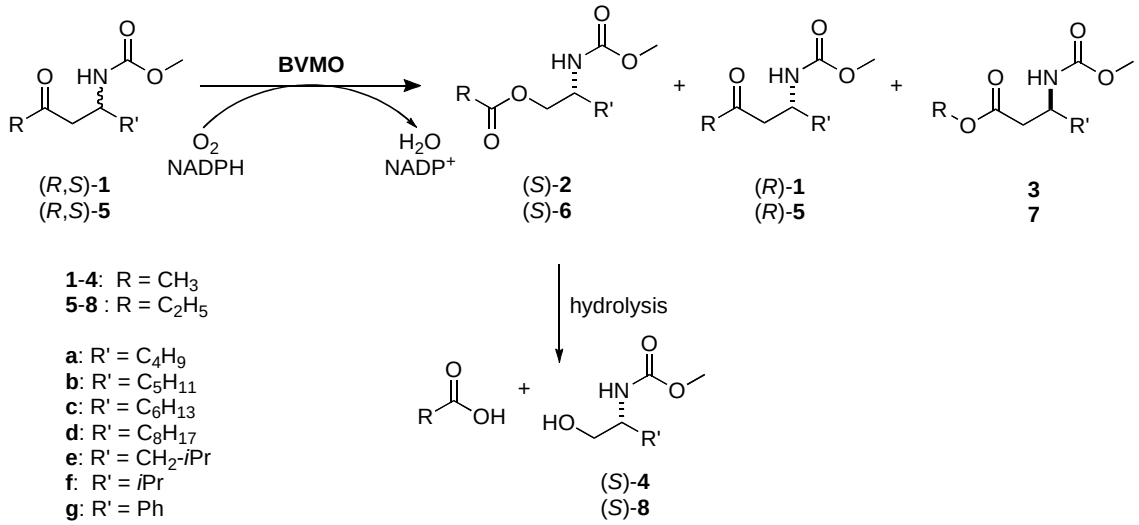

Scheme 1. Kinetic resolution of linear *N*-protected β-amino ketones using recombinant Baeyer-Villiger monooxygenases. The enzymatic oxidation yielded primarily the normal ester (**2** or **6**), which underwent hydrolysis to yield the β-amino alcohol (**4** or **8**). In few cases (see text) the abnormal esters (**3** or **7**) were also formed.

The utilization of whole-cells, expressing the desired BVMO, compared to isolated enzymes offers highly productive and "easy to handle" biocatalysts[43] combined with the advantages of endogenous co-factor regeneration, increased biocatalyst stability and renunciation of work

intensive enzyme purification. BVMO-mediated kinetic resolution was initially performed on a screening scale using 24-well plastic dishes in parallel format.[44] On the basis of these screening results, individual biotransformations were conducted as time-course experiments with selected biocatalysts in order to investigate the relationship between time, conversion, and enantiomeric excess in detail. For all substrates biotransformations were also performed in preparative scale in baffled Erlenmeyer flasks. Here, a higher oxygen input combined with a better substrate uptake due to a larger surface and an efficient distribution resulted in higher conversions and better enantiomeric excesses.

Table 1 summarizes the results from the pre-screening experiments with whole-cells expressing $CHMO_{Acineto}$, $CHMO_{Arthro}$, $CHMO_{Brachy}$, $CHMO_{Xantho}$, $CHMO_{Rhodo1}$, $CHMO_{Rhodo2}$, $CHMO_{Brevi1}$, CDMO, $HAPMO_{ACB}$ and PAMO using **1a, 1c**-**g** and **5a**, **5b** and **5e** as substrates.

Table 1. Multi-well plate screening of *N*-protected β-amino ketones with recombinant *E. coli* strains expressing Baeyer-Villiger monooxygenases of various bacterial origin.

Keton	Ester		Acineto	Arthro	Brachy	Xantho	Rhodo1	Rhodo2	Brevi1	CDMO	$HAPMO_{ACB}$	PAMO
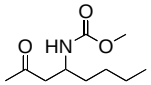	**2a**	% c[a]	35	58	53	64	45	42	37	50	14	26
		% ee_S[b]	52	>99	>99	>99	79	69	58	79	<1	22
		opt. $rot._S$ [c]	(+)	(–)	(–)	(–)	(+)	(+)	(+)	(+)	n.a.	(+)
		% ee_P[b]	96	73	89	57	95	95	>99	80	2	64
		opt. $rot._P$ [c]	(–)	(+)	(+)	(+)	(–)	(–)	(–)	(–)	n.a.	(–)
		E[d]	82	45	116	24	94	80	>200	21	1	6
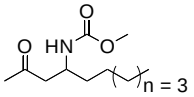	**2c**	% c[a]	3	28	16	17	8	5	30	81	74	traces
		% ee_S[b]	3	39	19	20	8	5	41	>99	27	
		opt. $rot._S$ [c]	(+)	(+)	(+)	(+)	(+)	(+)	(+)	(+)	(–)	
		% ee_P[b]	>99	>99	>99	>99	>99	>99	>99	24	10	
		opt. $rot._P$ [c]	(–)	(–)	(–)	(–)	(–)	(–)	(–)	(–)	(+)	
		E[d]	>200	>200	>200	>200	>200	>200	>200	9	2	
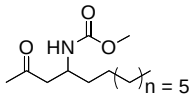	**2d**	% c[a]	n.c.	4	3	17	n.c.	n.c.	20	87	83	n.c.
		% ee_S[b]		4	3	20			25	>99	3	
		opt. $rot._S$ [c]		(+)	(+)	(+)			(+)	(+)	(+)	
		% ee_P[b]		>99	>99	>99			>99	15	9	
		opt. $rot._P$ [c]		(–)	(–)	(–)			(–)	(–)	(–)	
		E[d]		>200	>200	>200			>200	7	1	
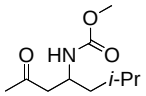	**2e**	% c[a]	44	96	80	95	67	63	31	45	n.c.	traces
		% ee_S[b]	45	>99	>99	>99	>99	98	9	56		
		opt. $rot._S$ [c]	(+)	(+)	(+)	(+)	(+)	(+)	(+)	(+)		
		% ee_P[b]	57	4	26	5	49	57	21	68		
		opt. $rot._P$ [c]	(–)	(–)	(–)	(–)	(–)	(–)	(–)	(–)		
		E[d]	6	4	10	4	14	15	2	9		

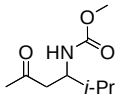	**2f**	% c[a]	2	66	25	43	15	13	4	92	41	traces
		% ee_S[b]	2	98	14	39	13	10	4	54	3	
		opt. $rot._S$ [c]	(–)	(–)	(–)	(–)	(–)	(–)	(+)	(–)	(–)	
		% ee_P[b]	67	52	43	53	71	67	97	5	6	
		opt. $rot._P$ [c]	(+)	(+)	(+)	(+)	(+)	(+)	(–)	(+)	(+)	
		E[d]	6	13	3	5	8	6	68	2	1	
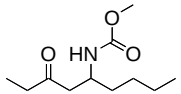	**6a**	% c[a]	n.c.	traces	traces	traces	n.c.	n.c.	n.c.	12	28	n.c.
		% ee_S[b]								13	2	
		opt. $rot._S$ [c]								(+)	(+)	
		% ee_P[b]								>99	6	
		opt. $rot._P$ [c]								(–)	(–)	
		E[d]								>200	1	
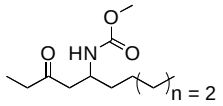	**6b**	% c[a]	n.c.	traces	traces	traces	n.c.	n.c.	n.c.	32	26	n.c.
		% ee_S[b]								42	3	
		opt. $rot._S$ [c]								(+)	(+)	
		% ee_P[b]								87	9	
		opt. $rot._P$ [c]								(–)	(–)	
		E[d]								22	1	
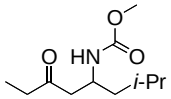	**6e**	% c[a]	n.c.	24	7	13	n.c.	n.c.	n.c.	10	n.c.	n.c.
		% ee_S[b]		31	7	15				11		
		opt. $rot._S$ [c]		(+)	(+)	(+)				(+)		
		% ee_P[b]		>99	>99	>99				>99		
		opt. $rot._P$ [c]		n.d.	n.d.	n.d.				(+)		
		E[d]		>200	>200	>200				>200		

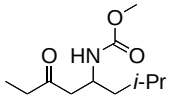	**7e**	% c[a]	n.c.	24	7	13	n.c.	n.c.	n.c.	10	n.c.	n.c.
		% ee_S[b]		31	7	15				11		
		opt. $rot._S$ [c]		(+)	(+)	(+)				(+)		
		% ee_P[b]		>99	>99	>99				>99		
		opt. $rot._P$ [c]		(–)	(–)	(–)				(+)		
		E[d]		>200	>200	>200				>200		
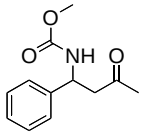	**2g**	% c[a]	75	100	100	100	82	73	15	69	n.c.	51
		% ee_S[b]	70	<1	<1	<1	>99	78	17	63		>99
		opt. $rot._S$ [c]	(+)	n.a.	n.a.	n.a.	(+)	(+)	(+)	(+)		(–)
		% ee_P[b]	24	2	2	5	22	30	>99	29		97
		opt. $rot._P$ [c]	(–)	(–)	(–)	(–)	(–)	(–)	(–)	(–)		(+)
		E[d]	3	1	1	1	9	4	>200	3		>200

Biotransformations were carried out at 24°C and monitored over 24 h. Chemical syntheses of β-amino ketones and the enzymatic syntheses of β-amino esters as standards for GC analysis as well as spectral data of all new compounds are described and given in the experimental section.; opt. rot. = optical rotation of substrate (S) or product (P); n.c. = no conversion; n.a. = not applicable; n.d. = not determined; [a] Conversion calculated from % ee_S (enantiomeric excess of substrate) and % ee_P (enantiomeric excess of product). [b] % ee_S and % ee_P were determined by chiral phase GC and calculated according to Chen *et al*.[45] [c] Sign of optical rotation is given in parentheses. [d] Enantioselectivity values were determined by computer fitting[46] of GC data from % ee_S and % ee_P.

In principle five different substrate structures can be distinguished: I) linear aliphatic 4-amino-2-ketones (**1a**, **1c**, **1d**); II) linear-branched aliphatic 4-amino-2-ketones (**1e**, **1f**); III) linear aliphatic 5-amino-3-ketones (**5a**, **5b**); IV) linear-branched aliphatic 5-amino-3-ketones (**5e**) and V) aryl-aliphatic 4-amino-2-ketones (**1g**). Comparing the results for type I substrates it becomes obvious, that all cyclohexanone-accepting enzymes ($CHMO_{Acineto}$, $CHMO_{Arthro}$, $CHMO_{Brachy}$, $CHMO_{Xantho}$, $CHMO_{Rhodo1}$, $CHMO_{Rhodo2}$) preferentially convert middle-chain 4-amino-2-ketones. While **1a** (C_8) is converted by all BVMOs with moderate to high enantioselectivities, conversion decreases dramatically with **1d** (C_{12}). Here, $CHMO_{Acineto}$, $CHMO_{Rhodo1}$ and $CHMO_{Rhodo2}$ showed even no activity. Presumably, **1d** is too bulky and cannot enter the active site. On the contrary, $HAPMO_{ACB}$ and CDMO revealed a complementary trend. While conversion for **1a** does not exceed 14% for $HAPMO_{ACB}$, **1c** and **1d** are converted much better (74% and 83% conversion, respectively). This is supported by earlier observations that both enzymes preferentially convert structurally more demanding ketones.[19, 27] Nevertheless, chain length variation does not seem to influence selectivity, since E-values for all three substrates and both enzymes remain rather poor. Investigating oxidation of **1a** in detail revealed that several BVMOs ($CHMO_{Arthro}$, $CHMO_{Brachy}$, $CHMO_{Xantho}$) convert this compound in an enantiocomplementary way. Thus, implementing $CHMO_{Brachy}$ and $CHMO_{Brevi1}$ in a kinetic resolution approach would give access to either the (*R*)- or (*S*)-enantiomer of substrate and product, both in high optical purity.

For type II substrates **1e** and **1f** the problem of sterical hindrance is even more prominent. In contrast to type I compounds, all BVMOs show moderate to high activity (conversion up to 95%, Table 1), while enantioselectivity is rather poor. Anyway, **1e** still seems to be preferred to **1f**. This might be explained by the location of the *i*-Pr group in vicinity to the carbonyl function. While for **1e** the *i*-Pr group is more distant due to an additional $–CH_2$ group, **1f** seems to be more compact. Probably, the proximity of the large terminal substitutent to the reacting center might be impedimental and therefore **1f** cannot be coordinated properly for catalysis. Thus, all cyclohexanone-converting BVMOs showed a reduced activity towards **1f**, in some cases even 20-fold lower (compare $CHMO_{Acineto}$ in Table 1). On the other hand, $HAPMO_{ACB}$ and CDMO again showed different results, which are consistent with those of **1a**, **1c** and **1d**. While **1e** is not converted at all by $HAPMO_{ACB}$, **1f** seemed to be a rather good substrate, since conversion reaches 41%. A similar effect could be observed with CDMO, where conversion increases two-fold from **1e** to **1f** (45% and 92%, respectively). Furthermore, it is worth mentioning that with the exception of $CHMO_{Brevi1}$ all other BVMOs oxidized the opposite enantiomers compared to **1e** and **1f**. While for **1e** the (–)-enantiomer is converted, for **1f** the (+)-enantiomer is preferred in all cases besides $CHMO_{Brevi1}$ that again oxidized the (-)-enantiomer. This fact might also be connected to the structural difference of both compounds. It is interesting that within this type of substrates $CHMO_{Brevi1}$ displays an enantiocomplementary behaviour compared to the other members of the BVMO collection studied. On the bases of protein sequences and biocatalytical performance all cyclohexanone- and cylopentanone-converting enzymes described so far can be clustered into two groups[47], giving access to antipodal lactones or esters. It can be noticed that $CHMO_{Brevi1}$ obviously possesses a borderline position as this behaviour was also observed in previous studies.[48]

Similar results could be obtained for the structurally more demanding type III and IV compounds, where the carboxylic function is shifted further into the center of the molecule. For

5a and **5b** only CDMO and $HAPMO_{ACB}$ showed activity, while **5e** is also accepted by $CHMO_{Arthro}$, $CHMO_{Brachy}$ and $CHMO_{Xantho}$. Interestingly, the formation of the two regioisomers **6e** and **7e** in high optical purity could be observed only for **5e**. Here, either the more substituted or the less substituted carbon center undergoes migration, leading to the 'normal' and 'abnormal' ester. Such regiodivergent biotransformations have been observed in previous studies on linear[29] and (fused) cyclic ketones.[49-54] For the other two substrates **5a** and **5b** maximum yield of the 'abnormal' ester did not go above 5%. Since the formation of regioisomeric esters is less likely using a chemical Baeyer-Villiger oxidation, it underscores the powerful capabilities of BVMOs and broadens their synthetic applicability in organic chemistry. Besides its high regioselectivity it is also noteworthy, that CDMO oxidized the opposite enantiomer of **5e** to give the 'abnormal' product **7e** compared to the cyclohexanone-converting BVMOs $CHMO_{Arthro}$, $CHMO_{Brachy}$ and $CHMO_{Xantho}$, which only generated (–)-**7e** (Table 1). Additionally, scaling the reaction (0.25 mmol substrate) and performing the biotransformation in a baffled Erlenmeyer flask (500 mL) even increased conversion of **5e** with CDMO from 9 to 20% (Table 3), probably due to a better substrate distribution and a higher oxygen input compared to a 24-well plastic plate.

Using **1g** as the only investigated aryl-aliphatic substrate revealed high activity for most of the BVMOs. Surprisingly, $HAPMO_{ACB}$ showed no conversion, although this enzyme is known to react preferentially on aromatic and aryl-aliphatic ketones. Nevertheless, PAMO, also an aryl-aliphatic-converting BVMO[55], proved to be highly selective against **1g**. Conversion even totally stopped at 50%, while for the other BVMOs it seemed that the preferred enantiomer is only converted with a slightly higher velocity than the non-preferred enantiomer, resulting in poor enantioselectivities. Furthermore, PAMO generated the enantiocomplementary product, compared to cycloketone-converting enzymes.

In order to optimize enantiomeric excess and enantioselectivities for all possible products, time-course experiments were performed. Here, samples were taken at different time intervals and conversions were stopped around 50%, when ideally only one substrate enantiomer is converted with a highly selective enzyme. For these experiments selected biocatalysts were used that showed satisfactory results in pre-screening experiments described above. The results of these biotransformations are shown in Figure 1 and all relevant data are compiled in Table 2. Best results for type I substrates **1a**, **1c** and **1d** could be achieved using $CHMO_{Brevi1}$ (E-values > 100), but also $CHMO_{Brachy}$, $CHMO_{Arthro}$ and $CHMO_{Rhodo1}$ turned out to produce excellent enantiomeric excesses (% ee > 80) and selectivities. Even after 48 h the less favored enantiomer is not converted at all by $CHMO_{Brevi1}$ and the reaction stopped at 50%. In comparison, CDMO and $HAPMO_{ACB}$, respectively, oxidized **1c** and **1d** very fast (less than 10 h for 50% conversion, data not shown), but this was accompanied with a loss of enantioselectivity as E-values were not higher than 13 (Table 2). Performing time-course experiments with **1e** showed an increased enantioselectivity using $CHMO_{Rhodo1}$ and $CHMO_{Rhodo2}$. Conversion was stopped around 60% and E-values could therefore be enhanced slighlty from 15 to 29 for $CHMO_{Rhodo2}$, suggesting that the (+)-enantiomer is only insignificantly faster oxidized compared to the (–)-enantiomer.

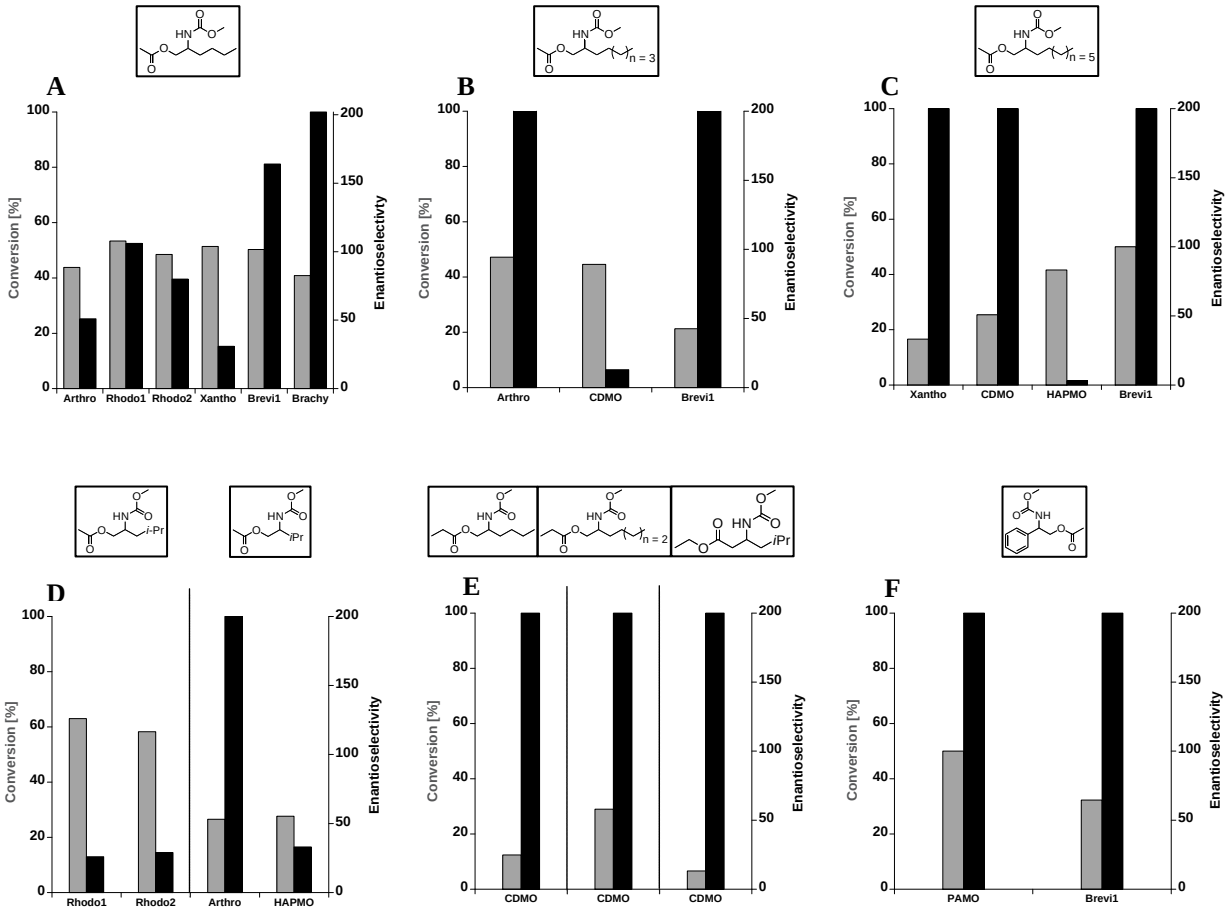

Figure 1. Conversions (grey) and enantioselectivites (black) achieved using different BVMOs recombinantly expressed in *E. coli* and **1a** (A), **1c** (B), **1d** (C), **1e** and **1f** (D), **5a**, **5b** and **5e** (E) and **1g** (F) as substrates.

Investigating the relationship between time and enantiomeric excess for the product of **1f** using $CHMO_{Arthro}$ on the other hand revealed that stopping conversion before 50% could lead to an improved enantioselectivity. After 24 h already 66% of **1f** had been oxidized and selectivity was rather low (E-value of 13,Table 1), while below 50% conversion enantioselectivity was much higher (E > 200).

Table 2. Microbial Baeyer-Villiger oxidations of the *N*-protected β-amino ketones **1a** and **1c**-**g** using recombinant whole cells of *E. coli* expressing BVMOs from different bacterial orgin.

Ester formed	BVMO	time [h]	conversion [%][a]	ee_S [%][b]	ee_P [%][b]	E[c]
2a	Arthro	6	44	72	92 (+)	51
	Rhodo1	42	53	>99	87 (–)	106
	Rhodo2	24	49	88	93 (–)	80
	Xantho	6	52	89	83 (+)	31
	Brevi1	42	51	97	95 (–)	164
	Brachy	6	41	68	98 (+)	>200
2b	Arthro	168	47	90	>99 (–)	>200
	CDMO	6	45	61	76 (–)	13
	Brevi1	168	21	27	99 (–)	>200
2c	Xantho	20	17	20	>99 (–)	>200
	CDMO	8	25	34	>99 (–)	>200
	$HAPMO_{ACB}$	6	42	25	35 (–)	3
	Brevi1	20	50	>99	>99 (–)	>200
2e	Rhodo1	20	61	>99	61 (–)	27
	Rhodo2	20	58	99	71 (–)	29
2f	Arthro	5	27	36	>99 (+)	>200
	$HAPMO_{ACB}$	20	28	35	91 (+)	33
2g	PAMO	6	50	>99	>99 (+)	>200
	Brevi1	120	32	48	>99 (–)	>200

Biotransformations were carried out at 24°C and monitored over 7 d. Samples were taken at definite time intervals. [a]Conversion calculated from % ee_S (enantiomeric excess of substrate) and % ee_P (enantiomeric excess of product). [b]% ee_S and % ee_P were determined by chiral phase GC and calculated according to Chen *et al*.[45]; sign of optical rotation is given in parentheses. [c]Enantioselectivity values were determined by computer fitting of GC[46] data from % ee_S and % ee_P.

Also linear and linear-branched aliphatic 5-amino-3-ketones were subjected to time-course experiments, but even after 7 d conversion could not be increased further (data not shown). The best results for **5a**, **5b** and **5e** could be obtained with CDMO (Table 1). However, preparative scale experiments in baffled shaking flasks (500 mL) could improve conversions up to three-fold without compromising enantioselectivity (Table 3). Obviously, these conditions led to a better substrate distribution and limitations in oxygen input are minimized due to an increase in surface area, which is necessary for a sufficient cell growth and enzyme activity.

With the exception of $HAPMO_{ACB}$, all other BVMOs oxidized **1g** quite fast, although nevertheless time-course experiments did not reveal an increase in selectivity at 50% conversion. Only two enzymes of the collection investigated converted this aryl-aliphatic compound in high selectivity. An excellent E-value (> 99% ee) at a conversion of 33% could be obtained with $CHMO_{Brevi1}$after 7 d, suggesting that the **1g**-(–)-enantiomer is not accepted and therefore not converted. PAMO oxidized **1g** highly selective with full conversion of the (+)-enantiomer after 6 h, without converting the (–)-enantiomer within the next days. Thus,

utilizing PAMO on one hand would yield the (+)-ester (50% conversion), but using $CHMO_{Brevi1}$ on the other hand gives access to the (–)-ester (32% conversion), both in very high optical purity (E > 200), as shown in Table 2.

Table 3. Preparative scale biotransformation (0.25 mmol substrate) of **5a**, **5b** and **5e** with CDMO recombinantly expressed in *E. coli*.

Ester	conversion [%][a]	ee_S [%][b]	ee_P [%][b]	E[c]
6a	35	54	>99 (–)	>200
6b	41	58	84 (–)	20
7e	20	22	>99 (+)	>200

Preparative biotransformations (0.25 mmol substrate) were carried out at 24°C. [a]Conversion calculated from % ee_S (enantiomeric excess of substrate) and % ee_P (enantiomeric excess of product). [b]% ee_S and % ee_P were determined by chiral phase GC and calculated according to Chen *et al*.[45] Sign of optical rotation is given in parentheses.
[d]Enantioselectivity values were determined by computer fitting of GC[46] data from % ee_S and % ee_P.

Aligning the crystal structures of PAMO[56] and a cyclohexanone monooxygenase from *Rhodococcus sp*.[57] a close homolog of $CHMO_{Rhodo}$ from *Rhodococcus* Phi1 (protein identity > 89 %), and performing docking experiments with **1g** displayed a possible reason for PAMO's high affinity and enantioselectivity towards only one enantiomer of this substrate. A comparison of the putative binding pockets of both enzymes revealed two amino acids in PAMO (Ser441 and Ala442) part of a loop segment ("bulge" 441-444) in proximity to the reactive peroxy group of the FAD (Figure 2A). In fact, the reduced space due to a stretched loop in PAMO might be the reason that only the (*R*)-enantiomer can be oxidized, whereas the (*S*)-enantiomer does not fit properly because of sterical hindrance (Figure 2B). These two additional amino acids are missing in $CHMO_{Rhodo}$ resulting in a larger binding pocket resulting in a rather unselective conversion of **1g**. Furthermore, the distance between the reaction center of (*R*)-**1g** and the C4a atom of FAD is about 4 Å (compared to the (*S*)-enantioer with 8 Å), which means that the reactive flavin peroxy-species is spatially close enough to the carbonyl group of the substrate to perform a Baeyer-Villiger oxidation. The relationship between the loop segment Ser441-Al442-Leu443-Ser444 of PAMO and its selectivity and combined thermostability was also outlined in previous studies on rational protein design.[10, 58-61]
Performing a protein sequence alignment of PAMO, $CHMO_{Rhodo1}$ and other cyclohexanone monooxygenases that were also subjected to kinetic resolution with *N*-protected β-amino-4-phenylbutan-2-one, it could be shown that the missing amino acids within the bulge among these monooxygenases might be also reasonable for the reduced enantioselectivity of CHMOs (Figure 3).

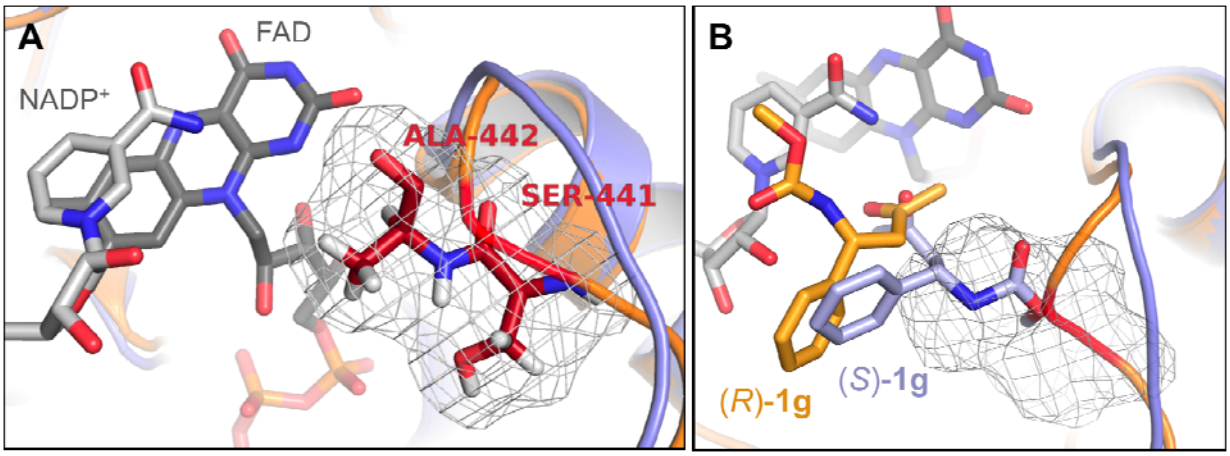

Figure 2. Comparison of both putative binding pockets of PAMO (orange) and CHMO (light blue) from *Rhodococcus sp*. aligned from both crystal structures[56, 57] (A) without and (B) with **1g** in both configurations ((*R*)-**1g** is marked in orange, (*S*)-**1g** in light blue). FAD (dark grey) and $NADP^+$ (light grey) are shown as sticks. Residues Ser441 and Ala442 and backbone amino acid chain are highlighted in red.

```
PAMO          PNLFFIAGPGSPSALSNMLVS
CHMO_Brevi2   PNLMFLYGPQSPSGFCNGTDF
CHMO_HI-31    PNMFMILGPNGP--FTNLPPT
CHMO_Rhodo1   PNWFMVLGPNGP--FTNLPPS
CHMO_Acineto  PNMFMVLGPNGP--FTNLPPS
CHMO_Brevi1   PNFLMSLGPQTP--YSNLVVP
```

Figure 3. Alignment of six BVMO protein sequences highlighting the loop segment 441-444 (green box, residues 441 and 442 are written in bold letters), which is closely related to PAMO's enantioselectivity in kinetic resolution of *N*-protected β-amino-4-phenylbutan-2-one. Code: phenylactone monooxygenase from *T. fusca* (PAMO: 1wx4), cyclohexanone monooxygenase from *Brevibacterium* sp. HCU (CHMO_Brevi2: AAG01290), cyclohexanone monooxygenase from *Rhodococcus* sp. HI-31 (CHMO_HI-31:), cyclohexanone monooxygenase from *Rhodococcus* sp. Phi1 (CHMO_Rhodo1:), cyclohexanone monooxygenase from *A. calcoaceticus* NCIMB 9871 (CHMO_Acineto: BAA86293), and cyclohexanone monooxygenase from *Brevibacterium* sp. HCU (CHMO_Brevi1: AAG01289).

Kinetic resolution of β-amino ketones can be an attractive tool in organic chemistry since two different optically active species are formed, which additionally differ in their configuration: besides the residual β-amino ketone also a β-aminoalkyl acetate is generated. Interestingly, this aminoalkyl acetate can undergo autohydrolysis to give enantiomerically pure *N*-protected β-amino alcohols, which are highly valuable building blocks in the pharmaceutical industry. Since ester hydrolysis proceeds without any conformational changes, the resulting β-amino alcohols possess the same absolute configuration as the aminoalkyl acetates. The maximum amount of generated *N*-protected β-amino alcohol observed was 56% after 7 d using **1c** as starting material and CDMO as biocatalyst. It seems that with a decrease in pH due to cell metabolism, the ester bond of the Baeyer-Villiger product is cleaved resulting in the formation of acetic acid and the corresponding β-amino alcohol. For all ketones, where alcohol production was detected (Figure 3), spontaneous ester hydrolysis started 30 h and 42 h, respectively, after substrate addition. This observation makes the kinetic resolution of linear

β-amino ketones even more sophisticated since a third interesting, bioactive and valuable compound can be generated in high optical purity.

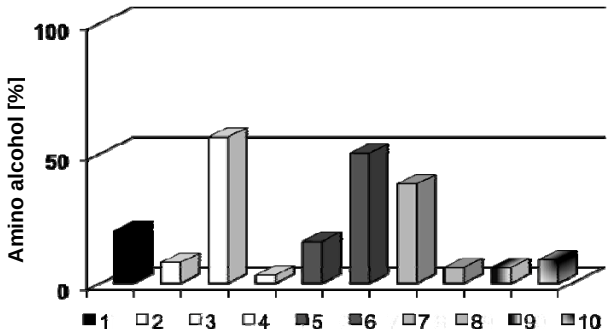

Figure 3. Formation of *N*-protected 2-amino alcohols after autohydrolysis of corresponding 2-amino esters. 1 = **4a**, $CHMO_{Arthro}$; 2 = **4c**, $CHMO_{Arthro}$; 3 = **4c**, CDMO; 4 = **4c**, $CHMO_{Brevi1}$; 5 = **4e**, $CHMO_{Rhodo1}$; 6 = **4e**, $CHMO_{Brachy}$; 7 = **4f**, $CHMO_{Arthro}$; 8 = **4f**, $CHMO_{Brachy}$; 9 = **8b**, CDMO; 10 = **8e**, $CHMO_{Arthro}$.

Conclusions

Within these studies we could demonstrate that BVMOs indeed can be a very attractive and useful biocatalytic tool to generate chiral synthons of high interest for pharmaceutical, food, and synthetic chemical industry. Besides formation of enantiomerically pure linear aliphatic β-aminoalkyl esters and residual β-amino ketones, respectively, they also proved to be capable of allowing access to compounds like β-amino alcohols, which do not belong to the common products usually associated with the enzymatic Baeyer-Villiger oxidation. Similar possibilities have been shown in earlier studies on the hydroxy-counterpart in beta-position of the carboxylic function.[29] Regarding this potential BVMOs seem to be widely applicable in organic chemistry since they are able to convert substituents with different inductive effects and electronic environments in vicinity to the carboxylic group. Moreover, the majority of investigated BVMOs, which goes along with the majority of recombinantly available BVMOs today, not only accepts *N*-protected β-amino ketones as substrates, they even oxidize them in a highly selective manner leading to optically active and enantiocomplementary products. Within the five different structural types of racemic substrates examined in this contribution, the short-chain linear aliphatic 4-amino-2-ketones as well as the aryl-aliphatic amino ketone revealed to be the best substrates regarding conversion and enantioselectivity. In both cases several BVMOs could be identified yielding the opposite enantiomers of product ester and residual ketone. For all other substrates the number of suitable BVMOs decreased, but still certain biocatalysts could be identified performing kinetic resolutions enantioselectively. Furthermore, it could be shown for linear-branched 5-amino-3-ketones, that BVMOs possess a regioselectivity, not accessible utilizing the chemical Baeyer-Villiger reaction, leading to the abnormal product in high enantiomeric excess. The excellent enantioselectivity combined with the chemo- and naturally occurring regioselectivity makes the enzymatic Baeyer-Villiger oxidation an essential strategy and method for the synthesis of optically active valuable compounds and solutions in the chemical industry.

Experimental Section

Chemical Synthesis

Unless otherwise stated, all chemicals and microbial growth media were purchased from commercial suppliers and used without further purification. All solvents were distilled prior to use. Flash column chromatography was performed on silica gel 60 from Merck (40-63 µm). NMR-spectra were recorded from $CDCl_3$ solution on a Bruker AC 200 (200 MHz) and chemical shifts are reported in ppm using TMS as internal standard. Combustion analysis was carried out in the Microanalytic Laboratory, University of Vienna, while mass spectra analysis was performed at the University of Greifswald. Analyses of purified products and sample measurements were performed on a Thermo Focus DSQ (quadropol, EI+) using a capillary column BGB5 (5% diphenyl-, 95% dimethylpolysiloxane, 30 m x 0.25 mm ID). Enantiomeric excesses were determined by chiral-phase GC (Thermo Trace and Focus) using a BGB 175 (2,3-diacetyl-6-*tert*-butyldimethylsilyl-γ-cyclodextrin, 30 m x 0.25 mm ID) or a hydrodex β-TBDAc column (30 m x 0.25 mm ID). Specific optical rotations, $[\alpha]_D^{20}$ were determined using a Perkin Elmer Polarimeter 241.

Bacterial Strains and Growth Conditions

E. coli containing the plasmids for the particular BVMOs were routinely cultivated on LB-agar (1% Bacto-Peptone, 0.5% Bacto-Yeast Extract, 1% NaCl, 1.5% agar) plates supplemented by ampicillin (200 µg mL^{-1}) and stored as frozen stocks (15 % glycerol) at –80°C. Liquid cultures were grown in standard LB media (1% Bacto-Peptone, 0.5% Bacto-Yeast Extract, 1% NaCl) supplemented with ampicillin (LB_{amp}) in baffled Erlenmeyer flasks on an orbital shaker (120 rpm at 37°C).

Substrate synthesis

General procedure for chemical syntheses of linear *N*-protected-β amino ketones: synthesis of **1a, 1c-1g** and **5a**, **5b** and **5e** was performed in two reaction steps: an aldol addition leading to α,β-unsaturated ketones followed by an *aza*-Michael addition. With the exception of 5-methyl-hexen-2-one, 3-octen-2-one, 3-decen-2-one and 4-phenyl-3-buten-2-one, which were commercially avalaible, all other α,β-unsaturated ketones were synthesized by aldol addition as described by Kourouli *et al*.[42], purified by vacuum distillation (> 99%) or medium pressure liquid chromatography (MPLC) and used as starting material in an *aza*-Michael-addition.[41] Here, methylcarbamate served as nitrogen donor, tributylphosphine as catalyst and TMSCl as reaction starter. All reactions were carried out in dry dichloromethane under vigorous stirring at room temperature or under reflux. After the reaction was completed (usually after 2-7 days, monitored by TLC), the mixture was quenched with saturated sodium bicarbonate and extracted three times with chloroform. The organic layers were combined, dried over anhydrous sodium sulphate, filtered and the solvent was evaporated. The crude products were purified via silica gel chromatography (petrol ether/ethyl acetate: 10:1 or 5:1). Both linear α,β-unsaturated ketones as well as *N*-protected-β-amino ketones were identified and analyzed by GCMS and $^1H/^{13}C$-NMR.

Physical and spectral data of chemically synthesized α,β-unsaturated ketones

3-dodecen-2-one ($C_{12}H_{22}O$): obtained from ethyl acetoacetate (12.87 g, 0.1mol) and *n*-decanal (7 g, 0.05 mol) as a colorless liquid (500 mg, yield 21%) as described by Kourouli *et al*.[42]

6-methyl-3-hepten-2-one ($C_8H_{14}O$): obtained from ethyl acetoactate (12.78 g, 0.1 mol) and *iso*-valeraldehyde (4.7 g, 0.05 mol) as a colorless liquid (4 g, yield 85%) as described by Kourouli *et al*.[42]

4-nonen-3-one ($C_9H_{16}O$): obtained from ethyl propionylacetate (14 g, 0.1 mol) and *n*-valeraldehyde (4.7 g, 0.05 mol) as a yellowish liquid (1.5 g, yield 38%) as described by Kourouli *et al*.[42]

4-decen-3-one ($C_{10}H_{18}O$): obtained from ethyl propionylacetate (14 g, 0.1 mol) and capronaldehyde (5 g, 0.05 mol) as a yellow liquid (2.5 g, yield 50%) as described by Kourouli *et al*.[42]

7-methyl-4-octen-3-one ($C_9H_{16}O$): obtained from ethyl propionylacetate (3 g, 0.2 mol) and *iso*-valeraldehyde (1.7 g, 0.2 mol) as a colorless liquid (1 g, yield 58%) as described by Kourouli *et al*.[42]

Physical and spectral data of chemically synthesized *N*-protected β-amino ketones

1a ($C_{10}H_{19}NO_3$): obtained from 3-octen-2-one (1.5 g, 10 mmol), methylcarbamate (900 mg, 12 mmol), (*n*-Bu)$_3$P (250 mg, 1 mmol) and TMSCl (1.4 g, 11 mmol) as a colorless solid (920 mg, 51%); mp: 38-40°C; specific rotation of sample obtained from enzymatic kinetic resolution: $[\alpha]_D^{20}$ = +33.4 (c 1.03, $CHCl_3$; ee = 94%); δ_H (200 MHz, $CDCl_3$, 25°C) 0.87 (t, *J* = 6.6 Hz, 3H), 1.21-1.51 (m, 6H), 2.14 (s, 3H), 2.64 (d, *J* = 5.4 Hz, 2H) 3.63 (s, 3H), 3.80-3.97 (m, 1H), 5.01-5.10 (m, 1H); δ_C (50 MHz, $CDCl_3$, 25°C) 13.9 (q), 22.4 (t), 28.4 (t), 30.5 (q), 34.2 (t), 47.8 (d), 48.0 (t), 51.9 (q), 156.6 (s), 207.8 (s); ESI-MS-TOF (70 eV) *m/z* (%): 236 (100), $[M+2H_2O-1]^-$, 200 (9) $[M-1]^-$, 193 (9) $[158+2H_2O-1]^-$, 182 (50) $[M-H_2O-1]^-$.

1c ($C_{12}H_{23}NO_3$): obtained from 3-decen-2-one (1.8 g, 10 mmol), methylcarbamate (900 mg, 12 mmol), (*n*-Bu)$_3$P (250 mg, 1 mmol) and TMSCl (1.4 g, 11 mmol) as a colorless solid (1.3 g, 61%); mp: 50-52°C; specific rotation of sample obtained from enzymatic kinetic resolution: $[\alpha]_D^{20}$ = +28.3 (c 1.20, $CHCl_3$; ee = 99%); δ_H (200 MHz, $CDCl_3$, 25°C) 0.88 (t, *J* = 7 Hz, 3H), 1.23-1.61 (m, 10H), 2.15 (s, 3H), 2.65 (d, *J* = 6 Hz, 2H), 3.64 (s, 3H), 3.82-3.98 (m, 1H), 5.09-5.18 (m, 1H); δ_C (50 MHz, $CDCl_3$, 25°C) 13.9 (q), 22.5 (t), 26.1 (q), 28.9 (t), 30.5 (t), 31.7 (t), 34.5 (t), 47.9 (d), 48.1 (t), 51.9 (q), 156.6 (s), 207.8 (s); combustion analysis: 63.14% C (calc.: 62.85% C); 9.99% H (calc.: 10.11% H); 6.09% N (calc.: 6.11% N).

1d ($C_{14}H_{27}NO_3$): obtained from 3-dodecen-2-one (770 mg, 3 mmol), methylcarbamate (300 mg, 4 mmol), (*n*-Bu)$_3$P (60 mg, 0.3 mmol) and TMSCl (400 mg, 3.7 mmol) as a colorless solid (280 mg, 51%); mp: 62-64°C; specific rotation of sample obtained from enzymatic kinetic resolution: $[\alpha]_D^{20}$ = +7.1 (c 0.56, $CHCl_3$; ee = 30%); δ_H (200 MHz, $CDCl_3$, 25°C) 0.86 (t, *J* = 6.6 Hz, 3H), 1.24-1.48 (m, 14H), 2.14 (s, 3H), 2.64 (d, *J* = 5.4 Hz, 2H), 3.63 (s, 3H), 3.83-3.94 (m, 1H), 4.99-5.08 (m, 1H); δ_C (50 MHz, $CDCl_3$, 25°C) 14.2 (q), 22.8 (t), 26.4 (q), 29.3 (t), 29.5 (t), 30.7 (t), 31.9 (t), 34.7 (t), 48.0 (d), 48.2 (t), 52.1 (q), 156.7 (s), 207.3 (s); combustion analyis: 66.01% C (calc.: 65.33% C), 10.43% H (calc.: 10.57% H), 5.44% N (calc.: 5.44% N).

1e ($C_{10}H_{19}NO_3$): obtained from 6-methyl-3-hepten-2-one (4 g, 30 mmol), methylcarbamate (2.7 g, 36 mmol), (*n*-Bu)$_3$P (600 mg, 3 mmol) and TMSCl (3.6 g, 33 mmol) as a yellow liquid (2.5 g, 52%); specific rotation of sample obtained from enzymatic kinetic resolution: $[\alpha]_D^{20}$ = +49.9 (c 0.70, $CHCl_3$; ee = 99%); δ_H (200 MHz, $CDCl_3$, 25°C) 0.89 (d, *J* = 6.6 Hz, 6H), 1.15-1.32 (m, 1H), 1.40-1.1.68 (m, 2H), 2.12 (s, 3H), 2.63 (d, *J* = 5.4 Hz, 2H), 3.62 (s, 3H), 3.85-4.08 (m 1H), 5.01-5.11 (m, 1H); δ_C (50 MHz, $CDCl_3$, 25°C) 22.1 (q), 23.1 (q), 25.1 (d), 30.7 (q), 43.7 (d), 46.3 (t), 48.3 (t), 52.1 (q), 156.6 (s), 208.0 (s); ESI-MS-TOF (70 eV) *m/z* (%): 236 (15) $[M+2H_2O-H]^-$, 182 (7) $[M-H_2O-1]^-$.

1f ($C_9H_{17}NO_3$): obtained from 5-methyl-3-hexen-2-one (5.6 g, 50 mmol), methylcarbamate (4.5 g, 60 mmol), (*n*-Bu)$_3$P (1.01 g, 5 mmol) and TMSCl (6 g, 55 mmol) as a yellow liquid (2.3 g, 34%); specific rotation of sample obtained from enzymatic kinetic resolution: $[\alpha]_D^{20}$ = –50.2 (c 0.43, $CHCl_3$; ee = 99%); δ_H (200 MHz, $CDCl_3$, 25°C) 0.91 (d, *J* = 6.8 Hz, 6H), 1.79-1.95 (m, 1H), 2.16 (s, 3H), 2.61 (d, *J* = 6 Hz, 2H), 3.63 (s, 3H), 3.69-3.89 (m, 1H), 5.02-5.10 (m, 1H); δ_C (50 MHz, $CDCl_3$, 25°C) 18.6 (q), 19.5 (q), 30.4 (q), 31.8 (d), 45.8 (t), 52.2 (d), 53.5 (q), 156.7 (s), 208.0 (s); ESI-MS-TOF (70 eV) *m/z* (%): 355 (25) $[2M-H_2O-H]^-$, 337 (20) $[2M-2H_2O-1]^-$, 222 (33) $[M+2H_2O-1]^-$.

1g ($C_{12}H_{15}NO_3$): obtained from 4-phenyl-3-buten-2-one (1.95 g, 13.3 mmol), methylcarbamate (1.2 g, 16 mmol), (*n*-Bu)$_3$P (270 mg, 1.3 mmol) and TMSCl (1.88 g, 14.7 mmol) as a yellow oil (810 mg, 35%); specific rotation of sample obtained from enzymatic kinetic resolution: $[\alpha]_D^{20}$ = –11.7 (c 1.84, $CHCl_3$; ee = 87%); δ_H (200 MHz, $CDCl_3$, 25°C) 2.02 (s, 3H), 2.77-3.05 (dd, *J* = 16.4 Hz and 6.6 Hz, 2H), 3.57 (s, 3H), 5.03-5.10 (m, 1H), 5.59-5.68 (m, 1H), 7.05-7.15 (m, 5H); δ_C (50 MHz, $CDCl_3$, 25°C) 14.1 (q), 48.9 (t), 51.4 (d), 52.2 (q), 126.9 (t), 126.9 (t), 128.3 (t), 128.3 (t), 128.6 (t), 141.2 (d), 156.3 (s), 206.8 (s).

5a ($C_{11}H_{21}NO_3$): obtained from 4-nonen-3-one (1.4 g, 10 mmol), methylcarbamate (900 mg, 12 mmol), (*n*-Bu)$_3$P (202 mg, 1 mmol) and TMSCl (1.2 g, 11 mmol) as a colorless solid (568 mg, 34%); mp: 40-42°C; specific rotation of sample obtained from enzymatic kinetic resolution: $[\alpha]_D^{20}$ = +16.8 (c 0.37, $CHCl_3$; ee = 54%); δ_H (200 MHz, $CDCl_3$, 25°C) 0.85 (t, *J* = 6.8 Hz, 3H), 1.03 (t, *J* = 7.4 Hz, 3H), 1.25-1.72 (m, 6H), 2.42 (q, *J* = 7.4 Hz, 2H), 2.63 (dd, *J* = 5.4 and 2.4 Hz, 2H), 3.64 (s, 3H), 3.81-3.99

(m, 1H), 5.04-5.17 (m, 1H); δ_C (50 MHz, $CDCl_3$, 25°C) 7.7 (q), 14.1 (q), 22.6 (t), 28.6 (t), 34.4 (t), 36.7 (t), 46.6 (d), 48.3 (t), 52.1 (q), 156.7 (s), 210.1 (s); combustion analysis or ESI-MS-TOF not applicable.
5b ($C_{12}H_{23}NO_3$): obtained from 4-decen-3-one (2.46 g, 16 mmol), methylcarbamate (1.44 g, 19 mmol), (*n*-Bu)$_3$P (324 mg, 1.6 mmol) and TMSCl (1.91 g, 17.6 mmol) as a colorless solid (1.2 g, 41%); mp: 44-46°C; specific rotation of sample obtained from enzymatic kinetic resolution: $[\alpha]_D^{20}$ = +23.8 (c 0.20, $CHCl_3$; ee = 58%); δ_H (200 MHz, $CDCl_3$, 25°C) 0.88 (t, *J* = 6.6 Hz, 3H), 1.03 (t, *J* = 7.2 Hz, 3H), 1.21-1.75 (m, 8H), 2.42 (q, *J* = 7.4 Hz, 2H), 2.62 (dd, *J* = 5.2 Hz and 2.8 Hz, 2H), 3.64 (s, 3H), 3.81-3.99 (m, 1H), 5.01-5.13 (m, 1H); δ_C (50 MHz, $CDCl_3$, 25°C) 7.7 (q), 14.1 (q), 22.7 (t), 26.1 (t), 31.7 (t), 34.6 (t), 36.7 (t), 46.6 (d), 48.3 (t), 52.1 (q), 156.7 (s), 210.7 (s); combustion analysis: 62.59% C (calc.: 62.85% C), 10.05% H (calc.: 10.11% H), 6.14% N (calc.: 6.11% N).
5e ($C_{11}H_{21}NO_3$): obtained from 7-methyl-4-octen-3-one (980 mg, 7 mmol), methylcarbamate (630 mg, 8.4 mmol), (*n*-Bu)$_3$P (141.6 mg, 0.7 mmol) and TMSCl (837 mg, 7.7 mmol) as a colorless liquid (351 mg, 30%); specific rotation of sample obtained from enzymatic kinetic resolution: $[\alpha]_D^{20}$ = +10.2 (c 0.60, $CHCl_3$; ee = 22%); δ_H (200 MHz, $CDCl_3$, 25°C) 0.91 (d, *J* = 6.4 Hz, 6H), 1.03 (t, *J* = 6.6 Hz, 3H), 1.20-1.27 (m, 1H), 1.41-1.72 (m, 2H), 2.41 (q, *J* = 7.2 Hz, 2H), 2.62 (d, *J* = 3.6 Hz, 2 H), 3.63 (s, 3H), 3.89-4.05 (m, 1H), 5.04-5.11 (m, 1H); δ_C (50 MHz, $CDCl_3$, 25°C) 7.7 (q), 22.1 (q), 23.2 (q), 25.1 (d), 36.7 (t) 43.8 (d), 46.4 (t), 46.9 (t), 52.1 (q), 156.7 (s), 210.7 (s); ESI-MS-TOF (70 eV) *m/z* (%): 250 (100) $[2M+2H_2O-H]^-$, 233 (60) $[M-H_2O]^-$, 204 (45) $[186+H_2O]^-$, 190 (50) $[172+H_2O]^-$, 181 (30) $[200-H_2O-1]^-$, 154 (50) $[172-H_2O]^-$, 139 (12) $[158-H_2O-1]^-$.

Biotransformations

All biotransformations were conducted using recombinant BVMOs from different bacterial origin expressed in *E. coli*. The following BVMOs were investigated for their substrate specificity towards linear aliphatic β-amino ketones:
Cyclohexanone monooxygenase from *A. calcoaceticus* NCIMB 9871 ($CHMO_{Acineto}$)[14] and seven other cyclohexanone monooxygenases ($CHMO_{Arthro}$ from *Arthrobacter sp*.[62], $CHMO_{Brachy}$ from *Brachymonas sp*.[63], $CHMO_{Brevi1}$ and $CHMO_{Brevi2}$ from *Brevibacterium sp*.[64], $CHMO_{Rhodo1}$ and $CHMO_{Rhodo2}$ from *Rhodococcus sp*.[62], $CHMO_{Xantho}$ from *Xanthobacter sp*. ZL5[17] as well as cyclopentanone monooxygenase (CPMO) from *Comamonas sp*. NCIMB 9872[18] and cylododecanone monooxygenase (CDMO) from *Rhodococcus ruber* SC1.[20] Also arylketone-converting BVMOs like the 4-hydroxyacetophenone monooxygenase from *P. putida* JD1 ($HAPMO_{PpJD1}$)[21], the 4-hydroxyacetophenone monooxygenase from *P. fluorescens* ACB ($HAPMO_{ACB}$)[22] as well as phenylacetone monooxygenase from *T. fusca* (PAMO)[28] have been investigated, followed by alkylketone-converting BVMOs from *P. putida* KT2440 ($BVMO_{PpKT2440}$)[24], *P. fluorescens* DSM 50106 ($BVMO_{Pfl}$)[23] and *M. tuberculosis* H37Rv ($BVMO_{Mtb5}$).[65] Since CPMO, $CHMO_{Brevi2}$, $HAPMO_{PpJD1}$, $BVMO_{PpKT2440}$, $BVMO_{Pfl}$ and BVMOMtb5 did not show activity against any substrate they were excluded from the results section.
Typical procedure for screening experiments
Analytical screening experiments were performed in 24-well plates. For this, precultures were inoculated with a single colony from a plate (LB_{amp}) and incubated at 37°C overnight (in case of CHMO from *Xanthobacter* sp. at 30°C) in an orbital shaker in a baffled Erlenmeyer flask. After 20 h LB_{amp} (20 mL) was inoculated with 1% of the overnight preculture and incubated at 37 and 30°C, respectively, until OD_{600nm} reached 0.6-0.8 (usually after 3 h). Then, BVMO expression was induced with either IPTG (0.1 mM, final concentration) or in case of $HAPMO_{ACB}$ and PAMO with L-arabinose (0.2% (w/v), final concentration). Protein expression was performed at 24°C for 2 h. Then, 1 mL bacterial culture was transferred into each well of the 24-well plate followed by subsequent substrate addition (1 mM, in dioxane). Biotransformations were carried out at 24°C and analyzed after 24 h. Samples were extracted with ethyl acetate supplemented with 1 mM of an internal standard (benzoic acid methylester), dried over anhydrous sodium sulphate and examined using GC analysis.

Conduction of time-course experiments

Time-course experiments were performed as described for screening experiments, with samples to be taken at definite time intervals (2, 4, 6, 8, 10, 24, 30 and 48 h).

Preparative scale experiments

For preparative scale experiments a baffled flask filled with LB_{amp} (500 mL) was inoculated with 1% of the overnight preculture and incubated at 37°C in an orbital shaker. At OD_{600nm} 0.6-0.8 protein expression was induced with IPTG (0.1 mM) or L-arabinose (0.2% (w/v)) followed by substrate addition (0.25 mmol, in dioxane,). Protein expression and subsequent biotransformations were performed at 24°C. At a conversion of about 50% the whole volume was extracted four times with ethyl acetate (100 mL each). The organic layers were combined, dried over anhydrous sodium sulphate and the organic solvent was evaporated. The crude product was purified via silica gel chromatography (petrol ether/ethyl acetate) and finally the amino ketone and the corresponding amino ester were analyzed via GC, GCMS and $^{1}H/^{13}C$-NMR.

Physical and spectral data of enzymatically synthesized *N*-protected β-amino esters

2a ($C_{10}H_{19}NO_4$): obtained enzymatically via biotransformation of **1a** (0.25 mmol, 51 mg) with $CHMO_{Brevi1}$ as a colorless liquid (32 mg, 63%); specific rotation of sample obtained from enzymatic kinetic resolution: $[\alpha]_D^{20}$ = –34.3 (c 1.60, $CHCl_3$; ee = 97%); δ_H (200 MHz, $CDCl_3$, 25°C) 0.87 (t, *J* = 6.6 Hz, 3H), 1.29-1.53 (m, 6H), 2.05 (s, 3H), 3.65 (s, 3H), 3.75-3.95 (m, 1H), 4.04 (d, *J* = 4.5 Hz, 2H), 4.66-4.79 (m 1H); δ_C (50 MHz, $CDCl_3$, 25°C) 13.9 (q), 20.8 (q), 22.4 (t), 27.9 (t), 31.5 (t), 50.2 (d), 52.1 (q), 66.1 (t), 156.6 (s), 171.0 (s).

2c ($C_{12}H_{23}NO_4$): obtained enzymatically via biotransformation of **1c** (0.25 mmol, 58 mg) with $CHMO_{Brevi1}$ as a colorless solid (24 mg, 42%); mp: 61-63°C; specific rotation of sample obtained from enzymatic kinetic resolution: $[\alpha]_D^{20}$ = –26.8 (c 1.65, $CHCl_3$; ee = 96%); δ_H (200 MHz, $CDCl_3$, 25°C) 0.86 (t, *J* = 6.8 Hz, 3H), 1.25-15.3 (m, 10H), 2.05 (s, 3H), 3.65 (s, 3H), 3.78-3.93 (m, 1H), 4.05 (d, *J* = 4.7 Hz, 2H), 4.64-4.78 (m, 1H); δ_C (50 MHz, $CDCl_3$, 25°C) 14.0 (q), 20.8 (q), 22.5 (t), 25.7 (t), 29.0 (t), 31.6 (t), 31.8 (t), 50,2 (d), 52.1 (q), 66.1 (t), 156.6 (s), 171.0 (s).

2d ($C_{14}H_{27}NO_4$): obtained enzymatically via biotransformation of **1d** (0.25 mmol, 65 mg) with $CHMO_{Brevi1}$ as a colorless solid (3mg, 5%); mp: 72-74°C; specific rotation of sample obtained from enzymatic kinetic resolution: $[\alpha]_D^{20}$ = –25.3 (c 0.15, $CHCl_3$; ee = 98%); δ_H (200 MHz, $CDCl_3$, 25°C) 0.88 (t, *J* = 6.6 Hz, 3H),1.16-1.55 (m, 14H), 2.07 (s, 3H), 3.67 (s, 3H), 3.77-3.93 (m, 1H), 4.06 (d, *J* = 4.5 Hz, 2H), 4.64-4.72 (m, 1H); δ_C (50 MHz, $CDCl_3$, 25°C) 14.1 (q), 20.8 (q), 22.6 (t), 25.8 (t), 29.2 (t), 29.4 (t), 29.9 (t), 31.3 (t), 31.8 (t), 49.4 (d), 51.8 (q), 66.1 (t), 156.6 (s), 171.0 (s).

2e ($C_{10}H_{19}NO_4$): obtained enzymatically via biotransformation of **1e** (0.25 mmol, 51 mg) with $CHMO_{Rhodo2}$ as a colorless liquid (23 mg, 45%); specific rotation of sample obtained from enzymatic kinetic resolution: $[\alpha]_D^{20}$ = –34.9 (c 1.15, $CHCl_3$; ee = 71%); δ_H (200 MHz, $CDCl_3$, 25°C) 0.91 (d, *J* = 6.6 Hz, 6H), 1.19-1.37 (m, 2H), 1.58-1.77 (m, 1H), 2.05 (s, 3H), 3.65 (s, 3H), 3.81-4.05 (m, 1H), 4.04 (d, *J* = 4.7 Hz, 2H), 4.67-4.72 (m, 1H); δ_C (50 MHz, CDCl, 25°C) 20.8 (q), 23.0 (q), 23.0 (q), 24.6 (d), 40.9 (t), 48.4 (d), 52.1 (q), 66.6 (t), 156.6 (s), 171.0 (s).

2f ($C_9H_{17}NO_4$): obtained enzymatically via biotransformation of **1f** (0.25 mmol, 47) with $CHMO_{Rhodo2}$ as a colorless liquid (18 mg, 38%); specific rotation of sample obtained from enzymatic kinetic resolution: $[\alpha]_D^{20}$ = +22.8 (c 0.90, $CHCl_3$; ee = 43%); δ_H (200 MHz, $CDCl_3$, 25°C) 0.93 (dd, *J* = 2.4 Hz and 6.8 Hz, 6H), 1.72-1.89 (m, 1H), 2.05 (s, 3H), 3.66 (s, 3H), 3.68-3.75 (m, 1H), 4.08 (d, *J* = 4.3 Hz, 2H), 4.69-4.75 (m, 1H); δ_C (50 MHz, $CDCl_3$, 25°C) 18.3 (q), 19.3 (q), 20.8 (q), 29.6 (d), 52.2 (q), 55.3 (d), 64.6 (t), 156.9 (s), 171.0 (s).

2g ($C_{12}H_{15}NO_4$): obtained enzymatically via biotransformation of **1g** (0.25 mmol, 56 mg) with PAMO as a yellow liquid (17 mg, 30%); specific rotation of sample obtained in from enzymatic resolution: $[\alpha]_D^{20}$ = +26.4 (c 0.85, $CHCl_3$; ee = 99%); δ_H (200 MHz, $CDCl_3$, 25°C) 2.05 (s, 3H), 3.67 (s, 3H), 4.28 (d, *J* = 5 Hz, 2H), 4.93-5.09 (m, 1H), 5.28-5.39 (m, 1H), 7.25-7.36 (m, 5H); δ_C (50 MHz, $CDCl_3$, 25°C) 30.6 (q), 48.9 (t), 51.4 (d), 52.2 (q), 126.2 (t), 126.2 (t), 127.5 (t), 128.6 (t), 128.6 (t), 141.2 (d), 156.3 (s), 206.8 (s).

6a ($C_{11}H_{21}NO_4$): obtained enzymatically via biotransformation of **5a** (0.25 mmol, 54 mg) with CDMO as a colorless liquid (3 mg, 6%); specific rotation of sample obtained from enzymatic kinetic resolution: $[\alpha]_D^{20}$ = –24.4 (c 0.15, $CHCl_3$; ee = 99%); δ_H (200 MHz, $CDCl_3$, 25°C) 0.92 (t, *J* = 6 Hz, 3H), 1.17 (t, *J* = 7.8 Hz, 3H), 1.33-1.51 (m, 6H), 2.34 (q, *J* = 7.8 Hz, 2H), 3.67 (s, 3H), 4.10-4.18 (m, 1H), 4.13-4.21 (m, 2H), 4.65 (m, 1H); δ_C (50 MHz, $CDCl_3$, 25°C) 9.1 (q), 14.1 (q), 22.7 (t), 27.8 (t), 29.7 (t), 31.9 (t), 49.4 (d), 52.5 (q), 66.7 (t), 156.6 (s), 174.2 (s).
6b ($C_{12}H_{23}NO_4$): obtained enzymatically via biotransformation of **5b** (0.25 mmol, 58 mg) with CDMO as a colorless solid (10 mg, 17%); mp: 53-55°C; specific rotation of sample obtained from enzymatic kinetic resolution: $[\alpha]_D^{20}$ = –26.5 (c 0.50, $CHCl_3$; ee = 84%); δ_H (200 MHz, $CDCl_3$, 25°C) 0.88 (t, *J* = 6.6 Hz, 3H), 1.14 (t, *J* = 7.6 Hz, 3H), 1.23-1.45 (m, 8H), 2.34 (q, *J* = 7.6 Hz, 2H), 3.66 (s, 3H), 3.78-3.95 (m, 1H), 4.09 (d, *J* = 7.2 Hz, 2H), 4.62-4.71 (m, 1H); δ_C (50 MHz, $CDCl_3$, 25°C) 9.1 (q), 14.0 (q), 22.5 (t), 25.4 (t), 27.5 (t), 31.5 (t), 31.8 (t), 50.3 (d), 52.1 (q), 66.0 (t), 156.6 (s), 174.4 (s).
7e ($C_{11}H_{21}NO_4$): obtained enzymatically via biotransformation of **5e** (0.25 mmol, 54 mg) with CDMO as a colorless liquid (3 mg, 6%); specific rotation of sample obtained from enzymatic kinetic resolution: $[\alpha]_D^{20}$ = +19.6 (c 0.15, $CHCl_3$; ee = 99%); δ_H (200 MHz, $CDCl_3$, 25°C) 0.89 (d, *J* = 6.6 Hz, 6H), 1.28 (t, *J* = 7.2 Hz, 3H), 1.40-1.47 (m, 2H), 1.53-1.68 (m, 1H), 2.51 (d, *J* = 4.8 Hz, 2H), 3.65 (s, 3H), 4.02-4.16 (m, 1H), 4.14 (q, *J* = 7.2 Hz, 2H), 4.98-5.07 (m, 1H); δ_C (50 MHz, $CDCl_3$, 25°C) 14.2 (q), 22.1 (q), 22,9 (q), 24.9 (d), 39.2 (d), 39.5 (t), 44.8 (t), 52.7 (q), 60.5 (t), 156.4 (s), 170.2 (s).

Computer Modeling

Computer modeling studies were performed using YASARA structure (version 9.7.24) and the AMBER03-force field with default settings.[66] AutoSMILES force field assignment was used for cofactors and substrates.[67] In order to get an active model of PAMO (pdb-code: 1W4X[56]) the missing $NADP^+$ was taken from a homologous cyclohexanone monooxygenase from *Rhodococcus* HI-31 (pdb-code: 3GWF[57]) after structural alignments using the MUSTANG algorithm.[68] Energy minimization was performed in a periodic water box at pH 7.0. Substrates were docked into the active site using Autodock4 and the Lamarckian genetic algorithm[69] with max. 50 million energy evaluations, max. 60.000 generations and default parameters. Analysis was carried out using YASARA structure. For visualization PyMol (DeLano Scientific, Palo Alto, CA, USA.; www.PyMol.org) was used.

Acknowledgement

The authors thank the Deutsche Bundesstiftung Umwelt (DBU, AZ 80006/871) for a scholarship to J. R. and the Austrian Science Fund FWF (Project No. 18945).

References

[1] G.-J. Brink, I. W. C. E. Arends, R. A. Sheldon, *Chem. Rev.* **2004**, *104*, 4105-4124.

[2] M. Renz, B. Meunier, *Eur. J. Org. Chem.* **1999**, 737-750.

[3] G. R. Krow, *Org. React.* **1993**, *43*, 251-296.

[4] A. Baeyer, V. Villiger, *Ber. Dtsch. Chem. Ges.* **1899**, *32*, 3625-3633.

[5] G. E. Turfitt, *Biochem. J.* **1948**, *42*, 376-383.

[6] G. Strukul, A. Varagnolo, F. Pinna, *J. Mol. Catal. A: Chemical* **1997**, *117*, 413-423.

[7] A. Gusso, C. Baccin, F. Pinna, G. Strukul, *Organometallics* **1994**, *13*, 3442-3451.

[8] C. M. Clouthier, M. M. Kayser, M. T. Reetz, *J. Org. Chem.* **2006**, *71*, 8431-8437.

[9] M. D. Mihovilovic, F. Rudroff, A. Winninger, T. Schneider, F. Schulz, M. T. Reetz, *Org. Lett.* **2006**, *8*, 1221-1224.

[10] M. Bocola, F. Schulz, F. Leca, A. Vogel, M. W. Fraaije, M. T. Reetz, *Adv. Synth. Catal.* **2005**, *347*, 979-986.

[11] M. T. Reetz, B. Brunner, T. Schneider, F. Schulz, C. M. Clouthier, M. M. Kayser, *Angew. Chem. Int. Ed.* **2004**, *43*, 4075-4078.

[12] N. M. Kamerbeek, D. B. Janssen, W. J. H. van Berkel, M. W. Fraaije, *Adv. Synth. Catal.* **2003**, *345*, 667-678.

[13] J. Rehdorf, U. T. Bornscheuer, *Encyclopedia of industrial biotechnology: bioprocess, bioseparation, and cell technology.*, Wiley & Sons, Inc., **2009**.

[14] Y.-C. J. Chen, O. P. Peoples, C. T. Walsh, *J. Bacteriol.* **1988**, *170*, 781-789.

[15] M. D. Mihovilovic, B. Müller, P. Stanetty, *Eur. J. Org. Chem.* **2002**, *22*, 3711-3730.

[16] M. D. Mihovilovic, *Curr. Opin. Chem.* **2006**, *10*, 1265-1287.

[17] J. B. van Beilen, F. Mourlane, M. A. Seeger, J. Kovac, Z. Li, T. H. M. Smits, U. Fritsche, B. Witholt, *Environ. Microbiol.* **2003**, *5*, 174-182.

[18] H. Iwaki, Y. Hasegawa, S. Wang, M. M. Kayser, P. C. K. Lau, *Appl. Environ. Microbiol.* **2002**, *68*, 5671-5684.

[19] H. Iwaki, S. Wang, S. Grosse, H. Bergeron, J. Nagahashi, J. Lertvorachon, J. Yang, Y. Konishi, Y. Hasegawa, P. C. K. Lau, *Appl. Environ. Microbiol.* **2006**, *72*, 2707-2720.

[20] K. Kostichka, S. M. Thomas, K. J. Gibson, V. Nagarajan, Q. Cheng, *J. Bacteriol.* **2001**, *183*, 6478-6486.

[21] J. Rehdorf, C. L. Zimmer, U. T. Bornscheuer, *Appl. Environ. Microbiol.* **2009**, *75*, 3106-3114.

[22] N. M. Kamerbeek, M. J. H. Moonen, J. G. M. van der Ven, W. J. H. van Berkel, M. W. Fraaije, D. B. Janssen, *Eur. J. Biochem.* **2001**, *268*, 2547-2557.

[23] A. Kirschner, J. Altenbuchner, U. T. Bornscheuer, *Appl. Microbiol. Biotechnol.* **2007**, *73*, 1065-1075.

[24] J. Rehdorf, A. Kirschner, U. T. Bornscheuer, *Biotechnol. Lett.* **2007**, *29*, 1393-1398.

[25] A. Völker, A. Kirschner, U. T. Bornscheuer, J. Altenbuchner, *Appl. Microbiol. Biotechnol.* **2008**, *77*, 1251-1260.

[26] L. N. Britton, A. J. Markovetz, *J. Biol. Chem.* **1977**, *252*, 8561-8566.

[27] N. M. Kamerbeek, J. J. Olsthoorn, M. W. Fraaije, D. B. Janssen, *Appl. Environ. Microbiol.* **2003**, *69*, 419-426.

[28] M. W. Fraaije, J. Wu, D. P. H. M. Heuts, E. W. van Hellemond, J. H. Lutje Spelberg, D. B. Janssen, *Appl. Microbiol. Biotechnol.* **2005**, *66*, 393-400.

[29] J. Rehdorf, A. Lengar, U. T. Bornscheuer, M. D. Mihovilovic, *Bioorg. Med. Chem. Lett.* **2009**, *19*, 3739-3743.

[30] A. Kirschner, U. T. Bornscheuer, *Angew. Chem. Int. Ed.* **2006**, *45*, 7004-7006.

[31] A. Rothaul, J. Brew.2007.

[32] Shivani, B. Pujala, A. K. Chakraborti, *J. Org. Chem.* **2007**, *72*, 3713-3722.

[33] N. Azizi, M. R. Saidi, *Org. Lett.* **2005**, *7*, 3649-3651.

[34] A. Heydari, M. Mehrdad, A. Maleki, N. Ahmadi, *Synthesis* **2004**, 1557-1558.

[35] D. Menche, F. Arikan, J. Li, S. Rudolph, *Org. Lett.* **2007**, *9*, 267-270.

[36] G. Liu, S. S. Stahl, *J. Am. Chem. Soc.* **2006**, *128*, 7179-7181.

[37] L. Dahlenburg, H. Treffert, F. Christian, F. W. Heinemann, A. Zahl, *Eur. J. Inorg. Chem.* **2007**, 1738-1751.

[38] J. V. Potetinova, T. L. Voyushina, V. M. Stepanov, *Bioorg. Med. Chem. Lett.* **1997**, *7*, 705-710.

[39] G. Sekar, R. M. Kamble, V. K. Singh, *Tetrahedron Asymm.* **1999**, *10*, 3663-3666.

[40] M. D. Mihovilovic, B. Müller, M. M. Kayser, J. D. Stewart, J. Fröhlich, P. Stanetty, H. Spreitzer, *J. Mol. Catal. B: Enzym* **2001**, *11*, 349-353.

[41] L.-W. Xu, C.-G. Xia, *Tetrahedron Lett.* **2004**, *45*, 4507-4510.

[42] T. Kourouli, P. Kefalas, N. Ragoussis, V. Ragoussis, *J. Org. Chem.* **2002**, *67*, 4615-4618.

[43] M. M. Kayser, G. Chen, J. D. Stewart, *Synlett* **1999**, 153-158.

[44] M. D. Mihovilovic, R. Snajdrova, A. Winninger, F. Rudroff, *Synlett* **2005**, *18*, 2751-2754.

[45] C.-S. Chen, Y. Fujimoto, G. Girdaukas, C. J. Sih, *J. Am. Chem. Soc.* **1982**, *104*, 7294-7299.

[46] K. Faber, H. Hönig, A. Kleewein *Free shareware programs ('Selectivity-1.0') for calculation of the enantiomeric ratio.*

[47] M. D. Mihovilovic, F. Rudroff, B. Grötzl, P. Kapitan, R. Snajdrova, J. Rydz, *Angew. Chem. Int. Ed.* **2005**, *44*, 3609-3613.

[48] F. Rudroff, J. Rydz, F. J. Ogink, M. Fink, M. D. Mihovilovic, *Adv. Synth. Catal.* **2007**, *349*, 1436-1444.

[49] R. Snajdrova, G. Grogan, M. D. Mihovilovic, *Bioorg. Med. Chem. Lett.* **2006**, *16*, 4813-4817.

[50] M. D. Mihovilovic, P. Kapitán, P. Kapitánová, *ChemSusChem* **2008**, *1*, 143-148.

[51] P. Cernuchová, M. D. Mihovilovic, *Org. Biomol. Chem.* **2007**, *5*, 1715-1719.

[52] V. Alphand, R. Furstoss, *J. Org. Chem.* **1992**, *57*, 1306-1309.

[53] F. Petit, R. Furstoss, *Tetrahedron Asymm.* **1993**, *4*, 1341-1352.

[54] A. Rioz-Martínez, G. de Gonzalo, D. E. Torres-Pazmiño, M. W. Fraaije, V. Gotor, *Eur. J. Org. Chem.* **2009**, 2526-2523.

[55] C. Rodríguez, G. de Gonzalo, M. W. Fraaije, V. Gotor, *Tetrahedron Asymm.* **2007**, *18*, 1338-1344.

[56] E. Malito, A. Alfieri, M. W. Fraaije, A. Mattevi, *Proc. Nat. Acad. Sci. USA* **2004**, *101*, 13157-13162.

[57] I. A. Mirza, B. J. Yachin, S. Wang, S. Grosse, H. Bergeron, A. Imura, H. Iwaki, Y. Hasegawa, P. C. Lau, A. M. Berghuis, *J. Am. Chem. Soc.* **2009**, *131*, 8848-8854.

[58] F. Schulz, F. Leca, F. Hollmann, M. T. Reetz, *Beilstein J. Org. Chem.* **2005**, *1*, 1-8.

[59] M. T. Reetz, M. Bocola, J. D. Carballeira, D. Zha, A. Vogel, *Angew. Chem. Int. Ed.* **2005**, *44*, 4192-4196.

[60] M. T. Reetz, D. Kahakeaw, J. Sanchis, *J. Mol. Biosyst.* **2009**, *5*, 115-122.

[61] M. T. Reetz, W. Sheng, *J. Am. Chem. Soc.* **2009**, *131*, 15424-15432.

[62] P. C. Brzostowicz, D. M. Walters, S. M. Thomas, V. Nagarajan, P. E. Rouvière, *Appl. Environ. Microbiol.* **2003**, *69*, 334-342.

[63] M. G. Bramucci, P. C. Brzostowicz, K. Kostichka, V. Nagarajan, P. E. Rouvière, S. M. Thomas.2003.

[64] P. C. Brzostowicz, K. L. Gibson, S. M. Thomas, M. S. Blasko, P. E. Rouvière, *J. Bacteriol.* **2000**, *18215*, 4241-4248.

[65] D. Bonsor, S. F. Butz, J. Solomons, S. Grant, I. J. S. Fairlamb, M. J. Fogg, G. Grogan, *Org. Biomol. Chem.* **2006**, *4*, 1252-1260.

[66] E. Krieger, T. Darden, S. Nabuurs, A. Finkelstein, G. Vriend, *Proteins* **2004**, *57*, 678-683.

[67] A. Jakalian, D. B. Jack, C. I. Bayly, *J. Comput. Chem.* **2002**, *23*, 1623-1641.

[68] A. S. Konagurthu, J. C. Whisstock, P. J. Stuckey, A. M. Lesk, *Proteins* **2006**, *64*, 559-574.

[69] G. M. Morris, D. S. Goodsell, R. S. Halliday, R. Huey, W. E. Hart, R. K. Belew, A. J. Olson, *J. Comput. Chem.* **1998**, *19*, 1639-1662.

Article III

Exploiting Regioselectivity of Baeyer-Villiger Monooxygenases – A Route to the Formation of β-Amino Acids

Jessica Rehdorf[*], Marko D. Mihovilovic[†] and Uwe T. Bornscheuer[*]

[*]Dipl.-Biochem. J. Rehdorf, Prof. Dr. U. T. Bornscheuer, Institute of Biochemistry, Department of Biotechnology & Enzyme Catalysis, Ernst-Moritz-Arndt University of Greifswald, Felix-Hausdorff-Str. 4, D-17487 Greifswald (Germany), Fax: (+49)3834-86-80066, Email: uwe.bornscheuer@uni-greifswald.de
[†]Prof. Dr. M. D. Mihovilovic, Institute of Synthetic Chemistry, Vienna University of Technology, Getreidemarkt 9/163-OC, A-1060 Vienna (Austria), Fax: (+43)1-58801-15499, Email: mmihovil@pop.tuwien.ac.at

Submitted to Angewandte Chemie International Edition 2009.

Keywords: β-amino acids, Baeyer-Villiger monooxygenases, kinetic resolution, regioselectivity, linear β-amino ketones

β-Amino acids are of growing interest owing to their unique pharmaceutical importance as building blocks of β-peptides, alkaloids, terpenoids or β-lactam antibiotics. Furthermore, they are valuable precursors for medical products such as the anti-cancer drug taxol or the potent anti-tumor depsipeptide cryptophycin.[1] As biologically active compounds and especially β-peptides have an auspicious potential due to their enhanced stability towards proteolytic enzymes this offers new possibilities to create drugs not rejected or degraded by the human body. Therefore, a plethora of chemical methods for the preparation of β-amino acids focussing on asymmetric synthesis have been developed.[2] However, chemical syntheses often lack the advantages of stereo- and enantioselectivity usually achieved by utilizing enzymes. So far, the main enzymatic paths for obtaining highly enantiopure β-amino acids are based on kinetic resolutions exploiting enzymes either acting on C-N bonds (e.g. acylases[3], amidases[4] or aminopeptidases[5]) or C-O bonds (e.g. hydrolytic enzymes like lipases[6] or esterases).[7] Besides kinetic resolutions, optically pure β-amino acids can also be obtained using aminomutases[8] or via reductive amination of ketones with β-aminotransferases.[9] We herein report a new enzymatic route to enantiopure β-amino acids under mild conditions using Baeyer-Villiger monooxygenases. For this, *N*-protected β-amino ketones served as racemic substrates in a kinetic resolution leading to an enrichment of *N*-protected β-amino esters, which are hydrolyzed in a second step to furnish optically pure *N*-protected β-amino acids and β-amino alcohols.

Baeyer-Villiger monooxygenases (BVMOs, 1.14.13.x) are flavoenzymes and belong to the class of oxidoreductases. They convert cyclic, aromatic and linear or aryl-aliphatic ketones into esters and lactones, respectively, using molecular oxygen instead of peracids, typically utilized in their chemical pendant.[10] Besides the flavin cofactor they also require reduction equivalents in form of NAD(P)H, that are crucial for catalysis. The high stereo-, chemo- and enantioselectivity of enzymatic-mediated Baeyer-Villiger reactions implicate a valuable advantage towards (metal)-based catalysts[11] used in chemical oxidations. Until recently,

mainly cyclic and bicyclic ketones have been subjected to desymmetrization and kinetic resolution approaches using BVMOs as biocatalysts.[12] In our previous work we could demonstrate that also linear aliphatic ketones like 4-hydroxy-2-ketones and 5-hydroxy-3-ketones can be accepted as substrates for BVMOs in kinetic resolutions[13] yielding enantiopure β-hydroxyalkyl acetates; these were then hydrolyzed enzymatically to yield optically active 1,2-diols. Only a few results for the conversion of aryl-aliphatic compounds bearing the carbonyl group in the side chain have been published for arylketone-converting enzymes.[14] Consequently, we then investigated, whether also β-amino ketones are accepted by BVMOs, which would yield the corresponding β-amino alcohols if the oxygen is inserted on the side of the more sterically hindered carbon atom next to the ketone functionality. Interestingly, we found that certain BVMOs incorporate the oxygen at the opposite site furnishing the regioisomeric ester, which after hydrolysis yields a β-amino acids.

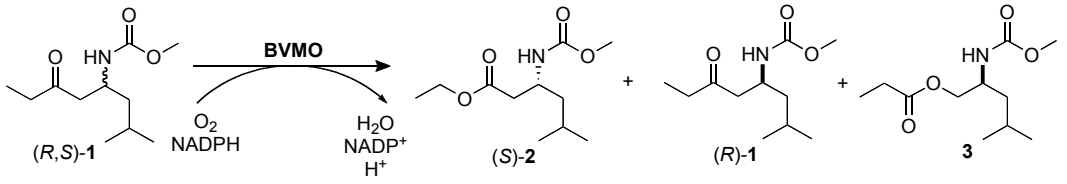

Scheme 1. Baeyer-Villiger monooxygenase (BVMO) catalyzed kinetic resolution of the aliphatic *N*-protected β-amino ketone **1** yields either the protected β-amino alcohol **3** or the β-amino acid **2** depending on the regioselectivity of the enzyme.

Within a collection of 16 BVMOs originating from different bacterial origin, four enzymes (CDMO, $CHMO_{Arthro}$, $CHMO_{Brachy}$ and $CHMO_{Xantho}$) were active against 5-amino-3-ketone **1** and showed high enantioselectivities (Table 1). In pre-screening experiments performed in 24-well microtiter plates all four enzymes proved to be able to insert oxygen on both sides of the ketone functionality, allowing access to the 'normal' and the 'abnormal' Baeyer-Villiger ester, which is less likely using peracids in a chemical oxidation. Whereas $CHMO_{Arthro}$, $CHMO_{Brachy}$ and $CHMO_{Xantho}$ generated both regioisomers **2** and **3** with high enantiomeric excess (>99% ee), CDMO showed a rather low E-value for **3**, although selectivity for **2** was very high (E > 200). Still, it is important that CDMO oxidized the ketone enantiomer ((–)-**1**) generating the opposite 'abnormal' ester ((+)-**2**), compared to the other three enzymes. Thus, biotransformations with *rac*-**1** using $CHMO_{Arthro}$ and CDMO would yield in (–)-**2** and (+)-**2**, both with high optical purity.

Table 1. Results of kinetic resolutions of **1** using various BVMOs[a].

Product	BVMO	conversion [%][b]	ee_P [%][c]	E[d]	rp [%][e]
2	CDMO	10	>99 (+)[f]	>200	42
	$CHMO_{Arthro}$	24	>99 (–)[f]	>200	37
	$CHMO_{Brachy}$	7	>99 (–)[f]	>200	66
	$CHMO_{Xantho}$	13	>99 (–)[f]	>200	42
3	CDMO	12	81	10	58
	$CHMO_{Arthro}$	24	>99	>200	63
	$CHMO_{Brachy}$	7	>99	>200	34
	$CHMO_{Xantho}$	13	>99	>200	58

[a]Biotransformations were carried out at 24°C using whole cells of *E. coli* expressing the desired BVMO. Screenings were performed in 24-well plastic dishes, reactions were stopped after 24 h and analysed by chiral phase GC. [b]Conversion calculated from $\%ee_S$ (enantiomeric excess of substrate) and $\%ee_P$ (enantiomeric excess of product). [c]$\%ee_P$ was determined by chiral phase GC and calculated according to Chen *et al*.[15] [d]Enantioselectivity values were determined by computer fitting of GC data[16] from $\%ee_S$ and $\%ee_P$. [e]% regioisomeric percentage determined by chiral GC. [f]Sign of optical rotation measured on a Perkin Elmer Polarimeter 241 is given in parenthesis. Further details are given in the experimental section.

Biotransformations of *rac*-**1** to (+)-**2** using CDMO as biocatalyst in a baffled shake flask (0.35 mmol substrate) revealed a constant increase in product formation within 96 h (Figure 1). However, increasing the reaction time using 24-well plastic dishes did not yield in a higher conversion as the reaction stopped around 10% (data not shown). Comparing these results indicated that an increased oxygen input due to a larger surface and better shaking conditions combined with a better substrate distribution led to higher conversions. Surprisingly, using CDMO in preparative scale biotransformation the ratio between 'normal' and 'abnormal' ester changed from 1:1 in 24-well microtiter plates to 1:3 in a flask.

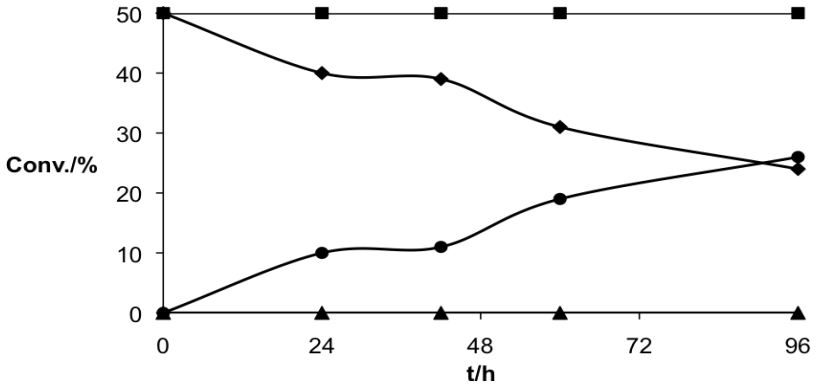

Figure 1. Time-dependent conversion of *rac*-**1** into **2** at 24°C using whole cells of *E. coli* expressing CDMO from *Rhodococcus ruber* SC1. ■: (+)-**1**, ◆: (–)-**1**, ●: (+)-**2**, ▲: (–)-**2**.

After isolation and purification of both Baeyer-Villiger products, ester hydrolysis was performed using *Candida antarctica* lipase B (CAL-B) yielding *N*-protected β-leucine (3.4 mg) and *N*-protected β-amino-4-methyl-1-propanol (4 mg), which even can be further oxidized to

α-leucine (Scheme 2). Since ester hydrolysis proceeded without any conformational changes, both products possess the same configuration as their corresponding esters. Interestingly, we also observed a spontaneous autohydrolysis of **3** combined with the increase of **5** starting 30 h after substrate addition. Since *E. coli* does not overexpress its own endogenous hydolytic enzymes like esterases or lipases, we assume that the decrease in pH due to cell metabolism might be a reason for ester bond cleavage. However, this autohydrolysis was not detected for the 'abnormal' ester.

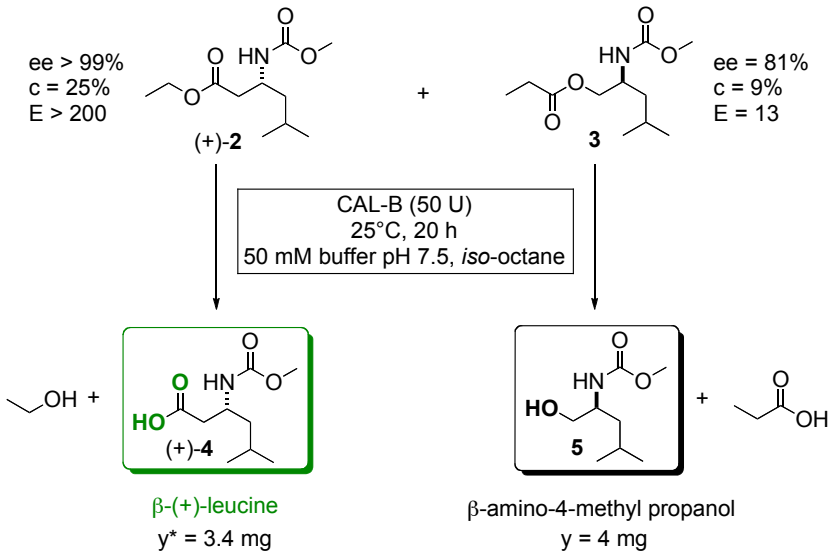

Scheme 2. Enzymatic hydrolysis of Baeyer-Villiger esters leading to the formation of the *N*-protected β-amino acid **4** and the *N*-protected β-amino alcohol **5**. (*yield refers to methylester after derivatisation of the β-amino acid with methanol and TMS-diazomethane)

These studies demonstrate the broad applicability of Baeyer-Villiger monooxygenases in synthetic chemistry due to the formation of highly valuable building blocks usually not associated with a Baeyer-Villiger oxidation. Indeed, kinetic resolution of β-amino ketones revealed, that the oxygen insertion process onto a carbon-carbon bond is a powerful methodology to generate five chemically different compounds, which also differ in their configuration. Combined with the regioselectivity of Baeyer-Villiger monooxygenases valuable optically active synthons all of high importance for the pharmaceutical industry can be synthesized. Furthermore, generating an 'abnormal' Baeyer-Villiger ester and therefore allowing access to β-amino acids is particularly interesting since common chemical strategies still lack this possibility. In this particular example four different enzymes proved to generate the regioisomeric Baeyer-Villiger ester in enantiocomplementary form and therefore allowing access to both β-amino acid enantiomers. Thus, with the enzymatic Baeyer-Villiger reaction new synthetic routes for the formation of β-amino acids could be discovered and this demonstrated to be a versatile and useful alternative to already established enzymes like hydrolases, acylases or aminomutases.

Experimental Section

Unless otherwise stated, all chemicals and microbial growth media were purchased from commercial suppliers and used without further purification. All solvents were distilled prior to use. Flash column chromatography was performed on silica gel 60 from Merck (40-63 µm). NMR-spectra were recorded from $CDCl_3$ solution on a Bruker AC 300 (300 MHz) and chemical shifts are reported in ppm using TMS as internal standard. Combustion analysis was carried out in the Microanalytic Laboratory, University of Vienna. General conversion control and analyses of purified products were performed on a GC Top 8000/MS Voyager (quadropol, EI^+) using a capillary column BGB5 (5% diphenyl-, 95% dimethylpolysiloxane, 30 m x 0.25 mm ID). Enantiomeric excesses were determined by chiral-phase GC using a hydrodex β-TBDAc column (30 m x 0.25 mm ID). Specific rotations, $[\alpha]_D^{20}$ were determined using a Perkin Elmer Polarimeter 241. Racemic *N*-protected 5-amino-3-ketone **1** was synthesized in two steps: first an α,β-unsaturated ketone was synthesized by an aldol addition[17], purified by vacuum destillation and used for the second step in an aza-Michael-addition.[18] The crude product was purified by flash chromatography. The Baeyer-Villiger products **2** and **3** were synthesized enzymatically in a preparative scale biotransformation. For this LB_{amp} (500 mL) was inoculated with 1% of an overnight preculture and incubated at 37°C in an orbital shaker. At an optical density of 0.6-0.8 at 600 nm protein expression was induced with IPTG (0.1 mM, final concentration) followed by substrate addition (80 mg, 0.35 mmol, in dioxane). Protein expression and subsequent biotransformation were performed at 24°C. Product extraction was carried out using ethyl acetate. The organic layers were combined, dried over Na_2SO_4 and the organic solvent was evaporated. The crude product was purified via silica gel chromatography (petrol ether and ethyl acetate) and finally the amino ketone and the corresponding amino ester were analyzed via GC, GCMS and $^1H/^{13}C$ NMR.

E. coli containing the plasmids for the CDMO from *Rhodococcus ruber* SC1[19], $CHMO_{Arthro}$ from *Arthrobacter sp.*[20], $CHMO_{Brachy}$ from *Brachymonas sp.*[21] and $CHMO_{Xantho}$ from *Xanthobacter sp.* ZL5[22] were used for substrate investigation. Analytical screening experiments were performed in 24-well plates. For this, LB_{amp} (20 mL) was inoculated with 1% of the overnight preculture and incubated at 37°C up to an optical density of 0.6-0.8 at 600 nm. BVMO expression was induced with IPTG (0.1 mM, final concentration). Protein expression was performed at 24°C for 2 h. Then, 1 mL bacterial culture was transferred into each well of the 24-well plate followed by subsequent substrate addition (1 mM, in dioxane). Biotransformations were carried out at 24°C and analyzed after 24 h. For this, samples were extracted with ethyl acetate supplemented with 1 mM of an internal standard (benzoic acid methylester), dried over Na_2SO_4 and examined using GC analysis. Time-course experiments were performed as described for screening experiments and samples were taken at defined time intervals (2, 4, 6, 8, 10, 24, 30 and 48 h), extracted with ethyl acetate and analyzed by GC.

Enzymatic syntheses of **4** and **5** were carried out in a glass vial (500 µL sodium phosphate buffer pH 7.5 50 mM, 500 µL *iso*-octane) at 25°C for 20 h using 40 mg CAL-B (immobilized, Novozyme 435, 50 U measured with tributyrin) and esters **2** and **3** as starting material. The organic phase was extracted twice with ethyl acetate (500 µL each), dried over Na_2SO_4 and directly analyzed by GC-MS. The aqueous phase was acidified with 25 µL 1N HCl and extracted twice with ether (500 µL each). Then, 100 µL methanol and 40 µL of diazomethane were added. After 30 min the reaction was stopped by adding 20 µL glacial acid, the solvent was evaporated under nitrogen stream and the residual compounds were dissolved in dichloromethane followed by GC-MS analysis.

Physical and spectral data

7-methyl-4-octen-3-one ($C_9H_{16}O$) was obtained from ethyl propionyl acetate (3 g, 0.2 mol) and *iso*-valeraldehyde (1.7 g, 0.2 mol) as a colorless liquid (1 g, yield 58%) as described by Kourouli *et al*.[17]

1 ($C_{11}H_{21}NO_3$): obtained from 7-methyl-4-octen-3-one (980 mg, 7 mmol), methylcarbamate (630 mg, 8.4 mmol), (n-Bu)$_3$P (141.6 mg, 0.7 mmol) and TMSCl (837 mg, 7.7 mmol) as a yellowish liquid (351 mg, 30%); specific rotation of sample obtained in BVMO-catalyzed kinetic resolution: $[\alpha]_D^{20}$ = +10.2 (c 0.60, $CHCl_3$; ee = 22%); ^{1}H NMR (200 MHz, $CDCl_3$, 25°C, TMS): δ = 0.9 (d, ^3J (H,H) = 6.4 Hz, 6H, 2CH_3), 1.0 (t, ^3J (H,H) = 6.6 Hz, 3H, CH_3), 1.2-1.3 (m, 1H, CH), 1.4-1.7 (m, 2H, CH_2), 2.4 (q, ^3J (H,H) = 7.2 Hz, 2H, CH_2), 2.6 (d, ^3J (H,H) = 3.6 Hz, 2 H, CH_2), 3.6 (s, 3H, CH_3), 3.9-4.1 (m, 1H, CH), 5.08 (m, 1H, NH); ^{13}C NMR (50 MHz, $CDCl_3$, 25°C): δ = 7.7 (q), 22.1 (q), 23.2 (q), 25.1 (d), 36.7 (t) 43.8 (d), 46.4 (t), 46.9 (t), 52.1 (q), 156.7 (s), 210.7 (s); ESI-MS-TOF (70 eV): *m/z* (%): 250 (100) $[2M+2H_2O-H]^-$, 233 (60) $[M-H_2O]^-$, 204 (45) $[C_9H_{16}NO_3+H_2O]^-$, 190 (50) $[C_8H_{14}NO_3+H_2O]^-$, 181 (30) $[C_{10}H_{18}NO_3-H_2O-1]^-$, 154 (50) $[C_8H_{14}NO_3-H_2O]^-$, 139 (12) $[C_7H_{12}NO_3-H_2O-1$ or $C_8H_{16}NO_2-H_2O-1]^-$.

2 ($C_{11}H_{21}NO_4$): obtained enzymatically via biotransformation of **1** (80 mg, 0.35 mmol) with CDMO as a colorless liquid (% c = 25, y = 16 mg, 20%); specific rotation of sample obtained in enzyme-catalyzed kinetic resolution: $[\alpha]_D^{20}$ = +19.6 (c 0.15, $CHCl_3$; ee = 99%); ^{1}H NMR (200 MHz, $CDCl_3$, 25°C, TMS): δ = 0.9 (d, ^3J (H,H) = 6.6 Hz, 6H, 2CH_3), 1.3 (t, ^3J (H,H) = 7.2 Hz, 3H, CH_3), 1.4-1.5 (m, 2H, CH_2), 1.5-1.7 (m, 1H, CH), 2.5 (d, ^3J (H,H) = 4.8 Hz, 2H, CH_2), 3.7 (s, 3H, CH_3), 4.0-4.2 (m, 1H, CH), 4.2 (q, ^3J (H,H) = 7.2 Hz, 2H, CH_2), 5.0 (m, 1H, NH); ^{13}C NMR (50 MHz, $CDCl_3$, 25°C): δ = 14.2 (q), 22.1 (q), 22,9 (q), 24.9 (d), 39.2 (d), 39.5 (t), 44.8 (t), 52.7 (q), 60.5 (t), 156.4 (s), 170.2 (s).

3 ($C_{11}H_{21}NO_4$): obtained enzymatically via biotransformation of **1** (80 mg, 0.35 mmol) with CDMO as a colorless liquid (% c = 9, y = 5.3 mg, 6.6%); δ_H (200 MHz, $CDCl_3$, 25°C) 0.9 (d, ^3J (H,H) = 6.6 Hz, 6H, 2CH_3), 1.1-1.2 (t, ^3J (H,H) = 7.4 Hz, 3H, CH_3), 1.2-1.4 (m, 2H, CH_2), 1.6-1.8 (m, 1H, CH), 2.2-2.4 (q, ^3J (H,H) = 7.8 Hz, 2H, CH_2), 3.7 (s, 3H, CH_3), 3.8-4.1 (m, 1H, CH), 4.2 (d, ^3J (H,H) = 4.8 Hz, 2H, CH_2), 4.8 (m, 1H, NH); δ_C (50 MHz, CDCl, 25°C)) 9.1 (q), 23.4 (q), 23.7 (q), 24.9 (d), 27.8 (t), 41.0 (t), 46.8 (d), 52.5 (q), 66.9 (t), 155.6 (s), 174.2 (s).

4 ($C_{10}H_{19}NO_4$): obtained enzymatically via biotransformation of **2** (10.5 mg, 70 µmol) with CAL-B as a yellowish liquid (y = 3.4 mg); δ_H (300 MHz, $CDCl_3$, 25°C, derivatized with MeOH and diazomethane) 0.9 (d, ^3J (H,H) = 6.6 Hz, 6H, 2CH_3), 1.2-1.4 (m, 2H, CH_2), 1.6-1.8 (m, 1H, CH), 2.3-2.7 (d, ^3J (H,H) = 4.8 Hz, 2H, CH_2), 3.7 (s, 3H, CH_3), 3.7 (s, 3H, CH_3), 4.2-4.3 (m, 1H, CH), 5.1 (m, 1H, NH); GC-MS (ESI-MS-quadropol): m/z (%): 217 (3) [M], 186 (4) $[C_9H_{16}NO_3]$, 174 (3) $[C_7H_{12}NO_4]$, 160 (100) $[C_6H_{10}NO_4]$, 144 (50) $[C_7H_{14}NO_2]$, 128 (100) $[C_6H_{13}NO]$, 118 (60) $[C_5H_7NO_3]$.

5 ($C_8H_{17}NO_3$): obtained enzymatically via biotransformation of **3** (5 mg, 28.6 µmol) with CAL-B as a yellowish liquid (y = 4 mg); δ_H (300 MHz, $CDCl_3$, 25°C) 0.9 (d, ^3J (H,H) = 6.6 Hz, 6H, 2CH_3), 1.2-1.4 (m, 2H, CH_2), 1.6-1.7 (m, 1H, CH), 3.5-3.8 (d, ^3J (H,H) = 5.4 Hz, 2H, CH_2), 3.6 (s, 3H, CH_3), 3.9-4.1 (m, 1H, CH), 4.8 (m, 1H, OH), 5.1 (m, 1H, NH); GC-MS (ESI-MS-quadropol): m/z (%): 174 (80) $[C_6H_{11}NO]$, 118 (12) $[C_4H_8NO_3]$, 102 (30) $[C_4H_7NO_2]$.

Acknowledgement

The authors thank the Deutsche Bundesstiftung Umwelt (DBU, AZ 80006/871) for a scholarship to J. R. and the Austrian Science Fund FWF (Project No. 18945).

References

[1] E. Juaristi, V. A. Soloshonok, *Enantioselective synthesis of β-amino acids.*, 2nd ed., Wiley-VCH, New York, **2005**.

[2] a) E. Juaristi, H. López-Riuz, *Curr. Med. Chem.* **1999**, *6*, 983-1004; b) S. Abele, D. Seebach, *Eur. J. Org. Chem.* **2000**, 1-15; c) F. Fülöp, *Chem. Rev.* **2001**, *101*, 2181-2204; d) M. Liu, M. P. Sibi, *Tetrahedron* **2002**, *58*, 7991-8035; e) G. Lelais, D. Seebach, *Biopolymers* **2004**, *76*, 206-243.

[3] H. Gröger, H. Trauthwein, S. Buchholz, K. Drauz, C. Sacherer, S. Godfrin, H. Werner, *Org. Biomol. Chem.* **2004**, *2*, 1977-1978.

[4] a) V. A. Soloshonok, N. A. Fokina, A. V. Rybakova, I. P. Shishkina, S. V. Galushko, A. E. Sorochinsky, V. P. Kukhar, *Tetrahedron Asymm.* **1995**, *6*, 1601-1610; b) D. Li, S. Cheng, D. Wei, Y. Ren, D. Zhang, *Biotechnol. Lett.* **2007**, *29*, 1825-1830.

[5] T. Heck, D. Seebach, S. Osswald, M. K. J. ter Wiel, H.-P. E. Kohler, B. Geueke, *ChemBioChem* **2009**, *10*, 1558-1561.

[6] a) S. Gedey, A. Liljeblad, L. Lázár, F. Fülöp, L. T. Kanerva, *Tetrahedron Asymm.* **2001**, *12*, 105-110; b) S. Gedey, A. Liljeblad, L. Lázár, F. Fülöp, L. T. Kanerva, *Can. J. Chem.* **2002**, *80*, 565-570.

[7] A. Liljeblad, L. T. Kanerva, *Tetrahedron* **2006**, *62*, 5831-5854.

[8] a) P. A. Frey, O. T. Magnusson, *Chem. Rev.* **2003**, *103*, 2129-2148; b) B. Wu, W. Szymanski, P. Wietzes, S. de Wildemann, G. J. Poelarends, B. L. Feringa, D. B. Janssen, *ChemBioChem*, **2009**, *10*, 338-344.

[9] A. Banerjee, M. Chase, R. A. Clayton, B. Landis, WO2005005633, United States, **2006**.

[10] A. Baeyer, V. Villiger, *Ber. Dtsch. Chem. Ges.* **1899**, *32*, 3625-3633.

[11] a) G. Strukul, A. Varagnolo, F. Pinna, *J. Mol. Catal. A: Chemical* **1997**, *117*, 413-423; b) C. Bolm, G. Schlinghoff, *Chem. Soc. Chem. Commun.* **1995**, 1247-1248.

[12] a) J. Rehdorf, U. T. Bornscheuer, in *Encyclopedia of industrial biotechnology: bioprocess, bioseparation, and cell technology.,* Vol. 1 (Ed: M. Flickinger), Wiley & Sons, Inc., **2009**; b) M. D. Mihovilovic, *Curr. Opin. Chem.* **2006**, *10*, 1265-1287.

[13] a) J. Rehdorf, A. Lengar, U. T. Bornscheuer, M. D. Mihovilovic, *Bioorg. Med. Chem. Lett.* **2009**, *19*, 3739-3743; b) A. Kirschner, U. T. Bornscheuer, *Angew. Chem. Int. Ed.* **2006**, *45*, 7004-7006.

[14] a) C. Rodrìguez, G. de Gonzalo, M. W. Fraaije, V. Gotor, *Tetrahedron Asymm*., **2007**, *18*, 1338-1344; b) K. Geitner, A. Kirschner, J. Rehdorf, M. Schmidt, M. D. Mihovilovic, U. T. Bornscheuer, *Tetrahedron Asymm*., **2007**, *18*, 892-895.

[15] C.-S. Chen, Y. Fujimoto, G. Girdaukas, C. J. Sih, *J. Am. Chem. Soc.* **1982**, *104*, 7294-7299.

[16] K. Faber, H. Hönig, A. Kleewein; Free shareware programs ('Selectivity-1.0') for calculation of the enantiomeric ratio. Available on the authors website: <http://borgc182.kfunigraz.ac.at./>.

[17] T. Kourouli, P. Kefalas, N. Ragoussis, V. Ragoussis, *J. Org. Chem.* **2002**, *67*, 4615-4618.

[18] L.-W. Xu, C.-G. Xia, *Tetrahedron Lett.* **2004**, *45*, 4507-4510.

[19] K. Kostichka, S. M. Thomas, K. J. Gibson, V. Nagarajan, Q. Cheng, *J. Bacteriol.* **2001**, *183*, 6478-6486.

[20] P. C. Brzostowicz, D. M. Walters, S. M. Thomas, V. Nagarajan, P. E. Rouvière, *Appl. Environ. Microbiol.* **2003**, *69*, 334-342.

[21] M. G. Bramucci, P. C. Brzostowicz, K. Kostichka, V. Nagarajan, P. E. Rouvière, S. M. Thomas, WO/2003/020890, **2003**.

[22] J. B. van Beilen, F. Mourlane, M. A. Seeger, J. Kovac, Z. Li, T. H. M. Smits, U. Fritsche, B. Witholt, *Environ. Microbiol.* **2003**, *5*, 174-182.

Article IV

Available online at www.sciencedirect.com
ScienceDirect
Tetrahedron: Asymmetry
Tetrahedron: *Asymmetry* 18 (2007) 892–895

Enantioselective kinetic resolution of 3-phenyl-2-ketones using Baeyer–Villiger monooxygenases

Kristian Geitner,[a] Anett Kirschner,[a] Jessica Rehdorf,[a] Marlen Schmidt,[a] Marko D. Mihovilovic[b] and Uwe T. Bornscheuer[a,*]

[a]*Department of Biotechnology and Enzyme Catalysis, Institute of Biochemistry, Greifswald University, Felix-Hausdorff-Str. 4, D-17487 Greifswald, Germany*

[b]*Institute of Applied Synthetic Chemistry, Vienna University of Technology, Getreidemarkt 9/163-OC, A-1060 Vienna, Austria*

Received 13 March 2007; accepted 26 March 2007
Available online 25 April 2007

Abstract—The enantioselective kinetic resolution of two 3-phenyl-2-ketones using four different Baeyer–Villiger monooxygenases (BVMO) expressed recombinantly in *Escherichia coli* was studied. The highest enantioselectivity ($E = 82$) was achieved for 3-phenyl-2-butanone using a BVMO originating from *Pseudomonas fluorescens*. A BVMO from *Pseudomonas putida* showed an opposite (*R*)-enantiopreference and $E = 12$.

1. Introduction

Baeyer–Villiger monooxygenases (BVMOs) belong to the class of oxidoreductases and convert aliphatic, arylaliphatic and cyclic ketones into esters and lactones, respectively, using molecular oxygen.[1–5] Thus, they mimic the chemical Baeyer–Villiger oxidation,[6] which is usually peracid-catalyzed and proceeds by a two-step process as initially proposed by Criegee.[7] Since it is becoming more and more important to perform Baeyer–Villiger oxidations in an enantioselective manner,[8] BVMOs represent a valuable alternative to metal-based chiral catalysts.[9] Until now, stereoselective Baeyer–Villiger oxidations using enzymes were described for prochiral or racemic mono- and bicyclic ketones[10–15] as well as racemic arylaliphatic ketones.[3,16] Recently, we have shown that aliphatic acyclic ketones such as 4-hydroxy-2-ketones could be enantioselectively ($E \sim 50$) converted by a BVMO from *Pseudomonas fluorescens* DSM 50106, which was recombinantly expressed in *Escherichia coli*.[17,18]

Herein we report, the kinetic resolution of two 3-phenyl-2-ketones using four different BVMOs (Scheme 1).

2. Results and discussion

Kinetic resolutions of the two 3-phenyl-2-ketones **1a** and **1b** (Scheme 1), which were synthesized according to the literature,[19] were carried out using resting cells of recombinant *E. coli* expressing four different BVMOs: cyclohexanone monooxygenase from *Acinetobacter calcoaceticus* NCIMB 9871 (CHMO[20]), cyclopentanone monooxygenase from *Comamonas* sp. NCIMB 9872 (CPMO[21]), a BVMO from *P. fluorescens* DSM 50106 (PF-BVMO) and a BVMO from *Pseudomonas putida* KT2440 (PP-BVMO).

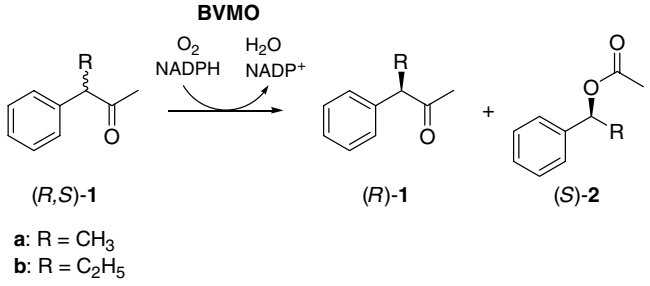

Scheme 1. Kinetic resolution of two 3-phenyl-2-ketones by Baeyer–Villiger monooxygenase-catalyzed oxidation.

After expression of the recombinant enzymes, cells were harvested by centrifugation, washed once with phosphate

* Corresponding author. Tel.: +49 3834 86 4367; fax: +49 3834 86 80066; e-mail: uwe.bornscheuer@uni-greifswald.de

0957-4166/$ - see front matter © 2007 Elsevier Ltd. All rights reserved.
doi:10.1016/j.tetasy.2007.03.025

buffer and used directly afterwards for biocatalysis reactions on an analytical scale. Cofactor recycling was ensured by employing the whole cell *E. coli* and glucose was added to each reaction vial. Therefore, the addition of cofactor NADPH was not necessary. For efficient uptake of the substrates **1a** and **1b** by the cells, β-cyclodextrin had to be included.[22,23] Reaction progress was monitored by GC analyses using a chiral column.

3-Phenyl-2-butanone **1a** was converted by all four enzymes to the corresponding 1-phenylethyl acetate **2a**, while PF-BVMO and PP-BVMO did not oxidize 3-phenyl-2-pentanone **1b** to 1-phenylpropyl acetate **2b** (Tables 1 and 2). The enzymes exhibited different activities and enantioselectivities towards **1a**, for example, CPMO showed the highest activity but only low enantioselectivity ($E < 3$). On the other hand, PF-BVMO exhibited significantly less activity but at the same time was the most selective, yielding the highest *E*-value (analytical scale: $E = 43$, preparative scale: $E = 82$). This value substantially exceeds the selectivity ($E \sim 7$) estimated for a BVMO from *Thermobifida fusca*.[16] Interestingly, PP-BVMO preferentially converted the (*R*)-enantiomer of **1a** ($E = 12$), while the three other BVMOs were (*S*)-selective.

Table 1. Whole cell biocatalysis reactions (analytical scale) with different BVMOs expressed in recombinant *E. coli* for ketone **1a** at 30 °C (CHMO: cyclohexanone monooxygenase from *Acinetobacter calcoaceticus* NCIMB 9871; CPMO: cyclopentanone monooxygenase from *Comamonas* sp. NCIMB 9872; PF-BVMO: BVMO from *P. fluorescens* DSM 50106; PP-BVMO: BVMO from *P. putida* KT2440)

Enzyme	Time (h)	Conversion[a] (%)	Enantiomeric excess		E[a]
			% ee_S	% ee_P	
CHMO	8	41	2.6	8.3 (*S*)	<3
CPMO	2	93	90	6.0 (*S*)	<3
PF-BVMO	8	46	75	90 (*S*)	43
PP-BVMO	2	50	72	71 (*R*)	12

[a] Calculated according to Chen et al.[24]

Table 2. Whole cell biocatalysis reactions (analytical scale) with different BVMOs expressed in recombinant *E. coli* for ketone **1b** at 30 °C. For abbreviations, see Table 1

Enzyme	Time (h)	Conversion[a] (%)	Enantiomeric excess		E[b]
			% ee_S	% ee_P	
CHMO	4	36	n.d.[c]	73 (*S*)	4.5
CPMO	2	44	n.d.[c]	48 (*R*)	4.0
PF-BVMO		No conversion			
PP-BVMO		No conversion			

[a] Calculated by the following equation: (peak areas of product enantiomers)/(peak areas of substrate enantiomers + peak areas of product enantiomers).

[b] Calculated according to Chen et al.[24]

[c] n.d.—not determined due to unsatisfactory separation of enantiomers by GC analysis.

A similar pattern was found for **1b**, for which CHMO and CPMO again exhibited only low enantioselectivity, but the *E*-values were slightly higher compared to **1a** ($E \sim 4$; Table 2). Increasing the length of the alkyl side chain from methyl to ethyl changed the enantiopreference of CPMO from (*S*)- to (*R*)-selectivity, while CHMO remained (*S*)-selective.

Using resting cells of *E. coli* JM109 pGro7 pJOE4072.6, biocatalysis with **1a** was also performed in preparative scale (1 mmol substrate), this time using shake flasks and only 0.5 equiv of β-cyclodextrin. Previous experiments with different cyclodextrin concentrations revealed that conversions only marginally decreased when reducing the amount of cyclodextrin to 0.5 equiv (data not shown). After 6 h at 30 °C, GC analysis showed 46% conversion. The enantiomeric excess of substrate and product was 80% ee and 94% ee, respectively, corresponding to an $E = 82$. For better separation of the ketone and ester during work-up, **2a** was enzymatically hydrolyzed to the corresponding alcohol using *Candida antarctica* lipase A (CAL-A). CAL-A was identified to be non-selective and therefore could be used without affecting the enantiomeric excess of the ester. Thus, 1-phenylethanol **3a** could be isolated in 35% yield and 93% ee. GC analysis of the substrate fraction revealed that a small amount of ester **2a** was still present. Interestingly, using an esterase from *P. fluorescens* instead of CAL-A, the ee-value of **2a** could be increased up to 99% since this enzyme preferentially hydrolyzes the (*R*)-ester (data not shown).

3. Conclusions

Herein, we have shown that arylaliphatic ketones were accepted as substrates by different Baeyer–Villiger monooxygenases. Only the BVMO from *P. fluorescens* DSM 50106 gave satisfactory enantioselectivity in the kinetic resolution of 3-phenyl-2-butanone yielding the corresponding (*S*)-acetate with 93% ee. On a preparative-scale reaction the corresponding chiral alcohol 1-phenylethanol was obtained in 35% yield and 93% ee. Interestingly, one enzyme showed opposite enantiopreference towards **1a** and the increase of the alkyl chain from methyl to ethyl gave no conversion using the BVMOs originating from *Pseudomonas* sp. but inverted the enantiopreference of CPMO.

4. Experimental

4.1. General

All chemicals were purchased from Sigma–Aldrich (Taufkirchen, Germany), Fisher Scientific (Schwerte, Germany), VWR (Darmstadt, Germany), ABCR (Karlsruhe, Germany) and Roth GmbH (Karlsruhe, Germany) unless otherwise specified. ^1H and ^{13}C NMR-spectra were recorded on a 300 MHz or 600 MHz (Bruker) instrument.

4.2. Synthesis of the starting material

3-Phenyl-2-butanone **1a** and 3-phenyl-2-pentanone **1b** were synthesized according to the literature[19] by conversion of the corresponding carboxylic acids with methyllithium. Synthesis of 1-phenylpropyl acetate **2b** was carried out by acetylation of 1-phenylpropanol with acetylchloride.[25] Structural identity was confirmed by NMR spectroscopy.

4.3. BVMO-production

Cyclohexanone monooxygenase (CHMO) from *Acinetobacter calcoaceticus* NCIMB 9871: *E. coli* BL21 (DE3) pKJE7 pMM4[26] was grown in 200 mL LB_{cm+amp} at 30 °C to an optical density of 0.5. Then, 0.5 mg/mL L-arabinose for induction of chaperone coexpression[27] and 0.1 mM IPTG for induction of CHMO expression were added. After further growth for 4 h at 30 °C, cells were harvested by centrifugation (10 min, 4400*g*, 4 °C) and washed once with sterile phosphate buffer (50 mM, pH 7.5).

Cyclopentanone monooxygenase (CPMO) from *Comamonas* sp. NCIMB 9872: expression of CPMO in *E. coli* DH5α pCMO206[28] was performed in 200 mL LB_{amp}. Cells were grown at 37 °C to an optical density of 0.5 where CPMO expression was induced by the addition of 0.1 mM IPTG. After further growth for 6 h at 25 °C, cells were harvested by centrifugation (10 min, 4400*g*, 4 °C) and washed once with sterile phosphate buffer (50 mM, pH 7.5).

BVMO from *P. fluorescens* DSM 50106 (PF-BVMO): *E. coli* JM109 pGro7 pJOE4072.6[18] was grown in 200 mL LB_{cm+amp} containing 0.5 mg/mL L-arabinose at 30 °C. At OD = 0.6, enzyme expression was induced by addition of L-rhamnose (0.2% (w/v) final concentration) and cells were further incubated at 30 °C for 4 h. Afterwards, cells were harvested by centrifugation (10 min, 4400*g*, 4 °C) and washed once with sterile phosphate buffer (50 mM, pH 7.5).

BVMO from *P. putida* KT2440 (PP-BVMO): expression of PP-BVMO in *E. coli* JM109 pGro7 pBVMO2440 was performed as described for PF-BVMO.

After expression of the recombinant BVMOs, the resting cells were used for biocatalysis reactions.

4.4. Biocatalysis reactions on an analytical scale

Recombinant *E. coli* cells carrying the BVMOs were resuspended in a sodium phosphate buffer (50 mM, pH 7.5) to a final OD of around 50. Aliquots (1 mL) of these cell suspensions were mixed in 2 mL Eppendorf (Hamburg, Germany) reaction vials with 15 μmol substrate, 15 μmol β-cyclodextrin and 10 μL of a sterile 1 M glucose solution. The vials were closed with air permeable caps (Lid_{Bac}, Eppendorf) and incubated in a thermoshaker (Eppendorf) at 1400 rpm. After certain time intervals, samples (300 μL) were taken, extracted twice with ethyl acetate and dried over anhydrous sodium sulfate. Excess solvent was removed under nitrogen and samples were analyzed via GC.

4.5. Biocatalysis reaction on a preparative scale

Recombinant *E. coli* cells containing the expressed PF-BVMO were resuspended in sodium phosphate buffer (50 mM, pH 7.5) to a final OD of around 20. To 100 mL of this suspension 1 mmol of substrate **1a**, 0.5 mmol β-cyclodextrin and 2 mL of a sterile 1 M glucose solution were added. The reaction mixture was incubated at 30 °C and 220 rpm. After four hours another 2 mL sterile glucose solution was added. The reaction was stopped after 6 h and extracted five times with 50 mL ethyl acetate. The combined organic phase was dried over anhydrous sodium sulfate and solvent was removed in vacuo.

For better separation of ketone **1a** and ester **2a**, the product mixture was hydrolyzed by *Candida antarctica* lipase A (CAL-A, Chirazyme L-5) in 60 mL of a 5:1 mixture of sodium phosphate buffer and hexane yielding unreacted **1a** and 1-phenylethanol **3a**. After 24 h, the reaction mixture was extracted four times with 30 mL of ethyl acetate. After drying over anhydrous sodium sulfate and evaporation of the organic solvent, the product was purified by column chromatography (hexane/ethyl acetate 5:1). Compound **3a** could be isolated in 35% yield (43 mg, 0.35 mmol).

4.6. Chiral GC analysis

GC analyses on a chiral stationary phase were carried out on a Shimadzu GC-14A gas chromatograph with a chiral β-cyclodextrin column (Hydrodex®-β-3P, Macherey-Nagel, Düren, Germany). Injection and detection temperature were set to 220 °C. Absolute configurations were determined by comparison of the retention times with those of optically active standards of (*R*)-**1a** and (*S*)-**2b** (see Table 3).

Table 3. GC analysis using a chiral column

Compound	T_{Column} (°C)	Retention times (min)
1a	100[a]	7.1/7.6[c]
2a	100[a]	6.7/9.7[d]
3a	100[a]	10.8/12.1[c]
1b	90[b]	35.6/36.1[c]
2b	90[b]	34.6/48.7[d]

[a] Column pressure: 125 kPa.
[b] Column pressure: 65 kPa.
[c] Elution order of enantiomers is (*R*) before (*S*).
[d] Elution order of enantiomers is (*S*) before (*R*).

Acknowledgements

Anett Kirschner thanks the Fonds der Chemischen Industrie (Frankfurt, Germany) and the Studienstiftung des Deutschen Volkes (Bonn, Germany) for stipends. We also thank Anette Riebel and Torge Vorhaben for their support during their practical courses.

References

1. Walsh, C. T.; Chen, Y. C. J. *Angew. Chem., Int. Ed. Engl.* **1988**, *27*, 333–343.
2. Mihovilovic, M. D.; Müller, B.; Stanetty, P. *Eur. J. Org. Chem.* **2002**, 3711–3730.
3. Kamerbeek, N. M.; Olsthoorn, J. J.; Fraaije, M. W.; Janssen, D. B. *Appl. Environ. Microbiol.* **2003**, *69*, 419–426.
4. Mihovilovic, M. D. *Curr. Org. Chem.* **2006**, *10*, 1265–1287.

5. Kamerbeek, N. M.; Janssen, D. B.; van Berkel, W. J. H.; Fraaije, M. W. *Adv. Synth. Catal.* **2003**, *345*, 667–678.
6. Baeyer, A.; Villiger, V. *Chem. Ber.* **1899**, *32*, 3625–3633.
7. Criegee, R. *Justus Liebigs Ann. Chem.* **1948**, *560*, 127–141.
8. Mihovilovic, M. D.; Rudroff, F.; Grötzl, B. *Curr. Org. Chem.* **2004**, *8*, 1057–1069.
9. Strukul, G. *Angew. Chem., Int. Ed.* **1998**, *37*, 1199–1209.
10. Mihovilovic, M. D.; Rudroff, F.; Grötzl, B.; Kapitan, P.; Snajdrova, R.; Rydz, J.; Mach, R. *Angew. Chem., Int. Ed.* **2005**, *44*, 3609–3613.
11. Taschner, M. J.; Black, D. J.; Chen, Q. Z. *Tetrahedron: Asymmetry* **1993**, *4*, 1387–1390.
12. Taschner, M. J.; Peddada, L. *J. Chem. Soc., Chem. Commun.* **1992**, 1384–1385.
13. Taschner, M. J.; Black, D. J. *J. Am. Chem. Soc.* **1988**, *110*, 6892–6893.
14. Carnell, A. J.; Roberts, S. M.; Sik, V.; Willetts, A. J. *J. Chem. Soc., Perkin Trans. 1* **1991**, 2385–2389.
15. Alphand, V.; Furstoss, R. *J. Org. Chem.* **1992**, *57*, 1306–1309.
16. Fraaije, M. W.; Wu, J.; Heuts, D. P. H. M.; van Hellemond, E. W.; Spelberg, J. H. L.; Janssen, D. B. *Appl. Microbiol. Biotechnol.* **2005**, *66*, 393–400.
17. Kirschner, A.; Bornscheuer, U. T. *Angew. Chem., Int. Ed.* **2006**, *45*, 7004–7006.
18. Kirschner, A.; Altenbuchner, J.; Bornscheuer, U. T. *Appl. Microbiol. Biotechnol.* **2007**, *73*, 1065–1072.
19. Rubottom, G. M.; Kim, C.-W. *J. Org. Chem.* **1983**, *48*, 1550–1552.
20. Donoghue, N. A.; Norris, D. B.; Trudgill, P. W. *Eur. J. Biochem.* **1976**, *63*, 175–192.
21. Griffin, M.; Trudgill, P. W. *Eur. J. Biochem.* **1976**, *63*, 199–209.
22. Hedges, A. R. *Chem. Rev.* **1998**, *98*, 2035–2044.
23. Saenger, W. *Angew. Chem., Int. Ed.* **1980**, *19*, 344–362.
24. Chen, C.-S.; Fujimoto, Y.; Girdaukas, G.; Sih, C. J. *J. Am. Chem. Soc.* **1982**, *104*, 7294–7299.
25. Krebsfänger, N.; Zocher, F.; Altenbuchner, J.; Bornscheuer, U. T. *Enzyme Microb. Technol.* **1998**, *22*, 641–646.
26. Chen, G.; Kayser, M. M.; Mihovilovic, M. D.; Mrstik, M. E.; Martinez, C. A.; Stewart, J. D. *New J. Chem.* **1999**, *23*, 827–832.
27. Lee, D. H.; Kim, M. D.; Lee, W. H.; Kweon, D. H.; Seo, J. H. *Appl. Microbiol. Biotechnol.* **2004**, *63*, 549–552.
28. Iwaki, H.; Hasegawa, Y.; Wang, S.; Kayser, M. M.; Lau, P. C. K. *Appl. Environ. Microbiol.* **2002**, *68*, 5671–5684.

Article V

Biotechnol Lett (2007) 29:1393–1398
DOI 10.1007/s10529-007-9401-y

ORIGINAL RESEARCH PAPER

Cloning, expression and characterization of a Baeyer-Villiger monooxygenase from *Pseudomonas putida* KT2440

Jessica Rehdorf · Anett Kirschner · Uwe T. Bornscheuer

Received: 26 February 2007 / Revised: 3 April 2007 / Accepted: 4 April 2007 / Published online: 26 May 2007

Abstract The gene encoding a Baeyer-Villiger monooxygenase and identified in *Pseudomonas putida* KT2440 was cloned and functionally expressed in *Escherichia coli*. The highest yield of soluble protein could be achieved by co-expression of molecular chaperones. In order to determine the substrate specificity, biocatalyses were performed using crude cell extract, growing and resting cells. Examination of aromatic, cyclic and aliphatic ketones revealed a high specificity towards short-chain aliphatic ketones. Interestingly, some open-chain ketones were converted to the alkylacetates, while for others formation of the ester products with oxygen on the other side of the keto group could also be detected yielding the corresponding methyl or ethyl esters.

Keywords Aliphatic ketones · Baeyer-Villiger monooxygenase · Cloning · Enzymatic reactions · *Pseudomonas putida*

J. Rehdorf · A. Kirschner · U. T. Bornscheuer (✉)
Department of Biotechnology and Enzyme Catalysis, Institute of Biochemistry, Greifswald University, Greifswald, Germany
e-mail: uwe.bornscheuer@uni-greifswald.de

Introduction

Baeyer-Villiger monooxygenases (BVMOs) belong to the class of oxidoreductases and convert aliphatic, cyclic and aromatic ketones into esters and lactones, respectively, using molecular oxygen (Mihovilovic et al. 2002). They are flavin-dependent (mostly FAD) and require NAD(P)H to catalyze this reaction. The cyclohexanone monooxygenase from *Acinetobacter calcoaceticus* NCIMB 9871, converting mono- and bicyclic ketones (Donoghue et al. 1976, Stewart 1998), is the best studied BVMO so far. Other BVMOs converting aromatic ketones (Kamerbeek et al. 2001, Tanner and Hopper 2000) or aliphatic open-chain ketones (Britton and Markovetz 1977, Malito et al. 2004) were also described. Recently, the gene of a BVMO from *Pseudomonas fluorescens* DSM 50106 was cloned and functionally expressed in *E. coli* (Kirschner et al. 2007). This enzyme preferentially accepts aliphatic acyclic 2-ketones and converts racemic 4-hydroxy-2-ketones with good enantioselectivities (Kirschner and Bornscheuer 2006). In 2004 the first crystal structure of a BVMO from *Thermobifida fusca*, the phenylacetone monooxygenase, was published (Malito et al. 2004).

In 2002 the complete genome sequence of *Pseudomonas putida* KT2440 was published (GenBank accession number: AE015451) (Nelson et al. 2002). 15 open reading frames encoding putative monooxygenases were determined. Sequence analysis on protein and nucleotide level revealed one monooxygenase

containing sequence motifs typical for Baeyer-Villiger monooxygenases (consensus sequence (FXGXX XHXXXW) and binding sites for cofactor and prosthetic group (GXGXXG-motifs)) (Fraaije et al. 2002). In this paper, we now describe the cloning, expression and the biocatalytical investigation of this newly found Baeyer-Villiger monooxygenase.

Materials and methods

Bacterial strains and plasmids

E. coli DH5α was from Clontech, *E. coli* JM109 was received from New England Biolabs, *E. coli* BL21 (DE3) and pET22b(+) were purchased from Novagen. *Pseudomonas putida* KT2440 was obtained from the FZ Jülich (Jülich, Germany). The Chaperone Plasmid Set containing the plasmids pG-KJE8, pGro7, pKJE7, pG-Tf2 and pTf16 was purchased from TaKaRa Bio Inc.

Construction of expression vectors

The BVMO gene was amplified from the genomic DNA from *Ps. putida* KT2440 without the stop codon using the polymerase chain reaction (PCR) with the oligonucleotides FW-*Pp*KT2440-gDNA (5′-GTA CAT CGA TGG GAT CCT CGG CGG-3′) and RV-*Pp*KT2440-gDNA (5′-GTA CGA GCT CCC ATA TGT CCT CTC ACA C-3′) and *Pwo* DNA polymerase (Roche). The restriction sites for *Nde*I and *Bam*HI (underlined) in the primer sequences were used to perform a directed cloning between the *Nde*I/*Bam*HI sites of the vector pJOE4072.6 (Kirschner et al. 2007). Hereby the BVMO gene was fused at the *C*-terminal end in frame to the six histidine codons (coding for a His-tag) following the *Bam*HI site in the vector. This plasmid was named pJOE-KT2440. For cloning into pET22b(+), a *Hin*dIII restriction site within the gene was deleted using QuikChange site-directed mutagenesis (Stratagene). The mutated pJOE-KT2440 was then digested with *Nde*I and *Hin*dIII and the resulting fragment, consisting of the BVMO gene and the His-tag, was cloned into pET22b(+). This construct was named pET22b(+)-KT2440. Constructs without *C*-terminal His-tags were obtained by introducing a TGA stop-codon into the *Bam*HI site using QuikChange site-directed mutagenesis.

Gene expression

E. coli JM109 was transformed with the pJOE construct, BL21 (DE3) with the pET22b(+) construct. In both cases expression was performed in 30 ml LB media containing 100 μg ampicillin/ml (LB_{amp}) at 25, 30 and 37°C. At an optical density (600 nm) of 0.6–0.7, BVMO expression was induced by the addition of L-rhamnose (0.2% w/v final concentration) for the pJOE construct and with 0.5 mM IPTG for the pET22b(+) construct. During growth for up to 24 h, samples were taken, centrifuged, resuspended in 200 μl sodium phosphate buffer (50 mM, pH 7.5) and disrupted on ice by sonication (Sonoplus, Bandelin, Germany; 50% pulse and 50% amplitude). Inclusion bodies were separated from the cell lysate by centrifugation for 10 min (4°C, 800 × *g*), treated with 0.2% (v/v) Triton X-100 (10 min, 37°C) and washed twice with sodium phosphate buffer. Cell debris were removed from the cell lysate by additional centrifugation at high speed (10 min, 4°C, 16,000 × *g*). Soluble and inclusion body fractions were analysed by SDS-PAGE and Western blotting.

Coexpression of the BVMO gene with chaperone encoding plasmids

E. coli JM109 and BL21 (DE3) cells were transformed with chaperone encoding plasmids and competent cells were prepared thereof. These were transformed with pJOE constructs (for JM109) or pET22b(+) constructs (for BL21 (DE3)) and selected on LB-plates containing 100 μg ampicillin/ml and 34 μg chloramphenicol/ml ($LB_{amp + cm}$). Expression was performed at 30°C as described before using $LB_{amp + cm}$ containing 0.5 mg L-arabinose/ml (in case of pGro7, pKJE7 and pTf16), 5 ng tetracycline/ml (in case of pG-Tf2) or L-arabinose and tetracycline (in case of pG-KJE8) in concentrations given above.

Biocatalysis and biotransformation

Substrate specificity was investigated using crude cell extract, growing and resting cells. For all experiments *E. coli* JM109 pJOE-KT2440 pGro7 cells were used.

Biocatalysis with crude cell extract

Cells were grown in 2x $YT_{amp + cm}$ medium at 37°C to an optical density (600 nm) of 0.6–0.7. BVMO expression was induced by the addition of L-rhamnose to 0.2% (w/v), chaperone expression (GroES/EL) by the addition of L-arabinose to 0.5 mg/ml. Expression was performed at 25°C overnight (~12 h). Cells were harvested at an optical density (600 nm) of 6–7, washed and resuspended in sterile sodium phosphate buffer (50 mM, pH 7.5). Cell disruption was performed by sonication on ice, cell debris were removed by centrifugation (30 min, 4°C, 10,000 × *g*). Biocatalysis reactions were performed in 2 ml reaction tubes closed with air permeable caps (Lid_{Bac}, Eppendorf) at 20, 25 and 30°C. For all investigated temperatures the same crude cell extract was used. To 900 µl crude cell lysate 50 µl FAD (1 mg/ml), 200 mM NADPH and 50 mM substrate (aliphatic, aromatic and cyclic ketones) were added. After defined time intervals (1, 2, 4 and 6 h) samples were taken, extracted with dichloromethane and dried over anhydrous sodium sulphate. Samples were analysed via GC-MS.

Biotransformation with resting cells

Cultivation and BVMO expression were performed as described for crude cell extract. At an optical density (600 nm) of 6–7, cells were harvested, washed twice with sterile sodium phosphate buffer (50 mM, pH 7.5) and resuspended in the same buffer. 10 mM substrate and 20 mM glucose for cofactor regeneration were added simultaneously. Biotransformation was performed in flasks (50 ml cell suspension; optical density 6–7) at 20, 25 and 30°C. Samples were taken at defined times (0.5, 1, 2, 4, 8, 24 and 32 h) and treated as above.

Biotransformation with growing cells

Cells were grown in 50 ml 2x $YT_{amp + cm}$ at 37°C to an optical density at 600 nm of 0.6–0.7. BVMO expression was induced by addition of L-rhamnose to 0.2% (w/v) and chaperone expression (GroES/EL) by the addition of L-arabinose to 0.5 mg/ml. Subsequently, 10 mM substrate was added. Expression and biotransformation were performed at 20, 25 and 30°C. After defined time intervals (1, 4, 8 and 24 h) samples were taken and treated as described above.

GC-MS analysis

GC-MS analyses were carried out on a GCMS-QP 2010 instrument (Shimadzu) with a BPX5 column (Macherey-Nagel). All substrates, methyl and ethyl esters were purchased from Fluka at GC standard purity. Other ester standards for GC-MS analysis were prepared enzymatically according to Kirschner et al. (2007). ^{1}H-NMR spectra were recorded in $CDCl_3$ on a 300 MHz (Bruker) instrument. The obtained NMR spectra of aliphatic esters matched literature data.

Results and discussion

Cloning and BVMO expression in *E. coli*

The gene of the BVMO from *Pseudomonas putida* KT2440 was successfully amplified by PCR from the genomic DNA and inserted into pJOE4072.6 and pET22b(+). The BVMO expression was performed in *E. coli* JM109 with pJOE-KT2440 and in BL21 (DE3) with pET22b(+)-KT2440. Different expression temperatures were investigated and the amount of BVMO in the soluble and inclusion body fraction was studied by SDS-PAGE and western blotting. For both systems, more enzyme was found in the pellet than in the soluble fraction revealing a problem with the proper folding of the BVMO in *E. coli*. Therefore, the BVMO was co-expressed at 30°C with different combinations of chaperones provided by the TaKaRa Chaperone Plasmid Set. It has already been reported that coexpression of molecular chaperones in the *E. coli* cytoplasm could significantly increase the yield of soluble protein (Lee et al. 2004). For co-expression in *E. coli* JM109, the GroES/GroEL complex (pGro7) as well as GroES/GroEL together with DnaK/DnaJ/GrpE (pG-KJE8) or the trigger factor (pG-Tf2) led to noticeably higher amounts of soluble BVMO (Fig. 1), whereas the DnaK/DnaJ/GrpE (pKJE7) alone or in combination with the trigger factor (pTf16) showed only a slightly positive effect on BVMO expression (data not shown). For coexpression in BL21 (DE3) no noticeably higher

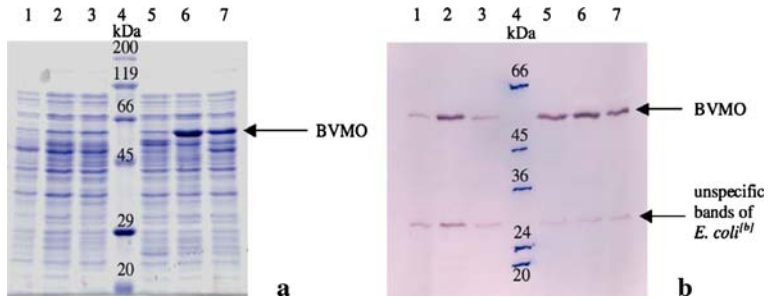

Fig. 1 SDS-PAGE and Western blot of the soluble fraction of BVMO expression in *E. coli* JM109 with and without coexpression of chaperones [a]; for detection of 6xHis tagged BVMO, the QIAexpress detection system using a Ni-NTA-alkaline phosphatase conjugate (Qiagen) was applied according to the manufacturer's instructions. *Notes*: [a] Lanes 1–3: expression without chaperones at 25, 30 and 37°C, respectively; lanes 5–7: chaperone coexpression with pG-KJE8, pGro7 and pG-Tf2 at 25°C, respectively; lane 4: (**a**) RotiMark Standard (Roth), (**b**) Low Range Marker (Sigma). [b] Western blot analysis of expression experiments with *E. coli* JM109 pJOE without an additional gene revealed a band of the same molecular weight assuming an *E. coli* host-protein with cross-reaction to the Ni-NTA-alkaline phosphatase conjugate (data not shown)

amount of soluble BVMO could be obtained (data not shown).

Substrate specificity

In order to investigate the substrate specificity of the BVMO from *Ps. putida* KT2440 biocatalytic reactions at 30°C using crude cell extract were performed. Different substrates (cyclic, aromatic and aliphatic open-chain ketones) were investigated. However, only aliphatic acyclic ketones were converted to the corresponding esters with good conversions, while oxidation of cyclic ketones (cyclohexanone, cyclopentanone and cycloheptanone) was rather low and aromatic ketones (acetophenone and derivatives) were not accepted at all (data not shown). In fact, a search in the protein sequence data base revealed that one of the closest homologs (52% sequence identity) with known substrate specificity is the prodrug activator EtaA from *Mycobacterium tuberculosis* (Fraaije et al. 2004). This enzyme was shown to convert aliphatic open-chain ketones as well as phenylacetone and benzylacetone, while typical BVMO substrates like acetophenone and cyclohexanone were not accepted. Interestingly, sequence identity with a BVMO from *Ps. fluorescens* DSM50106 with similar substrate specificity was only 25% (Kirschner et al. 2007).

Further experiments investigating the conversion of aliphatic open-chain ketones (C_8–C_{13}) were then performed at 20, 25 and 30°C using crude cell extract, growing and resting cells. When using whole cells expressing the BVMO, there was no need to add NADPH, which makes biotransformations cost-effective. Reaction courses were monitored via GC-MS analysis.

In Table 1, conversions at 25°C after 8 h reaction time for all investigated aliphatic acyclic ketones using the three different systems are summarized. As a control, biotransformations were also performed under the same reaction conditions using a pJOE-vector without the BVMO gene, but no ester formation could be detected. Additionally, no other by-product could be found and product esters were not further hydrolyzed by *E. coli* enzymes since no alcohol could be detected. However, especially for the shorter chain compounds (C_8, C_9) a significant loss of substrate and product due to evaporation was evident at 30°C.

Apparently, in all three systems the BVMO from *Ps. putida* KT2440 preferentially converted short-chain ketones like 2-decanone, 3-decanone and 4-decanone. Here conversions reached the highest values. A BVMO from *Ps. cepacia* also converts aliphatic open-chain ketones with good yields. However, in contrast to the BVMO from *Ps. putida* KT2440, this 2-tridecanone monooxygenase preferred medium-chain ketones from C_{12}–C_{14} and also converted cyclopentanone with high specific activity (Britton and Markovetz 1977).

Comparing biocatalysis with crude cell extract and biotransformation using whole cells, either growing

Table 1 Conversion of aliphatic acyclic ketones using crude cell extract, growing and resting cells

Substrate	Conversion [%]			Product composition
	Cell extract[a]	Growing cells[b]	Resting cells[c]	(for resting cells)
2-Octanone	0	0	4	Hexyl acetate
2-Nonanone	13	n.d.	22	Heptyl acetate
2-Decanone	12	36	93	Octyl acetate
3-Decanone	9	50	95	Heptyl propionate and ethyl caprylate (1:1)[d]
4-Decanone	12	62	100	Hexyl butyrate
2-Undecanone	5	3	35	Nonyl acetate and methyl decanoate (7:2)[e]
2-Dodecanone	2.5	0	5	Decyl acetate and methyl undecanoate (7:2)[f]
2-Tridecanone	0	6	6	Methyl laurate

n.d. = Not determined

[a] 50 mM substrate, 200 mM NADPH

[b] 10 mM substrate

[c] 10 mM substrate, 20 mM glucose for cofactor regeneration

[d] Crude cell extract: heptylpropionate only; growing cells: heptylpropionate and ethylcaprylate (1:1)

[e] Crude cell extract: nonylacetate only; growing cells: nonylacetate and methyldecanoate (5:2)

[f] Crude cell extract: decylacetate only

All values were measured after 8 h at pH 7.5 and 25°C

or resting, revealed that the latter system worked more efficiently at all investigated temperatures since conversions were higher and some ketones were oxidized even quantitatively. In the case of crude cell extract, sonication leading to the loss of the enzyme protecting physiological environment can influence enzyme activity and stability. This might be a possible explanation for reduced conversions. When using growing cells, substrate was added simultaneously to the time-point of induction of BVMO expression, whereas for resting cells the enzyme was first expressed before starting biotransformations. Conclusively, the reaction times for growing cells are much longer compared to resting cells. Another problem using growing cells was that 2-nonanone (or an unknown impurity in the substrate) seemed to have a harmful effect, since no conversion could be detected and no more growth could be observed after substrate addition. Thus, resting cells seemed to give best results working sufficiently and cost-effective.

Interestingly, conversion of some ketones did not only generate one ester product. According to Fig. 2, oxygen can be inserted on both sides of the keto group producing alkylacetates as well as the less favored methyl esters. With longer chain length the enzyme does not insert oxygen by migration of the higher substituted alkyl chain as typical for Baeyer-Villiger reactions. Instead, conversion into the methylesters seem to be preferred. Comparing these results to those of the BVMO from *Ps. fluorescens* DSM50106 it strikes that for this enzyme the migrating substituent during oxygen insertion depends on the position of the keto group. While here all 2-ketones became acetates, 3-ketones were converted into both ester products and 4-ketones gave propylesters only (unpublished results). In the case of EtaA from *Mycobacterium tuberculosis* insertion of oxygen depends on alkyl chain length and position of the keto group (Fraaije et al. 2004).

Examining the different results at 20, 25 and 30°C also revealed a correlation between reaction temperature and conversion. Biotransformations at 30°C using resting cells lead to a two-fold increase or quantitative conversion in comparison to 20°C after

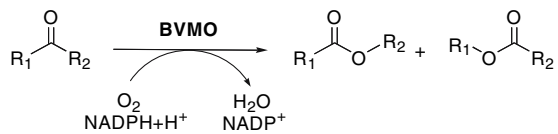

Fig. 2 BVMO catalyzed conversion of aliphatic open-chain ketones

the same reaction time (data not shown). At higher temperatures reaction times were shorter but, especially for the short-chain ketones, the effect of evaporation was also more evident.

Conclusion

In this study, the gene of a Baeyer-Villiger monooxygenase from *Pseudomonas putida* KT2440 was successfully amplified from genomic DNA and cloned into two different vectors. Performing coexpression of different chaperones with the BVMO successfully lead to soluble protein. Investigation of substrate specificity revealed a high preference towards short-chain aliphatic ketones. Comparing biocatalysis using crude cell extract and whole cells showed that resting cells worked most efficiently and gave the best results. Additionally, it was found that some acyclic ketones were converted not only to the alkylacetates, but also methyl- and ethylesters were obtained, indicating insertion of oxygen on both sides of the keto group.

Acknowledgements We thank the Deutsche Bundesstiftung Umwelt (Osnabrück, Germany) for a stipend to Jessica Rehdorf and the Fonds der Chemischen Industrie (Frankfurt, Germany) and the Studienstiftung des Deutschen Volkes (Bonn, Germany) for stipends to Anett Kirschner.

References

Britton LN, Markovetz AJ (1977) A novel ketone monooxygenase from *Pseudomonas cepacia*. J Biol Chem 252:8561–8566

Donoghue NA, Norris DB, Trudgill PW (1976) The purification and properties of cyclohexanone oxygenase from *Nocardia globerula* CL1 and *Acinetobacter calcoaceticus* NCIMB 9871. Eur J Biochem 63:175–192

Fraaije MW, Kamerbeek NM, Heidekamp AJ et al (2004) The produg activator EtaA from *Mycobacterium tuberculosis* is a Baeyer-Villiger monooxygenase. J Biol Chem 279:3354–3360

Fraaije MW, Kamerbeek NM, van Berkel WJH et al (2002) Identification of a Baeyer-Villiger monooxygenase sequence motif. FEBS Lett 518:43–47

Kamerbeek NM, Moonen MJH, van der Ven JGM et al (2001) 4-Hydroxyacetophenone monooxygenase from *Pseudomonas fluorescens* ACB. Eur J Biochem 268:2547–2557

Kirschner A, Altenbuchner J, Bornscheuer UT (2007) Cloning, expression and characterization of a Baeyer-Villiger monooxygenase from *Pseudomonas fluorescens* DSM 50106 in *E. coli*. Appl Microbiol Biotechnol 73:1065–1072

Kirschner A, Bornscheuer UT (2006) Baeyer-Villiger monooxygenase-catalyzed kinetic resolution of 4-hydroxy-2-ketones. Angew Chem Int Ed 45:7004–7006

Lee DH, Kim MD, Lee WH et al (2004) Consortium of fold-catalyzing proteins increases soluble expression of cyclohexanone monooxygenase in recombinant *Escherichia coli*. Appl Microbiol Biotechnol 63:549–552

Malito E, Alfieri A, Fraaije MW et al (2004) Crystal structure of a Baeyer-Villiger monooxygenase. Proc Natl Acad Sci USA 101:13157–13162

Mihovilovic MD, Müller B, Stanetty P (2002) Monooxygenase-mediated Baeyer-Villiger oxidations. Eur J Org Chem 2002:3711–3730

Nelson KE, Weinel C, Paulsen IT et al (2002) Complete genome sequence and comparative analysis of the metabolically versatile *Pseudomonas putida* KT2440. Environ Microbiol 4:799–808

Stewart JD (1998) Cyclohexanone monooxygenase: a useful reagent for asymmetric Baeyer-Villiger reactions. Curr Org Chem 2:211–232

Tanner A, Hopper DJ (2000) Conversion of 4-hydroxyacetophenone into 4-phenyl acetate by a flavin adenine dinucleotide-containing Baeyer-Villiger-type monooxygenase. J Bacteriol 182:6565–6569

Article VI

APPLIED AND ENVIRONMENTAL MICROBIOLOGY, May 2009, p. 3106–3114 Vol. 75, No. 10
0099-2240/09/$08.00+0 doi:10.1128/AEM.02707-08

Cloning, Expression, Characterization, and Biocatalytic Investigation of the 4-Hydroxyacetophenone Monooxygenase from *Pseudomonas putida* JD1[▽]†

Jessica Rehdorf, Christian L. Zimmer, and Uwe T. Bornscheuer*

Department of Biotechnology and Enzyme Catalysis, Institute of Biochemistry, Greifswald University, Felix-Hausdorff-Strasse 4, D-17487 Greifswald, Germany

Received 26 November 2008/Accepted 20 February 2009

While the number of available recombinant Baeyer-Villiger monooxygenases (BVMOs) has grown significantly over the last few years, there is still the demand for other BVMOs to expand the biocatalytic diversity. Most BVMOs that have been described are dedicated to convert efficiently cyclohexanone and related cyclic aliphatic ketones. To cover a broader range of substrate types and enantio- and/or regioselectivities, new BVMOs have to be discovered. The gene encoding a BVMO identified in *Pseudomonas putida* JD1 converting aromatic ketones (HAPMO; 4-hydroxyacetophenone monooxygenase) was amplified from genomic DNA using SiteFinding-PCR, cloned, and functionally expressed in *Escherichia coli*. Furthermore, four other open reading frames could be identified clustered around this HAPMO. It has been suggested that these proteins, including the HAPMO, might be involved in the degradation of 4-hydroxyacetophenone. Substrate specificity studies revealed that a large variety of other arylaliphatic ketones are also converted via Baeyer-Villiger oxidation into the corresponding esters, with preferences for *para*-substitutions at the aromatic ring. In addition, oxidation of aldehydes and some heteroaromatic compounds was observed. Cycloketones and open-chain ketones were not or poorly accepted, respectively. It was also found that this enzyme oxidizes aromatic ketones such as 3-phenyl-2-butanone with excellent enantioselectivity ($E \gg 100$).

Baeyer-Villiger monooxygenases (BVMOs; EC 1.14.13.x) belong to the class of oxidoreductases and convert aliphatic, cyclic, and/or aromatic ketones to esters or lactones, respectively, using molecular oxygen (29). Thus, they mimic the chemical Baeyer-Villiger oxidation, which is usually peracid catalyzed and was first described by Adolf Baeyer and Viktor Villiger in 1899 (2). All characterized BVMOs thus far are NAD(P)H dependent and require flavin adenine dinucleotide (FAD) or flavin mononucleotide (FMN) as prosthetic group, which is crucial for catalysis.

Today, BVMOs are increasingly recognized as valuable catalysts for stereospecific oxidation reactions. These enzymes display a remarkably broad acceptance profile for nonnatural substrates. Besides conversion of a wide range of aliphatic open-chain, cyclic, and aromatic ketones, they are also able to oxygenate sulfides (16), selenides (27), amines (33), phosphines, olefins (5), aldehydes, and borone- and iodide-containing compounds (Fig. 1) (7).

Therefore, recombinantly available BVMOs are powerful tools in organic chemistry and demonstrate a high potential as alternatives to existing chemical technologies, where some of these reactions are difficult to perform selectively using chemical catalysts.

Except for this promiscuity in reactivity, high enantioselectivities, as well as regio- and stereoselectivities, make them interesting for the pharmaceutical, food, and cosmetic industries, where enantiomerically pure compounds are valuable building blocks. In addition, renunciation of peracids when applying enzymatic driven Baeyer-Villiger oxidations turns them into an ecofriendly alternative and led to a considerable interest for biotransformations using BVMOs on an industrial scale (1, 8, 13–15) during the past decades.

Already in 1948 it was recognized that enzymes catalyzing the Baeyer-Villiger reaction exist in nature (39). This was concluded from the observation that a biological Baeyer-Villiger reaction occurred during the degradation of steroids by fungi. Still it took 20 years for the first BVMO to be isolated and characterized (10). Thus far, 22 BVMOs have been cloned, functionally expressed, and characterized. In Fig. 2 their genetic relationships are illustrated, and all BVMOs are sorted into different classes on the basis of their substrate specificity. Only two BVMOs, the 4-hydroxyacetophenone monooxygenase (HAPMO) from *Pseudomonas fluorescens* ACB (19) and phenylacetone monooxygenase (PAMO) from *Thermobifida fusca* (11), converting arylaliphatic and aromatic ketones were described. The latter is the only thermostable BVMO and served as a model to elucidate the enzymatic mechanism (28).

We report here the amplification, cloning, functional expression, and characterization of a HAPMO from *Pseudomonas putida* JD1 oxidizing a broad range of aromatic ketones and further substrates.

MATERIALS AND METHODS

Chemicals. All chemicals were of highest purity and purchased from Fluka (Buchs, Switzerland), Sigma-Aldrich (Taufkirchen, Germany), Roth GmbH

* Corresponding author. Mailing address: Department of Biotechnology and Enzyme Catalysis, Institute of Biochemistry, Greifswald University, Felix-Hausdorff-Str. 4, D-17487 Greifswald, Germany. Phone: 49-3834-86-4367. Fax: 49-3834-86-80066. E-mail: uwe.bornscheuer@uni-greifswald.de.

† Supplemental material for this article may be found at http://aem.asm.org/.

▽ Published ahead of print on 27 February 2009.

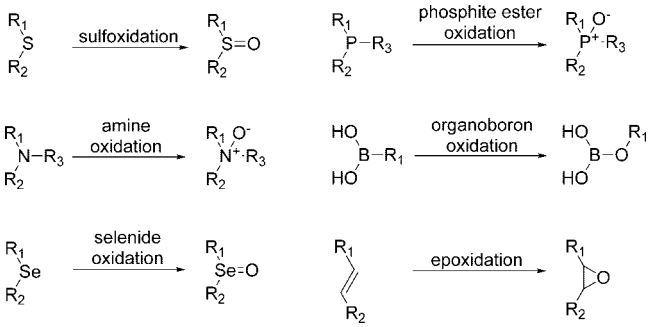

FIG. 1. Range of Baeyer-Villiger oxidations catalyzed by BVMOs.

(Karlsruhe, Germany), and Merck (Darmstadt, Germany) unless otherwise specified. Restriction enzymes were obtained from New England Biolabs (Beverly, MA), and NADPH was from Codexis (Jülich, Germany). DEAE-Sepharose FastFlow was from GE Healthcare (Uppsala, Sweden), and Reactive Red 120-Agarose was from Sigma-Aldrich. All β-hydroxyketones, as well as 4-hydroxy-4-phenyl-2-butanone, were synthesized according to the method of Kourouli et al. (23), and 3-phenyl-2-ketones and 1-phenylpropylacetate were synthesized according to the methods of Rubottom and Kim (35) and Krebsfänger et al. (24), respectively. Corresponding ester standards of β-hydroxyketones for gas chromatography-mass spectrometry (GC-MS) analysis were prepared enzymatically according to the method of Kirschner and Bornscheuer (22).

Bacterial strains, culture conditions, and plasmids. *P. putida* JD1 was kindly provided by David J. Hopper (Institute of Biological Sciences, University of Wales, Aberystwyth, Ceredigion, United Kingdom). *Escherichia coli* DH5α [Δ*lacU169*(ϕ80*lacZ*ΔM15) *hsdR17 recA1 end A1 gyrA96 thi-1 relA1*] was obtained from Clontech (Mountain View, CA). *E. coli* JM109 [*recA1 endA1 gyrA96 thi-1 hsdR17 supE44 relA* Δ(*lac-proAB*) F^- (*traD36 proAB*$^+$ *lacI*^{q} *lacZ*ΔM15)] was obtained from New England Biolabs (Beverly, MA). *E. coli* BL21(DE3) [F^- *ompT hsdSB* (r_B^- m_B^-) *gal dcm rne131* (DE3)] and Rosetta [F^- *ompT hsdSB*(r_B^- m_B^-) *gal dcm lacY1* (DE3)/pRARE (Cam^r)] and the plasmid pET22b(+) were purchased from Novagen (Darmstadt, Germany). *E. coli* BL21-CodonPlus (DE3)-RP [F^- *ompT hsdS* (r_B^- m_B^-) *dcm*$^+$ Tet^r *gal* λ(DE3) *endA* Hte (*argU proL*; Cam) (*argU ileY leuW*; Strep/Spec)] was from Stratagene (La Jolla, CA), and *E. coli* BL21 C41(DE3) [F^- *ompT gal hsdSB* (r_B^- m_B^-) *dcm lon* λDE3] was obtained from OverExpress. OneShot TOP10 cells [F^- *mcrA* Δ(*mrr-hsdRMS-mcrBC*) ϕ80*lacZ*ΔM15 Δ*lacX74 recA1 araD139* Δ(*ara-leu*)*7697 galU galK rpsL* (Str^r) *endA1 nupG*] for blue-white screening were purchased from Invitrogen (Paisley, United Kingdom). *E. coli* strains

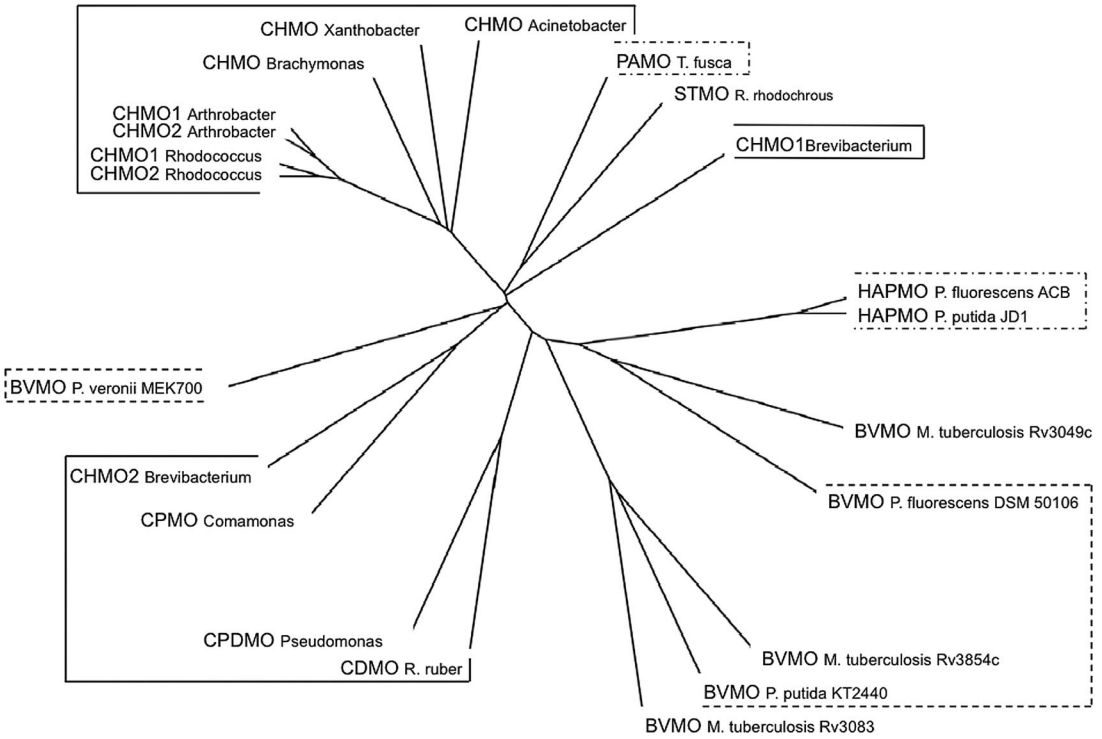

FIG. 2. Phylogenetic relationships within BVMOs. The sequences of 22 enzymes with confirmed BVMO activity were aligned, and an unrooted phylogenetic tree was generated using CLUSTAL W (v.1.81). Cycloketone-converting BVMO (solid lines), open-chain ketone-converting BVMO (dashed lines), and arylketone-converting BVMO (dash/dot lines). NCBI accession numbers of protein sequences: CHMO *Acinetobacter*, CHMO *Acinetobacter calcoaceticus* NCIMB 9871 (BAA86293); CHMO *Xanthobacter*, BVMO *Xanthobacter* sp. strain ZL5 (CAD10801); CHMO *Brachymonas*, CHMO *Brachymonas petroleovorans* (AAR99068); CHMO1 *Arthrobacter*, CHMO1 *Arthrobacter* sp. strain BP2 (AAN37479); CHMO2 *Arthrobacter*, CHMO2 *Arthrobacter* sp. strain L661 (ABQ10653); CHMO1 *Rhodococcus*, CHMO1 *Rhodococcus* Phi1 (AAN37494); CHMO2 *Rhodococcus*, CHMO2 *Rhodococcus* Phi2 (AAN37491); CHMO1 *Brevibacterium*, CHMO1 *Brevibacterium* sp. strain HCU (AAG01289); CHMO2 *Brevibacterium*, CHMO2 *Brevibacterium* sp. strain HCU (AAG01290); CPMO *Comamonas*, cyclopentanone monooxygenase *Comamonas* sp. strain NCIMB 9872 (BAC22652); CPDMO *Pseudomonas*, cyclopentadecanone monooxygenase *Pseudomonas* sp. strain HI-70 (BAE93346); CDMO *R. ruber*, cyclododecane monooxygenase *Rhodococcus ruber* SCI (AAL14233); BVMO *Mycobacterium tuberculosis* Rv3083, BVMO *M. tuberculosis* H37Rv (gene Rv3083) (CAA16141); BVMO *M. tuberculosis* Rv3049c, BVMO *M. tuberculosis* H37Rv (gene Rv3049c) (CAA16134); BVMO *M. tuberculosis* Rv3854c, BVMO *M. tuberculosis* H37Rv (gene Rv3854c) (CAB06212); BVMO *P. putida* KT2440, BVMO *P. putida* KT2440 (AAN68413); BVMO *P. fluorescens* DSM50106: BVMO *P. fluorescens* DSM50106 (AAC36351); BVMO *Pseudomonas veronii* MEK700, BVMO *P. veronii* MEK700 (ABI15711); STMO *Rhodococcus rhodochrous*, steroid monooxygenase *R. rhodochrous* (BAA24454); PAMO *T. fusca*, phenylacetone monooxygenase *T. fusca* (Q47PU3); HAPMO *P. fluorescens* ACB, 4-hydroxyacetophenone monooxygenase from *P. fluorescens* ACB (AAK54073); HAPMO *P. putida* JD1, 4-hydroxyacetophenone monooxygenase from *P. putida* JD1 (FJ010625 [the present study]).

were routinely cultured in LB medium and, when necessary, supplemented with ampicillin (100 μg/ml) or chloramphenicol (25 μg/ml). The Chaperone plasmid set containing the plasmids pG-KJE8, pGro7, pKJE7, pG-Tf2, and pTF16 was purchased from TaKaRa Bio, Inc. (Otsu, Japan).

Genetic methods and sequence analysis. Total genomic DNA (gDNA) from *P. putida* JD1 was amplified by using a GenomiPhi v.2 DNA amplification kit from GE Healthcare. Plasmid isolations (Fermentas, St. Leon-Roth, Germany), PCR purification, and gel extraction (Qiagen, Hilden, Germany) were performed according the protocols of the manufacturers. Standard procedures such as DNA cloning and manipulations were performed as described by Sambrook and Russell (36). DNA sequencing was conducted by GATC (Konstanz, Germany), and analyses were carried out using the software package VectorNTI from Invitrogen.

16S rRNA gene sequencing. The nearly full-length 16S rRNA gene of the *P. putida* JD1 strain was amplified by PCR using the eubacterial 16S rRNA gene primers 27f and 1492r as described by Lane (26). For further information, see the supplemental material.

Cloning of the HAPMO-encoding gene. Degenerate primers were designed on the basis of three peptides (including the N-terminal sequence) obtained by Edman degradation of the HAPMO as described by Tanner and Hopper (38) to perform gradient PCR using gDNA and Opti*Taq* DNA polymerase (Roboklon, Berlin, Germany). The sequences of the primers were as follows: PpJD1-4HAPMO-FW1deg, ATGCGCACCTAYAAYACCAC; PpJD1-4HAPMO-RV1deg, GCGCC GGTGCCGATSACSGCSACGCG; PpJD1-4HAPMO-RV2deg, ATCCAGGTGC CRTCRTCGCGGATGATGC; and PpJD1-4HAPMO-Cterm1deg, TACATGCA GAACATRTTSGGGAACTGSGGSACGGTCATRC. The PCR conditions were as follows: 3 min at 95°C; followed by 45 cycles consisting of 95°C for 1 min, 50 to 65°C for 30 s, and 72°C for 1.5 min; and a final extension step of 7 min at 72°C. Due to the use of degenerate primers the annealing step was performed between 55 and 65°C. The sequence of the PCR product was blasted in nonredundant databases. The most similar hit was the HAPMO from *P. fluorescens* ACB. Thus, it was assumed that the amplified product is indeed part of the sequence of the HAPMO gene from *P. putida* JD1. Since the missing C-terminal end of the gene could not be amplified using inverse PCR (32), SiteFinding-PCR was performed as an alternative approach as described Tan et al. (37). The cycler conditions are given in Table S1 in the supplemental material. As counter primers, two gene-specific primers were designed: GSP1 (AAAAAGCTTTTGCCTCGCTCAG) and GSP2 (TTGGCAGC TGCTCAAGGTCG). The amplified product was subcloned directly in the pCRII-TOPO vector, and OneShot TOP10 cells were transformed with this construct. After sequencing, the HAPMO gene was reamplified with nested PCR from gDNA using *Pfu*Plus DNA polymerase and primers incorporating restrictions sites (NdeI and BamHI [underlined in the sequences below]) for direct cloning into the expression vectors pET22b(+) and pJOE4072.6. The sequences of the primers were: FW1-HAPMO, TTCATCGGGCAGATGCACGG; FW2-HAPMO-NdeI, CATATGAG AACCTACAACACCACTTTGGC; RV1-HAPMO, TTGTAATTATTACCTGG CGGCCAG; and RV2-HAPMO-BamHI, GGATCCTCAGGAAAGGCAGTAGT CGG. The amplified product was subcloned into the pCRII-TOPO vector, digested with NdeI and BamHI (37°C, 3 h), and ligated into NdeI/BamHI-linearized pET22b(+) and pJOE4072.6, respectively. The plasmids were named pJOEPpJD1HAPMO and pET22b(+)PpJD1HAPMO and transformed into *E. coli* cells, followed by sequencing to confirm correct sequences.

Expression of 4-HAPMO in *E. coli*. *E. coli* JM109 was transformed with pJOE PpJD1HAPMO, and all BL21(DE3) strains, JM109 (DE3), and *E. coli* Rosetta were transformed with pET22b(+)PpJD1HAPMO. In all cases, expression was evaluated in 30 ml of LB or 2×YT medium (2% tryptone, 1% NaCl, 1% yeast extract) containing 100 μg of ampicillin/ml. For the expression in *E. coli* Rosetta, 25 μg of chloramphenicol/ml was also added. Induction, protein expression, and sample preparation for sodium dodecyl sulfate-polyacrylamide gel electrophoresis (SDS-PAGE) were performed according to the method of Rehdorf et al. (34).

Coexpression with molecular chaperones. *E. coli* JM109 and BL21(DE3) cells were transformed with chaperone-encoding plasmids (pGro7, pKJE7, pTf16, pG-KJE8, and pTf16). Cells were grown in 20 ml of LB containing 34 μg of chloramphenicol (LB_{cap})/ml at 37°C, and competent cells were prepared (36). These cells were transformed with pJOE constructs (for JM109) or pET22b(+) constructs [for BL21(DE3)] and selected on $LB_{cap+amp}$. Expression was performed at 30°C as described above using $LB_{cap+amp}$ containing L-arabinose (in case of pGro7, pKJE7, and pTf16) at 0.5 mg/ml or 5 ng of tetracycline/ml (in the case of pG-Tf2) or L-arabinose and tetracycline (in the case of pG-KJE8) in the concentrations given above.

Enzyme purification. Overexpressed HAPMO was purified to homogeneity in two chromatographic steps. For this, HAPMO was expressed in *E. coli* Rosetta (induction with 0.1 mM IPTG [isopropyl-β-D-thiogalactopyranoside] at an optical density at 600 nm of 1) using 2×YT-medium at 20°C for 6 h in a volume of 500 ml. Cells (4 g [wet weight]) were then harvested, washed twice with sterile sodium phosphate buffer (pH 7.0, 20 mM), and disrupted with a precooled French pressure cell (Polytec) at 96.5×10^3 kPa. The lysate was centrifuged for 30 min at 10,000 × *g* and 4°C. The supernatant (30 ml) was taken as crude extract, and purification steps were performed as described by Tanner and Hopper (38). Fractions containing HAPMO activity were pooled and concentrated (Amicon/Millipore, Schwalbach, Germany). All purification steps were performed at room temperature.

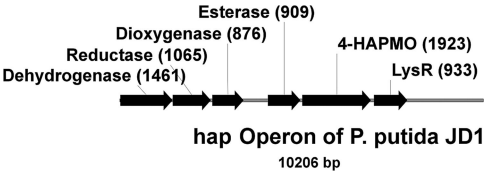

FIG. 3. Organization of the gene cluster of the 10.2-kb DNA fragment of *P. putida* JD1 amplified using SiteFinding-PCR. Dehydrogenase, putative 3-hydroxymuconic semialdehyde dehydrogenase; reductase, putative maleylacetate reductase; dioxygenase, putative hydroquinone dioxygenase; esterase, putative 4-hydroxyphenyl acetate hydrolase; 4-HAPMO, 4-hydroxyacetophenone monooxygenase; LysR, regulatory protein (LysR family).

Kinetic measurements. HAPMO activity was determined spectrophotometrically by monitoring the decrease of NADPH at 370 nm (ε = 1.96 mM/cm). Reaction mixtures (1 ml) contained 50 mM Tris-HCl buffer (pH 8.0), 312.5 μM NADPH, 28 mU of enzyme, and 10 μl of 0.1 mM 4-hydroxyacetophenone in dimethyl formamide. The reaction was started by adding NADPH to the mixture. One unit of HAPMO is defined as the amount of protein that oxidizes 1 μmol of NADPH per min. All kinetic measurements were performed at 30°C in air-saturated buffer. The kinetic parameters for all derivatives were determined by using at least six substrate concentrations ranging from 1 μM to 60 mM and a fixed concentration of 312.5 μM NADPH. The K_m and V_{max} for NADPH were determined by using a fixed concentration of 500 μM 4-hydroxyacetophenone and NADPH in a concentration range from 5 to 625 μM. All concentrations were measured in triplicate, and data were calculated according to the Hanes-Wolff equation.

Determination of protein concentration. The protein concentration was determined by using a BCA assay protein quantification kit from Uptima (Montluçon, France) with bovine serum albumin as a standard in sodium phosphate buffer (pH 7.0, 20 mM).

Effect of pH on activity. A total of 28 mU of purified enzyme was preincubated in acetate buffer (pH 4.0 to 5.5), phosphate buffer (pH 7.5 to 8.0), and Tris-HCl (pH 7.5 to 9.0) at 25°C for 30 min. The activity was measured spectrophotometrically as described above using 312.5 μM NADPH and 0.5 mM 4-hydroxyacetophenone.

Thermal stability. The half-life at various temperatures was studied by preincubating protein samples (28 mU of purified enzyme) in Tris-HCl buffer (pH 8.0, 50 mM) at 25, 30, and 35°C. After definite time intervals (10, 20, 30, and 40 min for 35°C; 0.5, 1, 2, and 3 h for 30°C; and 1, 2, 5, and 24 h for 25°C), samples were taken and centrifuged at 4°C, and the residual activity was assayed as described above.

SDS-PAGE. SDS-PAGE was carried out according to the method described by Laemmli (25).

Biocatalysis. Substrate specificity of HAPMO was investigated by using crude cell extract. For all experiments, *E. coli* Rosetta pET22b(+)PpJD14HAPMO cells were used. The following substrates were investigated: 4-hydroxy-2-octanone, 4-hydroxy-2-nonanone, 4-hydroxy-2-decanone, and 4-hydroxy-2-undecanone; 3-phenyl-2-butanone; 3-phenyl-2-pentanone; and 4-hydroxy-4-phenyl-2-butanone. 4-Hydroxyacetophenone served as positive control.

Cells were grown in $2\times YT_{cap+amp}$ medium at 37°C to an optical density at 600 nm of 1 to 1.5. HAPMO expression was induced by the addition of IPTG to a final concentration of 0.1 mM. Expression was performed at 20°C for 6 h. Cells were harvested and washed twice with sterile 50 mM Tris-HCl buffer (pH 8.0) and finally resuspended in the same buffer. Cell disruption was performed using a precooled French press (96.5×10^3 kPa), and cell debris was removed by centrifugation (30 min, 4°C, 10,000 × *g*). Biocatalysis reactions were performed in flasks at a volume of 5 ml at 25°C. To 5 ml of cell lysate 7 μmol of substrate and 0.2 mmol of NADPH were added. After defined time intervals (1, 2, 4, 6, and

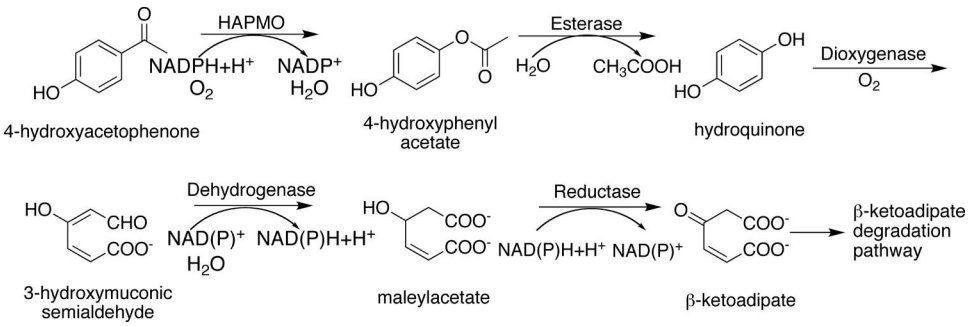

FIG. 4. Postulated degradation pathway of 4-hydroxyacetophenone catalyzed by the putative enzymes of the *P. putida* JD1 operon.

12 h) samples were obtained, extracted with ethyl acetate, and dried over anhydrous sodium sulfate. Samples were analyzed by GC and GC-MS.

GC and GC-MS analysis. Achiral GC-MS analyses were carried out on a GCMS-QP 2010 apparatus (Shimadzu Europa GmbH, Duisburg, Germany) with a BPX5 column (5% phenyl-/95% methylpolysilphenylen/siloxan; SGE GmbH, Darmstadt, Germany). The injection and detection temperatures were set to 220 and 300°C, respectively. Chiral analytics were done on a heptakis-(2,6-di-*O*-methyl-3-*O*-pentyl)-β-cyclodextrin column (Hydrodex-β-3P, 25 m by 0.25 mm; Macherey-Nagel, Düren, Germany) in a Hewlett-Packard GC 5890 series II (Agilent, Waldbronn, Germany). Injection and detection temperatures were set to 220°C.

Accession numbers. The nucleotide sequence of the amplified gene of 4-hydroxacetophenone monooxygenase from *P. putida* JD1 and the associated protein sequence, as well as a 16S rRNA gene sequence from *P. putida* JD1, have been deposited under GenBank accession numbers FJ010625 for the 4-hydroxyacetophenone monooxygenase and FJ010624 for the 16S rRNA gene.

RESULTS AND DISCUSSION

Amplification and cloning of the HAPMO gene. In 2000, three protein fragments, including the N-terminal sequence, of a Baeyer-Villiger monooxygenase from *P. putida* JD1 were determined by using Edman degradation, but the identification of the encoding gene and the recombinant expression were not reported. A BLAST search of these protein fragments revealed an identity of ~80% toward a BVMO from *P. fluorescens* ACB (GenBank accession no. AAK54073). On the basis of this sequence information, we then designed degenerate primers in order to perform PCR at different annealing temperatures. After sequencing of a 1.6-kb amplificate, identification of typical BVMO sequence motifs, and determination of the three known peptides, it was certain that the amplified sequence of 536 amino acids was indeed part of the HAPMO gene. Unfortunately, various PCR methods, including inverse PCR, failed to obtain the missing gene fragments, and the SiteFinding-PCR (see Fig. S1 in the supplemental material) was investigated (for a detailed method information, see the study by Tan et al. [37]). With this SiteFinding-PCR, a 10.2-kb fragment containing the whole HAPMO gene (1,920 bp) and several other open reading frames located up- and downstream could be identified. Analysis of these flanking genes suggests that HAPMO belongs together with four other putative enzymes (an esterase, a dioxygenase, a reductase, and a dehydrogenase) and a putative LysR regulator protein to an operon (Fig. 3). Since 4-hydroxyacetophenone can be considered the key substrate, the following biodegradation pathway in *P. putida* JD1 can be proposed (Fig. 4). First, 3-hydroxyacetophenone is converted into the corresponding ester by HAPMO, followed by the formation of a hydroquinone, which is further degraded via 3-hydroxymuconic semialdehyde and maleylacetate to β-ketoadipate, similar to the pathway described by Moonen et al. (30). Hence, the enzymatic Baeyer-Villiger oxidation is the key reaction to produce a substrate for the subsequent ring cleavage and further degradation. It has already been observed that in *Acinetobacter* sp. strain NCIMB 9871 and *Comamonas* sp. strain NCIMB 9872 the gene encoding the BVMO is clustered

TABLE 1. Purification of recombinant *P. putida* JD1 HAPMO from *E. coli*

Step	Vol (ml)	Total protein content (mg)	Total activity (U)	Sp act ($U/mg_{protein}$)	Purification factor	Yield (%)
Crude cell extract[a]	30	136	74	0.54	1	100
Q-Sepharose	60	13	97	7.5	15	131
Reactive Red	15	1.8	42	23.2	43	57

[a] Obtained from 4 g (wet weight) of *E. coli* Rosetta pET22b(+)PpJD1HAPMO.

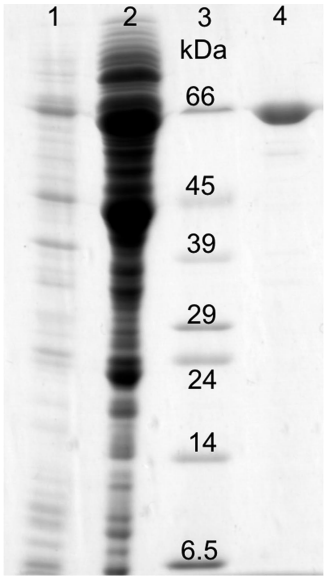

FIG. 5. Purification steps of HAPMO. Lanes: 1, lysate (1:10); 2, pooled active fractions from ion-exchange chromatography; 3, low-range marker (range, 6.5 to 66 kDa) from NEB; and 4, active fraction from affinity chromatography.

TABLE 2. Kinetic parameters of HAPMO from *P. putida* JD1[a]

Substrate	Structure	K_m (μM)	k_{cat} (s^{-1})	k_{cat}/K_m (10^3 $s^{-1} \cdot M^{-1}$)
Aromatic compounds				
4-Hydroxyacetophenone	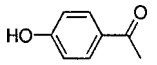	38.1	9.8	257
4-Fluoroacetophenone	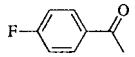	208	1.3	6.2
4-Chloroacetophenone	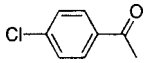	140	1.6	11
4-Aminoacetophenone	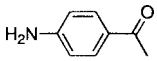	5.6	8.2	1,450
4-Methylacetophenone	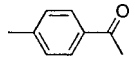	241	4.4	18.5
4-Methoxyacetophenone	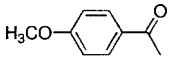	199	1.2	5.9
4-Nitroacetophenone	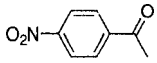	313	2.6	8.4
3′-Hydroxyacetophenone	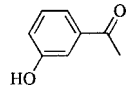	246	8.1	32.7
3-Aminoacetophenone	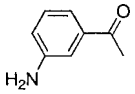	287	1.0	3.3
3-Methoxyacetophenone	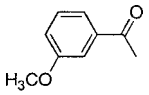	88.5	0.4	4.3
3-Nitroacetophenone	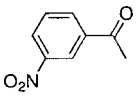	244	1.2	4.9
2′-Hydroxyacetophenone	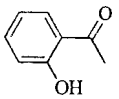	121	21.2	176
Acetophenone	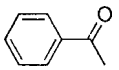	393	16.3	41.6
Propiophenone	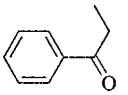	89.4	2.6	28.5
Butyrophenone	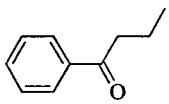	30,746	4.9	0.2
Benzaldehyde	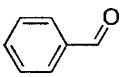	275	2.2	8.1
2-Phenylpropionaldehyde	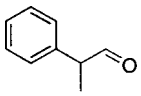	21,241	8.7	0.4
Trifluoroacetophenone	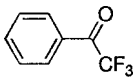	112	15.4	138
Methyl-4-tolyl sulfide	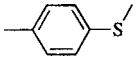	18,848	20	1.1
Heteroaromatic compounds				
2-Acetylpyrrole	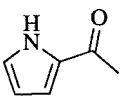	103	11.3	110

Continued on following page

TABLE 2—*Continued*

Substrate	Structure	K_m (μM)	k_{cat} (s^{-1})	k_{cat}/K_m (10^3 $s^{-1} \cdot M^{-1}$)
Aliphatic compounds				
2-Decanone	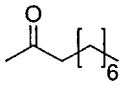	953	4.2	4.4
2,4-Pentanedione	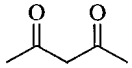	4,857	3.5	0.7

[a] All values were measured in Tris-HCl buffer (pH 8.0, 50 mM) at 30°C using a fixed NADPH concentration of 312 μM.

on the chromosome together with a hydrolase and a dehydrogenase (9, 17), which we also found for a BVMO from *P. putida* KT2440 (31).

Protein expression and purification. The expression of HAPMO was investigated using *E. coli* JM109 (with plasmid pJOEPpJD1HAPMO), various *E. coli* BL21(DE3) strains, and *E. coli* Rosetta [with plasmid pET22b(+)PpJD1HAPMO]. Different medium compositions and expression temperatures, as well as the addition of FMN, which is a precursor in the synthesis of FAD, were studied. Complex (LB medium supplemented with 2.5% [wt/vol] glucose and 2.5% [wt/vol] $K_2HPO_4 \cdot 3H_2O$) and 2×YT media were suggested to be optimal for these experiments. Adding FMN to the culture had no effect on HAPMO expression. The pET22b(+) vector yielded a higher amount of protein compared to the pJOE construct but, unfortunately, the majority of protein was produced as inclusion bodies. To overcome this problem, the expression temperature was lowered from 30 to 20°C. In addition, coexpression analysis using molecular chaperones was performed, but the expression of soluble protein was not improved (data not shown). A comparison of different *E. coli* strains [with the pET22b(+)PpJD1HAPMO construct] revealed that the Rosetta strain gave best results, since it supplies rare tRNAs, yielding the highest amounts of soluble HAPMO under optimized conditions at 20°C in complex medium after 6 h. The crude protein was purified to homogeneity in a two-step procedure using ion-exchange chromatography, followed by a 2′-ADP-based affinity chromatography with a recovery of 57% and a purification factor of 43 (Table 1 and Fig. 5).

pH optimum and thermal stability. The maximum activity was measured at pH 8 in Tris-HCl buffer, while at a pH of <6 the activity is very low (see Fig. S2 in the supplemental material). The highest thermal stability was found at 30°C. After 30 min at 35°C HAPMO possesses only 47% residual activity, and at 40°C it possesses even less than 1% (see Fig. S3 in the supplemental material). At 25°C HAPMO showed the highest activity and was found to be stable for at least 20 h.

Substrate specificity and kinetic measurements. In order to explore the substrate specificity, a wide range of potential substrates were investigated. It was found that HAPMO displays a broad substrate specificity among aromatic ketones (Table 2). Conversion of aromatic substrates was already reported for HAPMO from *P. fluorescens* ACB (19, 20). Open-chain and cyclic aliphatic ketones, which are good substrates for some known BVMOs (21, 34), were poorly accepted by HAPMO from *P. putida* JD1. Furthermore, the enzyme is strongly NADPH dependent. Oxidation of 4-hydroxyacetophenone does not occur with NADH as a cofactor. Substrates of HAPMO can be grouped into three classes: (i) aromatic, (ii) heteroaromatic, and (iii) aliphatic compounds (Table 2). The substances that did not show significant activity (<0.1 U/mg of protein) at a concentration of 5 mM were 2-acetylpyridine, 3-acetylpyridine, 4-acetylpyridine, 4-hydroxy-3-methoxyacetophenone, 1-indanone, cyclohexanone, cyclopentanone, acetylindole, progesterone, acetone, hydroxyacetone, dihydroxyacetone, (endo/exo)-acetylnorbornene, and 4-decanone.

Conversion of aromatic compounds. HAPMO from *P. putida* JD1 preferentially oxidizes acetophenone derivatives. Like HAPMO from *P. fluorescens* ACB, the highest catalytic activity could be observed with compounds bearing an electron-donating group in the *para* position of the aromatic ring. This suggests that the functional position at the aromatic ring (*para*, *meta*, or *ortho*) is crucial for substrate recognition and affinity and influences K_m and k_{cat} values, which is demonstrated for the three hydroxyacetophenone compounds (Table 2). Still, substitutions on the phenyl ring and modifications at the aceto function were accepted by HAPMO. Conversion of 4-hydroxyacetophenone (K_m = 47 μM) and acetophenone (K_m = 384 μM) was already reported by Tanner and Hopper (38), and K_m values correlate well with our data (Table 2). Also, compared to HAPMO from *P. fluorescens* ACB (18), most of the values were in the same range. Interestingly, 4-nitroacetophenone is not converted by *P. fluorescens* ACB HAPMO, whereas *P. putida* JD1 HAPMO oxidizes it with a K_m of 313 μM. A nitro group reduces the electron density of the aromatic ring through the negative mesomeric and inductive effect (−M and −I), while methyl, hydroxy, and amino functions possess a positive inductive (+I) or mesomeric effect (+M). The maximal turnover number for aromatic compounds was reached with 2′-hydroxyacetophenone (21.2 s^{-1}), followed by methyl-4-tolyl sulfide (20 s^{-1}), acetophenone (16.3 s^{-1}), and trifluoroacetophenone (15.4 s^{-1}). Kinetic data found for other aromatic substrates were in the same range (1.0 to 11.3 s^{-1}), which indicates that substitutions on the ring do not influence maximal turnover numbers significantly. Only in response to 3-methoxyacetophenone does HAPMO show a low activity. The lowest K_m values could be observed with 4-hydroxyacetophenone (38.1 μM) and 4-aminoacetophenone (5.6 μM), whereas for more bulky and hydrophobic substituents (4-methyl- and 4-methoxyacetophenone) the K_m values were much higher. The structure of the aceto function also influences the affinity and rate of catalysis: while benzaldehyde has

TABLE 3. Biocatalysis of β-hydroxy-2-ketones using crude cell extract (*E. coli* Rosetta pET22b(+)PpJD1HAPMO)[a]

Substrate[b]	Time (h)	ee_p (%)	Conversion (%)	E	Product
4-Hydroxy-2-octanone	4	12.4	2.4	1.3	4-Hydroxyhexylacetate
4-Hydroxy-2-nonanone	4	24.0	4.8	1.6	4-Hydroxyheptylacetate
4-Hydroxy-2-decanone	4	50.2	3.0	3.0	4-Hydroxyoctylacetate
4-Hydroxy-2-undecanone	4	6.4	8.6	1.1	4-Hydroxynonylacetate

[a] Experiments were carried out in Tris-HCl (pH 8.0, 50 mM) at 25°C in shake flasks. The ee_p (i.e., the enantiomeric excess of the product), the conversion, and the E value were each calculated as described by Chen et al. (3).

[b] The equation for substrates and products is 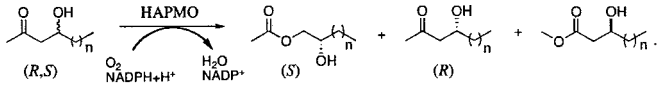

a K_m similar to that of acetophenone, the turnover number is much smaller. An additional methyl group (in propiophenone) increases the substrate affinity with a much lower K_m, but k_{cat} remains in the range of benzaldehyde. More bulky substituents such as butyrophenone lead to a drastic decrease in affinity, indicating that the propionyl residue might be optimal for catalysis.

HAPMO also catalyzes sulfoxidation. In addition to oxidation of ketones and aldehydes, some BVMOs are also able to catalyze the sulfoxidation of a variety of sulfides (6), which can be interesting chiral building blocks for the pharmaceutical chemistry. Here, methyl-4-tolyl sulfide was tested as a substrate for HAPMO. This prochiral sulfide was oxidized with a k_{cat} of 20 s^{-1}, while the K_m value was rather high (18.8 mM), which is in contrast to the affinity toward the corresponding ketone 4-methylacetophenone. This differs from the HAPMO from *P. fluorescens* ACB, which converts both methyl-4-tolyl sulfide and 4-methylacetophenone at similar K_m and k_{cat} values (20).

Conversion of heteroaromatic compounds. Thus far, only a few BVMOs have been tested for conversion of heteroaromatic compounds, and until now only the HAPMO from *P. fluorescens* ACB has been shown to be active against them (18). Here, three pyridine substrates and one pyrrole substrate were investigated. While the 2-, 3-, and 4-acetylpyridines are not converted, 2-acetylpyrrole is oxidized to the ester. Obviously, the pyrrole ring is preferred over the pyridine. With a K_m value of 103 μM, the affinity for 2-acetylpyrrole is even higher than for acetophenone and some derivatives.

Oxidation of aliphatic ketones. Although aliphatic cyclic ketones and open-chain ketones are known to be good substrates for some BVMOs (4, 21, 34), HAPMO is able to convert only a few of them. HAPMO showed no activity at all against cyclohexanone, cyclopentanone, and 4-decanone, while 2-decanone and 2,4-pentanedione were oxidized with turnover rates in the same range as some aromatic substrates. 2-Decanone was converted with a fivefold lower K_m value compared to 2,4-pentadione.

Biocatalysis. For kinetic resolution of several racemic substrates, crude cell extract was used. Although the use of crude cell extract requires the addition of expensive NADPH as a cofactor, which makes this system problematic from an economic point of view, it assures that the substrates and products are not further metabolized by the whole cells. Biotransformations using resting cells—facilitating cofactor regeneration by glucose addition—were also performed but gave results similar to those obtained with crude extract. The compounds investigated were grouped into (i) aliphatic open-chain racemic ketones (4-hydroxy-2-octanone, 4-hydroxy-2-nonanone, 4-hydroxy-2-decanone, and 4-hydroxy-2-undecanone) and (ii) arylaliphatic racemic substrates

TABLE 4. Biocatalysis of arylaliphatic ketones using crude cell extract [*E. coli* Rosetta pET22b(+)PpJD1HAPMO][a]

Substrate	Time (h)	ee_p (%)	Conversion (%)	E	Product
3-Phenyl-2-butanone[b]	4	99.2	45.6	>200	1-Phenylethylacetate
3-Phenyl-2-pentanone[b]	24	NC	NC	NC	1-Phenylpropylacetate
4-Hydroxy-4-phenylbutanone[c]	24	NC	NC	NC	1-Hydroxy-1-phenylethylacetate

[a] Experiments were carried out in Tris-HCl (pH 8.0, 50 mM) at 25°C in shake flasks. The ee_p (i.e., the enantiomeric excess of the product), conversion, and E values were calculated as described by Chen et al. (3). NC, no conversion.

[b] The equation for this substrate is 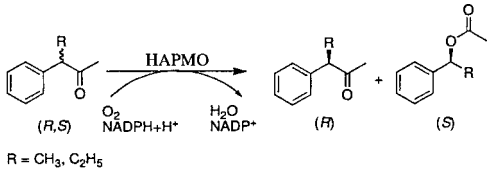

[c] The equation for this substrate is 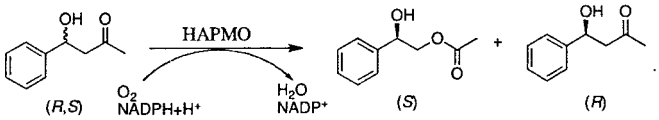

(3-phenyl-2-butanone, 3-phenyl-2-pentanone and 4-hydroxy-4-phenyl-2-butanone). The results for conversion, enantiomeric excess, and enantioselectivity are summarized in Tables 3 and 4. As already mentioned, aliphatic open-chain ketones are oxidized poorly by HAPMO (Table 3). Both enantiomeric excess and conversion were very low for all four substrates. A slight increase of the product enantiomeric excess could be observed for 4-hydroxy-2-decanone (50% ee), while conversion was highest for 4-hydroxy-2-undecanone (8.6%). Due to the structure of 4-hydroxy-2-ketones, two different products are possible (acetate or methyl ester), but with this HAPMO only the acetate was formed. With respect to enantioselectivity, 3-phenyl-2-butanone was converted with an exceptionally high E value of >200 at 45.6% conversion, with an enantiomeric excess for the product, 1-phenylethylacetate, of 99.2% ee (Table 4). The conversion could be further increased to 66% (data not shown) by the addition of an ion exchanger (Lewatit MP64) at pH 8.5, which allows then for a dynamic kinetic resolution. However, 3-phenyl-2-pentanone and 4-hydroxy-4-phenyl-2-butanone were not converted at all. This narrow substrate spectrum and high enantioselectivity for one compound matches results reported for BVMOs from *P. fluorescens* DSM50106 (22) and *P. putida* KT2440 (12), but the HAPMO from *P. putida* JD1 is far more selective.

In summary, we could successfully clone, express, and characterize a 4-hydroxyacetophenone monooxygenase from *P. putida* JD1. The key to successful identification of the encoding gene was the SiteFinding-PCR, which proved to be a powerful and reliable tool for amplifying the unknown flanking regions from gDNA. Besides the HAPMO from *P. fluorescens* ACB (which has only 83% sequence identity) and the PAMO from *T. fusca*, this HAPMO is actually the third described BVMO preferentially oxidizing arylaliphatic ketones. Interestingly, within this class, the HAPMO described here converts a broad range of *para*-substituted aromatic ketones bearing either electron-donating (OH, CH_3, and NH_2) or electron-withdrawing (NO_2) groups with very low K_m values and high k_{cat} values. Furthermore, HAPMO converts 3-phenyl-2-butanone into 1-phenylethylacetate with excellent selectivity, making it a versatile enzyme for biocatalysis.

ACKNOWLEDGMENT

We thank the Deutsche Bundesstiftung Umwelt for a stipend to Jessica Rehdorf.

REFERENCES

1. **Alphand, V., G. Carrea, R. Wohlgemuth, R. Furstoss, and J. M. Woodley.** 2003. Towards large-scale synthetic applications of Baeyer-Villiger monooxygenases. Trends Biotechnol. **21:**318–323.
2. **Baeyer, A., and V. Villiger.** 1899. Einwirkung des Caro'schen Reagens auf Ketone. Ber. Dtsch. Chem. Ges. **32:**3625–3633.
3. **Chen, C.-S., Y. Fujimoto, G. Girdaukas, and C. J. Sih.** 1982. Quantitative analysis of biochemical kinetic resolutions of enantiomers. J. Am. Chem. Soc. **104:**72947299.
4. **Chen, Y.-C. J., O. P. Peoples, and C. T. Walsh.** 1988. *Acinetobacter* cyclohexanone monooxygenase: gene cloning and sequence determination. J. Bacteriol. **170:**781–789.
5. **Colonna, S., N. Gaggero, G. Carrea, G. Ottolina, P. Pasta, and F. Zambianchi.** 2002. First assymetric epoxidation catalysed by cyclohexanone monooxygenase. Tetrahedron Lett. **43:**1797–1799.
6. **Colonna, S., N. Gaggero, G. Carrea, and P. Pasta.** 1998. Oxidation of organic cyclic sulfites to sulfates: a new reaction catalysed by cyclohexanone monooxygenase. Chem. Commun. **3:**415–416.
7. **de Gonzalo, G., G. Ottolina, F. Zambianchi, M. W. Fraaije, and G. Carrea.** 2006. Biocatalytic properties of Baeyer-Villiger monooxygenases in aqueous-organic media. J. Mol. Cat. B Enzymatic **39:**91–97.
8. **Doig, S. D., L. M. O'Sullivan, S. Patel, J. M. Ward, and J. M. Woodley.** 2001. Large scale production of cyclohexanone monooxygenase from *Escherichia coli* TOP10 pQR239. Enzyme Microb. Technol. **28:**265–274.
9. **Donoghue, N. A., and P. W. Trudgill.** 1975. The metabolism of cyclohexanol by *Acinetobacter* NCIMB 9871. Eur. J. Biochem. **60:**1–7.
10. **Forney, F. W., and A. J. Markovetz.** 1969. An enzyme system for aliphatic methyl ketone oxidation. Biochem. Biophys. Res. Commun. **37:**31–38.
11. **Fraaije, M. W., J. Wu, D. P. H. M. Heuts, E. W. van Hellmond, J. H. L. Spelberg, and D. B. Janssen.** 2005. Discovery of a thermostable Baeyer-Villiger monooxygenase by genome miming. Appl. Microbiol. Biotechnol. **66:**393–400.
12. **Geitner, K., A. Kirschner, J. Rehdorf, M. Schmidt, M. D. Mihovilovic, and U. T. Bornscheuer.** 2007. Enantioselective kinetic resolution of 3-phenyl-2-ketones using Baeyer-Villiger monooxygenases. Tetrahedron Asymm. **18:** 892–895.
13. **Hilker, I., V. Alphand, R. Wohlgemuth, and R. Furstoss.** 2004. Microbial transformations 56. Preparative scale asymmetric Baeyer-Villiger oxidation using a highly productive "two-in-one" resin-based in situ SFPR concept. Adv. Synth. Catal. **346:**203–214.
14. **Hilker, I., M. C. Gutierrez, R. Furstoss, J. Ward, R. Wohlgemuth, and V. Alphand.** 2008. Preparative scale Baeyer-Villiger biooxidation at high concentration using recombinant *Escherichia coli* and in situ substrate feeding and product removal. Nat. Protoc. **3:**546–554.
15. **Hilker, I., R. Wohlgemuth, V. Alphand, and R. Furstoss.** 2005. Microbial transformations 59: first kilogram scale asymmetric microbial Baeyer-Villiger oxidation with optimized productivity using a resin-based in situ SFPR strategy. Biotechnol. Bioeng. **92:**702–710.
16. **Holland, H. L., J.-X. Gu, A. Kerridge, and A. Willets.** 1999. Biotransformation of organic sulfides. Part 11. Preparation of functionalised phenyl propyl sulfoxides using *Helminthosporium* species and *Mortierella isabellina.* Biocatal. Biotrans. **17:**305–317.
17. **Iwaki, H., Y. Hasegawa, S. Wang, M. M. Kayser, and P. C. K. Lau.** 2002. Cloning and characterization of a gene cluster involved in cyclopentanol metabolism in *Comamonas* sp. strain NCIMB 9872 and biotransformations effected by *Escherichia coli*-expressed cyclopentanone 1,2-monooxygenase. Appl. Environ. Microbiol. **68:**5671–5684.
18. **Kamerbeek, N. M., D. B. Janssen, W. J. H. van Berkel, and M. W. Fraaije.** 2003. Baeyer-Villiger monooxygenases, an emerging family of flavin-dependent biocatalysts. Adv. Synth. Catal. **345:**667–678.
19. **Kamerbeek, N. M., M. J. H. Moonen, J. G. M. van der Ven, W. J. H. van Berkel, M. W. Fraaije, and D. B. Janssen.** 2001. 4-Hydroxyacetophenone monooxygenase from *Pseudomonas fluorescens* ACB. Eur. J. Biochem. **268:** 2547–2557.
20. **Kamerbeek, N. M., J. J. Olsthoorn, M. W. Fraaije, and D. B. Janssen.** 2003. Substrate specificity and enantioselectivity of 4-hydroxyacetophenone monooxygenase. Appl. Environ. Microbiol. **69:**419–426.
21. **Kirschner, A., J. Altenbuchner, and U. T. Bornscheuer.** 2007. Cloning, expression and characterization of a Baeyer-Villiger monooxygenase from *Pseudomonas fluorescens* DSM 50106 in *Escherichia coli*. Appl. Microbiol. Biotechnol. **73:**1065–1075.
22. **Kirschner, A., and U. T. Bornscheuer.** 2006. Baeyer-Villiger monooxygenase-catalyzed kinetic resolution of 4-hydroxy-2-ketones. Angew. Chem. Int. Edit. **45:**7004–7006.
23. **Kourouli, T., P. Kefalas, N. Ragoussis, and V. Ragoussis.** 2002. A new protocol for a regioselective aldol condensation as an alternative convenient synthesis of β-ketols and α,β-unsaturated ketones. J. Org. Chem. **67:**4615–4618.
24. **Krebsfänger, N., F. Zocher, J. Altenbuchner, and U. T. Bornscheuer.** 1998. Production, purification, characterization, and enantioselelectivity of a recombinant esterase from *Pseudomonas fluorescens*. Enzyme Microb. Technol. **22:**641–646.
25. **Laemmli, U. K.** 1970. Cleavage of structural proteins during assembly of the head of bacteriophage T4. Nature **27:**680–685.
26. **Lane, D. J.** 1991. 16S/23S rDNA sequencing, p. 115–175. *In* E. Stackebrandt and M. Goodfellow (ed.), Nucleic acid techniques in bacterial systematics. Wiley, Chichester, United Kingdom.
27. **Latham, J., J. A., B. P. Branchaud, Y.-C. J. Chen, and C. Walsh.** 1986. Allylic and propargylic phenyl selenide oxygenation by cyclohexanone oxygenase: [2,3]-sigmatraopic rearragement of the enzyme-generated selenidoxide. J. Chem. Soc. Chem. Commun. **1986:**528-530.
28. **Malito, E., A. Alfieri, M. W. Fraaije, and A. Mattevi.** 2004. Crystal structure of a Baeyer-Villiger monooxygenase. Proc. Natl. Acad. Sci. USA **101:**13157–13162.
29. **Mihovilovic, M. D., B. Müller, and P. Stanetty.** 2002. Monooxygenase-mediated Baeyer-Villiger oxidations. Eur. J. Org. Chem. **2002:**3711–3730.
30. **Moonen, M. J. H., N. M. Kamerbeek, A. H. Westphal, S. A. Boeren, D. B. Janssen, M. W. Fraaije, and W. J. H. van Berkel.** 2008. Elucidation of the 4-hydroxyacetophenone catabolic pathway in *Pseudomonas fluorescens* ACB. J. Bacteriol. **190:**5190–5198.

31. **Nelson, K. E., C. Weinel, I. T. Paulsen, and R. J. Dodson.** 2002. Complete genome sequence and comparative analysis of the metabolically versatile *Pseudomonas putida* KT2440. Environ. Microbiol. **4:**799–808.
32. **Ochman, H., A. S. Gerber, and D. L. Hartl.** 1988. Genetic application of an inverse polymerase chain reaction. Genetics **120:**621–623.
33. **Ottolina, G., S. Bianchi, B. Belloni, G. Carrea, and B. Danieli.** 1999. First asymmetric oxidation of tertiary amines by cyclohexanone monooxygenase. Tetrahedron Lett. **40:**8483–8486.
34. **Rehdorf, J., A. Kirschner, and U. T. Bornscheuer.** 2007. Cloning, expression and characterization of a Baeyer-Villiger monooxygenase from *Pseudomonas putida* KT2440. Biotechnol. Lett. **29:**1393–1398.
35. **Rubottom, G. M., and C.-W. Kim.** 1983. Preparation of methyl ketones by sequential treatment of carboxylic acids with methyllithium and chlorotrimethylsilane. J. Org. Chem. **48:**1550–1552.
36. **Sambrook, J., and D. W. Russell.** 2001. Molecular cloning: a laboratory manual, 3rd ed. Cold Spring Harbor Laboratory Press, New York, NY.
37. **Tan, G., Y. Gao, M. Shi, X. Zhang, S. He, Z. Chen, and C. An.** 2005. SiteFinding-PCR: a simple and efficient PCR method for chromosome walking. Nucleic Acids Res. **33:**e122.
38. **Tanner, A., and D. J. Hopper.** 2000. Conversion of 4-hydroxyacetophenone into 4-phenyl acetate by a flavin adenine dinucleotide-containing Baeyer-Villiger-type monooxygenase. J. Bacteriol. **182:**6565–6569.
39. **Turfitt, G. E.** 1948. The microbiological degradation of steroids. Biochem. J. **42:**376–383.

Erklärung

Hiermit erkläre ich, dass diese Arbeit bisher von mir weder an der Mathematisch-Naturwissenschaftlichen Fakultät der Ernst-Moritz-Arndt-Universität Greifswald noch einer anderen wissenschaftlichen Einrichtung zum Zwecke der Promotion eingereicht wurde.

Ferner erkläre ich, dass ich diese Arbeit selbständig verfasst und keine anderen als die angegebenen Hilfsmittel benutzt habe.

_____

Unterschrift

Lebenslauf

Name:	Jessica Rehdorf
Geburtstag:	22. August 1981
Geburtsort:	Berlin
Familienstand:	ledig
Nationalität:	Deutsch

Ausbildung

2007 - 2009	Promotion an der Ernst-Moritz-Arndt-Universität Greifswald im Arbeitskreis Biotechnologie & Enzymkatalyse, gefördert durch ein Stipendium der Deutschen Bundesstiftung Umwelt (DBU, Osnabrück) im Schwerpunkt „Nachhaltige Bioprozesse“ Betreuer: Prof. Uwe T. Bornscheuer Thema: Discovery of novel Baeyer-Villiger monooxygenases and their application in organic synthesis.
2008/2009	Gastwissenschaftlerin am Institut für Angewandte Synthesechemie der Technischen Universität Wien im Arbeitskreis von Prof. Marko D. Mihovilovic
2006	Diplomarbeit im Studiengang Biochemie Betreuer: Prof. Uwe T. Bornscheuer Thema: Klonierung, Expression und biochemische Charakterisierung einer Baeyer-Villiger Monooxygenase aus *Pseudomonas* sp.
2005	Projektmitarbeiterin am Robert-Koch-Institut in Berlin Thema: Molekulargenetik und Epidemiologie von Herpesviren bei Xenotransplantationen – Klonierung von Genen des Porcinen Lymphotropen Herpesvirus 1 sowie Transkriptions- und Expressionsanalysen.
2005	Gastwissenschaftlerin bei Chirotech Technology Limited Dowpharma (jetzt Dr. Reddy’s) in Cambridge, Großbritannien Thema: Discovery and application of novel alcohol dehydrogenases – purification and biocatalysis.
Apr. 2003	Wissenschaftliche Hilfskraft am Institut für Biochemie in der Arbeitsgruppe von Prof. J. Heinicke (Synthese von Phosphinverbindungen, NMR-Auswertungen)
Feb. 2003	Wissenschaftliche Hilfskraft am Institut für Mikrobiologie und Molekularbiologie in der Arbeitsgruppe von Prof. M. Hecker (Arbeit mit extrazellulären Proteasen aus *Staphylococcus aureus*)
2001 - 2006	Biochemiestudium an der Universität Greifswald, Abschluss Diplom
2001	Abitur (bilingual) und Latinum am Johann-Gottfried-Herder Gymnasium, Berlin
1992 - 2001	Besuch des Johann-Gottfried-Herder Gymnasiums, Berlin

Publikationen

1. J. Rehdorf and U. T. Bornscheuer (2009). Monooxygenases, Baeyer-Villiger applications in organic synthesis., In: *Wiley Encyclopedia of Industrial Biotechnology*, Ed.: M. Flickinger; Vol 1, in Druck.

2. J. Rehdorf, A. Lengar, U. T. Bornscheuer and M. D. Mihovilovic (2009). Kinetic resolution of aliphatic acyclic β-hydroxyketones by recombinant whole-cell Baeyer-Villiger monooxygenases – formation of enantiocomplementary regioisomeric esters, *Bioorg. Med. Chem. Lett*., **19**, 3739-3743.

3. J. Rehdorf, C. L. Zimmer and U. T. Bornscheuer (2009). Cloning, expression, characterization and biocatalytical investigation of 4-hydroxyacetophenone monooxygenase from *P. putida* JD1, *Appl. Environ. Microbiol*., **75**, 3106-3114.

4. K. Geitner, A. Kirschner, J. Rehdorf, M. Schmidt, M. D. Mihovilovic and U. T. Bornscheuer (2007). Enantioselective kinetic resolution of 3-phenyl-2-ketones using Baeyer-Villiger monooxygenases, *Tetrahedron Asymm*., **18**, 892-895.

5. J. Rehdorf, A. Kirschner and U. T. Bornscheuer (2007). Cloning, expression and characterization of a Baeyer-Villiger monooxygenase from *P. putida* KT2440, *Biotechnol. Lett*., **29**, 1393-1398.

6. J. Rehdorf, M. D. Mihovilovic, M. W. Fraaije and U. T. Bornscheuer (2009). Enzymatic synthesis of enantiomerically pure β-amino ketones, β-amino esters and β-amino alcohols with Baeyer-Villiger monooxygenases; eingereicht.

7. J. Rehdorf, M. D. Mihovilovic and U. T. Bornscheuer (2009). Exploiting regioselectivity of Baeyer-Villiger monooxygenases: a route to the formation of β-amino acids; eingereicht.

8. N. Giang-Son, R. Kourist, M. Paravidino, R. V. A. Orru, J. Rehdorf, A. Hummel, U. Hanefeld and U. T. Bornscheuer (2009). The substrate acceptance of esterases for tertiary alcohols is strongly affected by electronic interaction in the active site; eingereicht.
9. K. Geitner, J. Rehdorf, R. Snajdrova and U. T. Bornscheuer (2009). Scale-up of Baeyer-Villiger monooxygenase-catalyzed synthesis of enantiopure compounds; eingereicht.

Vorträge und Poster auf internationalen Konferenzen

Vortrag: “Discovery of novel Baeyer-Villiger monooxygenases and their application in organic chemistry“; Bioperspectives in Hannover (07. - 09. Oktober 2008).

Poster: “Kinetic resolution of aliphatic acyclic β-hydroxyketones by Baeyer-Villiger monooxygenases – formation of enantiocomplementary regioisomeric esters“; Biotrans in Bern (05. - 09. Juli 2009).

Poster: “Cloning, expression, characterization and biocatalytic invesrtigation of the 4-hydroxyacetophenone monooxygenase from *P. putida* JD1“; International Congress on Biocatalysis, BioCat, in Hamburg (31. August – 04. September 2008).